

Some pages of this thesis may have been removed for copyright restrictions.

If you have discovered material in AURA which is unlawful e.g. breaches copyright, (either yours or that of a third party) or any other law, including but not limited to those relating to patent, trademark, confidentiality, data protection, obscenity, defamation, libel, then please read our [Takedown Policy](#) and [contact the service](#) immediately

**ENZYMATIC PRODUCTION OF OLIGOSACCHARIDES IN
CENTRIFUGAL FIELDS**

PAUL ANDREW TACK

Doctor of Philosophy

ASTON UNIVERSITY

February 2001

This copy of the thesis has been supplied on condition that anyone who consults it is understood to recognise that its copyright rests with its author and that no quotation from this thesis and no information derived from it may be published without proper acknowledgement.

ASTON UNIVERSITY

ENZYMATIC PRODUCTION OF OLIGOSACCHARIDES
IN CENTRIFUGAL FIELDS

PAUL ANDREW TACK

PhD

FEBRUARY 2001

SUMMARY

The aims of this work have been to identify an enzymatic reaction system suitable to investigate and develop the high-speed centrifuge as a novel reaction system for performing such reactions. The production of galacto-oligosaccharides by the trans-galactosyl activity of the enzyme β -galactosidase on lactose monohydrate was identified as a model enzymatic system to elucidate the principles of this type of process. Galacto-oligosaccharides have attracted considerable commercial interest as food additives which have been shown to be beneficial to the health of the human gastrointestinal tract. The development of a single unit operation capable of controlling the biosynthesis of galacto-oligosaccharides whilst simultaneously separating the enzyme from the reaction products would reduce downstream processing costs.

This thesis shows for the first time that by using a combination of (a) immobilised or insolubilised β -galactosidase, (b) a rate-zonal centrifugation technique, and (c) various applied centrifugal fields, that a high-speed centrifuge could be used to control the formation of galacto-oligosaccharides whilst removing the enzyme from the reaction products. By layering a suspension of insolubilised β -galactosidase on top of a lactose monohydrate density gradient and centrifuging, the applied centrifugal fields generated produced sedimentation of the enzyme particles through the substrate. The higher sedimentation rate of the enzyme compared to those of the reaction products allowed for separation to take place. Complete sedimentation, or pelleting of the enzyme permits the possible recovery and re-use. Insolubilisation of the enzyme allowed it to be sedimented through the substrate gradient using much lower applied centrifugal fields than that required to sediment free soluble enzyme and this allowed for less expensive centrifugation equipment to be used.

Using free soluble and insolubilised β -galactosidase stirred-batch reactions were performed to investigate the kinetics of lactose monohydrate hydrolysis and galacto-oligosaccharide formation. Based on these results a preliminary mathematical model based on Michaelis-Menten kinetics was produced. It was found that the enzyme insolubilisation process using a chemical cross-linking agent did not affect the process of galacto-oligosaccharide formation.

Centrifugation experiments were performed and it was found that by varying the applied centrifugal fields that the yield of galacto-oligosaccharides could be controlled. The higher the applied centrifugal fields the lower the yield of galacto-oligosaccharides. By increasing the applied centrifugal fields the 'contact time' between the sedimenting enzyme and the substrate was reduced, which produced lower yields. A novel technique involving pulsing the insolubilised enzyme through the substrate gradient was developed and this was found to produce higher yields of galacto-oligosaccharide compared to using a single enzyme loading equivalent to the total combined activity of the pulses. Comparison of the galacto-oligosaccharide yields between stirred-batch and centrifugation reactions showed that the applied centrifugal fields did not adversely affect the trans-galactosyl activity of the insolubilised enzyme.

KEY WORDS: Applied Centrifugal Fields, Centrifugation, Galacto-oligosaccharide, β -Galactosidase, Insolubilisation, Lactose Monohydrate, Rate-Zonal Centrifugation, Transgalactosidation.

Dedicated to my mother and late father,
and to my family for their support.

ACKNOWLEDGEMENTS

The author wishes to thank the following:

Professor W. R. McWhinnie, Professor N. Slater and the Department of Chemical Engineering and Applied Chemistry for making the research facilities available.

Dr. E. L. Smith, my research supervisor for his advice, guidance and enthusiasm.

Dr. C. West for his helpful advice and useful discussions.

All the staff in the Department and in particular, Dr. D. E. Walton for his friendship and advice.

Finally, I would like to thank Mum, Karen, Dave, Lee, Gillian and Laura for their encouragement and support throughout this work.

LIST OF CONTENTS

	Page
Summary	2
1.0 Introduction	22
1.1 Bioreaction and Separation in Centrifugal Fields	22
1.1.1 Literature Survey	22
1.1.2 The Search for a Model Enzymatic Reaction System for use in the Centrifugal Bioreactor	26
1.2 Structure of the Thesis	27
2.0 Stirred-Batch Reaction Studies Using Soluble and Insolubilised β-Galactosidase	30
2.1 The Hydrolytic and Trans-Galactosyl Activity of β -Galactosidase	30
2.1.1 An Historical Perspective	30
2.1.2 Mechanism of Galacto-oligosaccharide Formation	33
2.1.3 The Effect of Galactose Inhibition and Mutarotation on β -Galactosidase Activity	37
2.2 Theory of Single-Substrate Kinetics	39
2.2.1 Introduction	39
2.2.2 Calculation of Kinetic Parameters using the Michaelis-Menten Equation	43
2.2.3 The Kinetics of Enzyme Inhibition	44
2.2.3.1 Determination of the Inhibition Constant, K_i , using the Dixon Plot Method	45
2.2.3.2 Effects of Enzyme Immobilisation and Insolubilisation on Enzyme Kinetic Parameters	46
2.3 The Industrial Use of Soluble and Immobilised β -Galactosidase	49
2.4 Stirred-batch Reactions using β -Galactosidase from <i>Aspergillus oryzae</i> (Biolactase F)	50
2.4.1 Properties of β -Galactosidase from <i>Aspergillus oryzae</i> (Biolactase F)	50
2.4.2 Stirred-batch Reactions Performed Using Soluble β -Galactosidase from <i>Aspergillus oryzae</i> (Biolactase F)	52
2.4.2.1 Determination of V_{max} and K_m for Soluble β -Galactosidase from <i>Aspergillus oryzae</i> (Biolactase F)	58
2.4.2.2 Determination of K_i for Soluble β -Galactosidase from <i>Aspergillus oryzae</i> (Biolactase F)	59
2.4.3 Stirred-batch Reactions Performed Using glutaraldehyde insolubilised β -Galactosidase from <i>Aspergillus oryzae</i> (Biolactase F)	59

2.4.3.1	Determination of V_{\max} and K_m for glutaraldehyde insolubilised β -Galactosidase from <i>Aspergillus oryzae</i> (Biolactase F)	64
2.4.3.2	Determination of K_i for glutaraldehyde insolubilised β -Galactosidase from <i>Aspergillus oryzae</i> (Biolactase F)	65
2.4.4	Comparison of the Results Obtained From Soluble and Glutaraldehyde Insolubilised β -Galactosidase Stirred-batch Reactions	65
2.4.5	Kinetic Modelling of Lactose Hydrolysis	67
2.4.5.1	Preliminary Study of Insolubilised β -Galactosidase Particles	72
3.0	Centrifugal Studies Using Soluble β-Galactosidase Enzyme	75
3.1	Development of the Centrifuge	75
3.2	Principles and Practices of Centrifugation	77
3.2.1	Introduction	77
3.2.2	Concepts of Sedimentation Theory	77
3.2.3	Calculation and Standardisation of the Sedimentation Coefficient	80
3.2.4	Sedimentation Theory Applied to Gradient Centrifugation	81
3.2.4.1	Calculation of the Force-time Integral	82
3.2.4.2	Determination of the Radial Position of Particles	84
3.2.4.3	Analysis of Gradient Medium	86
3.2.4.4	Standardising the Estimated Sedimentation Coefficient of a Particle in a Gradient Medium	87
3.2.5	Estimation of the Sedimentation Coefficient Using Isokinetic Gradients	87
3.2.6	The Relationship Between Sedimentation Coefficients and Molecular Parameters	89
3.2.6.1	The Partial Specific Volume	90
3.2.6.2	The Diffusion Coefficient	92
3.2.6.3	The Frictional Coefficient	93
3.2.7	Hydrostatic Pressure	95
3.2.8	Wall Effects	96
3.2.9	Droplet Sedimentation	98
3.2.10	The Swirling Effect	100
3.3	Classification of Centrifuges	100
3.3.1	Introduction	100

3.3.2	Industrial Centrifuges	102
3.3.3	Laboratory Centrifuges	106
3.3.3.1	Analytical Ultracentrifuges	106
3.3.3.2	Preparative Centrifuges	107
3.4	Normal Rate Separations	111
3.5	Centrifugation Studies With Soluble Free β -Galactosidase Using a Modified Version of the Normal Rate Separation Technique	112
3.5.1	Introduction	112
3.5.2	Beckman J2-MC Centrifuge Temperature Attainment and Control	113
3.5.3	Soluble Free β -Galactosidase Centrifugation Studies	113
3.5.4	Discussion of Results	117
4.0	Rate-Zonal Centrifugation Using Soluble β-Galactosidase Enzyme	119
4.1	Introduction	119
4.2	Practical Aspects of Rate-Zonal, or Density Gradient Centrifugation	121
4.2.1	Density Gradient Media	121
4.2.2	Density Gradient Preparation	122
4.2.3	Sample Loading and Convection During Rate-Zonal Centrifugation	125
4.2.4	Conditions During Centrifugation	126
4.2.5	Recovery of Fractions From the Gradient	126
4.2.6	Determining the Density Gradient Profile	128
4.2.7	Analytical Determination of Fraction Contents	128
4.3	Centrifugation Studies With Soluble Free β -Galactosidase Using the Rate-Zonal Separation Technique	129
4.3.1	Introduction and Experimental Programme	129
4.3.2	Density and Viscosity of Lactose Monohydrate Solutions	130
4.3.3	Reaction System Sedimentation Coefficients	131
4.3.3.1	β -Galactosidase Sedimentation Coefficient	132
4.3.3.2	Carbohydrate Sedimentation Coefficients	132
4.3.3.3	Comparison of the Reaction System Sedimentation Coefficients	133
4.3.4	The Formation and Stability of Lactose Monohydrate Density Gradients	133

4.3.4.1	The Formation Time (t_D) and the Stability Time (t_S) for a 10 to 40% ^{w/v} Lactose Monohydrate Continuous Density Gradient at 40°C	134
4.3.4.2	The Formation Time (t_D) and the Stability Time (t_S) for a 20 to 40% ^{w/v} Lactose Monohydrate Continuous Density Gradient at 40°C	138
4.3.4.3	Discussion of Lactose Monohydrate gradient Formation and Gradient Stability Results	140
4.3.5	Top-Layering of Soluble Free β -Galactosidase on a 10 to 40% ^{w/v} Lactose Monohydrate Continuous Density Gradient	141
4.3.6	Layering of Soluble Free β -Galactosidase Within a 10 to 40% ^{w/v} Lactose Monohydrate Density Gradient	143
4.3.7	Discussion of Results	145
5.0	Rate-Zonal Centrifugation Using Immobilised and Insolubilised β-Galactosidase Enzyme	147
5.1	Introduction	147
5.2	Methods of Immobilisation and Insolubilisation	149
5.2.1	Adsorption	149
5.2.1.1	Activity of Adsorbed Enzymes	150
5.2.1.2	Stability and Reversibility of Adsorption	151
5.2.1.3	Advantages and Disadvantages of Immobilisation by Adsorption	152
5.2.2	Covalent Binding	152
5.2.2.1	Covalent Bond Formation Between Enzymes and Support Materials	152
5.2.2.2	Activity of Covalently Bound Enzymes	156
5.2.2.3	Stability of Covalently Bound Enzymes	156
5.2.2.4	Advantages and Disadvantages of Immobilisation Using Covalent Binding	156
5.2.3	Entrapment	156
5.2.3.1	Methods For Enzyme Entrapment and Microencapsulation	157
5.2.3.2	Activity of Entrapped and Microencapsulated Enzymes	160
5.2.3.3	Stability of Entrapped and Microencapsulated Enzymes	161
5.2.3.4	Advantages and Disadvantages of Enzyme Entrapment and Microencapsulation Methods	161

5.2.4	Insolubilisation	161
5.2.4.1	Activity of Glutaraldehyde Insolubilised Enzymes	162
5.2.4.2	Stability of Glutaraldehyde Insolubilised Enzymes	163
5.2.4.3	Advantages and Disadvantages of Glutaraldehyde Insolubilisation	163
5.3	Centrifugation Studies With Immobilised and Insolubilised β -Galactosidase Using the Rate-Zonal Separation Technique	163
5.3.1	Introduction	163
5.3.2	Rate-Zonal Centrifugation Studies Using Blue Dextran	164
5.3.3	Rate-Zonal Centrifugation Studies Using Dextran Entrapped β -Galactosidase	172
5.3.4	Rate-Zonal Centrifugation Studies Using β -Galactosidase Covalently Linked to Industrial-Grade Dextran	177
5.3.5	Glutaraldehyde Insolubilisation of β -Galactosidase	179
5.3.5.1	Determination of the Density of Glutaraldehyde Insolubilised β -Galactosidase	180
5.3.5.2	Estimation of the Standard Sedimentation Coefficient ($S_{20,w}$) for Glutaraldehyde Insolubilised β -Galactosidase	181
5.3.5.3	Reproducibility of the Glutaraldehyde Insolubilisation Process, the Weight Equivalent and the Storage Stability of Insolubilised β -Galactosidase	184
5.3.6	Rate-Zonal Centrifugation Studies Using Glutaraldehyde Insolubilised β -Galactosidase	185
5.3.6.1	Reproducibility of Insolubilised β -Galactosidase Rate-Zonal Centrifugation Experiments	187
5.3.6.2	Rate-Zonal Centrifugation Experiments Using (a) Higher Lactose Monohydrate Concentration Density Gradients and (b) Performing Reactions at 25°C	199
5.3.6.3	Discussion of Results	201
6.0	Conclusions, Integrating Discussion and Recommendations for Further Work	204
6.1	Conclusions	204
6.1.1	Stirred-batch Reactions Performed Using Soluble Free and Glutaraldehyde Insolubilised β -Galactosidase From <i>Aspergillus oryzae</i>	204
6.1.2	Normal-Rate Centrifugation Studies Using Soluble β -Galactosidase	205
6.1.3	Rate-Zonal Centrifugation Studies Using Soluble β -Galactosidase	205

6.1.4	Rate-Zonal Centrifugation Studies Using Immobilised and Insolubilised β -Galactosidase	206
6.2	Integrating Discussion	207
6.2.1	A Comparison of Stirred-batch and Centrifugation Reactions Performed	207
6.2.2	A Novel Immobilised and Insolubilised Enzyme Centrifugation Reaction System	208
6.2.3	Pulsing of Insolubilised β -Galactosidase	209
6.2.4	The Applicability of the Centrifugal Reaction System to Industry	209
6.3	Recommendations for Further Work	209
7.0	Materials and Experimental Methods	211
7.1	Materials	211
7.2	Experimental Methods	212
7.2.1	Stirred-batch Reactions Using Soluble β -galactosidase from <i>Aspergillus oryzae</i> (Biolactase F)	212
7.2.1.1	Preparation of Soluble β -Galactosidase from <i>Aspergillus oryzae</i> (Biolactase F) Solutions	212
7.2.1.2	The Measurement of β -Galactosidase Activity	213
7.2.1.3	Preparation of Lactose Monohydrate Solutions	213
7.2.1.4	Preparation of Degassed HPLC-Grade Water	214
7.2.1.5	Stirred-batch Reactions Using Soluble β -Galactosidase from <i>Aspergillus oryzae</i>	214
7.2.1.6	Reaction Quenching Efficiency	216
7.2.1.7	HPLC Analysis of Stirred-batch Reaction Samples	217
7.2.2	Stirred-batch Reactions Using Glutaraldehyde Insolubilised β -Galactosidase from <i>Aspergillus oryzae</i> (Biolactase F)	219
7.2.2.1	Preparation of Glutaraldehyde Insolubilised β -Galactosidase from <i>Aspergillus oryzae</i> (Biolactase F)	219
7.2.2.2	Stirred-batch Reactions Using Insolubilised β -Galactosidase from <i>Aspergillus oryzae</i>	222
7.2.3	Rate-Zonal Batch Centrifugation Reactions	223
7.2.3.1	Preparation of Linear Lactose Monohydrate Density Gradients	223
7.2.3.2	Rate-Zonal Batch Centrifugation Reactions Performed Using Soluble and Insolubilised β -Galactosidase from <i>Aspergillus oryzae</i>	225

7.2.3.3	Further Experimental Methods	227
	References	228
Appendix A-1	Examples of stirred-batch reaction Excel spreadsheets	236
Appendix A-2	Kinetic model Excel spreadsheet calculations	251
Appendix A-3	Preparation of glutaraldehyde insolubilised β -galactosidase	268
Appendix A-4	Publications	273

LIST OF FIGURES

		Page
Figure 1.1	The enzymatic reaction of glutamic dehydrogenase (E.C.1.4.1.2.) ⁽²⁾ .	22
Figure 1.2	The formation of dextran and fructose by dextransucrase ⁽⁶⁾ .	24
Figure 1.3	Overview of the active enzyme centrifugal bioreaction system studied in this research project. Diagram A corresponds to the start of the reaction and B is the enzyme sedimenting during the reaction.	27
Figure 1.4	Structure of the thesis. The chapters highlighted in yellow are those where experimental work has been performed and the results presented.	29
Figure 2.1	The hydrolytic and trans-galactosyl activity of β -galactosidase ⁽³¹⁾ .	33
Figure 2.2	The hydrolytic and trans-galactosyl processes of the active site of β -galactosidase ^(40,41) . A is a lactose molecule at the active site, B is hydrolysis of the lactose molecule to release a glucose molecule, C is the β -galactosidase-galactose complex (R-O-H is the acceptor molecule, H ₂ O yields a galactose molecule and a saccharide yields a galacto-oligosaccharide molecule), and D is the release of either galactose or galacto-oligosaccharide.	35
Figure 2.3	The mutarotation of galactose in aqueous solution, the bracketed values give the % composition at equilibrium ⁽⁴⁴⁾ .	38
Figure 2.4	A graphical representation of a Michaelis-Menten-type enzymatic reaction.	43
Figure 2.5	The Lineweaver-Burk, or double reciprocal, plot ⁽⁴⁵⁾ .	44
Figure 2.6	Determination of the inhibition constant, K_i , using the Dixon plot method.	46
Figure 2.7	The microenvironment and bulk macroenvironment surrounding an idealised spherical immobilised/insolubilised particle ⁽¹⁹⁾ .	47
Figure 2.8	The % Relative enzyme activity of β -galactosidase from <i>Aspergillus oryzae</i> (Biolactase F) at varying pH and temperature ($^{\circ}$ C) values ⁽⁵²⁾ .	51
Figure 2.9a	% Galacto-oligosaccharides of Total Sugar and % Lactose monohydrate conversion for soluble Biolactase F (1.25 mg cm ⁻³ , 4 U cm ⁻³) stirred-batch reactions performed using 5 and 10% ^{w/v} lactose monohydrate, at 40 $^{\circ}$ C.	54
Figure 2.9b	% Galacto-oligosaccharides of Total Sugar and % Lactose monohydrate conversion for soluble Biolactase F (1.25 mg cm ⁻³ , 4 U cm ⁻³) stirred-batch reactions performed using 15 and 20% ^{w/v} lactose monohydrate, at 40 $^{\circ}$ C.	55
Figure 2.9c	% Galacto-oligosaccharides of Total Sugar and % Lactose monohydrate conversion for soluble Biolactase F (1.25 mg cm ⁻³ , 4 U cm ⁻³) stirred-batch reaction performed using 25% ^{w/v} lactose monohydrate, at 40 $^{\circ}$ C.	56
Figure 2.10	The hydrolysis of galacto-oligosaccharide formed during incubation of various initial lactose monohydrate (% ^{w/v}) concentrations with β -galactosidase from <i>Aspergillus oryzae</i> (1.25 mg cm ⁻³ , 4 U cm ⁻³), at 40 $^{\circ}$ C.	57
Figure 2.11	Determination of V_{max} and K_m for soluble Biolactase F using a Lineweaver-Burk, or double reciprocal plot.	58

Figure 2.12a	% Galacto-oligosaccharides of Total Sugar and % Lactose monohydrate conversion for insolubilised Biolactase F (1.25 mg cm^{-3} , 4 U cm^{-3}) stirred-batch reactions performed using 5 and 10% ^{w/v} lactose monohydrate, at 40°C.	60
Figure 2.12b	% Galacto-oligosaccharides of Total Sugar and % Lactose monohydrate conversion for insolubilised Biolactase F (1.25 mg cm^{-3} , 4 U cm^{-3}) stirred-batch reactions performed using 15 and 20% ^{w/v} lactose monohydrate, at 40°C.	61
Figure 2.12c	% Galacto-oligosaccharides of Total Sugar and % Lactose monohydrate conversion for insolubilised Biolactase F (1.25 mg cm^{-3} , 4 U cm^{-3}) stirred-batch reactions performed using 25 and 30% ^{w/v} lactose monohydrate, at 40°C.	62
Figure 2.12d	% Galacto-oligosaccharides of Total Sugar and % Lactose monohydrate conversion for insolubilised Biolactase F (1.25 mg cm^{-3} , 4 U cm^{-3}) stirred-batch reaction performed using 40% ^{w/v} lactose monohydrate, at 40°C.	63
Figure 2.13	Determination of V_{max} and K_m for glutaraldehyde insolubilised Biolactase F using a Lineweaver-Burk, or double reciprocal plot.	64
Figure 2.14	A comparison of theoretical and experimentally determined % lactose monohydrate conversion for stirred-batch reactions performed using soluble β -galactosidase from <i>Aspergillus oryzae</i> (1.25 mg cm^{-3} , 4 U cm^{-3}) at 40°C. Graph A is with an initial lactose monohydrate concentration of 5% ^{w/v} and Graph B is with an initial lactose monohydrate concentration of 20% ^{w/v} .	70
Figure 2.15	A comparison of theoretical and experimentally determined % lactose monohydrate conversion for stirred-batch reactions performed using insolubilised β -galactosidase from <i>Aspergillus oryzae</i> (1.25 mg cm^{-3} , 4 U cm^{-3}) at 40°C. Graph A is with an initial lactose monohydrate concentration of 5% ^{w/v} and Graph B is with an initial lactose monohydrate concentration of 20% ^{w/v} .	71
Figure 2.16	Scanning electron microscope images of insolubilised β -galactosidase particles. Photograph A shows a cluster of particles, Photograph B is a magnified single particle and Photograph C shows the surface texture.	73
Figure 3.1	Diagrammatic representation of the volume-radius relationship expressed in Equations (3.21) and (3.22), and based on six fractions collected. r_{men} = radius to the meniscus (cm), $r_{(\text{fraction } x)}$ = radial contribution of the fraction/s (cm), r_T = internal radius of the cylindrical part of the tube (cm), r_b = the internal radius of the hemispherical bottom (cm), h = radial length of the hemispherical bottom including the tube thickness (cm), and V = the total summed volumes of the fractions up to the one being considered (cm^3).	86
Figure 3.2	Diagram of the forces exerted on particles in a cylindrical tube used in a swing-out rotor. The particles inside the inner cone do not collide with the tube wall. The radius of the tube is r_T , L is the length, R is the maximum radius (r_{max}) of the rotor, and θ is the angle subtended by the two ends of the chord defining the width of a plane within the tube ⁽⁶⁵⁾ .	97
Figure 3.3	Droplet sedimentation ⁽⁶⁵⁾ .	99
Figure 3.4	Classification of centrifuges ⁽³⁾ .	101
Figure 3.5	The Sharples AS 26 tubular-bowl centrifuge ⁽⁶²⁾ , the lettering is described in the text.	102

Figure 3.6	The disk-type Centrifuge ⁽⁶²⁾ .	103
Figure 3.7	The decanter, or solid-bowl scroll centrifuge ⁽⁶²⁾ .	104
Figure 3.8	The Rousselet SC-KSA basket-type filtering centrifuge ⁽⁷⁹⁾ .	105
Figure 3.9	The analytical ultracentrifuge fitted with a quartz optical system ⁽⁶⁶⁾ .	107
Figure 3.10	Separation in a fixed-angle rotor. A, the initial orientation of the particle-containing medium before centrifugation; B, as the rotor begins to move the liquid in the tube begins to reorientate; C, the particles sediment down the tube; and D, the tubes reorientates as gravity becomes stronger than the centrifugal force ⁽⁶⁷⁾ .	108
Figure 3.11	Separations in a swing-out rotor. At rest the buckets containing the centrifuge tubes hang vertically, A. As the rotor begins to move they move out so that they are perpendicular to the axis of rotation, B. During centrifugation the particles sediment down the tube, C. When the rotor stops the tubes return to the vertical position, D.	109
Figure 3.12a	Batch-type zonal rotor (Beckman Instruments) ⁽³⁾ .	110
Figure 3.12b	Diagrammatic representation of the operation of a batch-type zonal rotor, the lettering is described in the text ⁽⁶⁶⁾ .	111
Figure 3.13	The normal rate separation, or differential pelleting.	112
Figure 3.14	Reaction system used to determine galacto-oligosaccharide distribution profiles.	114
Figure 3.15	Galacto-oligosaccharide distribution profiles obtained for β -galactosidase (1.25 mg cm^{-3} , 4 U cm^{-3}) loaded on 20% ^{w/v} lactose monohydrate and centrifuged at 9-, 11- and 13 000 r.p.m. for 0, 30 60, 90 and 120 minutes, at 40°C.	115
Figure 3.16	Protein sedimentation profiles of β -galactosidase (5 mg cm^{-3} , 16 U cm^{-3}) loaded on 20% ^{w/v} lactose monohydrate and centrifuged at 9-, 11- and 13 000 r.p.m. for 0, 30 60, and 90 minutes, at 40°C.	116
Figure 4.1	An illustration of rate-zonal and isopycnic gradient separation ⁽⁶⁵⁾ .	119
Figure 4.2	The general principles of the rate-zonal technique used in this research.	120
Figure 4.3	Examples of the different types of gradient profiles.	123
Figure 4.4	The under-layering density gradient technique.	123
Figure 4.5	The Biocomp Gradient Master automatic continuous gradient former ⁽⁶⁶⁾ .	124
Figure 4.6	Methods for collecting density gradient fractions after centrifugation: A is the tube bottom piercing method; B is the withdrawal of the fractions from the top downwards using a graduated pipette; C is where fractions are removed by being pumped out; and D is the bottom displacement method using a dense liquid.	127
Figure 4.7	The relationship of viscosity to lactose monohydrate concentration at 40°C.	130

Figure 4.8	The relationship of density to lactose monohydrate concentration at 40°C.	131
Figure 4.9	The profiles for an under-layered lactose monohydrate (10 to 40% ^{w/v}) step gradient incubated in a waterbath for 0, 30, 60, 90 and 180 minutes, at 40°C.	135
Figure 4.10	The profiles for an under-layered lactose monohydrate (10 to 40% ^{w/v}) step gradient centrifuged at 13 000 r.p.m (26 122 g max) for 0, 30, 60, 90 and 180 minutes, at 40°C.	136
Figure 4.11	Comparison of the profiles for under-layered lactose monohydrate (10 to 40% ^{w/v}) step gradients, A corresponds to gradients incubated in a waterbath for 0, 30, 60, 90 and 180 minutes, at 40°C (Figure 4.9), and B corresponds to gradients centrifuged at 13 000 r.p.m (26 122 g max) for 0, 30, 60, 90 and 180 minutes, at 40°C (Figure 4.10).	137
Figure 4.12	The diffusion coefficient for lactose monohydrate at 40°C determined by extrapolation of literature values ^(91,92) .	138
Figure 4.13	The profiles for an under-layered lactose monohydrate (20 to 40% ^{w/v}) step gradient centrifuged at 13 000 r.p.m (26 122 g max) for 0, 30, 60, 90 and 180 minutes, at 40°C.	139
Figure 4.14	The movement of β-galactosidase (5 mg cm ⁻³ , 16 U cm ⁻³) top-layered on a 10 to 40% ^{w/v} lactose monohydrate density gradient and centrifuged at 13 000 r.p.m (26 122 g max) for 0, 30, 90, and 180 minutes, at 40°C.	141
Figure 4.15	Comparison of the β-galactosidase profile with the density gradient profile after 180 minutes centrifugation at 13 000 r.p.m (26 122 g max), at 40°C.	142
Figure 4.16	Comparison of the β-galactosidase distribution profiles for 10 to 40% ^{w/v} lactose monohydrate density gradients layered with β-galactosidase (5 mg cm ⁻³ , 16 U cm ⁻³) in 17.5% ^{w/v} lactose monohydrate and centrifuged at 13 000 r.p.m. (26 122 g max) for 0 and 180 minutes, at 40°C.	144
Figure 4.17	Comparison of β-galactosidase and density gradient distribution profiles after centrifugation at 13 000 r.p.m (26 122 g max) for 180 minutes, at 40°C.	145
Figure 5.1	Different methods of enzyme immobilisation; A is adsorption, B is covalent binding, C is entrapment, and D is membrane confinement.	147
Figure 5.2	Enzyme insolubilisation using a chemical cross-linking agent.	148
Figure 5.3	Enzyme immobilisation using maleic anhydride copolymer ⁽⁹⁴⁾ .	153
Figure 5.4	Enzyme immobilisation using cyanogen bromide activated Sepharose ⁽⁹³⁾ .	154
Figure 5.5	Enzyme immobilisation using Procion Blue MX-R activated dextran.	155
Figure 5.6	The reaction scheme for polyacrylamide formation (without stoichiometry).	157
Figure 5.7	The chemical structure of dextran ⁽³⁾ .	158
Figure 5.8	The microencapsulation of enzyme molecules in a semi-permeable nylon membrane.	159
Figure 5.9	A diagrammatic representation of a liposome microencapsulated enzyme ⁽¹⁰⁴⁾ .	160

Figure 5.10	The reaction scheme for the insolubilisation of an enzyme using glutaraldehyde (pentane-1,5 dial) ⁽¹⁹⁾ .	162
Figure 5.11a	A comparison of the position of blue dextran with the corresponding lactose monohydrate density gradient after centrifugation at 13 000 r.p.m. (26 122 g max) for 0 minutes, at 40°C.	166
Figure 5.11b	A comparison of the position of blue dextran with the corresponding lactose monohydrate density gradient after centrifugation at 13 000 r.p.m. (26 122 g max) for 30 minutes, at 40°C.	167
Figure 5.11c	A comparison of the position of blue dextran with the corresponding lactose monohydrate density gradient after centrifugation at 13 000 r.p.m. (26 122 g max) for 60 minutes, at 40°C.	168
Figure 5.11d	A comparison of the position of blue dextran with the corresponding lactose monohydrate density gradient after centrifugation at 13 000 r.p.m. (26 122 g max) for 90 minutes, at 40°C.	169
Figure 5.11e	A comparison of the position of blue dextran with the corresponding lactose monohydrate density gradient after centrifugation at 13 000 r.p.m. (26 122 g max) for 180 minutes, at 40°C.	170
Figure 5.11f	A comparison of the movement of 1% ^{w/v} blue dextran (1 cm ³) to the corresponding 10-40% ^{w/v} lactose monohydrate density gradient profile (36 cm ³), during centrifugation at 13 000 r.p.m. (26 122 g max) for 0 and 180 minutes, at 40°C. A is at 0 minutes and B is at 180 minutes. Blue dextran movement monitored by absorbance measurements at 617.6 nm of the gradient fractions.	171
Figure 5.12	The particle size distribution for β -galactosidase immobilised using industrial-grade dextran.	172
Figure 5.13	Lactose monohydrate density gradients (10-40% ^{w/v} , 36 cm ³) top-layered with a solution of industrial-grade dextran/ β -galactosidase particles (1 cm ³ of bulk solution, equivalent to 5mg cm ⁻³ (16 U cm ⁻³) β -galactosidase and 10 mg cm ⁻³ of industrial-grade dextran) and centrifuged at 13 000 r.p.m (26 122 g max) for 0, and 30 minutes, at 40°C. A is after 0 minutes and B is after 30 minutes.	173
Figure 5.14	A comparison of the chromatograms obtained for the bottom fraction of the β -galactosidase/dextran and the soluble free β -galactosidase centrifugation experiments, performed at 13 000 r.p.m. (26 122 g max) for 30 minutes, at 40°C. A is for top-layered soluble free β -galactosidase (5 mg cm ⁻³ , 16 U cm ⁻³ , 1 cm ³) and B is for top-layered β -galactosidase/dextran conjugate (1 cm ³ of bulk solution, equivalent to 5mg cm ⁻³ (16 U cm ⁻³) of β -galactosidase and 10 mg cm ⁻³ of industrial-grade dextran).	174
Figure 5.15	Comparison of the galacto-oligosaccharide distribution profile with the dextran distribution profile for top-layered β -galactosidase/dextran conjugate (1 cm ³ of bulk, solution equivalent to 5mg cm ⁻³ (16 U cm ⁻³) β -galactosidase and 10 mg cm ⁻³ of industrial-grade dextran) loaded on to a 10-40% ^{w/v} lactose monohydrate density gradient and centrifuged at 13 000 r.p.m. (26 122 g max) for 30 minutes, at 40°C.	175
Figure 5.16	Comparison of the galacto-oligosaccharide distribution profiles for the top-layered β -galactosidase/dextran conjugate (1 cm ³ of bulk, solution equivalent to 5mg cm ⁻³ (16 U cm ⁻³) β -galactosidase and 10 mg cm ⁻³ of industrial-grade dextran) and the soluble free β -galactosidase (5mg cm ⁻³ , 16 U cm ⁻³), loaded	

- on to a 10-40%^{w/v} lactose monohydrate density gradient and centrifuged at 13 000 r.p.m. (26 122 g max) for 30 minutes, at 40°C. 176
- Figure 5.17** Lactose monohydrate density gradients (10-40%^{w/v}, 36 cm³) top-layered with a solution of triazine linked β-galactosidase/dextran particles (1 cm³) and centrifuged at 9 000 r.p.m (12 520 g max) for 0, and 30 minutes, at 40°C. A is after 0 minutes and B is after 30 minutes. 178
- Figure 5.18** Comparison of the galacto-oligosaccharide distribution profiles for the top-layered triazine linked β-galactosidase/dextran particles (1 cm³), loaded on to a 10-40%^{w/v} lactose monohydrate density gradient and centrifuged at 9 000 (12 520 g max) and 13 000 r.p.m. (26 122 g max) for 30 minutes, at 40°C. 178
- Figure 5.19** The particle size distribution for glutaraldehyde insolubilised β-galactosidase. 180
- Figure 5.20** Determination of the density of glutaraldehyde insolubilised β-galactosidase using a cesium chloride density gradient (5-50%^{w/w}) centrifuged at 12 000 r.p.m (22 258 g max) for 30 minutes, at 40°C. 182
- Figure 5.21** Estimation of the standard sedimentation coefficient for glutaraldehyde insolubilised β-galactosidase. A is after 0 minutes of centrifugation at 9 000 r.p.m.(12 520 g max), B is after 2 minutes of centrifugation at 9 000 r.p.m., C is after 4 minutes of centrifugation at 9 000 r.p.m., and D is after 15 minutes of centrifugation at 9 000 r.p.m. Measurements were taken from the actual tubes to eliminate errors due to photographic distortion and light reflection. 183
- Figure 5.22** The protein distribution profiles for insolubilised β-galactosidase (12 mg cm⁻³, 38.4 U cm⁻³, 1 cm³) top-layered on to a lactose monohydrate density gradient (10-40%^{w/v}, 36 cm³) and centrifuged at 9 000 r.p.m. (12 520 g max) for 0 and 30 minutes, at 40°C. Relative protein concentration determined by absorbance measurement at 280 nm. 186
- Figure 5.23a** Galacto-oligosaccharide distribution profiles for insolubilised β-galactosidase concentrations of 1.25 , 6, (2x) 6 - pulsing and 12 mg cm⁻³ (4, 19.2, (2x) 19.2 and 38.4 U cm⁻³ respectively) top-layered on to lactose monohydrate density gradients (10-40%^{w/v}) and centrifuged at 9 000 r.p.m. (12 520 g max) for 30 minutes, at 40°C. 188
- Figure 5.23b** % Lactose monohydrate conversion profiles for insolubilised β-galactosidase concentrations of 1.25 , 6, (2x) 6 - pulsing and 12 mg cm⁻³ (4, 19.2, (2x) 19.2 and 38.4 U cm⁻³ respectively) top-layered on to lactose monohydrate density gradients (10-40%^{w/v}) and centrifuged at 9 000 r.p.m. (12 520 g max) for 30 minutes, at 40°C. 189
- Figure 5.24a** Galacto-oligosaccharide distribution profiles for insolubilised β-galactosidase concentrations of 1.25 , 6, (2x) 6 - pulsing and 12 mg cm⁻³ (4, 19.2, (2x) 19.2 and 38.4 U cm⁻³ respectively) top-layered on lactose monohydrate density gradients (10-40%^{w/v}) and centrifuged at 11 000 r.p.m. (18 703 g max) for 30 minutes, at 40°C. 190
- Figure 5.24b** % Lactose monohydrate conversion profiles for insolubilised β-galactosidase concentrations of 1.25 , 6, (2x) 6 - pulsing and 12 mg cm⁻³ (4, 19.2, (2x) 19.2 and 38.4 U cm⁻³ respectively) top-layered on lactose monohydrate density gradients (10-40%^{w/v}) and centrifuged at 11 000 r.p.m. (18 703 g max) for 30 minutes, at 40°C. 191

- Figure 5.25a** Galacto-oligosaccharide distribution profiles for insolubilised β -galactosidase concentrations of 1.25 , 6, (2x) 6 - pulsing and 12 mg cm⁻³ (4, 19.2, (2x) 19.2 and 38.4 U cm⁻³ respectively) top-layered on to lactose monohydrate density gradients (10-40%^{w/v}) and centrifuged at 13 000 r.p.m. (26 122 g max) for 30 minutes, at 40°C. 192
- Figure 5.25b** % Lactose monohydrate conversion profiles for insolubilised β -galactosidase concentrations of 1.25 , 6, (2x) 6 - pulsing and 12 mg cm⁻³ (4, 19.2, (2x) 19.2 and 38.4 U cm⁻³ respectively) top-layered on to lactose monohydrate density gradients (10-40%^{w/v}) and centrifuged at 13 000 r.p.m. (26 122 g max) for 30 minutes, at 40°C. 193
- Figure 5.26** A comparison of both the galacto-oligosaccharide distribution profiles and the % lactose monohydrate conversion profiles obtained for 1.25 mg cm⁻³ (4 U cm⁻³) insolubilised β -galactosidase, top-layered on to a lactose monohydrate density gradient (10-40%^{w/v}) and centrifuged at 9-, 11- and 13 000 r.p.m. (12 520, 18 703 and 26 122 g max respectively) for 30 minutes at 40°C. A is the galacto-oligosaccharide distribution profiles and B is the % Lactose monohydrate conversion profiles. 194
- Figure 5.27** A comparison of both the galacto-oligosaccharide distribution profiles and the % lactose monohydrate conversion profiles obtained for 6 mg cm⁻³ (19.2 U cm⁻³) insolubilised β -galactosidase, top-layered on to a lactose monohydrate density gradient (10-40%^{w/v}) and centrifuged at 9-, 11- and 13 000 r.p.m. (12 520, 18 703 and 26 122 g max respectively) for 30 minutes at 40°C. A is the galacto-oligosaccharide distribution profiles and B is the % Lactose monohydrate conversion profiles. 195
- Figure 5.28** A comparison of both the galacto-oligosaccharide distribution profiles and the % lactose monohydrate conversion profiles obtained for (2x) 6 mg cm⁻³ (pulsing) ((2x) 19.2 U cm⁻³) insolubilised β -galactosidase, top-layered on to a lactose monohydrate density gradient (10-40%^{w/v}) and centrifuged at 9-, 11- and 13 000 r.p.m. (12 520, 18 703 and 26 122 g max respectively) for 30 minutes at 40°C. A is the galacto-oligosaccharide distribution profiles and B is the % Lactose monohydrate conversion profiles. 196
- Figure 5.29** A comparison of both the galacto-oligosaccharide distribution profiles and the % lactose monohydrate conversion profiles obtained for 12 mg cm⁻³ (38.4 U cm⁻³) insolubilised β -galactosidase, top-layered on to a lactose monohydrate density gradient (10-40%^{w/v}) and centrifuged at 9-, 11- and 13 000 r.p.m. (12 520, 18 703 and 26 122 g max respectively) for 30 minutes at 40°C. A is the galacto-oligosaccharide distribution profiles and B is the % Lactose monohydrate conversion profiles. 197
- Figure 5.30** A comparison of the galacto-oligosaccharide distribution profile results obtained for duplicate experiments using insolubilised β -galactosidase (6 mg cm⁻³ (19.2 U cm⁻³), 1 cm⁻³), for reactions performed at 9-, 11- and 13 000 r.p.m. (12 520, 18 703 and 26 122 g max respectively) using a lactose monohydrate density gradient (10-40%^{w/v}) centrifuged for 30 minutes at 40°C. A is at 9-, B is at 11- and C is at 13 000 r.p.m.. 198
- Figure 5.31** Comparison of Galacto-oligosaccharide of Total Sugar (%^{w/v}) results for centrifugation reactions performed using (a) 6 mg cm⁻³ (19.2 U cm⁻³) insolubilised β -galactosidase from *Aspergillus oryzae* layered onto a 10 to 40%^{w/v} lactose monohydrate gradient and centrifuged at 2 000 r.p.m. (618 g max) for 30 minutes at 25 °C, and (b) 6 mg cm⁻³ (19.2 U cm⁻³) insolubilised β -galactosidase from *Aspergillus oryzae* layered onto a 10 to 40%^{w/v} lactose

	monohydrate gradient and centrifuged at 9 000 r.p.m. (12 520 g max) for 30 minutes at 40 °C.	200
Figure 7.1	The apparatus used to perform stirred-batch reactions.	215
Figure 7.2	The high performance liquid chromatograph (HPLC) used to analyse samples.	217
Figure 7.3	A typical chromatogram obtained of products formed during hydrolysis of lactose monohydrate by β -galactosidase from <i>Aspergillus oryzae</i> .	218
Figure 7.4	The formation of glutaraldehyde insolubilised β -galactosidase from <i>Aspergillus oryzae</i> .	220
Figure 7.5	The effect of settling time on the narrowing of insolubilised β -galactosidase particle size distribution.	221
Figure 7.6	Insolubilised β -galactosidase from <i>Aspergillus oryzae</i> after 30 minutes settling time.	222
Figure 7.7	Beckman polycarbonate centrifuge tubes (50 cm ³).	224
Figure 7.8	The under-layering of lactose monohydrate solutions.	224
Figure 7.9	Beckman J2-MC High Speed Centrifuge.	225
Figure 7.10	Beckman JS13.1 Swing-out Rotor.	226

LIST OF TABLES

		Page
Table 2.1	A typical range of galacto-oligosaccharide compounds formed by the trans-galactosyl activity of β -galactosidase ⁽³¹⁾ .	36
Table 2.2	The enzymatic activities present in Biolactase F (1 unit (U) is defined as the amount of enzyme which converts 1 μ mole of substrate in 1 minute at the stated conditions of pH and temperature).	52
Table 2.3	Comparison of the maximum galacto-oligosaccharide yields (% ^{w/v}) obtained using various initial lactose monohydrate concentrations (% ^{w/v}), and performed at various temperatures ($^{\circ}$ C).	53
Table 2.4	Comparison of the experimentally determined kinetic parameters for soluble and insolubilised β -galactosidase (Biolactase F).	66
Table 2.5	Comparison of the maximum galacto-oligosaccharide yields obtained during stirred-batch reactions using soluble and insolubilised β -galactosidase (1.25 mg cm ⁻³ , 4 U cm ⁻³) performed using various initial lactose monohydrate concentrations, at 40 $^{\circ}$ C.	66
Table 3.1	Sedimentation coefficients of marker particles used in isokinetic gradient centrifugation ⁽⁶⁷⁾ .	89
Table 3.2	Molecular parameters of various proteins ^(65,67) .	90
Table 3.3	Calculation of the partial specific volume of a fictitious protein using amino acid analysis ⁽⁵⁸⁾ .	91
Table 3.4	Comparison of % Galacto-oligosaccharide of Total Sugar to Protein concentration obtained at Radial Positions of 9.9 and 12.8 cm, after centrifugation at 9 000, 11 000 and 13 000 r.p.m. (12 520, 18 703 and 26 122 g max respectively).	117
Table 4.1	Commonly used gradient material, properties and uses ⁽⁶⁵⁾ .	122
Table 5.1	Support materials commonly used for enzyme adsorption ⁽⁹⁴⁾ .	150
Table 5.2	The % binding of β -fructofuranosidase to DEAE-Sephadex and CM-Sephadex at varying pH ⁽¹⁹⁾ .	151
Table 5.3	Reproducibility of the β -galactosidase insolubilisation process.	184
Table 5.4	Comparison of the results obtained for Galacto-oligosaccharide of Total Sugar (% ^{w/v}) at various rotation speeds and using different insolubilised enzyme loadings. The reactions were performed using a 10-40% ^{w/v} lactose monohydrate gradient centrifuged for 30 minutes at 40 $^{\circ}$ C.	201
Table 5.5	Comparison of the results obtained for % Lactose Monohydrate Conversion at various rotation speeds and using different insolubilised enzyme loadings. The reactions were performed using a 10-40% ^{w/v} lactose monohydrate gradient centrifuged for 30 minutes at 40 $^{\circ}$ C.	202
Table 6.1	Comparison of equivalent % Galacto-oligosaccharide of Total Sugar values for stirred-batch and centrifugation reactions performed using a	

soluble/insolubilised enzyme concentration of 1.25 mg cm^{-3} (4 U cm^{-3}), at 40°C . Centrifuge data was taken from reactions performed at 9 000 r.p.m. ($12\ 520 \text{ g max}$) for 30 minutes, at 40°C using a 10-40%^{w/v} lactose monohydrate gradient.

208

Table 7.1 The materials used in this research project.

211

1.0 INTRODUCTION

This chapter describes the background to this research and gives the initial research objectives. The evolution of the experimental programme is reported and the structure of the thesis is presented.

1.1 Bioreaction and separation in centrifugal fields

Centrifugation is a technique designed to utilise centrifugal forces which are greater than the force of gravity to effect the sedimentation of particles suspended in a fluid, at a rate depending on their size and density. Such sedimentation only occurs if the density of the particles is greater than that of the fluid. Centrifugation is mainly used for the separation, purification, characterisation and/or the clarification of solids and liquids. The purpose of this research project was to investigate and develop the centrifuge as a novel reaction system for performing enzymatic reactions. A literature survey was carried out to determine the reported use of the centrifuge as a reaction system for performing chemical and enzymatic reactions: there are only a few instances in the literature concerning such studies.

1.1.1 Literature survey

In 1967, Cohen, Giraud and Messiah ⁽¹⁾ studied the behaviour of an enzyme in an applied centrifugal field using the rate-zonal technique. The rate-zonal technique is used to separate two or more sample components based upon the differences in their sedimentation rates in an applied centrifugal field; this technique is described in detail in Chapter 4. Cohen *et al.* studied the reaction of glutamic dehydrogenase (E.C.1.4.1.2) which is summarised in Figure 1.1.

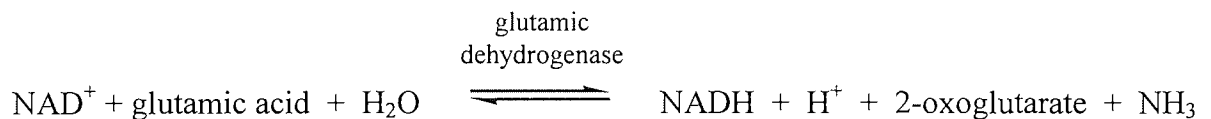


Figure 1.1. The enzymatic reaction of glutamic dehydrogenase (E.C.1.4.1.2.) ⁽²⁾.

Within a sample cell a small volume of the buffered enzyme was layered onto the top of a glutamic acid solution, which acted as both the supporting solution and the substrate solution. This was then centrifuged using an analytical ultracentrifuge: the analytical

ultracentrifuge is described in Section 3.3.3.1. At uniform time intervals the sample cell was photographed using light at a wavelength of 334nm, which is the wavelength of light only absorbed by NADH. The decrease in the optical density due to the absorbance of light was directly proportional to the NADH concentration and the distribution of the NADH within the sample cell at any time interval could thus be determined. The results obtained were used to determine the sedimentation rate of the glutamic dehydrogenase based upon the fact that NADH was only synthesised where the enzyme was present in the cell. This was the first example of an active enzyme centrifugal bioreaction system found in the literature.

The work of Cohen *et al.* was not intended to investigate the use of the centrifuge as a novel bioreaction system, but to use it as an analytical tool to elucidate characteristics of enzyme-molecule complexes formed during enzymatic reactions. For example, during a polymerisation reaction, the molecular weight of the complex will be proportional to its sedimentation rate and data can be obtained for the enzyme-molecule complexes and the changes that occur under the influence of various enzyme activators and inhibitors⁽³⁾.

In 1975, Parts and Elbing⁽⁴⁾ studied the polymerisation of acrylonitrile to polyacrylonitrile in centrifugal fields. Acrylonitrile was uniformly dispersed in a sample cell containing solutions of hydrogen peroxide and iron[III] nitrate. The decomposition of the hydrogen peroxide by the ferric nitrate initiated the polymerisation reaction and the formation of polyacrylonitrile. The sample cell was placed in an analytical ultracentrifuge and centrifugal fields ranging from 2 000 to 180 000g were applied. The reaction was monitored by the measurement of the level of sedimented polyacrylonitrile deposited at the base of the sample cell. Parts and Elbing found that the rate of polymerisation was lower in all of the applied centrifugal fields compared to that obtained at the normal gravitational field of 1g. When centrifuged at 180 000g for 597 minutes it was found that 51.2% of the monomer had polymerised, but the same degree of conversion was found to occur after 50 minutes at 1g. Experiments were performed at 2 000g, 6 000g and 23 000g and these confirmed that the rate of polymerisation decreased as the applied centrifugal fields increased. This was because as the polymer particles formed their mass increased, which caused the particles to sediment to the base of the sample cell where they were subsequently covered by further polymer particles. The sedimentation rate of the polymer particles was greater as the applied centrifugal fields was increased. This process effectively cut off the supply of further

monomer to these particles and hence the rate of polymerisation decreased. In 1979, Carezza, Tavan and Palma ⁽⁵⁾ monitored the radiation-induced polymerisation of vinyl chloride under various applied centrifugal fields and found similar results to those of Parts and Elbing ⁽⁴⁾.

In 1992, Setford ⁽³⁾ investigated the principle of using the centrifuge as a bioreaction system for performing enzymatic reactions. The enzymatic reaction that he studied was the formation of dextran and fructose by the action of the enzyme dextransucrase on the substrate sucrose; the reaction scheme is shown in Figure 1.2.

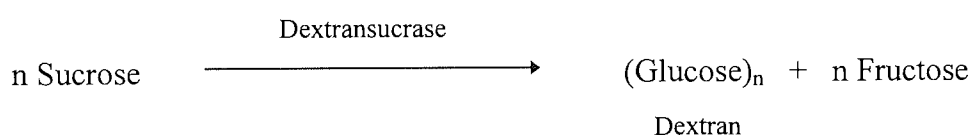


Figure 1.2. The formation of dextran and fructose by dextransucrase ⁽⁶⁾.

Setford overlaid buffered solutions of dextransucrase onto the top of sucrose substrate solutions contained within centrifuge tubes and centrifuged them at various rotation speeds at 25°C, the optimum temperature for the enzyme. Batch reactions were performed using a high speed centrifuge capable of generating a maximum relative centrifugal force (RCF) of 57 000g at the tube base. Further batch reactions were performed using a similar high speed centrifuge fitted with a zonal rotor capable of performing rate-zonal centrifugation, details of which are given in Section 3.3.3.2 and in Chapter 4. Setford found that under the influence of the applied centrifugal fields the enzyme could be sedimented through the substrate solution towards the base of the centrifuge tube or the wall of the zonal rotor. It was also found that the use of rate-zonal centrifugation techniques produced the most stable reaction environment. High molecular weight dextran was produced as the enzyme sedimented through the sucrose substrate and this rapidly sedimented to the base of the tube or the rotor wall due to its high sedimentation rate. The fully sedimented dextran formed a gel which increased in thickness as more dextran was produced. The fructose formed, having a low molecular weight and hence a very low sedimentation rate, effectively remained at the

position within the substrate solution where it was formed. Hence, the reaction products had been separated and the use of the centrifuge as a bioreaction and separation system had been demonstrated.

The enzymatic reaction system chosen by Setford had several experimental drawbacks which made it unsuitable for fully investigating the processes underlying, and the potential of, the centrifuge as a novel enzymatic bioreactor. The first drawback was the non-ideal sedimentation of the enzyme produced by its interaction with the dextran formed. Ideally, the enzyme layered onto the top of the substrate should have sedimented as a discrete band through the substrate, but it was found that the dextran particles formed entrapped the enzyme molecules and transported them to the gel layer. This produced an artificially high sedimentation rate for the enzyme, which reduced the contact time with the substrate and imposed diffusional limitations on the activity of the enzyme, thus limiting further conversion of the substrate. The dextran product formed was therefore contaminated with the enzyme and this required thermal quenching of the dextran product to denature the active enzyme content.

Setford found that the most stable reaction environment was to use a rate-zonal technique where the enzyme was layered onto the top of a sucrose density gradient. A density gradient is formed by layering solutions of increasing density within the centrifuge tube or rotor, so that the substrate density gradually increases the further it is away from the centre of rotation, or the closer it is to the base of the centrifuge tube or rotor wall. The formation of dextran by the sedimenting enzyme removed glucose molecules from the sucrose gradient which affected the sucrose gradient profile and hence the stability of the reaction system. Also, smearing of the dextran gel down the walls of the centrifuge tubes towards the base of the tube would be expected to create turbulence and disrupt the gradient.

The aims of this research project were; to identify an enzymatic reaction system suitable to investigate and develop the high speed centrifuge as a novel reaction system for performing such reactions, to determine the reaction conditions required to produce sedimentation of the enzyme through a suitable substrate medium, to monitor the formation of reaction products, to effect bioreaction and separation of the enzyme from the reaction products in a single unit operation. Based on preliminary results, centrifugation experiments were performed to

develop a novel reaction system using the enzyme in either an immobilised or insolubilised state. Various methods used for enzyme immobilisation and insolubilisation were assessed and their efficacy for use with a centrifugal bioreaction system was investigated.

1.1.2 The search for a model enzymatic reaction system for use in the centrifugal bioreactor

A search was conducted to identify a suitable enzymatic reaction system that would allow the use of the centrifuge as a novel bioreaction system to be investigated and to overcome the experimental drawbacks of the enzymatic reaction used by Setford^(3,6). In 1996, West⁽⁷⁾ based at Aston University investigated the use of a batch chromatographic system for combined bioreaction and separation. The enzyme reaction studied was the conversion of lactose monohydrate (milk sugar) to glucose, galactose and galacto-oligosaccharides by the enzyme β -galactosidase (lactase), isolated from *Aspergillus oryzae*: full details of the reaction are given in Chapter 2. The galacto-oligosaccharides produced are intermediate compounds that are ultimately hydrolysed to yield further glucose and galactose. There is currently considerable industrial interest in the use of galacto-oligosaccharides as food additives, which have been shown to be beneficial to the health of the human gastrointestinal tract: optimisation of yields of such oligosaccharides is consequently of commercial importance.

It was decided that this would be an ideal model enzyme reaction system to investigate the potential of a centrifuge as a novel bioreactor, particularly since no instances were found in the literature concerning the behaviour of the β -galactosidase reactions in centrifugal fields. A diagrammatic representation of the proposed reaction system is shown in Figure 1.3. In principle, the reaction system involves layering a solution of β -galactosidase on top of a lactose monohydrate substrate solution contained within a centrifuge tube. The centrifuge tube is then placed in a centrifuge and can be subjected to various centrifugal forces. The enzyme is allowed to fully sediment to the bottom of the tube and fractions can then be taken from the tube and analysed to determine the distribution of the substrate, enzyme and reaction products within the tube. Allowing the enzyme to fully sediment should effect separation from the reaction products.

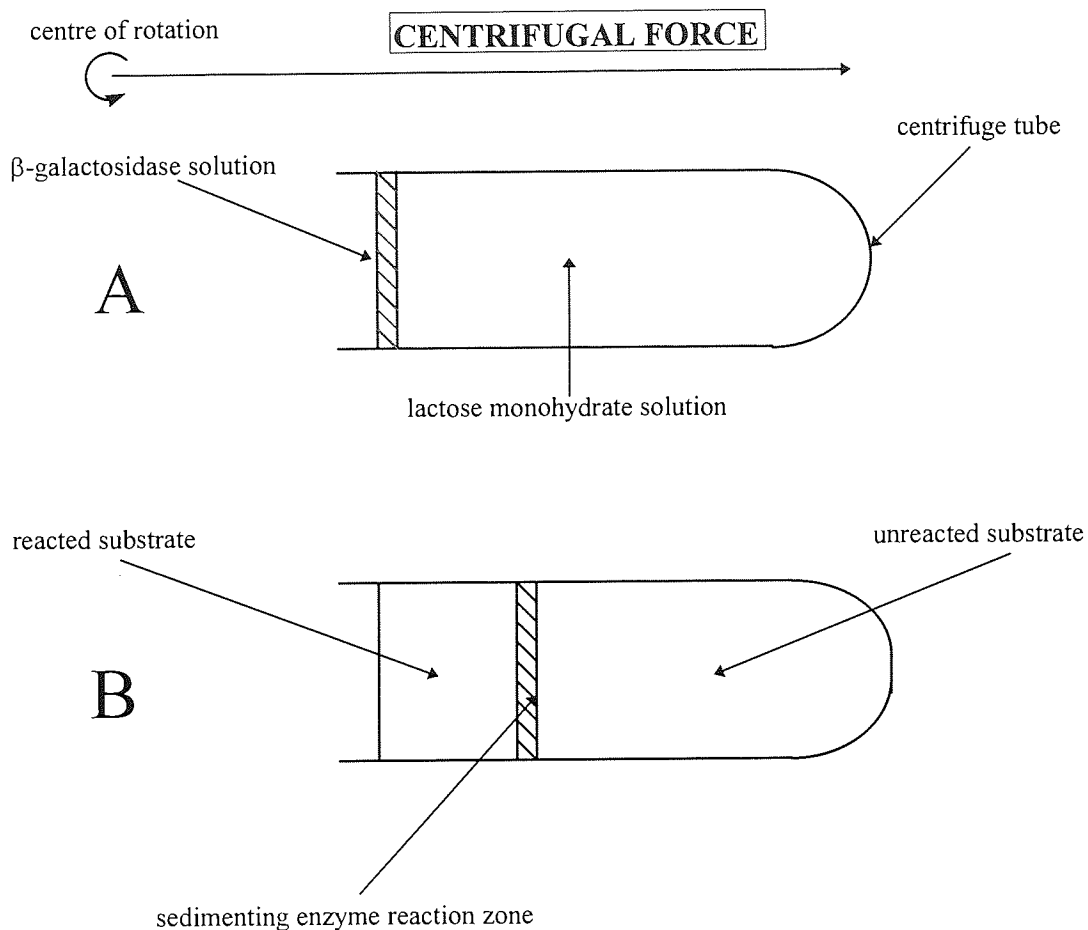


Figure 1.3. Overview of the active enzyme centrifugal bioreaction system studied in this research project. Diagram A corresponds to the start of the reaction and B is the enzyme sedimenting during the reaction.

As the experiments were performed the research project evolved and novel modifications were made to the basic reaction system presented in Figure 1.3. The structure of the thesis introduced below, reflects the evolution of the project.

1.2 Structure of the thesis

The thesis consists of seven chapters followed by the references and appendices. Each chapter starts with a short summary describing the contents of the associated chapter. Every chapter contains the theory and literature survey associated with the experimental work presented in that chapter. This provides the reader with the necessary information to fully appreciate the particular experimental results presented in each chapter, without having to refer back to an initial extensive literature survey.

Chapter 1 is a general introduction to the research performed in this project and describes the background to the thesis and introduces the initial research objectives. The model enzymatic reaction chosen to be studied in the centrifugal bioreaction system is described and the reason for its choice is explained. The overall structure to the thesis is also presented.

Chapter 2 describes stirred-batch reactions performed using the β -galactosidase enzyme chosen for the centrifugal studies. These experiments were performed to allow the β -galactosidase reaction to be fully understood using a conventional reaction system and to allow these results to be compared to the results obtained using the centrifugal bioreaction system. This chapter also includes the results of kinetic studies, and a preliminary mathematical model for the reactions of β -galactosidase is presented.

Chapter 3 describes the historical development of the centrifuge and the principles and practices of centrifugation. The initial centrifugal studies using soluble, free β -galactosidase and using a modified version of the normal rate separation technique are presented.

Chapter 4 introduces the concept of rate-zonal centrifugation techniques and also describes the practical aspects associated with this technique. The reasons for using this technique in preference to the normal rate technique are discussed and experimental results obtained using free, soluble β -galactosidase using the rate-zonal technique are presented.

Chapter 5 describes the theory and practical aspects of enzyme immobilisation and insolubilisation. Results obtained from novel centrifugal bioreaction experiments performed using immobilised and insolubilised β -galactosidase are presented and the reasons for using such a system are discussed.

Chapter 6 gives the conclusions of this research project and an integrated discussion allows the results obtained from all of the experimental work performed to be compared. This is followed by recommendations for further work.

Chapter 7 describes the materials used and details the experimental methods performed.

The structure of the thesis is shown diagrammatically in Figure 1.4.

Chapter 1	Introduction Bioreaction and separation in centrifugal fields Literature survey Structure of thesis
Chapter 2	STIRRED-BATCH REACTION STUDIES USING SOLUBLE AND INSOLUBILISED β-GALACTOSIDASE
Chapter 3	CENTRIFUGAL STUDIES USING SOLUBLE β-GALACTOSIDASE
Chapter 4	RATE-ZONAL CENTRIFUGATION USING SOLUBLE β-GALACTOSIDASE
Chapter 5	RATE-ZONAL CENTRIFUGATION USING IMMOBILISED AND INSOLUBILISED β-GALACTOSIDASE
Chapter 6	Conclusions and integrating discussion Recommendations for further work
Chapter 7	Materials and experimental methods

Figure 1.4. Structure of the thesis. The chapters highlighted in yellow are those where experimental work has been performed and the results presented.

2.0 STIRRED-BATCH REACTION STUDIES USING SOLUBLE AND INSOLUBILISED β -GALACTOSIDASE

In this chapter, the hydrolytic and trans-galactosyl activity of β -galactosidase is discussed. The industrial production and uses of galacto-oligosaccharides are reported. The kinetics of single-substrate enzyme-catalysed reactions is described. The results obtained from stirred-batch reaction studies performed using soluble and insolubilised β -galactosidase are presented. A preliminary mathematical model based on Michaelis-Menten-type kinetic behaviour is presented.

2.1 The hydrolytic and trans-galactosyl activity of β -galactosidase

2.1.1 An historical perspective

Galactose-containing oligosaccharides, or galacto-oligosaccharides, are naturally occurring compounds that are found in many types of food including fruit, vegetables and milk. Oligosaccharides are usually defined as glycosides containing between three to ten sugar moieties although certain disaccharides possess similar properties⁽⁸⁾. Lactose and certain galacto-oligosaccharides can act as substrates for β -galactosidases (EC 3.2.1.23), and this enzyme is found widely in micro-organisms, animals and plants⁽⁹⁾. β -Galactosidase, also known as lactase, is a hydrolase which attacks the glycosidic bond of lactose. The hydrolytic activity of β -galactosidase breaks down lactose to yield equimolar amounts of glucose and galactose⁽¹⁰⁾.

Experiments performed in the 1950's reported the trans-galactosyl activity of β -galactosidase to produce galacto-oligosaccharides. This trans-galactosyl activity proceeded in tandem with the normal hydrolytic activity. In 1951, Wallenfels⁽¹¹⁾ reported the formation of three galacto-oligosaccharides during the hydrolysis of lactose by β -galactosidase isolated from *Aspergillus oryzae*. In 1952, Aronson⁽¹²⁾ incubated β -galactosidase, isolated from *Saccharomyces fragilis*, with various concentrations of lactose. In addition to the hydrolytic products, four galacto-oligosaccharides were isolated. In 1953, Roberts and McFarren⁽¹³⁾ observed the formation of ten different galacto-oligosaccharides, whilst hydrolysing the lactose contained in whey, using β -galactosidase isolated from *Saccharomyces fragilis*. In

1957, Roberts and Pettinatti ⁽¹⁴⁾ found that the yield of galacto-oligosaccharides was dependent upon the initial lactose concentration. Experiments they performed using β -galactosidase, isolated from *Saccharomyces fragilis*, showed that the higher the initial lactose concentration, the higher the yield of galacto-oligosaccharides. This relationship was maintained up to a lactose concentration of 35%^{w/v}, and at higher concentrations there was no significant increase in the galacto-oligosaccharide yields. In 1958, Pazur, Tipton, Budovich and Marsh ⁽¹⁵⁾ identified three disaccharides in addition to the ten galacto-oligosaccharides identified by Roberts and McFarren, using similar reaction conditions. The three different disaccharides consisted of galactose-galactose and galactose-glucose conjugates. By 1985, twenty individual galacto-oligosaccharides had been isolated and the structures determined using ¹³C nuclear magnetic resonance spectroscopy (NMR) ⁽¹⁶⁾.

The main reasons for enzymatic lactose hydrolysis are (a) to remove lactose from a product making it suitable for consumption by people with low levels of intestinal β -galactosidase, or lactose intolerance, (b) to increase its value by conversion to glucose/galactose syrup, which has a higher degree of sweetness and can be used for product sweetening, and (c) to minimise the formation of crystals as glucose and galactose are less prone to crystallisation than lactose ^(17,18,19). The galacto-oligosaccharides formed during lactose hydrolysis can be regarded as intermediate compounds because they are ultimately hydrolysed to yield glucose and galactose as the reaction reaches equilibrium. Up until the last fifteen years these intermediate compounds were regarded as undesirable and their presence in the product stream was minimised by allowing the reaction to reach equilibrium, although this considerably increased the process time. In the 1980's there was a resurgence of interest in the mechanisms of enzymatic galacto-oligosaccharide formation, mainly driven by commercial considerations as described below.

In the early 1980's, the use of β -galactosidase to produce low lactose milk, yoghurt and other dairy products was a well established industrial process. The Japanese had performed extensive research in this area, driven by the requirement to offer these products to a large lactose intolerant population. At this time there was an increasing interest in the spectrum of sugars present in these products. In 1982, Toba, Watanabe and Adachi ⁽²⁰⁾ investigated the range and concentrations of galacto-oligosaccharides present in low lactose yoghurts. They found that the yoghurts contained less than 0.1% galacto-oligosaccharides. Flaschel, Raetz

and Renken ⁽²¹⁾ investigated the kinetics of lactose hydrolysis using β -galactosidase from *Aspergillus niger* and proposed a simple model based on Michaelis-Menten-type kinetics. This model was designed to be used by industry in the processing of whey. The model was based on the kinetics of glucose liberation, but did not incorporate the role of glucose in the trans-galactolysation process. In 1984, Betschart and Prenosil ⁽²²⁾ developed a technique involving high performance liquid chromatography (HPLC) to enable the identification and quantification of the products of enzymatic lactose hydrolysis. Prior to this technique, paper chromatography was used and this offered only qualitative analysis. Jeon and Mantha ⁽²³⁾ improved on this technique by extending the range of galacto-oligosaccharides detected. The HPLC provided a simple and fast method for monitoring the hydrolytic and trans-galactosyl activity of β -galactosidase in more detail than was previously available.

In the mid 1980's the terms 'functional foods' and 'nutraceuticals' were proposed in Japan to describe foods or food components that impart a physiological benefit that enhanced overall health ^(8,17,24,25). The potential benefits to health of galacto-oligosaccharides were recognised and this led to a considerable amount of research into the process of galacto-oligosaccharide formation. Galacto-oligosaccharides were found to promote the growth of bifidobacteria in the human intestinal tract. These bacteria improve the intestinal environment by suppressing the growth of putrefractive and harmful bacteria ^(8,17,26,27,28,29). In 1987, Yang and Tang ⁽³⁰⁾ and Prenosil, Strucker and Bourne ^(31,32) performed extensive studies into the formation of galacto-oligosaccharides during lactose hydrolysis and proposed mathematical models for the hydrolytic and trans-galactosyl activity of β -galactosidase. During the 1990's, the use of galacto-oligosaccharides as a prebiotic food additive increased and by 1995 the annual production had reached 15 000 tonnes world-wide ⁽⁸⁾. A prebiotic compound is a non-digestible food ingredient that beneficially affects the host by selectively stimulating the growth and/or activity of one or a limited number of bacterial species already resident in the colon ⁽⁸⁾. The production was predominantly based in Japan, where the Yakult Honsha Corporation (Tokyo) alone produced 6 500 tonnes per year marketed under the trade-name Oligomate[®] ⁽¹⁸⁾. The industrial process used was a two stage decoupled system consisting of a stirred-batch reaction followed by chromatographic product isolation ⁽³³⁾. In 1998, the market for a whole range of functional foods/nutraceuticals reached nearly £55 000 million within the United States, £2 400 million in Japan and in excess of £1 200 million in Europe ⁽²⁵⁾. These values are expected to rise as the food industry conglomerates release more

products. The use of galacto-oligosaccharides can be expected to rise in line with this future expansion.

2.1.2 Mechanism of galacto-oligosaccharide formation

Many researchers have proposed reaction schemes for the hydrolytic and trans-galactosyl activity of β -galactosidase. Prenosil, Stuker and Bourne ⁽³¹⁾ produced probably the most detailed and cited model. A simplified version based on this model is presented in Figure 2.1. Figure 2.1 does not show the possible complex range of chemical linkages formed within the galacto-oligosaccharide products (see Table 2.1).

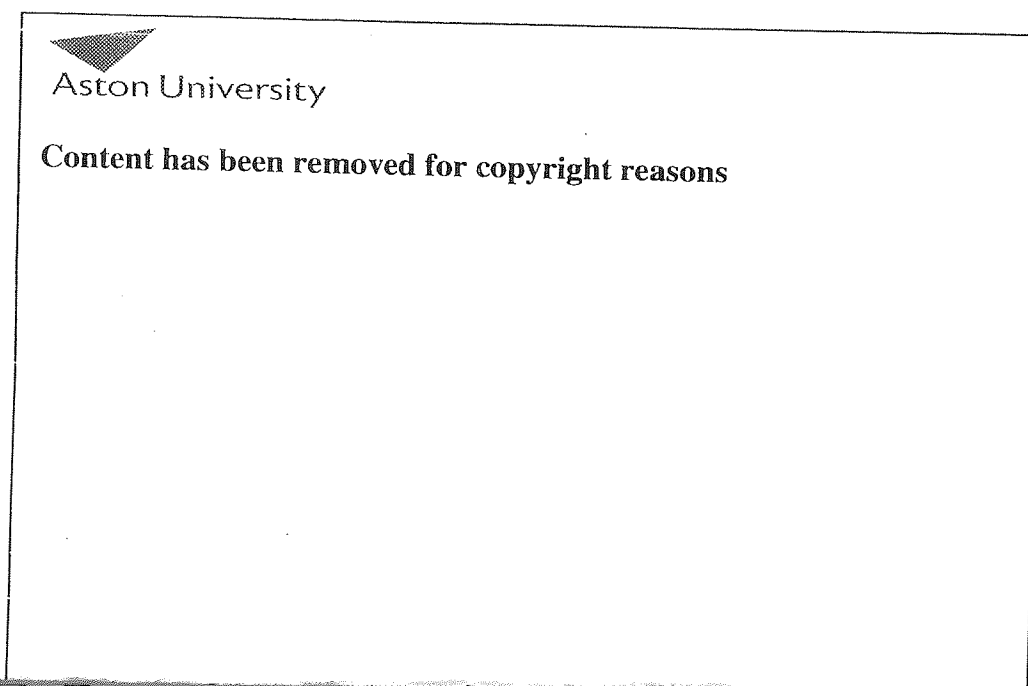


Figure 2.1. The hydrolytic and trans-galactosyl activity of β -galactosidase ⁽³¹⁾.

Figure 2.1 is limited to the formation of hexasaccharides, but the trans-galactolysation process can produce higher oligosaccharides. Prenosil, Stuker and Bourne ⁽³²⁾ reported that during the hydrolysis of lactose by β -galactosidase from *Aspergillus oryzae*, the highest galacto-oligosaccharides detected were pentasaccharides. The relative ratio of tri- : tetra- : pentasaccharides was found to be approximately 14 : 4 : 1, obtained at lactose conversions between 48 to 64%. The trans-galactosyl activity of β -galactosidase varies considerably

depending upon the source of the enzyme. β -Galactosidases from *Aspergillus oryzae*, *Bacillus circulans* and *Lactobacillus bulgaricus* have been reported to exhibit the highest trans-galactosyl activity⁽¹⁷⁾. The trans-galactosyl activity of β -galactosidase is enhanced when the initial lactose concentration is high, which results in a lower water activity environment^(8,12,14,17,27,31,34). Low water activity means that there is a reduced number of water molecules available to act as an acceptor. This allows other molecules to act as acceptors and produce galacto-oligosaccharides. This effect is analogous to enzymatic reactions performed in virtually non-aqueous environments where the water activity is extremely low. An example of this is the formation of sucrose-containing polyesters produced by the transesterification activity of Proleather, an alkaline protease from *Bacillus amyloliquifaciens*, in anhydrous pyridine. In aqueous solution Proleather exhibits proteolytic activity, but acts in reverse when in a low water environment⁽³⁵⁾.

The molecular weight of β -galactosidase varies depending upon the source organism. β -Galactosidases isolated from *Escherichia coli* and *Aspergillus oryzae* have reported molecular weights of 540 000 and 90 000 daltons respectively^(36,37,38). The differences in the molecular weights and amino acid sequences indicate a wide variety of tertiary structures. The quaternary structure forms a functional region, or active site, where the catalytic activity takes place. The chemical groups associated with the active site are not definitively known, but based upon inhibition experiments with sulfahydryl reagents and pH activity studies, Wallenfels and Mahotra⁽³⁹⁾ proposed a mechanism for β -galactosidase activity. For β -galactosidase with a pH optimum of 7 they concluded that the catalytic mechanism involved a sulfahydryl group (methionine) acting as an acid and an imidazole group (histidine) providing nucleophilic assistance for breaking the glycosidic linkage. This was confirmed by Proctor who found that β -galactosidase activity was inhibited when iodoacetate was added, iodoacetate reacting with both sulfahydryl and histodyl groups to render them catalytically inactive⁽³⁹⁾. Figure 2.2 shows a diagrammatic representation of the hydrolytic and trans-galactosyl processes of the active site of β -galactosidase^(40,41). Shukla⁽⁴¹⁾ described the hydrolysis process as a S_N2 -like displacement mechanism. The methionine group acts as a general acid to protonate the galactosidic oxygen atom. The histidine group acts as a nucleophile, which attacks the C1 carbon to remove the galactosyl group and release glucose. In the removal of the galactosyl group the sulfahydryl anion (S^-) acts as a general

base to remove a proton from a water molecule, which assists in the OH^- attack at the C1 position. If water is the acceptor molecule then the galactose is released, but if the OH group is part of a saccharide then a galacto-oligosaccharide molecule is released. The rate of trans-galactolysation for a specific acceptor is known to be influenced by the structural features of that acceptor ^(40,41). The general mechanism shown in Figure 2.2 is applicable to β -galactosidase from various sources with differing pH optima, however the catalytic groups involved may vary ⁽⁴¹⁾.

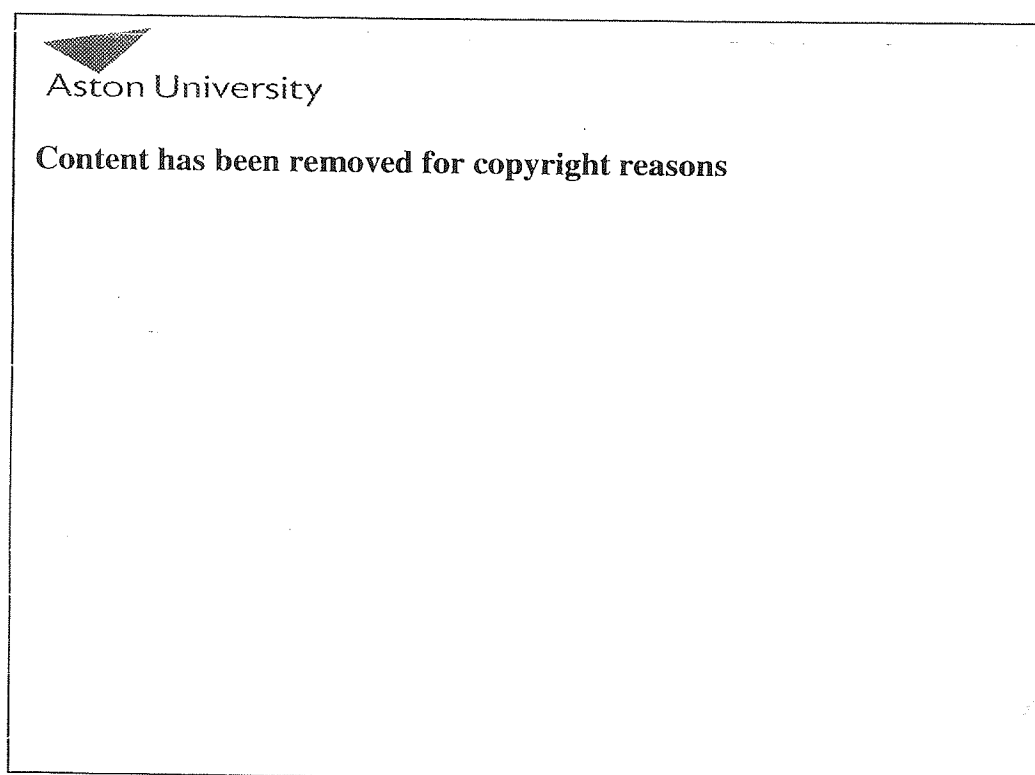


Figure 2.2. The hydrolytic and trans-galactosyl processes of the active site of β -galactosidase ^(40,41). A is a lactose molecule at the active site, B is hydrolysis of the lactose molecule to release a glucose molecule, C is the β -galactosidase-galactose complex (R-O-H is the acceptor molecule, H_2O yields a galactose molecule and a saccharide yields a galacto-oligosaccharide molecule), and D is the release of either galactose or galacto-oligosaccharide.

A typical range of galacto-oligosaccharide compounds formed by the trans-galactosyl activity of β -galactosidase is shown in table 2.1. A more comprehensive list is presented by Preņosil, Stuker and Bourne ⁽³¹⁾. Non-enzymatic (chemical) hydrolysis of lactose does not yield galacto-oligosaccharides, only glucose and galactose ⁽⁷⁾.

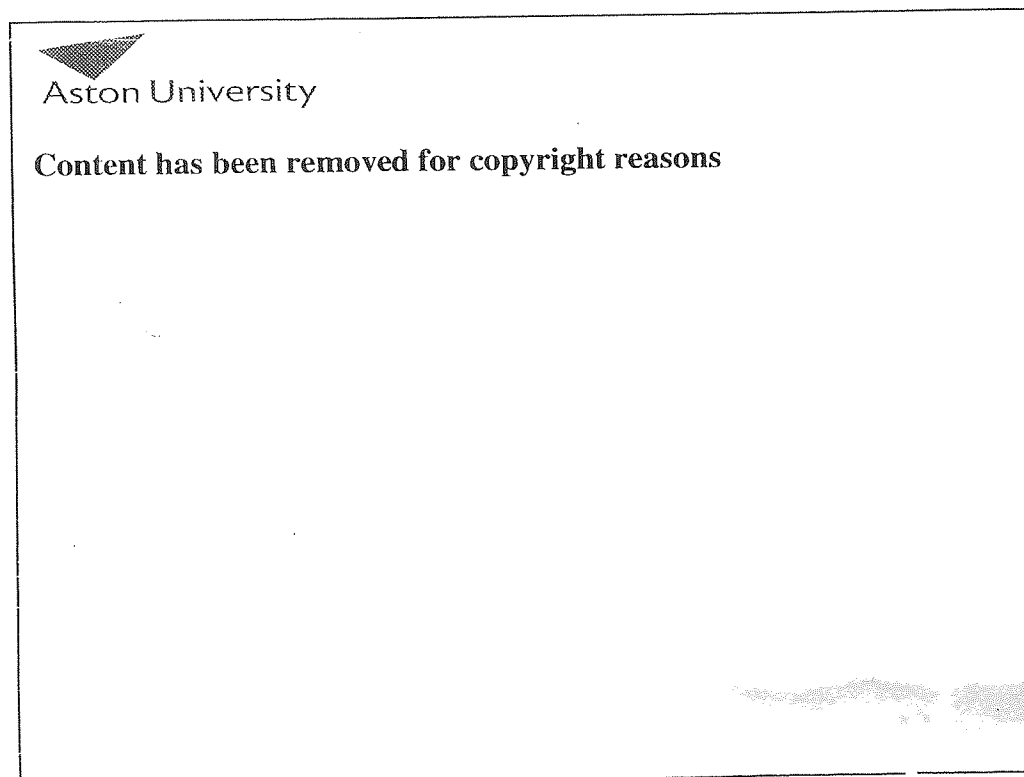


Table 2.1. A typical range of galacto-oligosaccharide compounds formed by the trans-galactosyl activity of β -galactosidase ⁽³¹⁾.

2.1.3 The effect of galactose inhibition and mutarotation on β -galactosidase activity.

Galactose acts a competitive inhibitor for β -galactosidase and it has been reported that a concentration of only 5mM can decrease the activity of the soluble enzyme by 50%^(42,43). In solution monosaccharides can exist as either pyranoses or furanoses, and these can be in either α or β forms. The interconversion between the α and β forms is known as mutarotation, or anomerisation. Pure forms of α and β monosaccharides mutarotate until equilibrium is reached and this can be monitored by optical rotation measurements. Pyranose ring structures usually exist as two chair (C) conformations, 1C_4 and 4C_1 , although less commonly skew (S) and boat (B) forms are formed. Furanose ring structures exist as two conformational forms which are envelope (E) and twist (T). With galactose there is an initial fast mutarotation, followed by a slow mutarotation. The fast mutarotation has been attributed to the furanose interconversion, whilst the slow mutarotation has been linked to the pyranose interconversion⁽⁴⁴⁾. The process of galactose mutarotation is shown in Figure 2.3. Mutarotation is produced by the protonation of the ring oxygen which promotes cleavage of the bond between the ring oxygen and C1 to give an acyclic intermediate, which re-cyclises to either the α or β forms. The rate of mutarotation varies depending upon the pH of the solution, with mildly acidic and basic solutions accelerating the speed at which equilibrium conditions are reached. The equilibrium composition of galactose in aqueous solution is as follows⁽⁴⁴⁾:

α -Furanose	1.0%
β -Furanose	3.1%
α -Pyranose	32.0%
β -Pyranose	63.9%

The α -pyranose form of galactose has been reported to have approximately 12 times the competitive inhibition effect on β -galactosidase isolated from *Aspergillus niger*⁽²¹⁾.

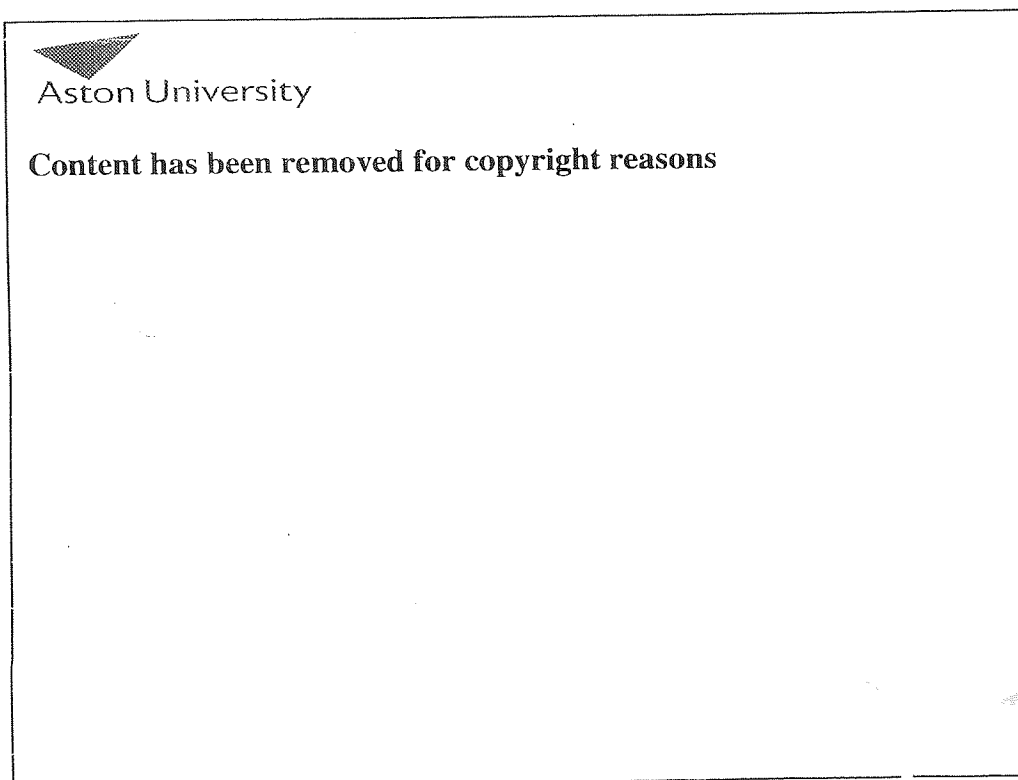


Figure 2.3. The mutarotation of galactose in aqueous solution, the bracketed values give the % composition at equilibrium ⁽⁴⁴⁾.

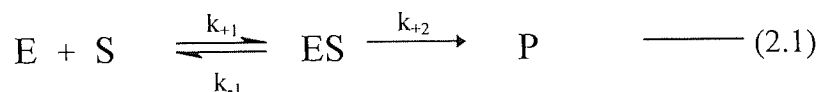
Modelling of the hydrolysis of lactose by β -galactosidase is complicated by mutarotation of galactose, especially due to the vast difference in the inhibitory effect of the α and β forms. The hydrolysis of lactose by β -galactosidase yields only β -galactose and the rate of mutarotation to the α form is determined by the pH of the reaction environment. To produce a workable model the mutarotation of galactose needs to be fully investigated over a range of reaction conditions.

2.2 Theory of single-substrate kinetics

This section introduces the theory of enzyme single substrate kinetics and the use of the Michaelis-Menten equation to calculate kinetic parameters. The kinetics of enzyme inhibition is described and a method for calculating this parameter is presented. The effects of immobilisation or insolubilisation on an enzyme's kinetic parameters are discussed.

2.2.1 Introduction

For an enzymatic reaction to occur, the reactant molecules must contain sufficient energy to cross a potential energy barrier, the activation energy. Enzymes catalyse a reaction by forming a transition state with the reactant, which has a lower free energy than that in an uncatalysed reaction. The lowering of the activation energy is primarily achieved by the binding energy between the enzyme and the substrate to form a bound complex, and the formation of this complex allows the catalytic reaction to proceed to completion. Michaelis and Menten illustrated this process with the following kinetic model ⁽¹⁹⁾:



where:

- E = enzyme molecule.
- S = substrate molecule.
- ES = enzyme-substrate complex.
- P = product molecule.
- k_{+1} , k_{-1} and k_{+2} = the rate constants.

This model assumes that none of the product reverts back to the substrate and this is valid at the initial stages of the reaction where the concentration of the product is low, and where the reaction is effectively irreversible.

The rate of reaction (v) is the rate at which the product is formed and is given by the following expression:

$$v = \frac{d[P]}{dt} = k_{+2}[ES] \quad \text{————— (2.2)}$$

where: [] indicates the molar concentration (mol dm⁻³).

The rate of change of the concentration of ES is equal to the rate of its formation minus the rate of its breakdown and this may be expressed as:

$$\frac{d[ES]}{dt} = k_{+1}[E][S] - (k_{-1} + k_{+2})[ES] \quad \text{————— (2.3)}$$

Assuming “steady-state kinetic conditions”, that is [S] and [P] are changing, but [ES] does not change (a constant flux of S “through” the enzyme), then the following applies;

$$0 \approx k_{+1}[E][S] - (k_{-1} + k_{+2})[ES] \quad \text{————— (2.4)}$$

or,

$$\frac{d[ES]}{dt} \approx 0 \quad \text{————— (2.5)}$$

Since $d[ES]/dt \approx 0$, then the rate of formation of [ES] must equal the rate of breakdown of [ES]. Also, from the conservation of matter the following applies;

$$[E] = [E]_0 - [ES] \quad \text{————— (2.6)}$$

where the total enzyme at the beginning of the reaction, $[E]_0$, is present either as the free enzyme, $[E]$, or as the enzyme-substrate complex, $[ES]$.

Assuming “steady-state kinetic conditions”, then the rate of formation of $[ES]$ must equal the rate of breakdown of $[ES]$ and the following are true:

- 1.) Rate of formation of $[ES] = k_{+1}[E][S]$
- 2.) Rate of breakdown of $[ES] = (k_{-1} + k_{+2})[ES]$
- 3.) $k_{+1}[E][S] = (k_{-1} + k_{+2})[ES]$

Rearranging the above and solving for $[ES]$ gives:

$$[ES] = \frac{k_{+1}[E][S]}{(k_{-1} + k_{+2})} \quad \text{————— (2.7)}$$

Substituting for $[E]$ in (2.7) using (2.6) gives:

$$[ES] = \left(\frac{k_{+1}}{(k_{-1} + k_{+2})} \right) [S] \{ [E]_0 - [ES] \} \quad \text{—— (2.8)}$$

Expanding the RHS of (2.8):

$$[ES] = \left(\frac{k_{+1}}{k_{-1} + k_{+2}} \right) [S] [E]_0 - \left(\frac{k_{+1}[ES][S]}{(k_{-1} + k_{+2})} \right) \quad \text{—— (2.9)}$$

Rearranging Equation (2.9) gives:

$$[\text{ES}] \left(1 + \frac{k_{+1}}{k_{-1} + k_{+2}} [\text{S}] \right) = \left(\frac{k_{+1}}{k_{-1} + k_{+2}} \right) [\text{E}]_0 [\text{S}] \quad \text{--- (2.10)}$$

Combining Equation (2.2) with Equation (2.10) and expressing for the rate of reaction (v) gives:

$$v = \frac{k_{+2} \left(\frac{k_{+1}}{k_{-1} + k_{+2}} \right) [\text{E}]_0 [\text{S}]}{1 + \left(\frac{k_{+1}}{k_{-1} + k_{+2}} \right) [\text{S}]} \quad \text{--- (2.11)}$$

Equation (2.11) can be simplified to give:

$$v = \frac{(k_{+2} [\text{E}]_0) [\text{S}]}{\left(\frac{k_{-1} + k_{+2}}{k_{+1}} \right) + [\text{S}]} \quad \text{--- (2.12)}$$

The maximum reaction velocity (V_{max}) and the Michaelis constant (K_m) can be expressed as:

$$V_{\text{max}} = (k_{+2} [\text{E}]_0) \quad \text{and} \quad K_m = \frac{k_{-1} + k_{+2}}{k_{+1}}$$

The simplified form of the Michaelis-Menten equation shown in (2.13) is derived by inserting the V_{\max} and K_m into Equation (2.12):

$$v = \frac{V_{\max}[S]}{[S] + K_m} \quad \text{————— (2.13)}$$

where: v = rate of reaction ($\text{mol dm}^{-3} \text{s}^{-1}$).
 V_{\max} = the maximum reaction velocity (mol s^{-1}).
 K_m = the Michaelis constant (mol dm^{-3}).

2.2.2 Calculation of kinetic parameters using the Michaelis-Menten equation

The Michaelis-Menten equation can be used to determine the kinetic parameters V_{\max} and K_m . V_{\max} is the maximum reaction velocity and K_m , the Michaelis constant, is the substrate concentration at which half of the enzyme active sites are occupied. The K_m value is also a measure of the affinity of an enzyme towards a particular substrate and this can be used to identify a particular enzyme⁽⁴⁵⁾. If an enzyme exhibits Michaelis-Menten-type kinetics then a graph of initial reaction velocity, v_0 , determined at various initial substrate concentrations and plotted against the substrate concentration, $[S_0]$, will have the form of a rectangular hyperbola, as shown in Figure 2.4⁽⁴⁶⁾.

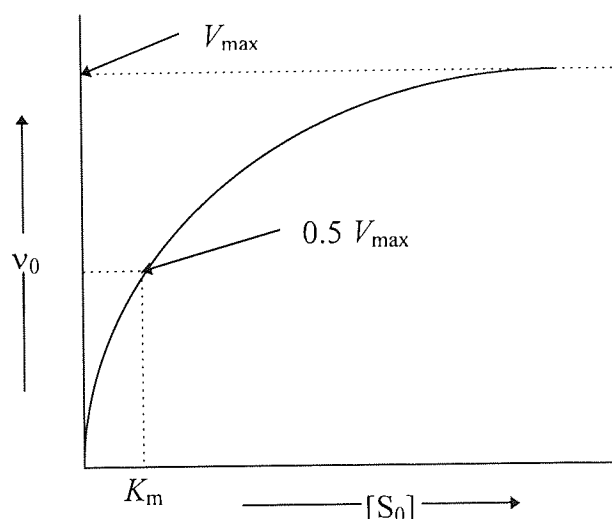


Figure 2.4. A graphical representation of a Michaelis-Menten-type enzymatic reaction.

This type of plot is not entirely satisfactory for determining V_{\max} and K_m unless there are sufficient data points to accurately define the plateau region. If an enzyme obeys the Michaelis-Menten equation then the Lineweaver-Burk plot, or double-reciprocal plot, can be used to produce a straight line graph, allowing a more accurate determination of V_{\max} and K_m . A diagrammatic representation of the Lineweaver-Burk plot is shown in Figure 2.5.

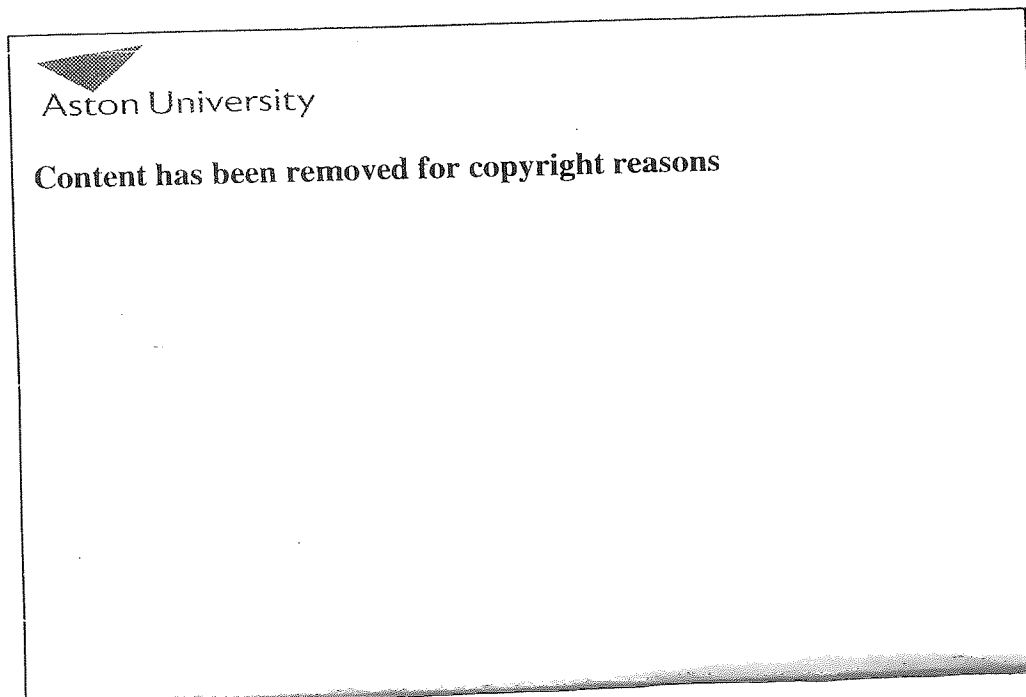


Figure 2.5. The Lineweaver-Burk, or double reciprocal, plot ⁽⁴⁵⁾.

2.2.3 The kinetics of enzyme inhibition

Competitive inhibition is where an inhibitor compound competes for an enzyme's active site with the substrate and this process can be either reversible or irreversible. The effect of a competitive inhibitor on the enzyme activity depends upon; the inhibitor concentration, the substrate concentration and the relative affinities of the inhibitor and substrate for the active site. A Michaelis-Menten plot for an enzyme in the presence of a fixed concentration of a competitive inhibitor shows a straightening of the usual rectangular hyperbola ⁽⁴⁵⁾. This produces an apparent increase in the K_m value and this is represented by K'_m . With the Lineweaver-Burk plot there is an increase in the slope of the line, which becomes steeper as the concentration of the inhibitor increases. The dissociation constant for the reaction

between the enzyme and the inhibitor is known as the inhibition constant, or K_i and K_i can be represented by the following expression:

$$K_i = \frac{[E][I]}{[EI]} \quad \text{————— (2.14)}$$

The Michaelis -Menten equation shown in equation (2.13) can be modified to incorporate the apparent increase in K_m resulting from the presence of a competitive inhibitor and this can be written as ^(45,46,47):

$$v = \frac{V_{\max}[S]}{[S] + K_m \left(1 + \frac{[I]}{K_i} \right)} \quad \text{————— (2.15)}$$

The inhibition constant is a measure of the potency of a compound to inhibit the activity of a particular enzyme and can be used along with other kinetic parameters to identify a particular enzyme.

2.2.3.1 Determination of the inhibition constant, K_i , using the Dixon plot method.

In 1953, Dixon proposed a graphical means of calculating the inhibition constant, K_i ⁽⁴⁵⁾. The Dixon plot involves incubating a fixed concentration of an enzyme, $[E_0]$, with different concentrations of the relevant substrate $[S]_{1,etc}$, in the presence of various inhibitor concentrations. Plotting the reciprocal of the initial velocity, v_0 , against the initial inhibitor concentration, I_0 , produces linear plots and at the point where the lines intersect is equivalent to the inhibition constant. An example of a typical Dixon plot is shown in Figure 2.6 ^(45,46).

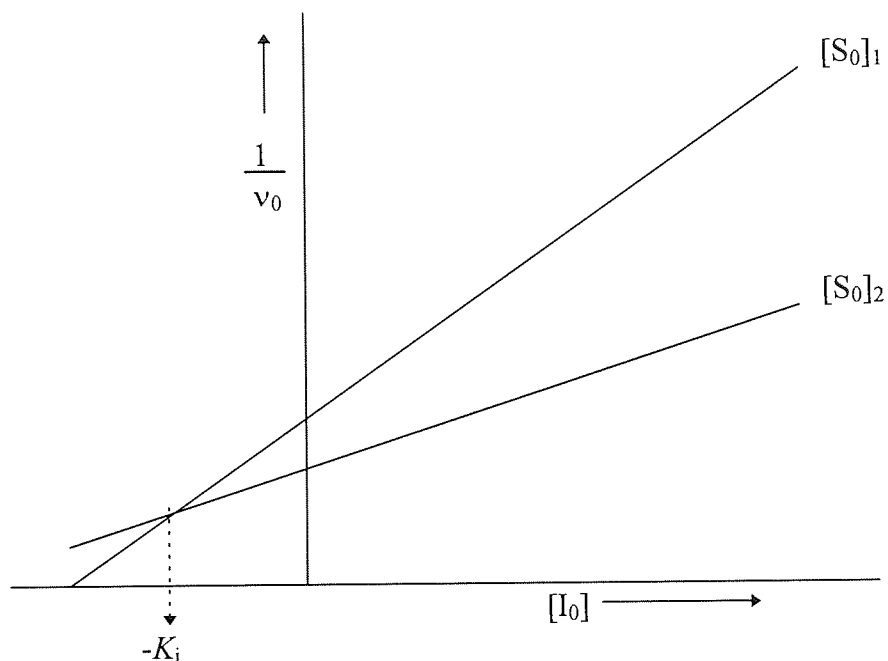


Figure 2.6. Determination of the inhibition constant, K_i , using the Dixon plot method.

2.2.3.2 Effects of enzyme immobilisation and insolubilisation on enzyme kinetic parameters.

The kinetic behaviour of an immobilised or insolubilised enzyme can vary significantly to that of the soluble free enzyme. The immobilisation/insolubilisation process can produce conformational changes to the enzyme and also introduce partitional and diffusional problems. In 1968, Lilly et al postulated that around a particle there is an unstirred layer of solution, ranging in thickness from 10-100 μm ⁽⁴⁶⁾. This layer is described as the microenvironment and the surrounding solution is the bulk macroenvironment; this is shown in Figure 2.7.

Within the microenvironment there is a partition layer (~20nm thick) which is affected by the charge and hydrophobicity of the particle surface ⁽¹⁹⁾. A partitioning of substrate and product/s can occur between the bulk solution and the microenvironment. Molecules of opposite charge to the particle surface are partitioned into the microenvironment and those molecules with the same charge as the particle are partitioned into the bulk macroenvironment.



Aston University

Content has been removed for copyright reasons

Figure 2.7. The microenvironment and bulk macroenvironment surrounding an idealised spherical immobilised/insolubilised particle ⁽¹⁹⁾.

The effect of solute partition can be quantified by the calculation of the electrostatic partition coefficient (Λ) which is represented by the following equation ⁽¹⁹⁾:

$$\Lambda = \frac{[C_0^{n+}]}{[C^{n+}]} = \frac{[A^{n-}]}{[A_0^{n-}]} \quad \text{————— (2.16)}$$

where: Λ = electrostatic partition coefficient.

$[C_0^{n+}]$ = cation concentration in the bulk macroenvironment (mol dm^{-3}).

$[C^{n+}]$ = cation concentration in the microenvironment (mol dm^{-3}).

$[A_0^{n-}]$ = anion concentration in the bulk macroenvironment (mol dm^{-3}).

$[A^{n-}]$ = anion concentration in the microenvironment (mol dm^{-3}).

The value of Λ for a particular reaction system can be used to calculate the apparent Michaelis constant, K_m^{app} , for an immobilised enzyme using the following expressions:

$$K_m^{\text{app}} = K_m \Lambda \quad (\text{for a positively charged substrate}) \quad \text{—————} \quad (2.17)$$

or,

$$K_m^{\text{app}} = K_m / \Lambda \quad (\text{for a negatively charged substrate}) \quad \text{—————} \quad (2.18)$$

Similarly, the electrostatic partition coefficient can be used to calculate the apparent inhibition constant, K_i^{app} , by replacing K_m with K_i in expressions (2.17) and (2.18). Solute partition can produce an apparent increase or decrease of the kinetic parameters V_{max} , K_m and K_i depending upon the charged status of the immobilised/insolubilised particle, the substrate charge, and the ionic strength of the media.

The apparent kinetic parameters described in (2.17) and (2.18) above can be further affected by diffusion factors. The substrate contained within the microenvironment may be rapidly utilised by the enzyme and the reaction velocity will then be dependent upon the rate at which the substrate contained within the bulk macroenvironment diffuses through the microenvironment and the partition layer. Usually, the substrate concentration surrounding the immobilised/insolubilised enzyme particle will be lower than that of the bulk macroenvironment, which produces a reduction in the reaction velocity compared to that expected for the bulk solution. The apparent values of V_{max} and K_m will be affected and the new K_m (K'_m) value can be calculated using the following equation ⁽¹⁹⁾:

$$K'_m = K_m^{\text{app}} + V'_{\text{max}} \cdot \delta l / D \quad \text{—————} \quad (2.19)$$

where: K'_m = the apparent Michaelis constant corrected for diffusional effects.
 V'_{max} = the maximum reaction velocity corrected for diffusional effects.
 δl = the thickness of the unstirred layer (cm).

D = diffusion coefficient ($\text{cm}^2 \text{s}^{-1}$).

Equation (2.19) refers to external diffusion and the effects of internal diffusion must also be considered. Internal diffusion is the transport of substrate and product/s within the pores or interstitial spaces of an immobilised/insolubilised enzyme particle. Internal and external diffusion problems can make the effects of product inhibition more severe due to the high localised concentration of the inhibitor compared to that found in the bulk macroenvironment.

2.3 The industrial use of soluble and immobilised β -galactosidase.

β -Galactosidase, especially of fungal origin, is used widely by the dairy industries. Most of the population of Northern Europe are lactose tolerant, but up to 97% of Thai, Chinese, Japanese and Black American populations are reportedly lactose intolerant⁽¹⁹⁾. This creates a large world-wide market for low-lactose products. On an industrial-scale, β -galactosidase from *Kluyveromyces fragilis* is used for the treatment of milk and β -galactosidase from *Aspergillus oryzae* is used to treat whey. β -galactosidase is also used in the production of ice cream and sweetened flavoured milk drinks. The soluble enzyme is added to the milk or whey and incubated for 24 hours at 5°C until approximately 50% of the lactose has been hydrolysed, giving a sweeter product that will not crystallise if frozen. If the lactose content within ice cream and other frozen dairy products is not reduced an unpleasant grainy texture is produced^(17,19). Immobilised β -galactosidase is not generally used in the manufacture of low-lactose dairy products due to the fouling produced by the colloidal nature of milk and whey^(48,49).

Over the past 15 years, a recognition of the potential health benefits of galacto-oligosaccharides has created a large world-wide market. In 1987, Honsha⁽³³⁾ patented a process for the industrial-scale production of galacto-oligosaccharides. The process involved the incubation of a lactose-containing solution with β -galactosidase from *Aspergillus oryzae*; the reaction was then thermally quenched and the reaction products were separated chromatographically. The product marketed as Oligomate 50[®] contained a minimum of

55%^{w/v} galacto-oligosaccharides and is used today as a food additive and a supplement to infant milk formulas. By 1995, 15 000 tonnes of Oligomate 50[®] was being produced in Japan ⁽⁸⁾. In Europe, Borculo Whey Products (The Netherlands) markets a galacto-oligosaccharide syrup (TOS-Syrup) which is added to milk beverages, confectionery and health drinks ^(8,50).

2.4 Stirred-batch reactions using β -galactosidase from *Aspergillus oryzae* (Biolactase F).

2.4.1 Properties of β -galactosidase from *Aspergillus oryzae* (Biolactase F).

The β -galactosidase used in all of this research was isolated from *Aspergillus oryzae* and was produced by Biocon Biochemicals Limited (Co. Cork, Ireland) under the trade-name Biolactase F. This enzyme has a reported effective pH range of 2.5-7.0 with an optimum range at 4.5-5.5, and an optimum temperature range at 55-60°C ^(43,51). Begum, Canuto, Hussain and Petrou ⁽⁵²⁾ performed stirred-batch reactions to confirm the pH and temperature optima for this enzyme and the results obtained are presented in Figure 2.8. The results obtained correlate closely to the literature values and confirm the broad effective pH and temperature range of this enzyme. The profile of the plots obtained may indicate the overlapping of differing enzyme activities.

Biolactase F is a comparatively crude product that possibly contains contaminating enzymes and growth medium compounds. Experiments were performed to determine the purity of Biolactase F by incubating solutions of the enzyme (10 mg cm⁻³, 1 cm³) with starch, maltose, raffinose and glucose (all 1%^{w/v}, 2 cm³) at 40°C for 30 minutes. The reactions were thermally quenched by placing the solutions in boiling water for 5 minutes, and the solution was then analysed by HPLC to determine the product profiles. A solution of the enzyme was incubated with lactose so that the relative activities of any contaminating enzymes could be related to the β -galactosidase activity. The analytical procedure is fully detailed in Chapter 7. The results obtained are presented in Table 2.2. Table 2.2 shows that Biolactase F exhibits enzyme activity other than that of β -galactosidase. A comparison of the concentrations of the reaction products formed showed that these contaminating enzymes were present in extremely low concentrations and therefore no attempt was made to remove them from Biolactase F solutions used in stirred-batch and centrifugation reaction studies.



Aston University

Content has been removed for copyright reasons

Temperature (°C)

Figure 2.8. The % Relative enzyme activity of β -galactosidase from *Aspergillus oryzae* (Biolactase F) at varying pH and temperature (°C) values ⁽⁵²⁾.

Substrate	Reaction products detected	Possible contaminating enzyme/s	Relative activity
lactose (control)	galacto-oligosaccharides, glucose, galactose	β -galactosidase	extremely high ($\sim 32 \text{ U cm}^{-3}$)
starch	maltose, glucose	β -amylase, α -glucosidase, amyloglucosidase	very low ($\sim 0.5 \text{ U cm}^{-3}$)
raffinose	sucrose, glucose, fructose	α -galactosidase, β -fructosidase	very low ($\sim 0.3 \text{ U cm}^{-3}$)
sucrose	glucose, fructose	β -fructosidase	very low ($\sim 0.1 \text{ U cm}^{-3}$)

Table 2.2. The enzymatic activities present in Biolactase F (1 unit (U) is defined as the amount of enzyme which converts 1 μmole of substrate in 1 minute at the stated conditions of pH and temperature).

β -Galactosidase from *Aspergillus oryzae* has a reported molecular weight of 90 000 daltons^(7,36,37) and the approximate molecular weights of β -amylase, α -glucosidase, amyloglucosidase, α -galactosidase and β -fructosidase are 57 000, 68 500, 97 000, 26 000 and 97 000 daltons respectively⁽³⁷⁾. The variation in the molecular weights of the enzymes present in Biolactase F will have no effect on stirred-batch reaction studies, but will produce broadening of the soluble enzyme band during centrifugation studies. The protein content of Biolactase F was determined using the Bio-Rad protein assay method (Bio-Rad Laboratories Ltd, Herts) and found to be 22.4%.

2.4.2 Stirred-batch reactions performed using soluble β -galactosidase from *Aspergillus oryzae* (Biolactase F)

Stirred-batch reactions were performed using soluble Biolactase F (1.25 mg cm^{-3} , 4 U cm^{-3}) incubated with various initial concentrations of lactose monohydrate (5, 10, 15, 20 and 25%^{w/v}) at 40°C (1 unit (U) is defined as the amount of enzyme which converts 1 μmole of

lactose monohydrate in 1 minute at the stated conditions of pH and temperature). The pH of the substrate solutions ranged from 4.4 to 5.2 and as shown in Figure 2.8 the enzyme activity is high and fairly constant over this range, and therefore the solutions were not buffered. Samples were taken at timed intervals and chemically quenched using sodium hydroxide. The samples were then analysed by HPLC and the raw data was entered into an Excel spreadsheet (see Appendix A-1) to determine the concentrations of the substrate and reaction products after various incubation times. The full experimental protocols used are presented in Chapter 7. A reaction temperature of 40°C was used as this was both the maximum attainable temperature for the centrifuge and the chosen reaction temperature used to perform subsequent centrifugal studies. A limited number of reactions were performed at 25°C and 55°C to determine the effects of temperature on galacto-oligosaccharide formation. Figure 2.9a shows the % Galacto-oligosaccharides of Total Sugar and % Lactose monohydrate conversion against Reaction time (minutes), for stirred-batch reactions performed using soluble Biolactase F (1.25 mg cm⁻³, 4 U cm⁻³) incubated with initial lactose monohydrate concentrations of 5 and 10%^{w/v}, at 40°C. Figure 2.9b shows the results obtained for lactose monohydrate concentrations of 15 and 20%^{w/v} and Figure 2.9c shows the results obtained for 25%^{w/v} lactose monohydrate.

Table 2.3 shows a comparison of the maximum galacto-oligosaccharide yields obtained using various initial lactose monohydrate concentrations, and performed at different temperatures.

Temperature (°C)	Initial Lactose Monohydrate Concentration (% ^{w/v})				
	5	10	15	20	25
25	11.3%	16.4%	19.1%	20.0%	21.4%
40	8.0%	14.4%	17.9%	21.2%	22.0%
55	8.2%	12.3%	15.3%	17.7%	20.4%

Table 2.3. Comparison of the maximum galacto-oligosaccharide yields (%^{w/v}) obtained using various initial lactose monohydrate concentrations (%^{w/v}), and performed at various temperatures (°C).

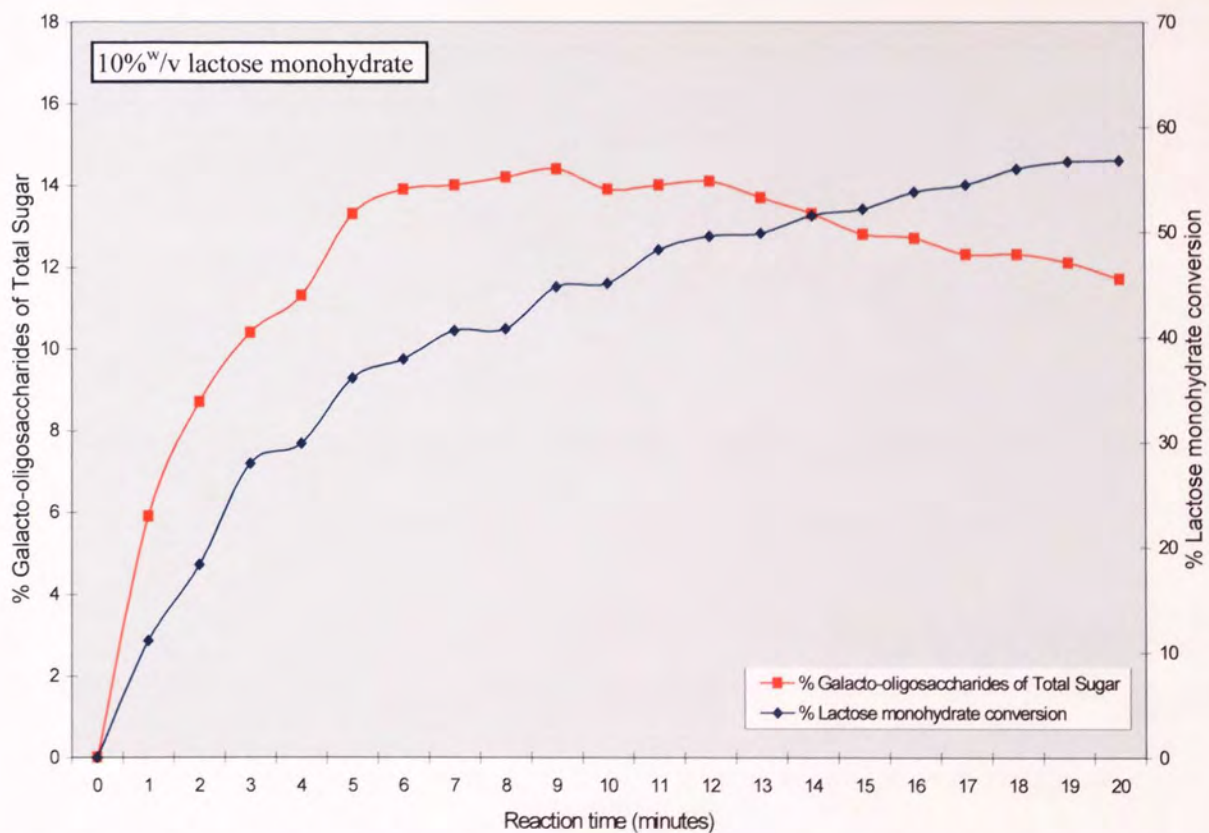
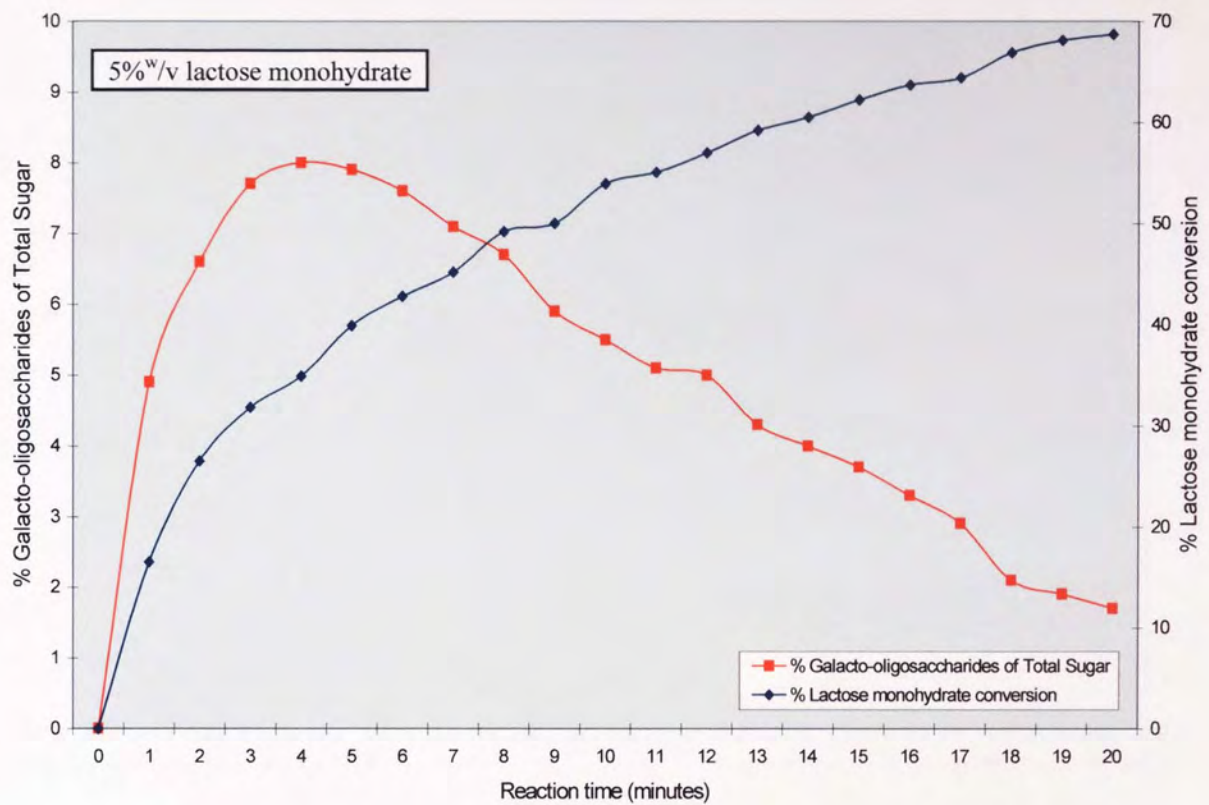


Figure 2.9a. % Galacto-oligosaccharides of Total Sugar and % Lactose monohydrate conversion for soluble Biolactase F (1.25 mg cm^{-3} , 4 U cm^{-3}) stirred-batch reactions performed using 5 and 10%^{w/v} lactose monohydrate, at 40°C.

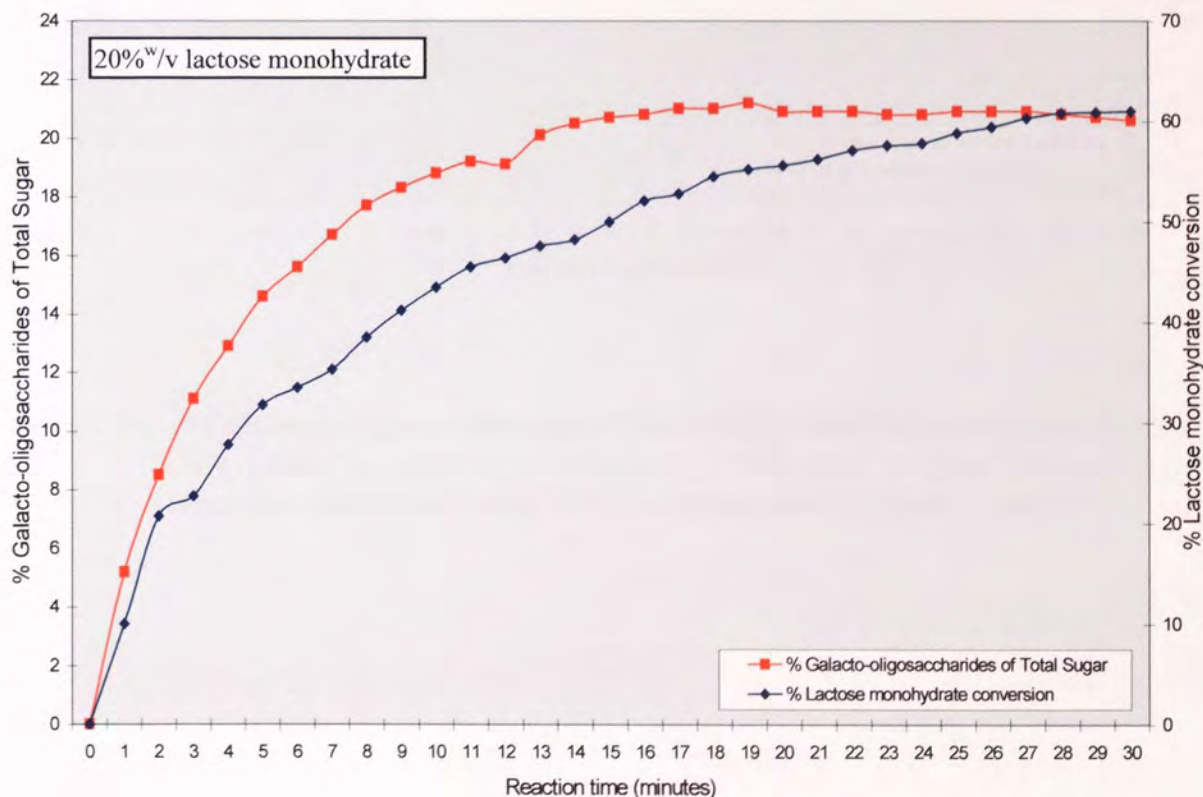
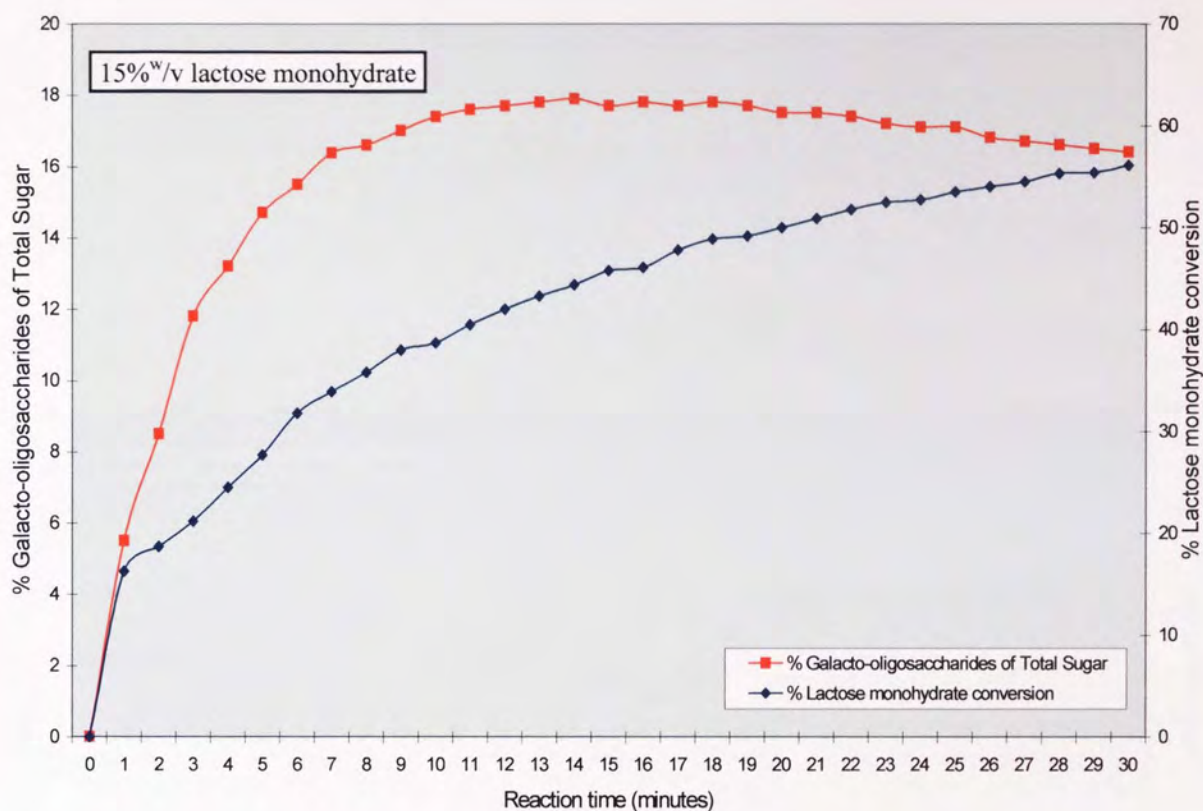


Figure 2.9b. % Galacto-oligosaccharides of Total Sugar and % Lactose monohydrate conversion for soluble Biolactase F (1.25 mg cm^{-3} , 4 U cm^{-3}) stirred-batch reactions performed using 15 and 20%^{w/v} lactose monohydrate, at 40°C.

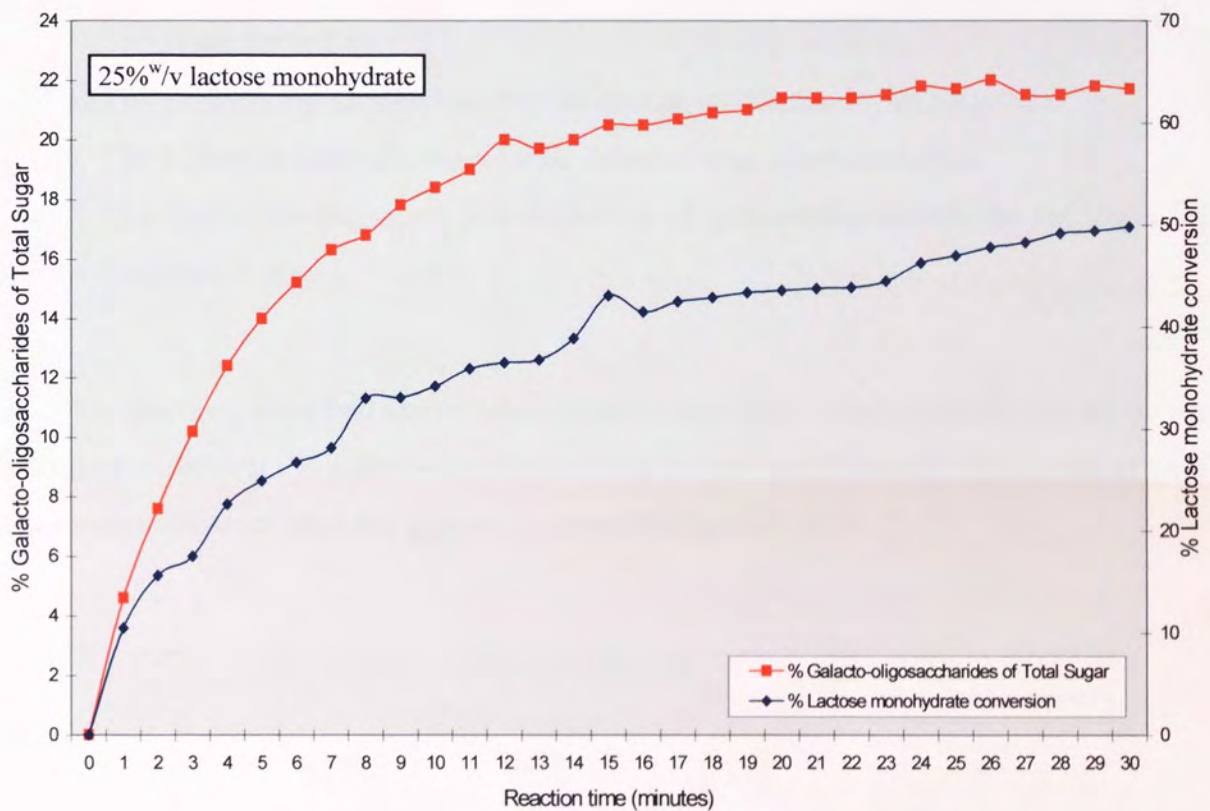


Figure 2.9c. % Galacto-oligosaccharides of Total Sugar and % Lactose monohydrate conversion for soluble Biolactase F (1.25 mg cm^{-3} , 4 U cm^{-3}) stirred-batch reaction performed using 25%^w/v lactose monohydrate, at 40°C.

The results obtained from the stirred-batch reactions performed at 40°C and those obtained for 25°C and 55°C can be summarised as follows:

1. Maximum galacto-oligosaccharide yields are achieved at lactose monohydrate conversions between 40-55%.
2. The higher the initial lactose monohydrate concentration the greater the yield of galacto-oligosaccharide.
3. Similar maximum galacto-oligosaccharide yields were obtained at 25°C, 40°C and 55°C (see Table 2.3).
4. The galacto-oligosaccharides formed consist predominantly of galactose.
5. The highest galacto-oligosaccharide detected was a tetrasaccharide.
6. The higher the degree of polymerisation of galacto-oligosaccharide the lower the yield (tri- > tetra-).

All of the reactions described above were repeated over longer reaction times and the results obtained showed that the galacto-oligosaccharides formed are ultimately hydrolysed to yield galactose and glucose, and this process is shown in Figure 2.10.

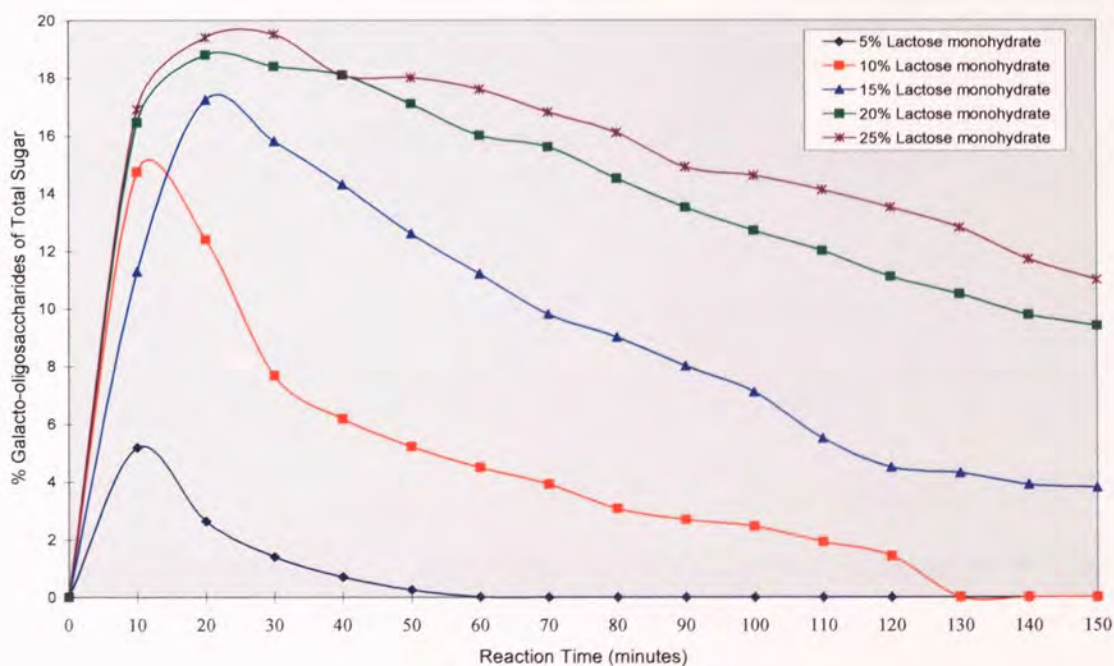


Figure 2.10. The hydrolysis of galacto-oligosaccharide formed during incubation of various initial lactose monohydrate (%^{w/v}) concentrations with β -galactosidase from *Aspergillus oryzae* (1.25 mg cm⁻³, 4 U cm⁻³), at 40°C.

2.4.2.1 Determination of V_{\max} and K_m for soluble β -galactosidase from *Aspergillus oryzae* (Biolactase F)

The results obtained from the stirred-batch reactions performed using soluble β -galactosidase from *Aspergillus oryzae* (Biolactase F) were used to determine the values of V_{\max} and K_m at 40°C. The data used to calculate V_{\max} and K_m was that obtained for glucose, as glucose is the reaction product least affected by the trans-galactosyl activity of the enzyme. The method used was a Lineweaver-Burk plot, or double reciprocal plot and is outlined in Section 2.2.2 and diagrammatically represented in Figure 2.5. The initial velocity, v_0 , was determined for glucose production at various initial lactose monohydrate concentrations, with a fixed enzyme concentration and the reciprocal of the initial velocity was plotted against the reciprocal of initial lactose monohydrate concentration. The graph obtained is presented in Figure 2.11.

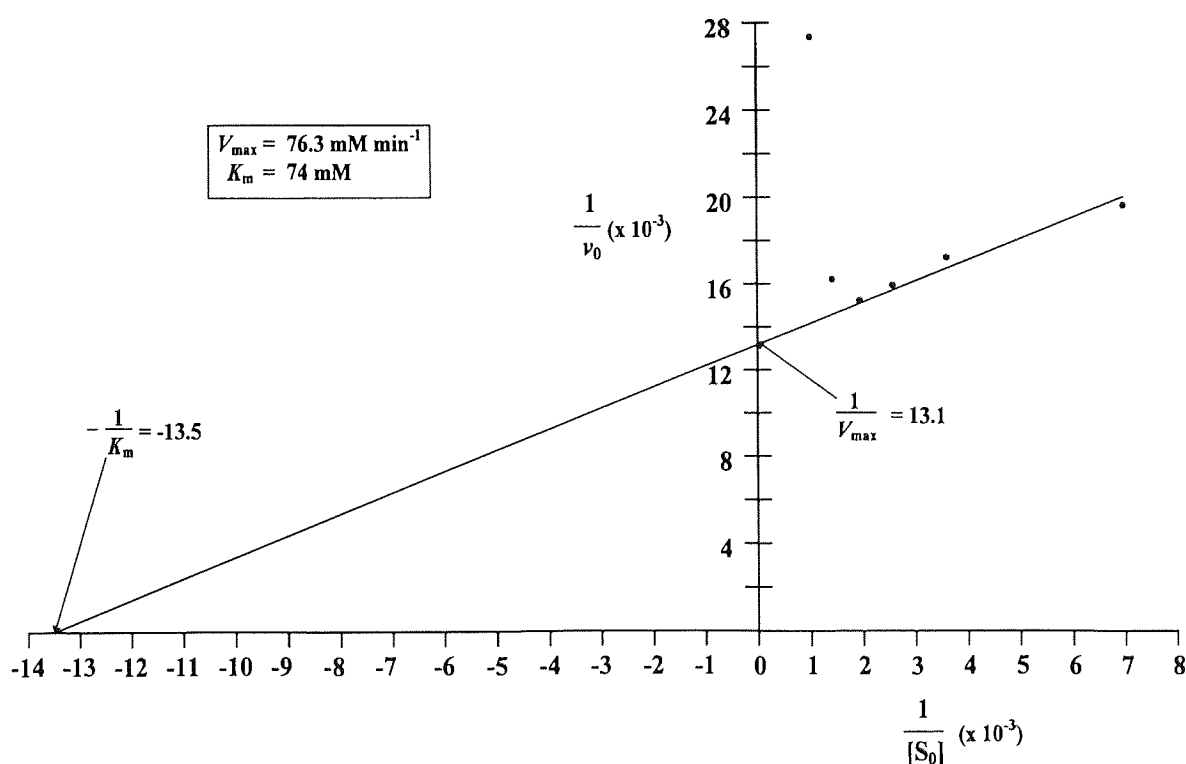


Figure 2.11. Determination of V_{\max} and K_m for soluble Biolactase F using a Lineweaver-Burk, or double reciprocal plot.

The values of V_{\max} and K_m for Biolactase F were determined to be 76.3 mM min^{-1} and 74 mM respectively and these values were similar to those reported in the literature (38,41,43,51).

Figure 2.11 clearly shows that substrate inhibition is taking place at the higher initial lactose monohydrate concentrations, as is shown by the distinctive feature of the highest lactose monohydrate data points curving sharply upward as the $1/v$ axis is approached⁽⁵³⁾. Generally, substrate inhibition occurs when a molecule of the substrate binds to one site on the enzyme and another molecule of the substrate binds to a separate site on the enzyme to form a dead-end complex. This can be regarded as a form of uncompetitive inhibition, with the extra substrate molecule being the inhibitor⁽⁴⁶⁾.

2.4.2.2 Determination of K_i for soluble β -galactosidase from *Aspergillus oryzae* (Biolactase F)

The inhibition constant, K_i , was determined for β -galactosidase from *Aspergillus oryzae* (Biolactase F) using the Dixon Plot method, which is described in Section 2.2.3.1. Stirred-batch reactions were performed using two different lactose monohydrate concentrations, 10 and 15%^{w/v}, and for each substrate concentration either 25mM or 50mM galactose was initially added. The Biolactase F enzyme concentration was fixed (1.25 mg cm⁻³, 4 U cm⁻³) and at timed intervals samples were removed and analysed by HPLC to determine the rate of lactose conversion. Using the Dixon Plot the value of K_i was determined to be 4.3mM (0.0043M).

2.4.3 Stirred-batch reactions performed using glutaraldehyde insolubilised β -galactosidase from *Aspergillus oryzae* (Biolactase F)

Stirred-batch reactions were performed as described in Section 2.4.2, except that glutaraldehyde insolubilised β -galactosidase (Biolactase F) was used. Sufficient insolubilised β -galactosidase was added to give an equivalent activity to that obtained for 1.25 mg cm⁻³ (4 U cm⁻³) of the soluble enzyme. The raw data generated by the HPLC was inserted into a spreadsheet to determine the concentration of the substrate and reaction products, and to monitor the overall mass balance; examples of the type of spreadsheets produced are shown in Appendix A-1. Figure 2.12a shows the % Galacto-oligosaccharides of Total Sugar and % Lactose monohydrate conversion against Reaction time (minutes), for stirred-batch reactions performed using glutaraldehyde insolubilised β -galactosidase incubated with initial lactose monohydrate concentrations of 5 and 10%^{w/v}. Figure 2.12b

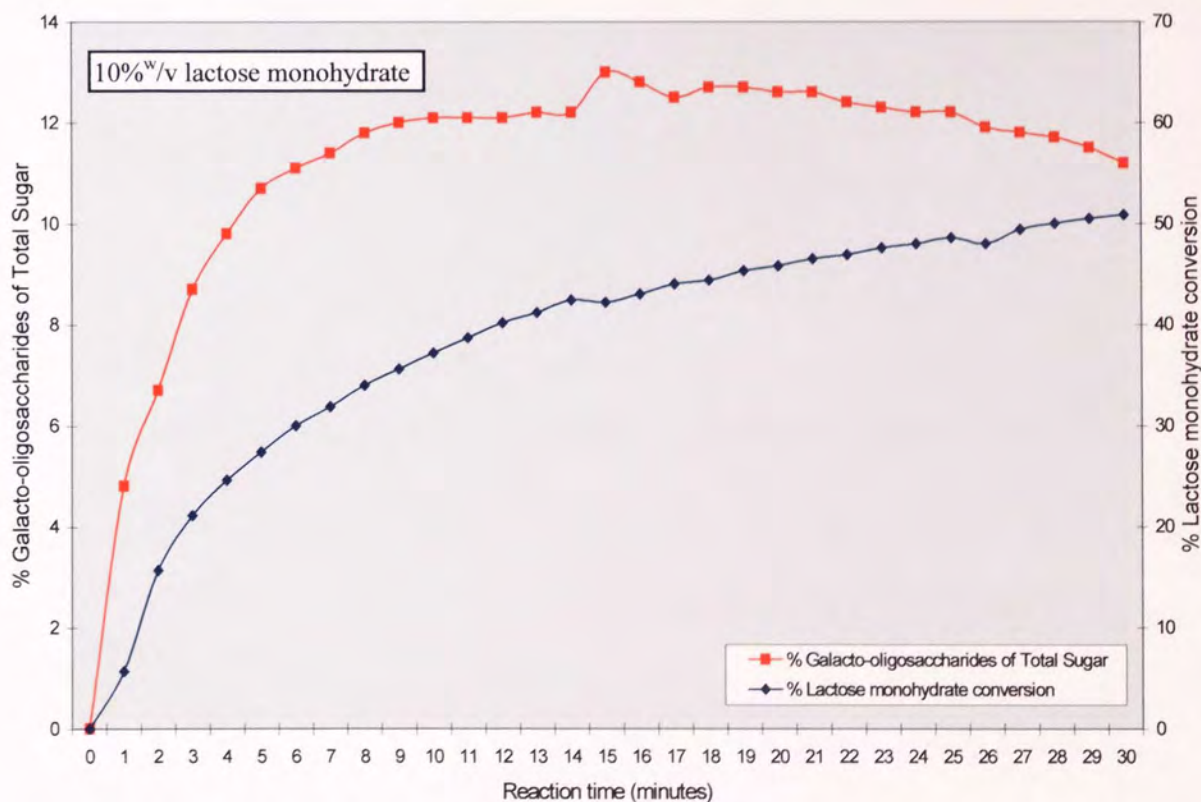
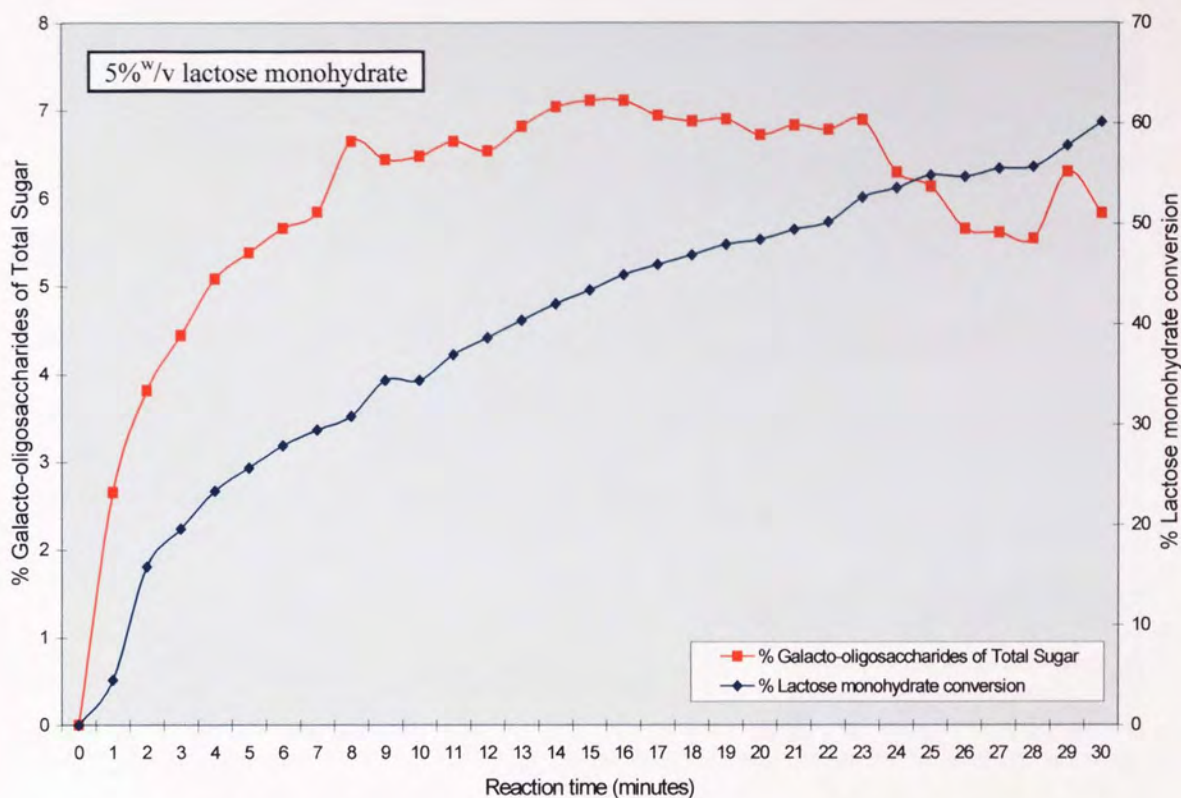


Figure 2.12a. % Galacto-oligosaccharides of Total Sugar and % Lactose monohydrate conversion for insolubilised Biolactase F (1.25 mg cm^{-3} , 4 U cm^{-3}) stirred-batch reactions performed using 5 and 10%^{w/v} lactose monohydrate, at 40°C.

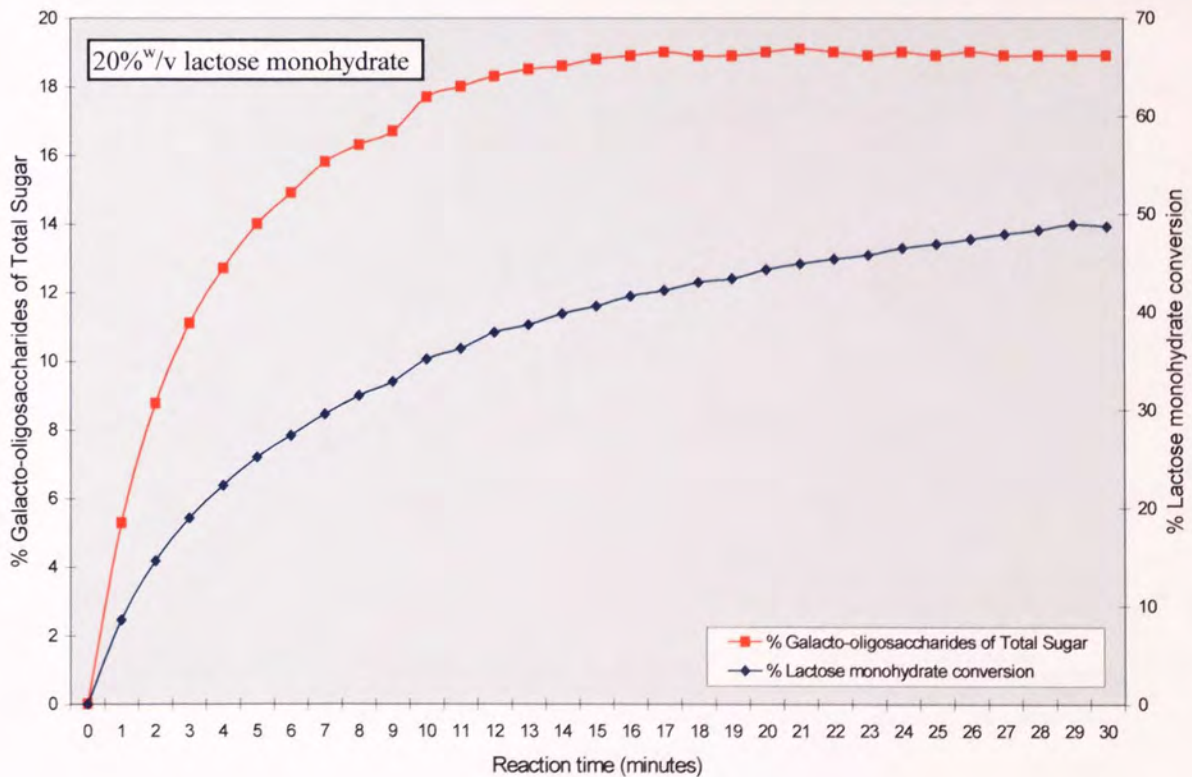
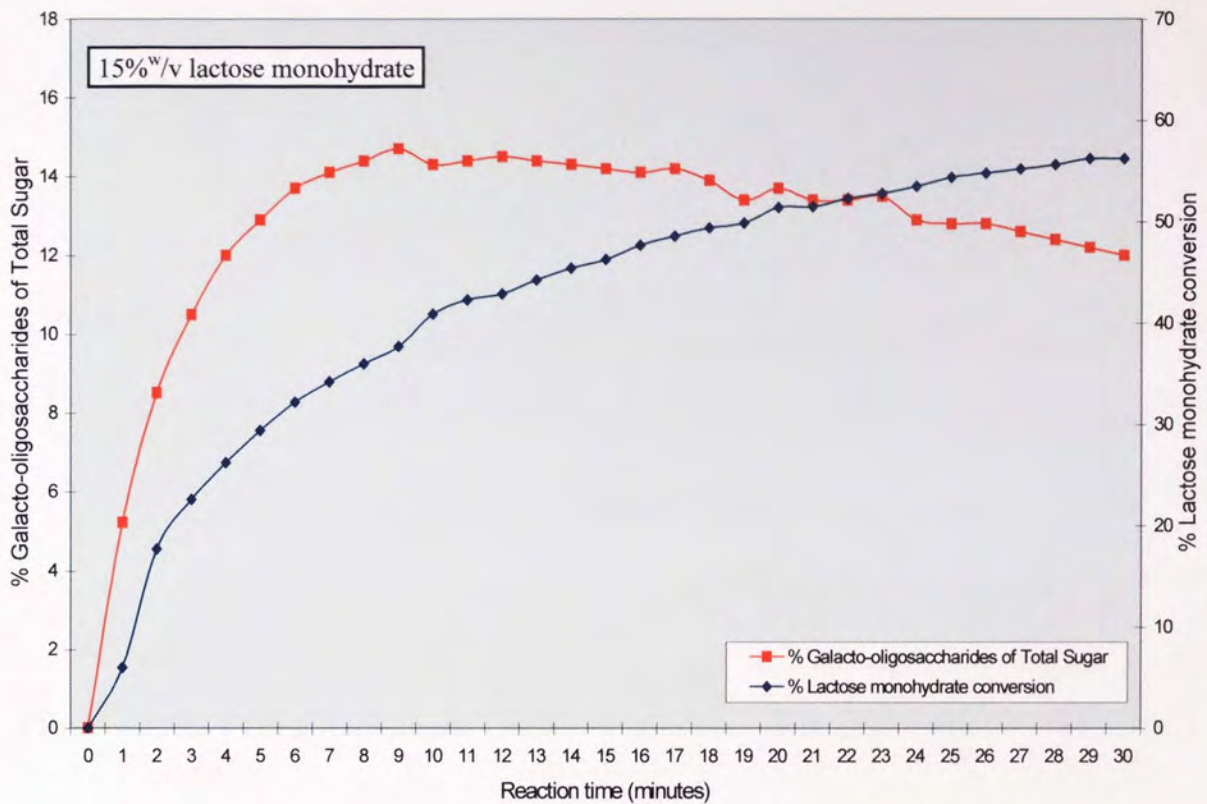


Figure 2.12b. % Galacto-oligosaccharides of Total Sugar and % Lactose monohydrate conversion for insolubilised Biolactase F (1.25 mg cm^{-3} , 4 U cm^{-3}) stirred batch reactions performed using 15 and 20%^{w/v} lactose monohydrate, at 40°C.

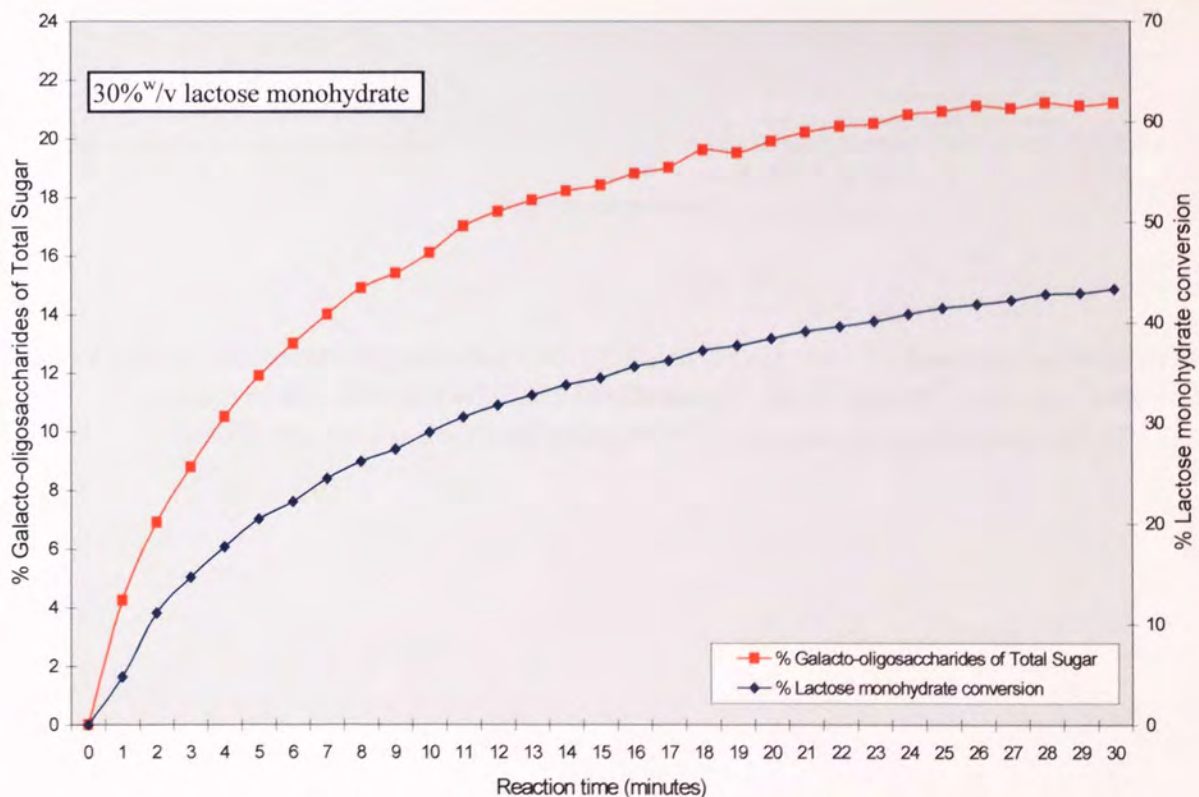
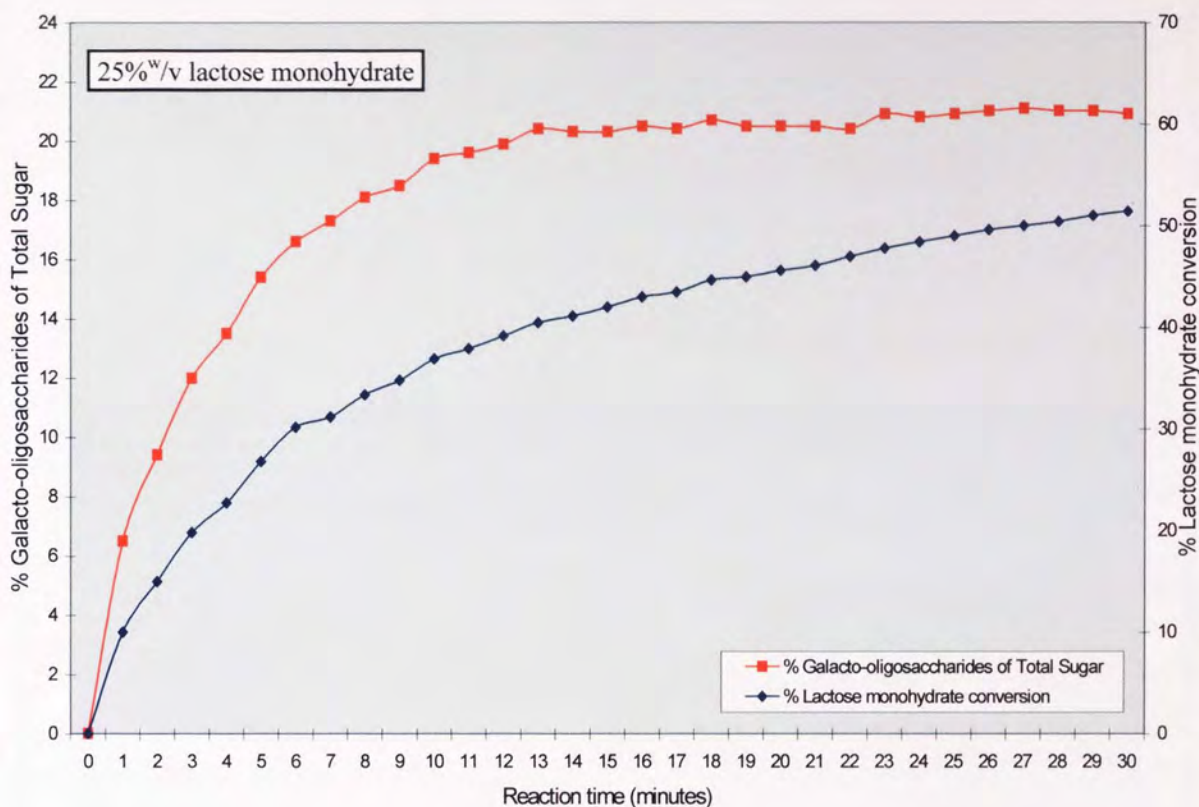


Figure 2.12c. % Galacto-oligosaccharides of Total Sugar and % Lactose monohydrate conversion for insolubilised Biolactase F (1.25 mg cm^{-3} , 4 U cm^{-3}) stirred-batch reactions performed using 25 and 30%^{w/v} lactose monohydrate, at 40°C.

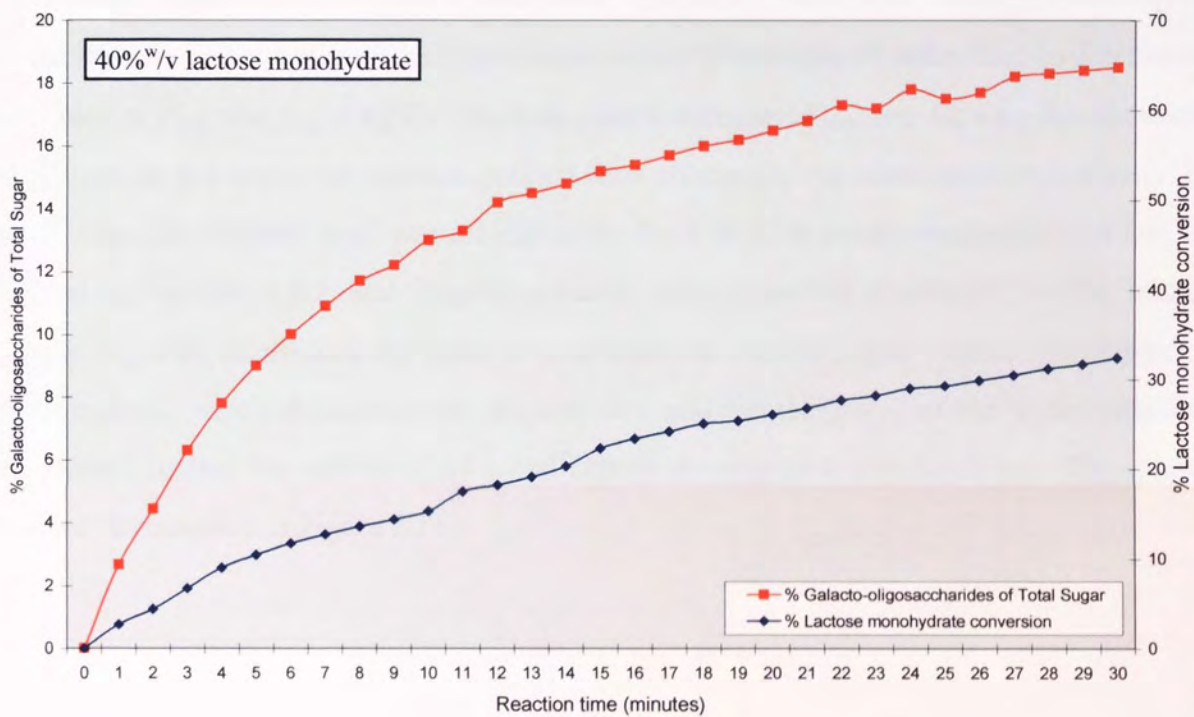


Figure 2.12d. % Galacto-oligosaccharides of Total Sugar and % Lactose monohydrate conversion for insolubilised Biolactase F (1.25 mg cm^{-3} , 4 U cm^{-3}) stirred-batch reaction performed using $40\% \text{ w/v}$ lactose monohydrate, at 40°C .

shows the results obtained for lactose monohydrate concentrations of 15 and 20%^{w/v}, Figure 2.12c shows the results obtained for 25 and 30%^{w/v} and Figure 2.12d shows the results for 40%^{w/v}.

2.4.3.1 Determination of V_{max} and K_m for glutaraldehyde insolubilised β -galactosidase from *Aspergillus oryzae* (Biolactase F)

The results obtained from the stirred-batch reactions performed using glutaraldehyde insolubilised β -galactosidase from *Aspergillus oryzae* (Biolactase F) were used to determine the values of V_{max} and K_m at 40°C. The data used to calculate V_{max} and K_m was that obtained for glucose, as glucose is the reaction product least affected by the trans-galactosyl activity of the enzyme. The method used was a Lineweaver-Burk plot, or double reciprocal plot and is outlined in Section 2.2.2 and diagrammatically represented in Figure 2.5. The initial velocity, v_0 , was determined for glucose production at various initial lactose monohydrate concentrations, with a fixed enzyme concentration and the reciprocal of the initial velocity was plotted against the reciprocal of initial lactose monohydrate concentration. The graph obtained is presented in Figure 2.13.

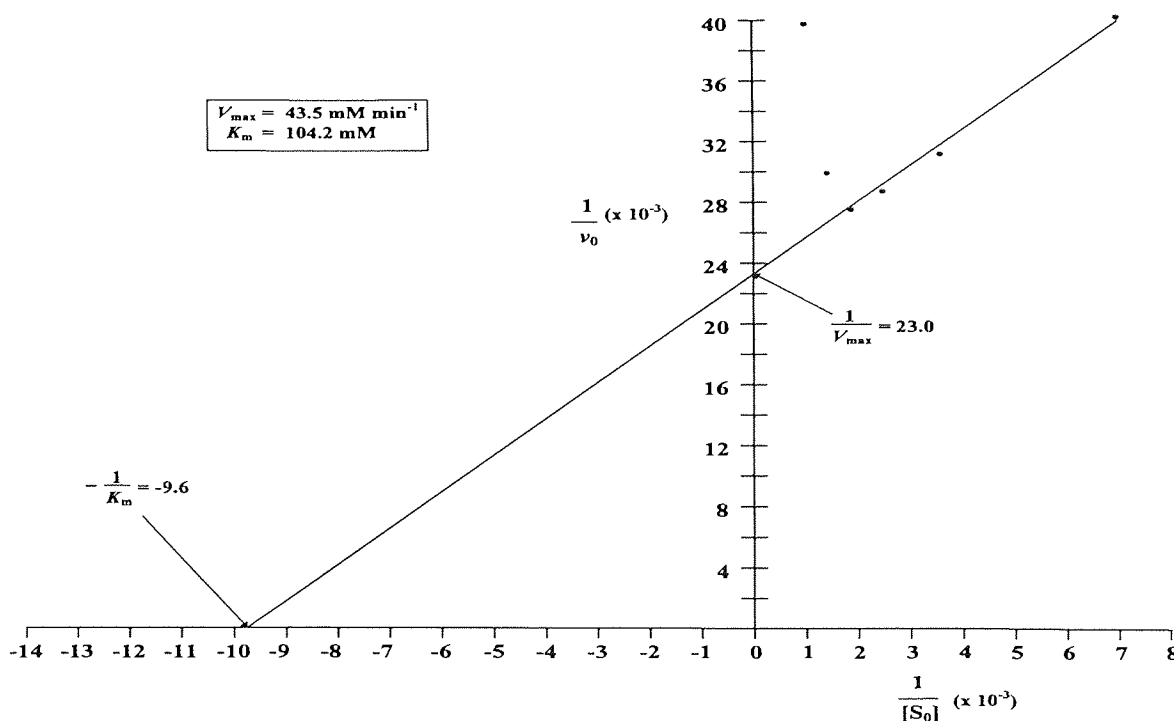


Figure 2.13. Determination of V_{max} and K_m for glutaraldehyde insolubilised Biolactase F using a Lineweaver-Burk, or double reciprocal plot.

The values of V_{\max} and K_m for glutaraldehyde insolubilised Biolactase F were determined to be 43.5 mM min^{-1} and 104 mM respectively. Figure 2.13 clearly shows that substrate inhibition is taking place, which is demonstrated by the upward curvature of the higher substrate concentration data points as the $1/v$ axis is approached.

2.4.3.2 Determination of K_i for glutaraldehyde insolubilised β -galactosidase from *Aspergillus oryzae* (Biolactase F)

The inhibition constant, K_i , was determined for glutaraldehyde insolubilised β -galactosidase from *Aspergillus oryzae* (Biolactase F) using the Dixon Plot method, which is described in Section 2.2.3.1. Stirred-batch reactions were performed using two different lactose monohydrate concentrations, 10 and 15%^{w/v}, and for each substrate concentration either 25mM or 50mM galactose was initially added. The insolubilised Biolactase F enzyme concentration was fixed (a soluble enzyme equivalent of 1.25 mg cm^{-3} , 4 U cm^{-3}) and at timed intervals samples were removed and analysed by HPLC to determine the rate of lactose conversion. Using the Dixon Plot the value of K_i was determined to be 2.5mM (0.0025M).

2.4.4 Comparison of the results obtained from soluble and glutaraldehyde insolubilised β -galactosidase stirred-batch reactions

A comparison of both the % Galacto-oligosaccharides of Total Sugar and the % Lactose monohydrate conversion for soluble β -galactosidase and glutaraldehyde insolubilised β -galactosidase shows:

1. The rate of lactose monohydrate conversion is slower for the insolubilised β -galactosidase.
2. For a given % Lactose monohydrate conversion the % Galacto-oligosaccharides of Total Sugar is slightly lower for the insolubilised β -galactosidase.
3. The insolubilisation process does not greatly affect the hydrolytic and trans-galactosyl activity of β -galactosidase from *Aspergillus oryzae* (Biolactase F).

Table 2.4 shows a comparison of the experimentally obtained values for V_{\max} , K_m and K_i for soluble and glutaraldehyde insolubilised Biolactase F.

Biolactase F	Kinetic parameter		
	V_{\max} (mM min ⁻¹)	K_m (mM)	K_i (mM)
Soluble	76.3	74	4.3
Insolubilised	43.5	104	2.5

Table 2.4. Comparison of the experimentally determined kinetic parameters for soluble and insolubilised β -galactosidase (Biolactase F).

The soluble and insoluble β -galactosidase V_{\max} values presented in Table 2.4 show a lower V_{\max} value for the insolubilised enzyme and this may be possibly explained by the diffusion and partition effects resulting from the insolubilisation process. The lower V_{\max} value correlates with the slightly slower rate of lactose monohydrate conversion and galacto-oligosaccharide formation obtained with the insolubilised enzyme. A comparison of the maximum galacto-oligosaccharide yields obtained using various initial lactose monohydrate concentrations for soluble and insolubilised β -galactosidase, at 40°C, is shown in Figure 2.5.

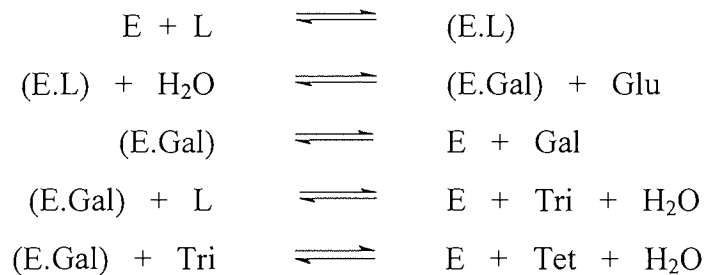
State of enzyme	Initial Lactose Monohydrate Concentration (% ^w /v)				
	5	10	15	20	25
Soluble	8.0%	14.4%	17.9%	21.2%	22.0%
Insolubilised	7.1%	12.9%	14.5%	19.1%	21.1%

Table 2.5. Comparison of the maximum galacto-oligosaccharide yields obtained during stirred-batch reactions using soluble and insolubilised β -galactosidase (1.25 mg cm⁻³, 4 U cm⁻³) performed using various initial lactose monohydrate concentrations, at 40°C.

Table 2.4 shows that the values obtained for K_m and K_i for both the soluble and insolubilised enzyme are comparatively close, which confirms that the insolubilisation process does not adversely affect the catalytic action of the enzyme.

2.4.5 Kinetic modelling of lactose hydrolysis

Producing a kinetic model for the hydrolysis of lactose by β -galactosidase is hindered by the complexity of the reaction. The reaction is complicated by the formation of galacto-oligosaccharides, which are intermediate compounds that are ultimately hydrolysed to yield glucose and galactose. The rate of galacto-oligosaccharide formation and its yield are dependent on the initial lactose concentration, the complete hydrolysis of lactose to yield glucose and galactose being favoured by low initial lactose concentrations. Increasing the complexity further is the variation in the inhibitory effect of galactose due to mutarotation. The rate of mutarotation depends upon the specific reaction conditions and the origin of the particular β -galactosidase used ^(21,44). Based on research performed by Prenosil, Strucker and Bourne ⁽³¹⁾, and Yang and Tang ⁽³⁰⁾ a simplified reaction scheme for the hydrolytic and trans-galactosyl activity of β -galactosidase can be proposed and is as follows:



where: E = enzyme
 L = lactose
 Gal = galactose
 Glu = glucose
 Tri = trisaccharide
 Tet = tetrasaccharide

The reaction scheme presented above ignores the effects of mutarotation and only considers galacto-oligosaccharides up to tetrasaccharides, because higher saccharides were not detected during the stirred-batch experiments performed as part of this research. Flaschel, Raetz and Renken ⁽²¹⁾ produced a model for lactose hydrolysis which considered mutarotation, but ignored galacto-oligosaccharide formation. In 1974, Weetall, Havewala, Pitcher, Detar, Vann and Yaverbaum ⁽⁵⁴⁾ produced a model for lactose hydrolysis in batch reactions based on Michaelis-Menten kinetics with competitive inhibition. The effects of mutarotation and galacto-oligosaccharide formation were ignored. This model was used to predict the hydrolysis of lactose contained in acid whey and stirred-batch reactions were performed using fungal β -galactosidase (Lactose-M, Miles Laboratories, New York) to compare with the calculated model values. The acid whey contained 15-20% solids of which 70-80% was lactose, thus giving a possible lactose range of 10.5-16%.

The expression used by Weetall, Havewala, Pitcher, Detar, Vann and Yaverbaum ⁽⁵⁴⁾ is derived as follows using Equation (2.15), which may be written as:

$$\frac{-d[L]}{dt} = \frac{V_{\max} [L]}{[L] + K_m \left(1 + \frac{[Gal]}{K_i} \right)} \quad (2.20)$$

where: $[L]$ = lactose concentration (mol dm^{-3}).

$[Gal]$ = galactose concentration (mol dm^{-3}).

Assuming $[L]_0 - [L] = [Gal]$

and $[L] = [L]_0$ at $t = 0$.

Separating the variables, $[L]$ and t , substituting for $[Gal]$ and then integrating gives:

$$V_{\max} \int_0^t dt = - \int_{[L]_0}^{[L]} \left(1 + \frac{K_m}{[L]} + \frac{K_m}{K_i} \cdot \frac{[L]_0}{[L]} - \frac{K_m}{K_i} \right) d[L] \quad (2.21)$$

which is expressed as:

$$V_{\max} \cdot t = \left(1 - \frac{K_m}{K_i} \right) \cdot ([L]_0 - [L]) + \left(\frac{K_m}{K_i} \cdot [L]_0 + K_m \right) \cdot \ln \frac{[L]_0}{[L]} \quad (2.22)$$

The expression (2.22) may be used to estimate kinetic constants or to approximate lactose conversion in a batch reactor of reaction time t , having fixed the enzyme concentration $[E]_0$.

Using the kinetic parameters obtained for soluble and insoluble β -galactosidase from *Aspergillus oryzae* an Excel spreadsheet was constructed based on Equation (2.22). The spreadsheet was used to calculate the theoretical values of lactose monohydrate hydrolysis, for reactions performed using various initial lactose monohydrate concentrations incubated with soluble and insolubilised β -galactosidase from *Aspergillus oryzae* at 40°C, and using a fixed enzyme concentration of 1.25 mg cm⁻³ (4 U cm⁻³). The kinetic parameters K_m and K_i obtained experimentally for the soluble and insolubilised enzyme were inserted into the appropriate spreadsheets. In the spreadsheets, the V_{\max} values used were based upon glucose formation results obtained from the stirred-batch reactions. Based on glucose formation, the V_{\max} value for soluble and insolubilised β -galactosidase from *Aspergillus oryzae* was 76.3 and 43.5 mM min⁻¹ respectively. Examples of the spreadsheet are presented in Appendix A-2. The theoretical values calculated were compared to the actual results obtained from the stirred-batch reactions, described in 2.4.2 and 2.4.3. Figure 2.14 shows a comparison of the theoretical and actual lactose monohydrate conversions for soluble β -galactosidase from *Aspergillus oryzae* using; initial lactose monohydrate concentrations of 5 and 20%^{w/v}, an enzyme concentration of 1.25 mg cm⁻³ (4 U cm⁻³), and a reaction temperature of 40°C. Figure 2.15 shows a comparison of the theoretical and actual lactose monohydrate

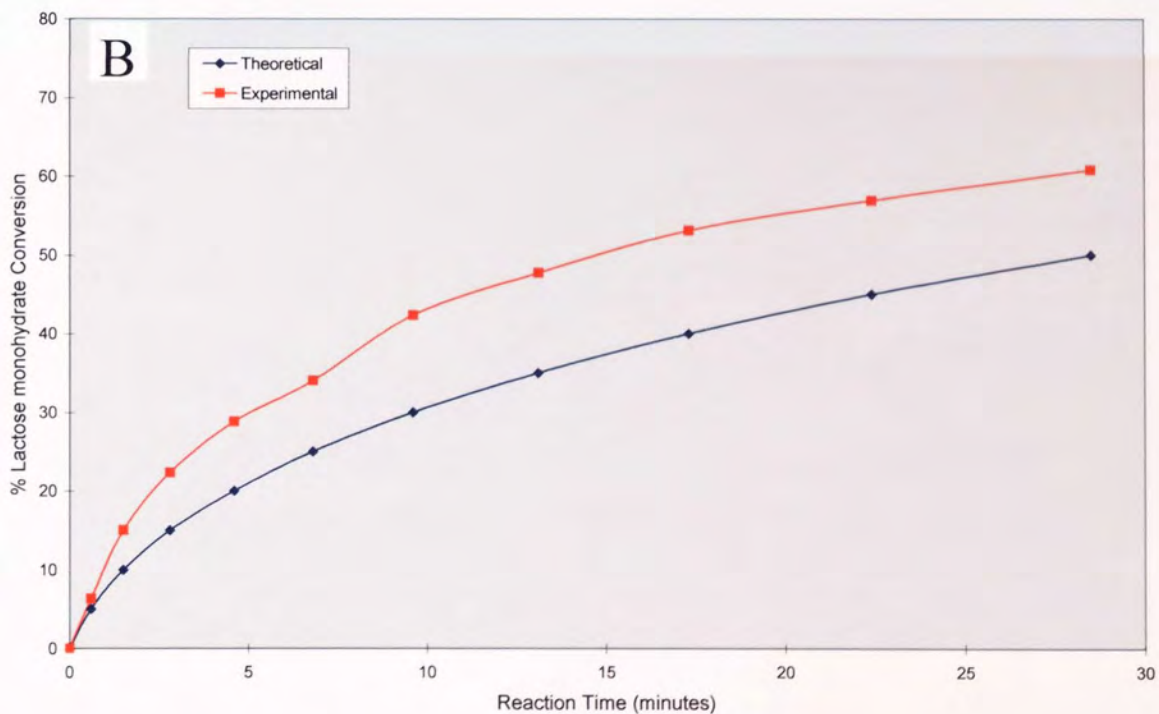
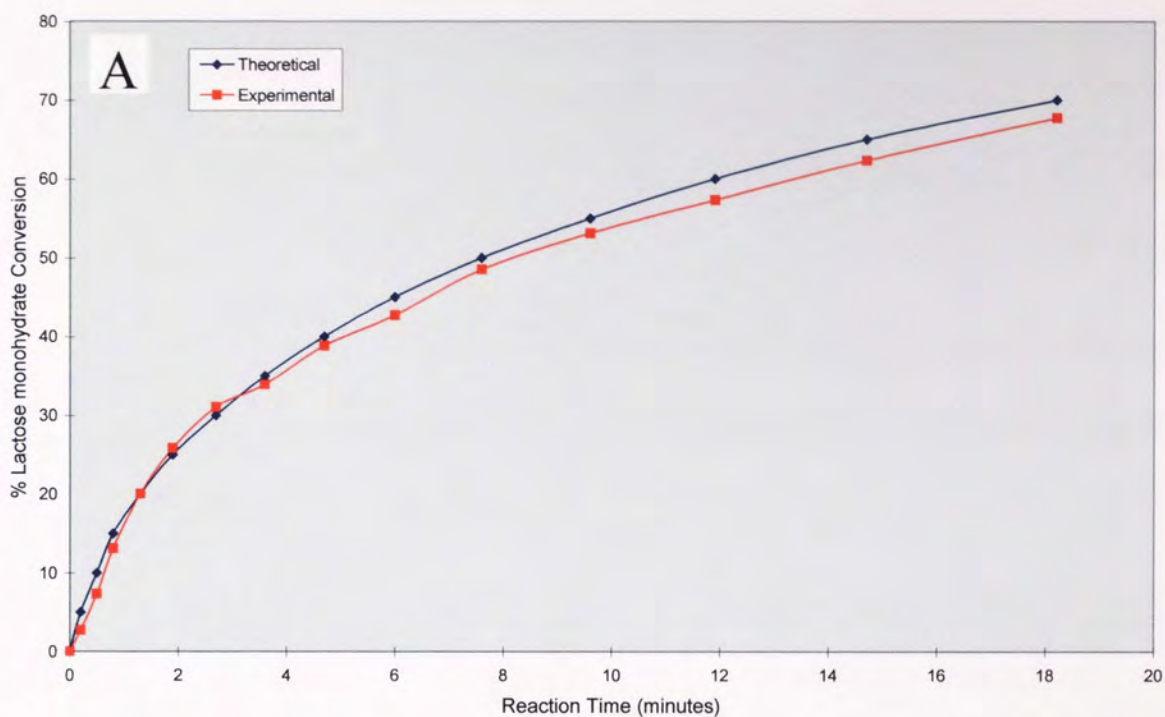


Figure 2.14. A comparison of theoretical and experimentally determined % lactose monohydrate conversion for stirred-batch reactions performed using soluble β -galactosidase from *Aspergillus oryzae* (1.25 mg cm^{-3} , 4 U cm^{-3}) at 40°C . Graph A is with an initial lactose monohydrate concentration of $5\% \text{ w/v}$ and Graph B is with an initial lactose monohydrate concentration of $20\% \text{ w/v}$.

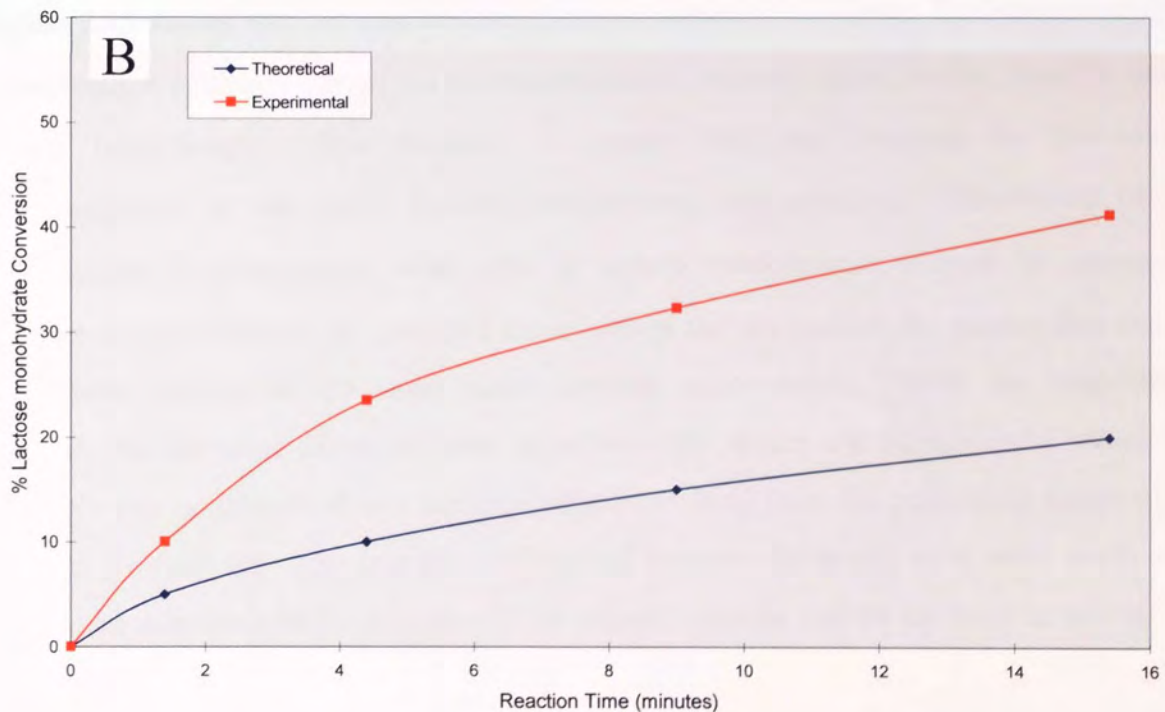
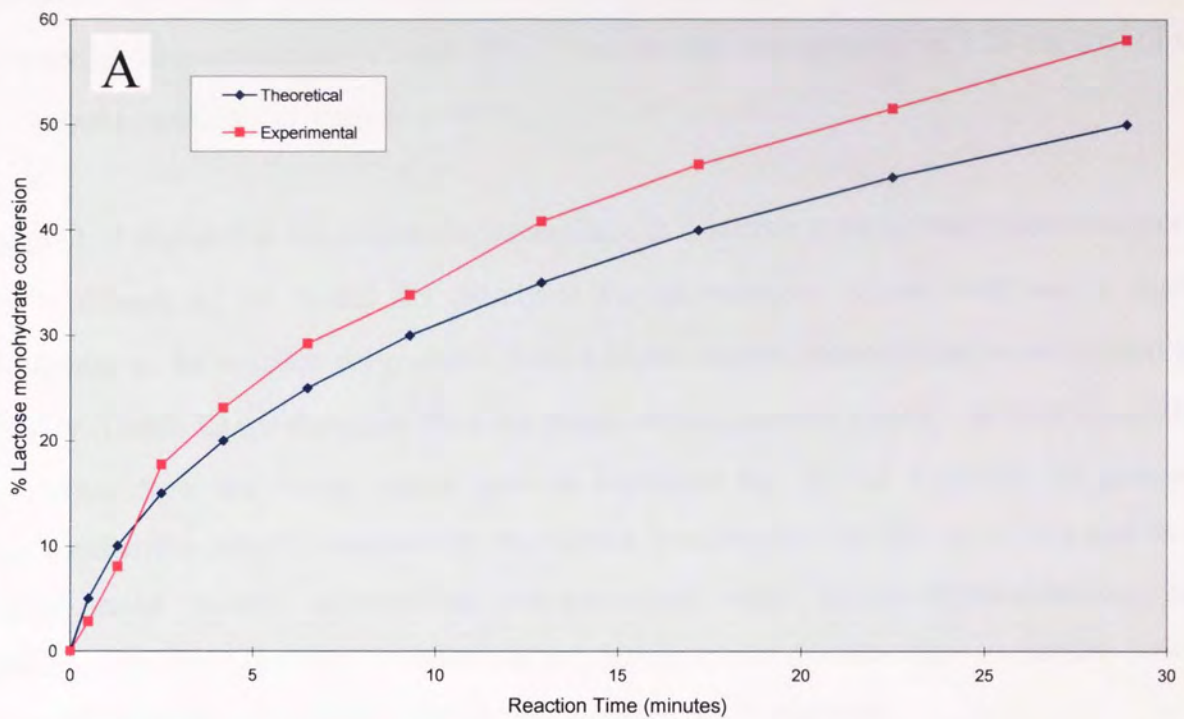


Figure 2.15. A comparison of theoretical and experimentally determined % lactose monohydrate conversion for stirred-batch reactions performed using insolubilised β -galactosidase from *Aspergillus oryzae* (1.25 mg cm^{-3} , 4 U cm^{-3}) at 40°C . Graph A is with an initial lactose monohydrate concentration of $5\% \text{ w/v}$ and Graph B is with an initial lactose monohydrate concentration of $20\% \text{ w/v}$.

conversions for insolubilised β -galactosidase from *Aspergillus oryzae* using; initial lactose monohydrate concentrations of 5 and 20%^{w/v}, an enzyme concentration of 1.25 mg cm⁻³ (4 U cm⁻³), and a reaction temperature of 40°C.

Figure 2.14 shows that for soluble β -galactosidase at a lactose monohydrate concentration of 5%^{w/v} (Graph A) the model fits closely to the experimental values, with only a slight divergence as the reaction progresses. With a higher lactose monohydrate concentration of 20%^{w/v} (Graph B) the deviation from the model values is much greater. In both cases, the divergence from the model values may be explained by; (a) the formation of galacto-oligosaccharides which compete with the lactose monohydrate for the active site and with higher initial lactose monohydrate concentrations more galacto-oligosaccharides are produced, (b) the incorporation of lactose monohydrate into galacto-oligosaccharides during trans-galactosylation, and (c) the effects of mutarotation of galactose.

Figure 2.15 shows that for insolubilised β -galactosidase at the lower lactose monohydrate concentration of 5%^{w/v} (Graph A) the experimentally derived values deviate from the model almost immediately. This deviation is greater than that observed for the soluble β -galactosidase at the same lactose monohydrate concentration. Incubation of the insolubilised β -galactosidase with 20%^{w/v} lactose monohydrate (Graph B) shows the greatest divergence from the predicted model values and is considerably greater than that for the soluble enzyme at the same initial substrate concentration. With the insolubilised enzyme, the increased degree of poor fit between the model and experimental values was probably due to diffusional and partition effects resulting from the particulate nature of the enzyme. To fully accommodate these effects and improve the model more work needs to be performed to investigate the structure of the enzyme particles and the microenvironment.

2.4.5.1 Preliminary study of insolubilised β -galactosidase particles

Samples of the insolubilised β -galactosidase particles were observed using a Cambridge Stereoscan Model 90 Scanning Electron Microscope (SEM) (Cambridge Instruments, Cambridge, UK) to determine the morphology and size range of the particles. The results obtained are shown in Figure 2.16. Figure 2.16 (Photographs A and B) shows that the

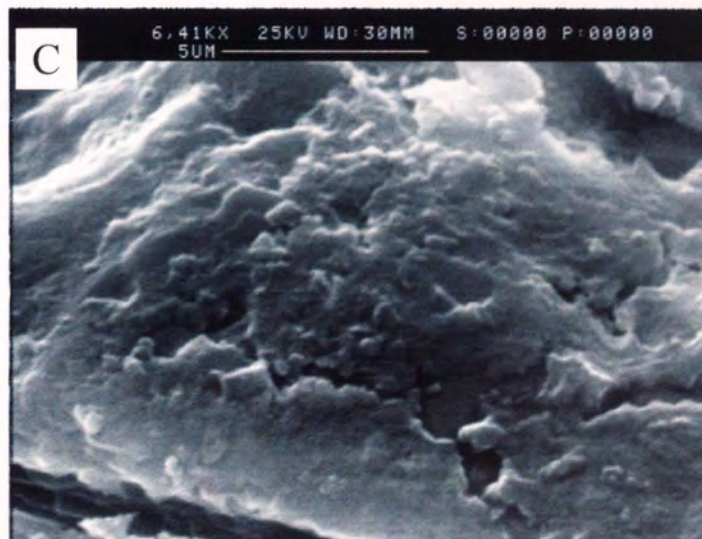
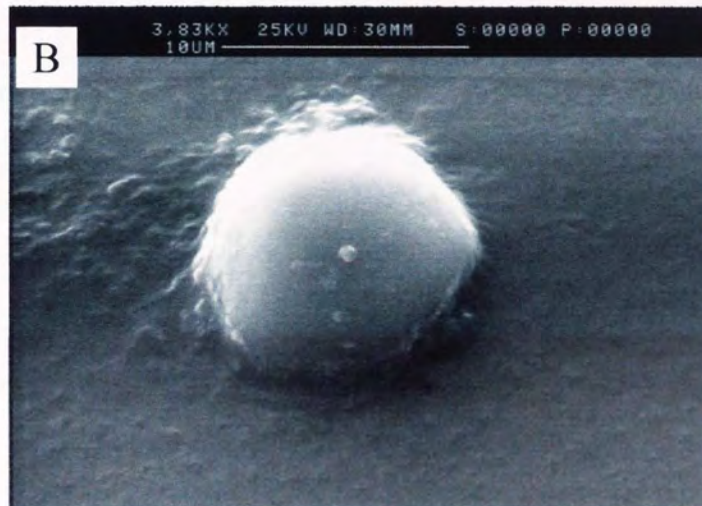


Figure 2.16. Scanning electron microscope images of insolubilised β -galactosidase particles. Photograph A shows a cluster of particles, Photograph B is a magnified single particle and Photograph C shows the surface texture.

particles were comparatively spherical in shape. The particles observed ranged in size from approximately 10 to 30 μ m and confirmed the results obtained using the laser particle sizer (see Figure 5.19). At a magnification of 6 410x the surface texture of a particle (Photograph C) showed no obvious porous structure and this indicates that diffusional limitations due to the movement of substrate/product/s through the particle is minimal. The almost spherical shape of the particles would seem to show that they are formed during the insolubilisation process and the mechanical grinding process just re-disperses the agglomerated particles.

Drying experiments were performed to determine the approximate water content of the insolubilised particles. A suspension of insolubilised β -galactosidase particles was centrifuged at 13 000 r.p.m to form a densely pelleted material at the bottom of the centrifuge tube, so that the majority of the liquid present was contained in the supernatant. The supernatant was decanted and the surface of the pelleted material was gently blotted using absorbent paper towel. The centrifuge tube containing the pelleted material was weighed and then dried using a laboratory air dryer at \sim 35-40 $^{\circ}$ C until constant weight was achieved. The water content of the pelleted material was calculated to be 83.5%. This high water content value would indicate that the particles may exist as a hydrogel, which is a water-rich colloidal system where the insolubilised particle structure consists of chemically-linked colloidal particles⁽⁵⁵⁾. Typically, colloidal particles are defined as particles with a size ranging from 1 to 500 nm in diameter⁽⁵⁶⁾. Although, the resolution limit of a scanning electron microscope is \sim 6nm it was not possible to achieve this with the insolubilised particles due to the focused electron beam vaporising the sample⁽⁵⁷⁾.

3.0 CENTRIFUGAL STUDIES USING SOLUBLE β -GALACTOSIDASE

In this chapter, the historical development of the centrifuge is discussed. The theoretical principles upon which centrifugation and sedimentation theory are based will be described. The different types of centrifuge, and their uses are discussed. The centrifugal separation technique known as normal rate separation is described. Centrifugal studies performed with soluble, free β -galactosidase, and using a modified version of the normal rate separation technique are presented.

3.1 Development of the centrifuge

The basic principles upon which centrifugation and sedimentation theory are based originate from Stokes' Law, which was published in 1856^(58,59). Stokes' equation was initially used by physicists to calculate the radius of a spherical droplet sedimenting under the influence of the earth's gravitational field. Centrifugation is a technique designed to utilise centrifugal forces, which exceed that of the force of gravity, to speed up the sedimentation rate of the particles, allowing faster separation, and analysis of small particles. In terms of centrifugation, the word particle describes all of the materials that are present in a sample, except for the medium in which the material is suspended⁽⁵⁹⁾.

The application of centrifugal forces to effect separation was first used on an industrial-scale over 120 years ago. The industries predominantly associated with this early use were those involved with the manufacture of sugar and milk products. In 1877, the Swedish engineer DeLaval invented the first continuous centrifugal separator, which was designed to separate cream from milk⁽⁶⁰⁾. The types of centrifugal separators increased as new applications were discovered. Rapid developments in industrial centrifuges occurred during World War II, driven by research in the field of isotope separation and enrichment. Today, centrifuges are widely used in the oil, chemical, biochemical, pharmaceutical and food industries^(3,60,61,62). In the oil industry centrifuges are used on oil platforms to remove salt water and other contaminants from lubricating oils. The pharmaceutical industry utilises centrifuges to recover products such as penicillin from solvents. The food industry use centrifuges to remove impurities from coffee, tea and fruit juices, as well as extracting edible proteins from both animal and vegetable products^(60,61). The centrifuge is also used for environmentally beneficial applications, such as sludge dewatering and heavy metal removal from wastewater

⁽⁶⁴⁾. Industrial centrifugal separators may be required to process tonnes of materials under an extreme range of operating conditions, such as temperatures from -62°C to 230°C ⁽⁶⁰⁾. Industrial centrifuges have become an integral part of product recovery and downstream processing.

The laboratory-scale centrifuge was first used as an analytical tool by Dumansky in 1913 ⁽⁵⁸⁾. He attempted to compare particle size determinations obtained using a laboratory centrifuge, with those obtained using an optical microscope. This proved unsuccessful due to the non-ideal sedimentation of the particles produced by the mechanical limitations of the centrifuge. During the 1920's Svedberg and Pedersen, researchers at the University of Uppsala in Sweden, were responsible for improving the design of laboratory centrifuges ^(58,60,65). Their improvements allowed higher centrifugal forces to be achieved, reduced the level of vibration during use, and incorporated the ability to control operational temperature. In 1923, they developed a small optical centrifuge which was capable of centrifugal forces equivalent to 150 times that of the force of gravity, or 150g. This type of centrifuge is now known as an analytical centrifuge, as distinct from a preparative centrifuge which is designed solely for separation. The inclusion of an optical system allowed the progress of sedimenting particles to be recorded on film, using either changes in refractive index or optical absorption to visualise the boundaries of sedimenting particles ⁽⁵⁸⁾.

The application of the laboratory centrifuge in the field of biochemistry, which required the separation and analysis of biological macromolecules such as proteins, led to rapid development. By 1933 certain centrifuges were capable of producing centrifugal forces up to 19 000g, and by 1934 centrifugal forces reaching 900 000g had been achieved, although this equipment usually exploded after several experimental runs due to mechanical failure ⁽⁵⁸⁾. By the 1970's the laboratory centrifuge had reached its zenith for the separation and analysis of biological macromolecules ⁽⁶⁵⁾, with certain centrifuges capable of attaining 500 000g ^(57,66). Over the past 20 years the introduction of new methods for defining the characteristics of macromolecules such as; gel and zonal electrophoresis, laser particle sizing, chromatographic systems linked to mass spectrometry (GC-MS, LC-MS), and chromatographic techniques have reduced the use of the centrifuge as an analytical tool. Although the popularity of the analytical centrifuge has declined, the use of the preparative centrifuge for the separation of materials has increased.

3.2 Principles and practices of centrifugation

3.2.1 Introduction

In a gravitational field of force, a particle suspended in a liquid medium possessing a lower density tends to migrate through the fluid in a downward direction. For a given medium and fixed external conditions, the rate of this particle sedimentation depends upon its mass, shape, size, the difference in density that exists between the particle and the liquid medium, and the viscosity of the liquid. Sedimentation does not occur if the density of the particles is lower than that of the liquid medium, or if the transport of the particles is counteracted by the effects of back diffusion. Back diffusion results from the concentration gradient produced by the partial sedimentation of the particles into the medium. The effects of back diffusion can be overcome by subjecting the medium containing the particles to fields of force exceeding that of gravity. Centrifuges are capable of generating very high gravitational fields, which enables the particles to sediment through the medium. Centrifuges achieve high gravitational forces by rapidly rotating the particles around a fixed axis, generating a relative centrifugal field or RCF, which is designated as the 'g' value. This 'g' value is a measure of the applied centrifugal field relative to the earth's gravitational force.

3.2.2 Concepts of Sedimentation Theory

The basic principles of sedimentation theory originate from Stokes' Law. As the sedimentation of a spherical particle placed in a gravitational field reaches a constant velocity, the net force on the particle is equal to the force resisting its motion through the liquid. This resisting force is called the frictional or drag force. If the sedimentation of a spherical particle in a gravitational field is considered, Stokes' equation can be expressed as:

$$\frac{1}{6} \pi d^3 (\rho_p - \rho_m) g = 3 \pi d \eta v \quad \text{————— (3.1)}$$

where v = sedimentation rate or velocity of the sphere (cm sec^{-1}).

d = diameter of the sphere (cm).

ρ_p = density of the spherical particle (g cm^{-3}).

ρ_m = density of the liquid medium (g cm^{-3}).

η = viscosity of the liquid medium ($\text{g cm}^{-1} \text{sec}^{-1}$).

g = gravitational force ($\text{g cm}^{-2} \text{sec}^{-2}$).

If this equation is solved for v :

$$v = \frac{\frac{1}{6} \pi d^3 (\rho_p - \rho_m) g}{3 \pi d \eta} \quad \text{————— (3.2)}$$

If this expression is simplified:

$$v = \frac{d^2 (\rho_p - \rho_m) g}{18 \eta} \quad \text{————— (3.3)}$$

The expression given in Equation (3.3) is known as Stokes' Law. From Stokes' Law it can be seen that:

1. The sedimentation rate of a given particle is proportional to the square of the diameter, d , of the particle.
2. The sedimentation rate is proportional to the difference that exists between the density of the particle and the density of the liquid medium, $(\rho_p - \rho_m)$.
3. The sedimentation rate is zero when the density of the of the particle is equal to the density of the liquid medium.
4. The sedimentation rate decreases as the viscosity, η , increases.
5. The sedimentation rate increases as the gravitational force, g , increases.

Stoke's Law applies to 1g sedimentation, thus Equation (3.3) can be written as follows:

$$v = \frac{dr}{dt} \quad \text{————— (3.4)}$$

$$\text{where } \frac{dr}{dt} = \frac{d^2 (\rho_p - \rho_m) g}{18 \eta} = \text{rate of particle movement (cm sec}^{-1}\text{)}.$$

The sedimentation rate, v , is used to characterise a particle and can be determined using an analytical centrifuge, as explained by the following equation:

$$v = \frac{dr}{dt} = S \times \omega^2 r \quad \text{————— (3.5)}$$

where S = sedimentation coefficient (sec).

ω = time rate of angular motion about an axis, rotor speed (radians sec^{-1}).

r = distance between the particle and the centre of rotation (cm).

$\frac{dr}{dt}$ = the rate of movement of the particle (cm sec^{-1}).

The sedimentation rate of a particle per unit of centrifugal force is known as the sedimentation coefficient and using Equation (3.5) can be written as:

$$S = \frac{1}{\omega^2 r} \frac{dr}{dt} \quad \text{————— (3.6)}$$

which can be expressed as:

$$S = \frac{\frac{dr}{dt}}{\omega^2 r} \quad \text{————— (3.7)}$$

which can be written as:

$$S = \frac{v}{\omega^2 r} \quad \text{————— (3.8)}$$

The rotor speed, ω , can be calculated from the speed at which the centrifuge is being operated, which is expressed in revolutions per minute, or r.p.m., from the following equation:

$$\omega = \text{r.p.m.} \times \frac{2\pi}{60} = \text{r.p.m} \times 0.10472 \quad \text{---(3.9)}$$

the value obtained for ω can then be inserted into Equation (3.7). Sedimentation coefficients are expressed in Svedbergs, or S, where 1S is equivalent to 10^{-13} seconds. A particle whose sedimentation coefficient is measured at 10^{-12} seconds has a value of 10S. Typical values of S for enzymes range from 2 to 25 ^(57,59,67).

3.2.3 Calculation and standardisation of the sedimentation coefficient

Using an analytical centrifuge the sedimentation rate, or v , of a particle in an homogeneous medium can be measured. The corresponding values of the gravitational field and the speed of rotation, g and ω respectively, can be calculated. The equation given for the sedimentation coefficient, or S, in (3.7) can be expressed as:

$$\frac{dr}{r} = S \omega^2 dt \quad \text{--- (3.10)}$$

Integration of both sides gives:

$$\ln(r) = S \omega^2 t + \text{Constant} \quad \text{--- (3.11)}$$

Plotting $\ln(r)$ against t gives a straight line having the slope of $(S\omega^2)$, which can be inserted into expression (3.12) to calculate S:

$$S = \frac{\text{slope}}{\omega^2} \quad \text{———— (3.12)}$$

Deviations from linearity usually indicate that the concentration of the sedimenting particles is too high, which causes a concentration gradient of the particles to be formed in the centrifuge cell ^(57,58,59,65,68).

The standard or normalised sedimentation coefficient, or $S_{20,w}$, is defined as that equivalent to centrifugation in water at 20°C, where both the density and viscosity of the medium surrounding the particles are standardised ^(65,68,69). Standardisation of the sedimentation coefficient allows comparison of values obtained using various media and reaction conditions. Sedimentation coefficients, $S_{T,m}$, obtained experimentally in a medium of density, $\rho_{T,m}$, and viscosity, $\eta_{T,m}$, at a temperature, T, can be corrected to standard coefficients using the equation:

$$S_{20,w} = S_{T,m} \left(\frac{\rho_p - \rho_{20,w}}{\eta_{20,w}} \times \frac{\eta_{T,m}}{\rho_p - \rho_{T,m}} \right) \quad \text{———— (3.13)}$$

3.2.4 Sedimentation theory applied to gradient centrifugation

Sedimentation coefficients determined using an analytical centrifuge are based upon the movement of particles through an homogeneous medium. Typically, most centrifugal separations, except for normal rate separations, use the rate-zonal technique, which is described in detail in Chapter 4. The rate-zonal technique involves the sedimentation of particles through a supporting density gradient formed by the medium. As the particles sediment through the medium they encounter differing environments produced by the variation in the viscosity and density of the medium. The gravitational forces exerted on the sedimenting particles also varies as they move further away from the centre of rotation. With

a gradient only the situations at the start and at the end of an experiment are known. If all of these aspects are coupled together the following expression can be written:

$$S_{20,w} \int_0^t \omega^2 dt = \left(\frac{\rho_p - \rho_{20,w}}{\eta_{20,w}} \right) \int_i^r \left(\frac{\eta_{T,m}}{\rho_p - \rho_{T,m}} \right) \times \frac{dr}{r} \quad \text{--- (3.14)}$$

If this equation is integrated between the limits from time zero to a fixed time, t (sec), and during that interval the particles move from an initial position, i (cm), to a final position, r (cm), then both integrals can be evaluated. These integrals cannot be solved analytically, but can be determined numerically using an iterative process. For the calculations it is essential that the medium gradient must be unaffected during the centrifugation.

The calculations are performed stepwise, in which each step corresponds to a fraction collected from the gradient on completion of an experimental run. Sedimentation coefficients are equated to specific fractions, and these values are related to fractions containing the maximum concentrations of the sedimenting particles. Resolving Equation (3.14) is best achieved by dividing the calculation into a series of steps, which are:

1. Determination of the force-time integral, $\int_0^t \omega^2 dt$.
2. Determination of the radial movement of the particles, $\frac{dr}{r}$.
3. Analysing the effect of the gradient on sedimentation, $\frac{\eta_{T,m}}{\rho_p - \rho_{T,m}}$.
4. Standardising the estimated coefficients to water at 20°C, $S_{20,w}$.

3.2.4.1 Calculation of the force-time integral.

Many modern ultracentrifuges display the force-time integral during operation, but in most cases the value must be calculated. The force-time integral consists of contributions from

the acceleration period, or A , the actual run period, or P , and the deceleration period, or D .
The run period contribution is given by the equation:

$$\omega_p^2 (60P) = (2\pi Q / 60)^2 (60P) = \frac{(\pi Q)^2 P}{15} \quad \text{—————} \quad (3.15)$$

where ω_p = rotor speed during the actual run period, (radians sec⁻¹).

$60P$ = ω^2 is linear during this time period (minutes)⁽⁶⁵⁾.

P = the actual run period, (minutes).

Q = the average rotor speed during the actual run period, r.p.m, ($\pi\omega / 30$).

If it is assumed that the acceleration is constant, then the angular velocity during acceleration, ω_a , can be expressed as:

$$\omega_a = k_a t \quad \text{—————} \quad (3.16)$$

where k_a = acceleration (radians sec⁻¹).

The value of ω^2 is linear during the time period $60A$, thus the acceleration is given by:

$$k_a = \frac{\omega_p}{60A} = \frac{2\pi Q / 60}{60A} = \frac{2\pi Q}{60^2 A} \quad \text{—————} \quad (3.17)$$

Combining Equations (3.16) and (3.17) gives:

$$\int_0^{60A} \omega_a^2 dt = \int_0^{60A} (k_a^2 t^2) dt = \left(\frac{2\pi Q}{60^2 A} \right)^2 \int_0^{60A} t^2 dt =$$

$$= \frac{(2\pi Q)^2}{60^4 A^2} \times \frac{(60A)^3}{3} = \frac{(\pi Q)^2 A}{45} \quad \text{————— (3.18)}$$

By inference the equation for deceleration is given by:

$$\int_0^{60D} \omega_d^2 dt = \frac{(\pi Q)^2 D}{45} \quad \text{————— (3.19)}$$

Combining Equations (3.15), (3.18) and (3.19) the force-time equation can be expressed as:

$$\int_0^t \omega^2 dt = \frac{(\pi Q)^2 \times [P + (A + D) / 3]}{15} \quad \text{————— (3.20)}$$

and this value can be inserted into Equation (3.14).

3.2.4.2 Determination of the radial position of particles

To determine the radial position of the particles zone at the start and end of centrifugation the volume-radius relationship is used. Analysis of the samples taken allows the particle zone mass centre to be assigned to a specific fraction, and using the volume-radius relationship the radial position of the fraction can be determined. This research has been limited to the use of

centrifuge tubes and a swing-out rotor, so the equations presented are specific to that system. The volume-radius relationship is given by ⁽⁶⁵⁾:

$$R = r_{\text{men}} + (V/\pi r_{\text{T}}^2) \quad \text{————— (3.21)}$$

- where R = the total radius from the centre of rotation (cm).
 r_{men} = the radius of the meniscus from the centre of rotation (cm).
 V = the total summed volumes of the fractions up to the one being considered (cm³).
 r_{T} = the internal radius of the cylindrical part of the tube (cm).

The volume-radius relationship for the hemispherical bottom of the tube is expressed as:

$$V = (\pi r_{\text{b}}^2 h) - (1/3\pi h^3) \quad \text{————— (3.22)}$$

- where r_{b} = the internal radius of the hemispherical bottom (cm).
 h = the radial length of the hemispherical bottom including the thickness of the tube wall (cm).

Equation (3.22) is solved for h and this is added to the calculated radii for fractions collected up to the rounded bottom of the tube. A diagrammatic representation of the volume-radius relationship based on Equations (3.21) and (3.22) is shown in Figure 3.1. The initial and final radial positions of the particles, i and r , can be inserted into Equation (3.14).

Alternatively, the volume-radius relationship can be determined empirically by adding a successive fraction volume to the tube and measuring the radial distance to the centre of

rotation. The smaller the fraction volumes, the more accurately the particle zone mass centre can be determined.

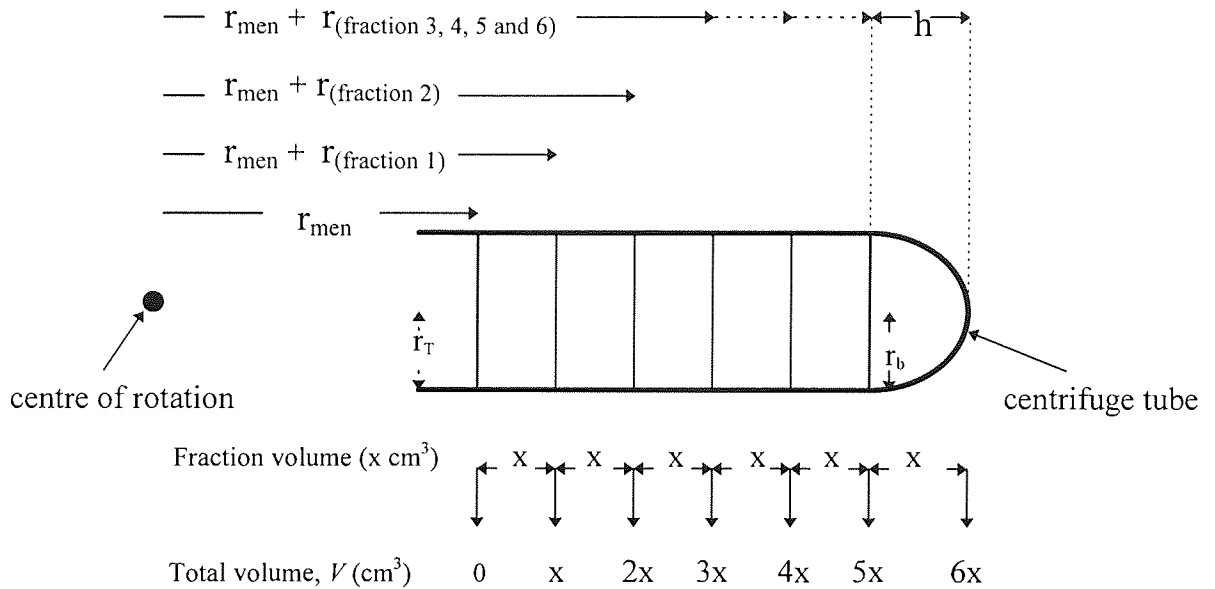


Figure 3.1. Diagrammatic representation of the volume-radius relationship expressed in Equations (3.21) and (3.22), and based on six fractions collected. r_{men} = radius to the meniscus (cm), $r_{(fraction\ x)}$ = radial contribution of the fraction/s (cm), r_T = internal radius of the cylindrical part of the tube (cm), r_b = the internal radius of the hemispherical bottom (cm), h = radial length of the hemispherical bottom including the tube thickness (cm), and V = the total summed volumes of the fractions up to the one being considered (cm^3).

3.2.4.3 Analysis of the gradient medium

After the completion of a gradient centrifugation experiment the contents of the centrifuge tube are divided into a number of fractions and the fraction/s containing the particles identified. The volume-radius relationship is used to assign a radial position to each of the fractions, and this can be related to the fraction containing the particle zone mass centre. The density of each fraction can be determined using refractive index, or using an electronic density meter. The viscosity of each fraction can be measured using a glass viscometer, or by using a rotational viscometer. A value for the density of the particle material itself, preferably determined in the same gradient medium as that used in the actual experiments, is

required. The protocol for determining the density of the particle material is given in Chapter 7. The experimentally obtained values can be inserted into the term:

$$\frac{\eta_{T,m}}{\rho_p - \rho_{T,m}} \quad \text{—————} \quad (3.23)$$

The final values required to allow the sedimentation coefficient to be determined are that for dr and r . The term dr is the radial increment, in cm, equivalent to the volume of a sample fraction and r is the radial position of the particle within a fraction, and is taken as the average radius of the fraction, in cm.

3.2.4.4 Standardising the estimated sedimentation coefficient of a particle in a gradient medium

The values obtained using Equations (3.20), (3.21), (3.23) and the values of dr and r can be inserted into Equation (3.14), and the value of $S_{20,w}$ calculated. Standardisation of the sedimentation coefficient allows comparison of values obtained for different particles, and for values obtained using different gradient medium.

3.2.5 Estimation of the sedimentation coefficient using isokinetic gradients.

The sedimentation coefficient of a particle can be estimated using an isokinetic gradient medium ⁽⁶⁵⁾. In 1961, Martin and Ames ⁽⁷⁰⁾ suggested that a density and viscosity gradient could be constructed to produce a uniform sedimentation velocity by compensating for the centrifugal force along the centrifuge tube; this is known as an isokinetic gradient. In a gradient the viscosity increases towards the bottom of a centrifuge tube; with an isokinetic gradient the linear increase in radial distance is offset by a linear increase in viscosity, which makes the sedimentation rate of the particle independent of the radial position ⁽⁷⁰⁾. In general, the shape of an isokinetic gradient is convex and exponential if the relationship between the medium concentration and the viscosity is logarithmic.

An example of an isokinetic gradient is that of a 5-20%^(w/w) linear sucrose gradient, which is widely used for the separation of macromolecules ^(59,71,72). This type of gradient can be used experimentally to calculate the sedimentation coefficient of a particle by comparing the sedimentation distance of a marker particle with a known sedimentation coefficient, with that of the sedimentation distance of the particle. The relationship is described as:

$$\frac{S_1}{S_2} = \frac{r_1}{r_2} \quad \text{————— (3.24)}$$

which can be rearranged to give the expression:

$$S_1 = S_2 \times \frac{r_1}{r_2} \quad \text{————— (3.25)}$$

- where
- S_1 = the unknown sedimentation coefficient (Svedbergs, S).
 - S_2 = the known sedimentation coefficient of marker particle (Svedbergs, S).
 - r_1 = sedimented distance of particle (cm).
 - r_2 = sedimented distance of marker particle (cm).

A list of commonly used marker particles for this comparative method is shown in Table 3.1. The accuracy of the estimated sedimentation coefficient can be increased by using two marker particles, one of a lower molecular weight, and one of a higher molecular weight to that of the particle under test. This method also allows the estimation of the molecular weight of a test particle by direct comparison to the molecular weights of the marker particles used.

Content has been removed for copyright reasons

Table 3.1. Sedimentation coefficients of marker particles used in isokinetic gradient centrifugation ⁽⁶⁷⁾.

3.2.6 The relationships between sedimentation coefficients and molecular parameters

The sedimentation coefficient is a function of particle size, density and shape. For macromolecules the size is given by its molecular weight (M), the density by the partial specific volume (\bar{v}), and the shape determined by the frictional coefficient ratio (f/f_0). The frictional coefficient ratio is a measure of how much the macromolecule deviates from the shape of a perfect sphere. The four parameters s , M , \bar{v} and f/f_0 are inter-related as shown below ⁽⁶⁵⁾:

$$S = M^{\frac{2}{3}} \left(\frac{1 - \bar{v}\rho}{\sqrt{\bar{v}}} \right) / [(N\pi 6\eta \sqrt[3]{0.75 / (N\pi)} (f/f_0)] \quad \text{--- (3.26)}$$

where S = sedimentation coefficient (Svedbergs, S).

M = molecular weight.

\bar{v} = the partial specific volume of the particle (g cm^{-3}).

ρ = the average density of the medium through which the particle has sedimented (g cm^{-3}).

N = Avogadro's number (6.022169×10^{23} molecules mole⁻¹).

f/f_0 = the frictional coefficient ratio of the particle.

If any three parameters are known then the fourth can be calculated by transposition of Equation (3.26). Table 3.2 gives examples of the sedimentation coefficients, partial specific volumes, frictional coefficients and molecular weights for different types of protein.

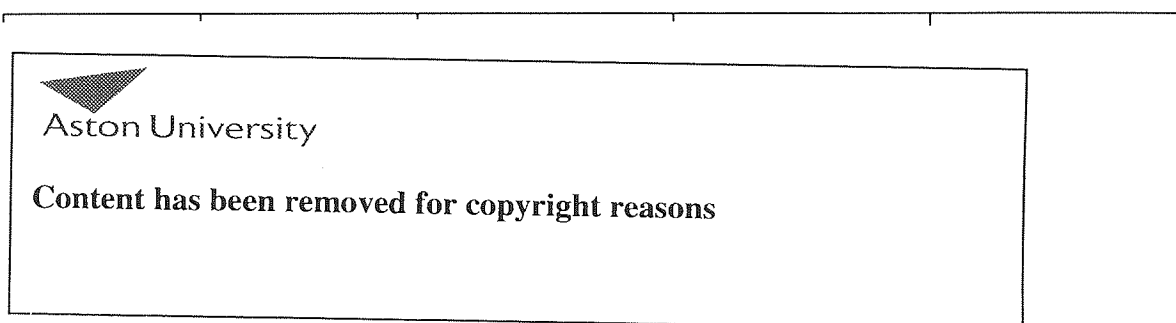


Table 3.2. Molecular parameters of various proteins ^(65,67).

3.2.6.1 The Partial Specific Volume

The partial specific volume is defined as the volume increase resulting from the addition of one gram of the solute species to an infinite volume of water. This can be regarded as the contribution per gram of dissolved material to the total volume of the solution ⁽³⁾. McCall ⁽⁶⁹⁾ proposed a simple method for calculating the 'apparent' partial specific volume based upon the volume contribution of 1 kg of the solute to 100 kg of the solution; this can be expressed as:

$$\bar{v}_{\text{app}} = \frac{100/\rho - [(100 - n)/\rho_0]}{n} \quad \text{————— (3.27)}$$

where \bar{v}_{app} = the apparent partial specific volume (m³/kg).

ρ = the density of the solution (kg m⁻³).

ρ_0 = the density of the solvent (kg m⁻³).

n = the percentage concentration of the solute.

Provided that the solutions are very dilute, \bar{v}_{app} may be used instead of \bar{v} without serious error^(3,58,73). The solution and solvent density can be experimentally determined at the required temperature using a density bottle, or by using an electronic density meter. For proteins, \bar{v}_{app} is considered independent of concentration^(3,73).

The partial specific volume of a protein can be calculated from a knowledge of the amino acid composition of the specific protein. An amino acid analyser is used to determine the % by weight of individual amino acids contained within the protein. The individual partial specific volumes of each amino acid are available in the literature⁽⁵⁸⁾. It is assumed that the partial specific volume of the protein is an additive property of the partial specific volumes of the constitutive amino acids, and this assumption is used to calculate the answer. An example of this technique using a fictitious protein which contains only five amino acids is presented in Table 3.3.

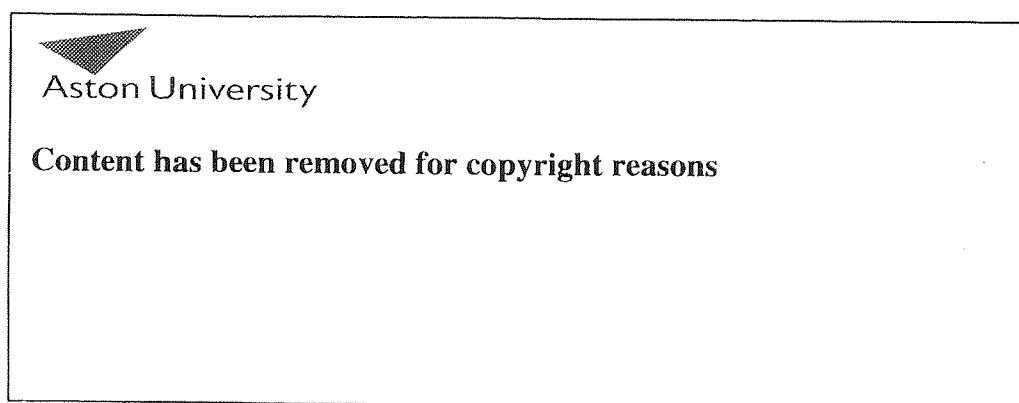


Table 3.3. Calculation of the partial specific volume of a fictitious protein using amino acid analysis⁽⁵⁸⁾.

The reciprocal of the partial specific volume is equal to the particle density (ρ_p) of a given particulate.

3.2.6.2 The Diffusion Coefficient

Diffusion is the transfer of material from a region of higher to lower concentration. The rate of diffusion, dm/dt , is proportional to the concentration gradient, dc/dr , and the cross-sectional area A through which it occurs. The relationship is shown in the following expression:

$$dm/dt \propto -A dc/dr \quad \text{————— (3.28)}$$

The negative sign in the expression is because material diffuses in the opposite direction to the concentration gradient. The diffusion coefficient (D) is a proportionality factor that can be added to Equation (3.28) as follows:

$$dm/dt = -DA dc/dr \quad \text{————— (3.29)}$$

A knowledge of the diffusion coefficient allows the molecular weight of a particle to be determined using the Svedberg equation given below ⁽⁶⁸⁾:

$$MW = \frac{RT}{D(1-\bar{v}\rho)} \frac{dr/dt}{\omega^2 r} \quad \text{————— (3.30)}$$

where MW = molecular weight of the particle.
 R = the gas constant ($8.314 \text{ J mol}^{-1} \text{ K}^{-1}$).
 T = temperature ($^{\circ}\text{K}$).

D = diffusion coefficient ($\text{cm}^2 \text{sec}^{-1}$).

\bar{v} = the partial specific volume of the particle (cm^3/g).

ρ = density of the medium (g cm^{-3}).

The expression given in (3.30) can be simplified by using Equation (3.7) to replace part of the expression with the sedimentation coefficient of the particle, (S), as follows:

$$MW = \frac{RTS}{D(1-\bar{v}\rho)} \quad \text{————— (3.31)}$$

The diffusion coefficient can be determined using data obtained from an analytical ultracentrifuge, where the spread of the sedimenting particles is visually monitored over a period of time. The diffusion coefficient can be converted to the standard state, that of pure water at 20°C by using the equation:

$$D_{20,W} = D_{\text{OBS}} \left(\frac{293.16}{T} \right) \left(\frac{\eta_{T, \text{SOLV}}}{\eta_{T, W}} \right) \quad \text{— (3.32)}$$

where $D_{20,W}$ = the corrected diffusion coefficient (water at 20°C).

D_{OBS} = the experimentally observed diffusion coefficient.

T = the temperature at which the diffusion coefficient was observed (°K).

$\eta_{T, \text{SOLV}}$ = the viscosity of the medium at T.

$\eta_{T, W}$ = the viscosity of water at T.

3.2.6.3 The Frictional Coefficient

The shape of sedimenting particles is given by the frictional coefficient ratio, f/f_0 , which indicates how much the particles deviate from the shape of a perfect sphere. The value of

f/f_0 , can be calculated using Equation (3.26) if the parameters, S , M and \bar{v} for the particles are known. Alternatively, the values of f and f_0 can be determined independently and the ratio calculated. The value of the frictional coefficient, f , can be determined if the diffusion coefficient, D , for the particles is known. The expression for calculating f is:

$$f = k_b T/D \quad \text{————— (3.33)}$$

where k_b = the Boltzman constant ($1.318 \times 10^{-23} \text{ J}^{-1} \text{ K}^{-1}$).

The term f_0 relates to the frictional coefficient of an equivalent ‘ideal’ particle, that is, a perfectly spherical non-hydrated particle. The value of f_0 can be calculated using the following expression^(58,65):

$$f_0 = 6\pi\eta_r \left(\frac{3 \text{ MW } \bar{v}_r}{4\pi N} \right)^{1/3} \quad \text{————— (3.34)}$$

where η_r = the viscosity of the medium at $T^\circ\text{C}$, the same medium and temperature used for the test particle.

\bar{v}_r = the partial specific volume of the ‘ideal’ particles, determined at the same temperature as for the test particles.

MW = the molecular weight of the ‘ideal’ particle.

N = Avogadro’s number ($6.022169 \times 10^{23} \text{ molecules mole}^{-1}$).

The value of the frictional coefficient ratio should be 1 if the test particle is perfectly spherical and non-hydrated. The greater the asymmetry of the test particles, the higher the value above 1 of the frictional coefficient ratio.

The frictional coefficient, f , can also be used to estimate particle size using Stokes' equation:

$$f = 6 \pi \eta r_p \quad \text{————— (3.35)}$$

where η = viscosity of the medium ($\text{g cm}^{-1} \text{sec}^{-1}$).

r_p = the radius of the particle (cm).

Substituting for f with Equation (3.33), (3.35) can be written as:

$$k_b T/D = 6 \pi \eta r_p \quad \text{————— (3.36)}$$

The calculated value of the particle size is only an estimate as the equation assumes that the particle is spherical.

3.2.7 Hydrostatic Pressure

A spinning centrifuge rotor generates hydrostatic pressure within the medium in which the particles are suspended. The hydrostatic pressure generated is dependent upon the rotation speed and the height of the liquid column. The hydrostatic pressure at any point within the liquid column can be calculated using the equation ⁽⁶⁵⁾:

$$P = \rho \omega^2 (r^2 - r_{\text{men}}^2) \quad \text{————— (3.37)}$$

where P = the hydrostatic pressure (N m^2).

- ω = the angular velocity (radians sec^{-1}).
 r = the distance from the centre of rotation (m).
 r_{men} = the distance of the meniscus from the centre of rotation (m).

The angular velocity in Equation (3.37) can be replaced by rotations per minute (r.p.m.) as follows:

$$P = \rho(1.10 \times 10^{-2} \text{ r.p.m.}^2) (r^2 - r_{\text{men}}^2) \quad \text{—————} \quad (3.38)$$

The pressures generated can be very high; for example, the pressure at the bottom of a 1cm column of water 8cm from the centre of rotation and centrifuged at 50 000 r.p.m. is equivalent to $112 \times 10^6 \text{ Nm}^2$, or 120 atmospheres. The high pressures generated can have significant effects on the permeability of biological membranes, and disassociate complexes such as ribosomes and cytoskeleton proteins^(65,67).

3.2.8 Wall Effects

The centrifugal force is radial in direction which means that sedimenting particles try to move radially away from the centre of rotation. Ideally, the vessel containing the medium and particles should be sector-shaped, to accommodate the radial movement of the particles. The analytical centrifuge has a sector-shaped cell which means that it does not suffer from wall effects. Most centrifugation work involves the use of a centrifuge tube which is usually narrow and parallel-sided. The radial movement of the particles during sedimentation tends to lead to their collision with the wall of the tube, which interrupts the sedimentation process. This is known as the wall effect and this is most noticeable when fixed-angle and swing-out rotors are used^(74,75,76). This research has used the swing-out rotor and centrifuge tubes and so the wall effects specific to this system will be discussed. In the case of swing-out rotors, only those particles contained within a cone reach the bottom of the centrifuge tube without colliding with the walls; this is shown diagrammatically in Figure 3.2.



Aston University

Content has been removed for copyright reasons

Figure 3.2. Diagram of the forces exerted on particles in a cylindrical tube used in a swing-out rotor. The particles inside the inner cone do not collide with the tube wall. The radius of the tube is r_T , L is the length, R is the maximum radius (r_{max}) of the rotor, and θ is the angle subtended by the two ends of the chord defining the width of a plane within the tube ⁽⁶⁵⁾.

The wall effect can be calculated using the following parameters:

1. radius of the tube, r_T (cm).
2. length of the tube, L , + radius of the hemispherical bottom, r_b (cm).
3. distance from the centre of rotation to the bottom of the tube, R (cm).
4. volume of the solution unaffected by the walls, V (cm³).

For the system shown in Figure 3.2, and neglecting the small contribution from the hemispherical bottom of the centrifuge tube, the total volume of the cone subtended from the centre of rotation to the bottom of the tube is given by:

$$\pi r_T^2 (R/3) \quad \text{————— (3.39)}$$

This includes the volume outside the tube which extends from the meniscus to the centre of rotation and this is calculated by:

$$\pi [(r_T - (r_T / R))^2 [R - (R + r_b)] / 3 \quad \text{————— (3.40)}$$

Subtracting the volume outside the tube from the total volume and rearranging the expression gives:

$$V = \pi r_T^2 \{3 - [3(L + r_b) / R] + [(L + r_b) / R]\} / 3 \quad \text{———— (3.41)}$$

The terms contained within the curly brackets represent the proportion of particles that hit the centrifuge tube walls. Increasing the radial position of the tube without increasing the tube diameter or length reduces the proportion of the particles that collide with the wall. Particles that reach the centrifuge tube walls are then subjected to less centrifugal force than those remaining within the cone. The particles that reach the walls may adhere to it which would adversely affect the separation efficiency of the centrifugation ⁽⁷⁷⁾, and also any bioreaction taking place. It has been reported that the wall effects do not appear to affect the rate-zonal sedimentation of small (< 10S) proteins ⁽⁶⁵⁾.

3.2.9 Droplet Sedimentation

When a sample containing particles is layered on top of a medium, diffusion between the layers occurs. The medium usually contains a low molecular weight solute which rapidly diffuses into the sample layer. The diffusion rate of the particles in the sample layer into the medium is less than that of the medium solute into the sample layer. Over time, the density of the sample layer rises and may exceed that of the medium. If the density of the sample layer is considerably higher than that of the medium then the phenomena known as droplet sedimentation can occur. The higher density of the sample layer causes it to 'stream' into the

medium and this produces an increase in the local density of the medium. If a medium of uniform density is used then the sample layer will continue to tumble uncontrollably to the bottom of tube because the medium is unable to support the sample layer^(58,65). The process of droplet sedimentation is shown in Figure 3.3.

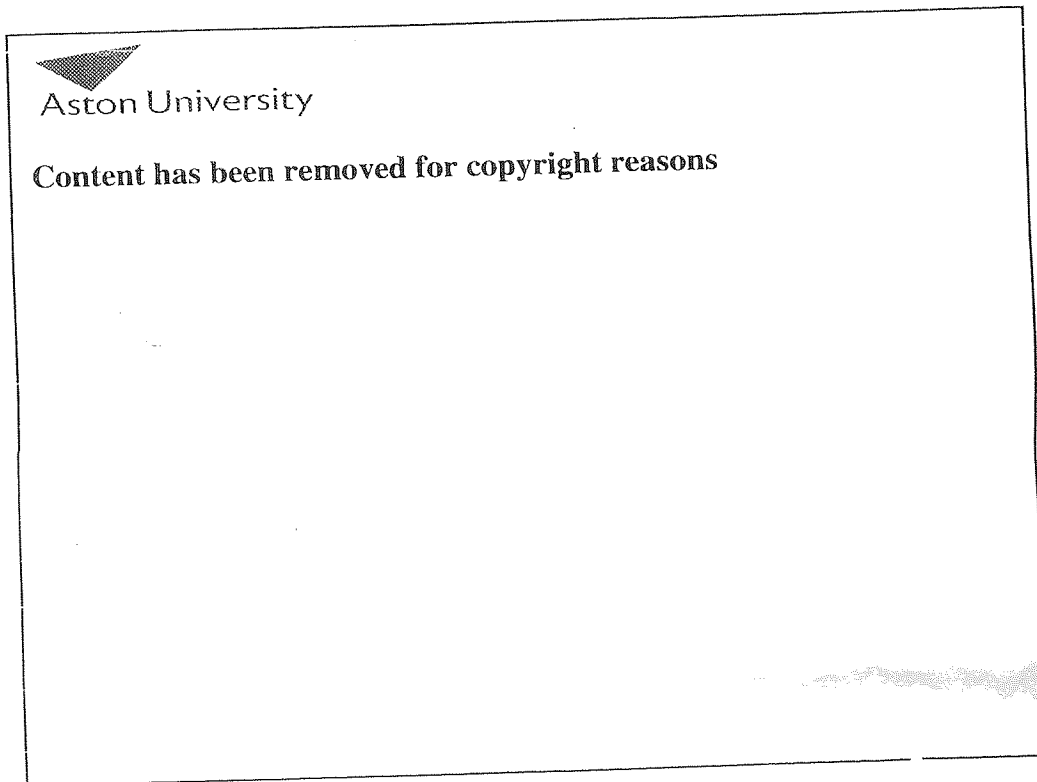


Figure 3.3. Droplet sedimentation⁽⁶⁵⁾.

If droplet sedimentation occurs then the sample layer does not sediment as a distinct zone. The effects of droplet sedimentation can be reduced by; using low sample concentrations, applying centrifugal force immediately after the sample is layered on top of the medium, minimising vibrational disruption during centrifugation, and using a density gradient medium. Using a density gradient medium stabilises the sedimenting zone of particles because any increase in the sample layer density, due to medium solute diffusion, is less than the density of gradient medium supporting the sedimenting layer. The steeper the rise in the medium gradient towards the bottom of the centrifuge tube, the greater the stability of the sedimenting sample layer. For maximum stability the sample concentration loaded onto a medium should be less than 10% of the medium concentration at the sample/medium interface ⁽⁵⁹⁾. Using a sample concentration over this value can cause broadening of the sedimenting particle zone.

3.2.10 The Swirling Effect

Swirling or vortexing of the centrifuge tube contents during acceleration and deceleration can produce serious disturbance to the medium and the sedimenting particle zone. The changes in the angular velocity of the rotor are accompanied by an angular momentum called the Coriolis forces which cause rotational movement of the fluid within the centrifuge tube. The main methods for counteracting this effect are; to reduce the rate of acceleration and deceleration of the rotor, use a steeper density gradient medium, and to increase the distance from the centre of rotation ⁽⁶⁵⁾.

3.3 Classification of centrifuges

3.3.1 Introduction

Primarily, centrifuges can be classified into two main groups which are industrial and laboratory. The classification of centrifuges showing the two areas of use is presented in Figure 3.4 ⁽³⁾. Industrial centrifuges can be either settling or filtering machines depending upon the mode of operation. Settling centrifuges separate materials according to their sedimentation properties and phase density differences. Filtering centrifuges use centrifugal fields to force liquid through a filtering medium where particulate material is retained. Laboratory centrifuges have far less capacity than that of industrial centrifuges and have been

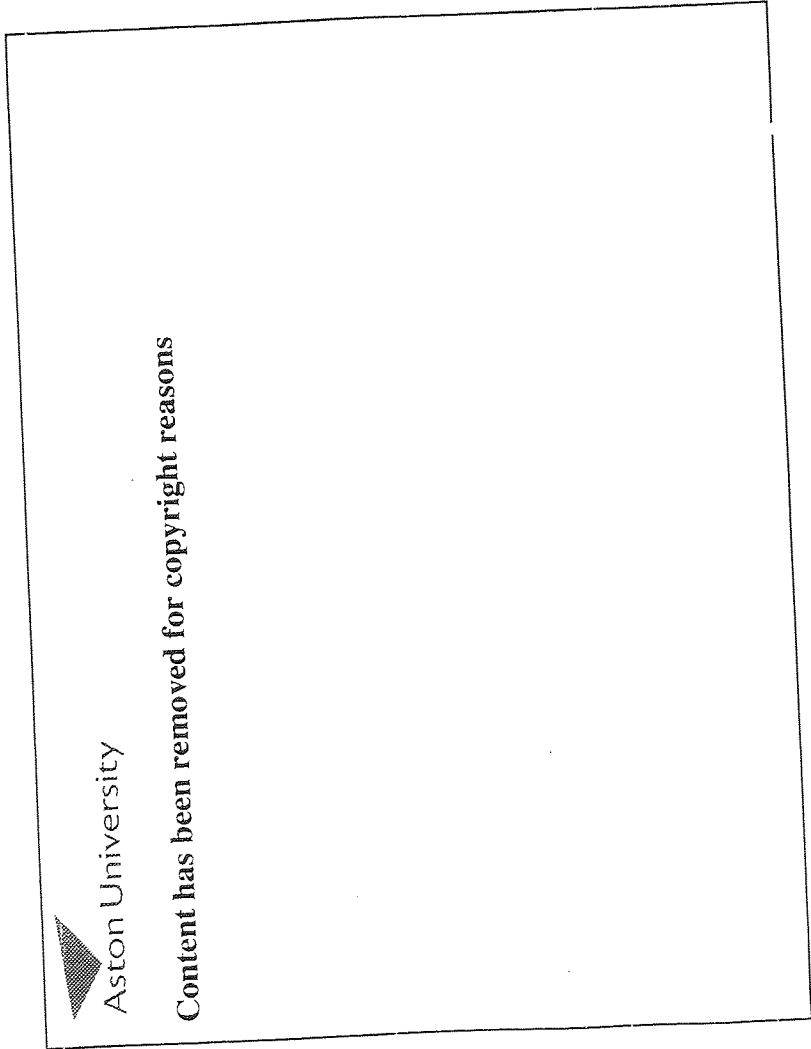


Figure 3.4. Classification of centrifuges (3).

developed for small-scale preparative work, and for research and development. Laboratory-scale centrifuges are often used in the pharmaceutical industries for separation and purification of low volume/high value products.

3.3.2 Industrial Centrifuges

Industrial centrifuges can be classified as either settling or filtering machines depending on their mode of action. Settling machines are either tubular, disk-type, or decanter and are used primarily to clarify liquids, concentrate emulsions and to separate immiscible liquids such as oil and water ⁽⁷⁸⁾. The tubular-bowl centrifuge is used for particle size ranges of 0.1 to 200 μm and up to 10% solids content of the in-going slurry; a diagram of a tubular-bowl centrifuge is shown in Figure 3.5 ⁽⁶²⁾.

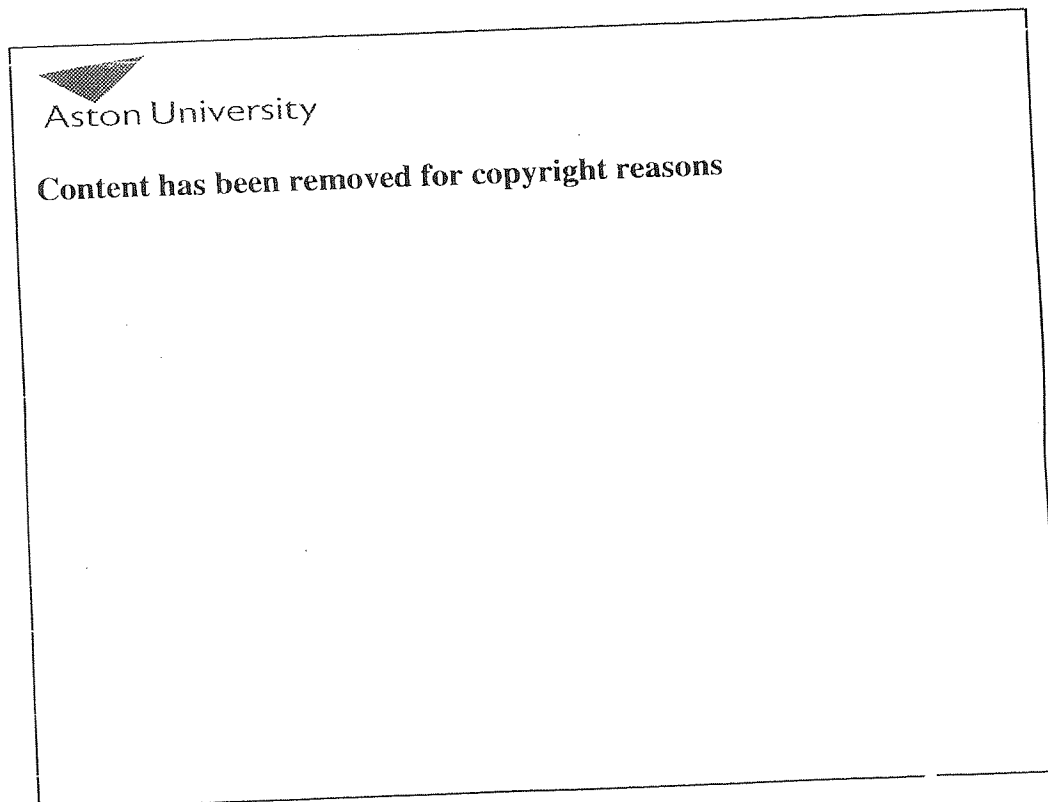


Figure 3.5. The Sharples AS 26 tubular-bowl centrifuge ⁽⁶²⁾, the lettering is described in the text.

The main component of the centrifuge is a cylindrical bowl, or rotor (A), which is suspended by a flexible shaft (B) driven by an overhead motor (C). The inlet to the bowl is through the bottom bearing (D). The feed consisting of solids and light and heavy phases enters via the nozzle (E). During operation the solids sediment to the bowl wall and the phases separate into the heavy phase located at zone G, and the light phase located at the central zone H. The two liquid phases are kept separate as they exit the bowl by an adjustable ring. The Sharples AS 26 Tubular Bowl Centrifuge (Pennwalt Limited, Surrey, UK) has a throughput of between 390 to 2400 dm³ h⁻¹ (62).

Larger throughputs can be achieved using the disk-type centrifuge which is shown in Figure 3.6.

Effluent Effluent

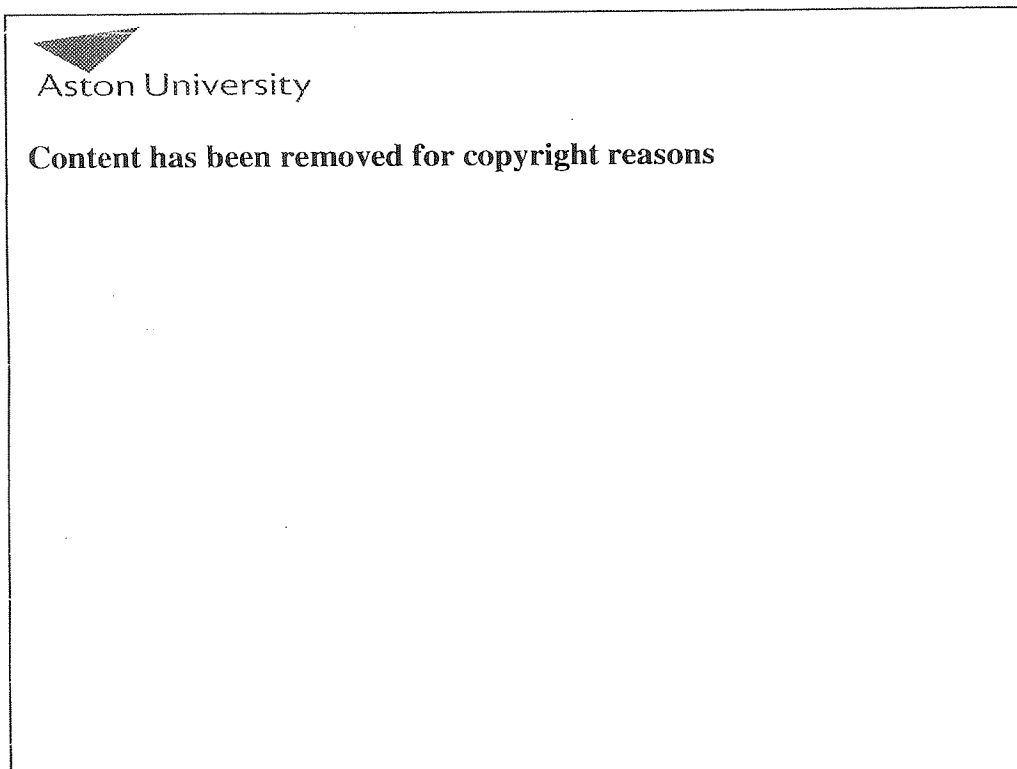


Figure 3.6. The disk-type Centrifuge (62).

The disk-type centrifuge consists of a central inlet pipe surrounded by a stack of stainless-steel conical discs. Each disk is separated by a spacer so that a stack can be built up. The medium to be separated flows outward from the central feed pipe, then upwards and inwards at an angle of 45° to the axis of rotation. The close packing of the cones allows rapid

sedimentation and the angle of the cones is sufficiently large that the aggregated solids slide radially down the cones and eventually accumulate on the inner wall of the rotor. Ideally, the sedimented solids should form a sludge which can flow rather than a hard particulate sediment. The sediment can be continually discharged or allowed to build up before being removed via discharge nozzles arranged around the circumference of the rotor. Disk-type centrifuges are commonly used to clarify fruit juices, dewater kaolin clay, and purify oil ⁽⁶⁰⁾. This type of industrial centrifuge can handle feed rates of between 45 to 1800 dm³ min⁻¹ ⁽⁶²⁾.

The decanter centrifuge, or the solid-bowl scroll centrifuge, is designed to handle coarse material such as sewage sludge. A diagram of the decanter centrifuge is shown in Figure 3.7.

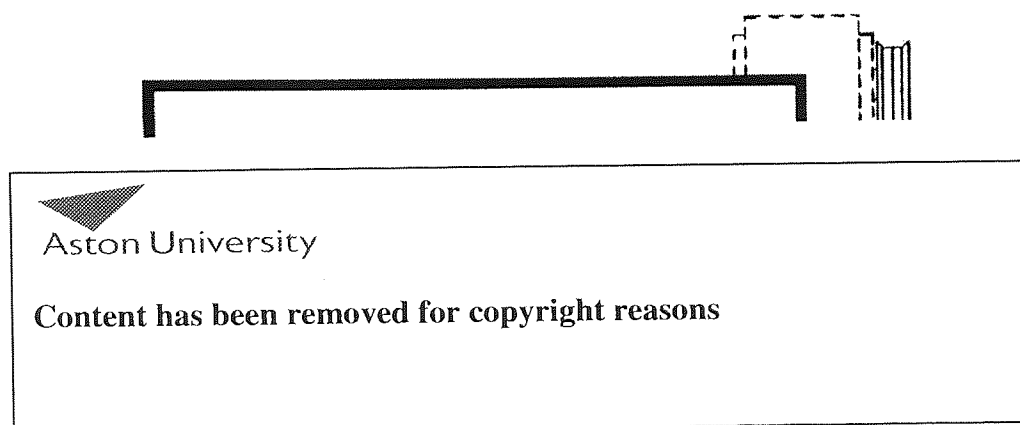


Figure 3.7. The decanter, or solid-bowl scroll centrifuge ⁽⁶²⁾.

The sewage slurry is fed through the spindle of an Archimedean screw within the horizontal rotating solids bowl. The solids settling on the walls of the bowl are fed to the conical end of the bowl and the slope of the cone allows excess liquid to be removed from the solids before it is discharged. The liquid phase is discharged from the other end of the bowl. The centrifuge usually operates at between 2 000 to 4 000 r.p.m. because of the lack of balance within the bowl assembly. This type of centrifuge is capable of handling 200 000 dm³ h⁻¹ of liquid and can process 40 tonnes h⁻¹ of solid material ⁽⁶²⁾.

Filtering centrifuges contain perforated metal plates or fabric material through which the process medium passes. A cake of solid material forms on the filter during the centrifugation process. The solid material can be removed from the filter using a knife, although some systems are designed to continuously discharge the solid material ⁽⁶⁰⁾. Figure 3.8 shows the Rousselet SC-KSA basket-type centrifuge, Rousselet UK Ltd, Harrogate, UK.

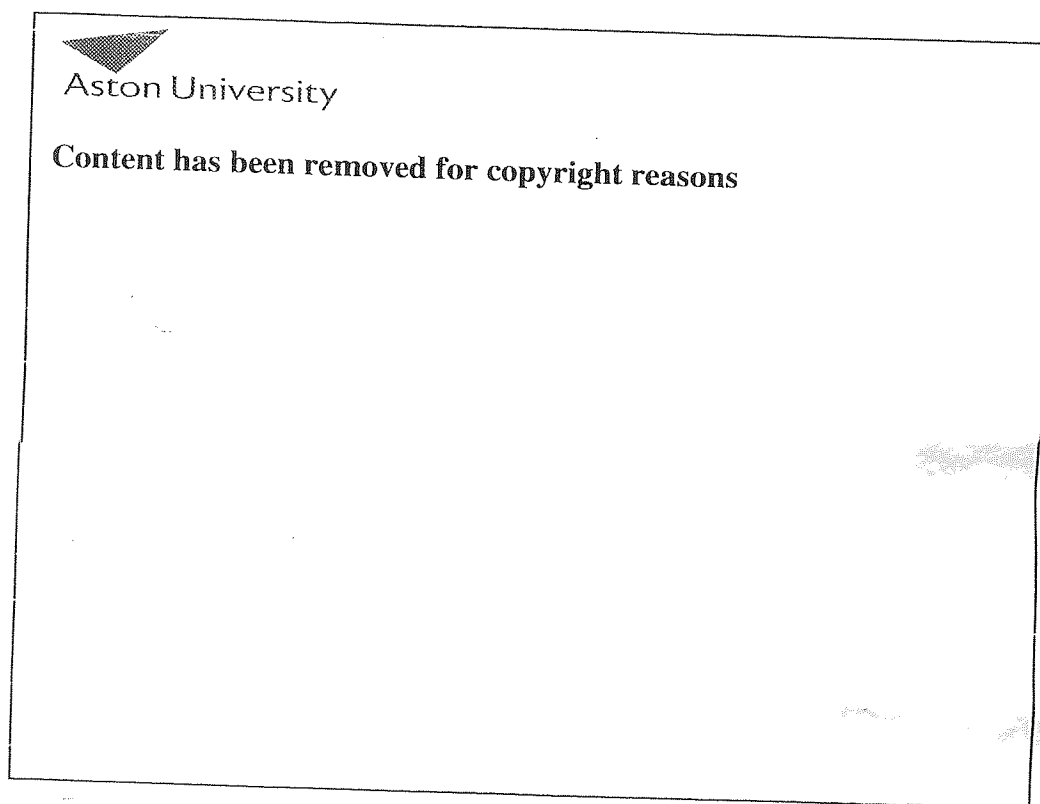


Figure 3.8. The Rousselet SC-KSA basket-type filtering centrifuge ⁽⁷⁹⁾.

The basket-type filtering centrifuge is used mainly for separating mould mycelia or crystalline compounds from liquid medium. The filter bag is usually made from nylon or

cotton. A continuous feed is used, and when the basket is filled with the solids filter cake it is possible to wash the cake before removing it. This type of centrifuge is normally operated at speeds up to 4 000 r.p.m. and can handle feed rates of 50 to 300 dm³ min⁻¹, and accommodate 30 to 500 dm³ of solid material⁽⁶²⁾. The principles of operation of the push, screw conveyor and the self discharge centrifuges are similar to that of the basket-type centrifuge, but they have been primarily designed to constantly discharge the solid material for continuous operation.

3.3.3 Laboratory Centrifuges

Laboratory centrifuges may be classed as either analytical or preparative centrifuges. Laboratory centrifuges are further classified according to their operational speed range. Low speed centrifuges are defined as those having maximum rotational speeds below 10 000 r.p.m.. High speed centrifuges have a maximum rotation speed of 20 000 r.p.m. and super-speed centrifuges can attain 30 000 r.p.m.. Ultracentrifuges are the fastest of all the centrifuges and are capable of reaching speeds up to 120 000 r.p.m.^(57,66).

3.3.3.1 Analytical Ultracentrifuges

The analytical ultracentrifuge has made a major contribution to the characterisation of biological macromolecules in terms of their molecular properties such as; molecular weight, sedimentation and diffusion coefficients, and their density. Data from these measurements have also allowed the determination of shape, frictional coefficients and the partial specific volume factors of a wide variety of particles⁽⁸⁰⁾. Analytical ultracentrifuges are fitted with sophisticated optical systems that allow the sedimentation behaviour of particles to be observed during a centrifugal run. The most widely used type of optical system is the Schlieren. The Schlieren optical system measures the differences in refractive index between the medium and the medium containing particles, which allows the movement of the particles to be visualised and photographed. A simplified diagram of the analytical ultracentrifuge is shown in Figure 3.9. The basic design of the optical rotor has not appreciably altered since the original work of Svedberg was performed^(3,68). The use of the analytical ultracentrifuge has declined over the last 30 years as new, cheaper, and simpler, methods of macromolecule characterisation such as gel and zonal electrophoresis, mass spectrometry, and laser particle sizing, have been introduced.

Aston University

Content has been removed for copyright reasons

Figure 3.9. The analytical ultracentrifuge fitted with a quartz optical system ⁽⁶⁶⁾.

3.3.3.2 Preparative Centrifuges

This group of centrifuges is classified according to the type of rotor used, namely fixed angle rotors, swing-out rotors, zonal rotors and continuous flow zonal rotors. Fixed-angle and swing-out rotors are usually made from aluminium alloys, but the zonal rotors which have higher sample capacities are made from titanium alloys ^(3,57,65,67).

The fixed-angle rotors hold centrifuge tubes at a fixed angle and when the rotor begins to turn the liquid reorientates. At the end of run the liquid again reorientates as gravity becomes stronger than the applied centrifugal forces; this process is shown in Figure 3.10. The angle of the tubes in the rotor ranges from 10° to 50° but the most widely used system has an angle of 35° to the vertical. Systems with a 35° tube angle have been found to be most suitable for separating large, slowly diffusing macromolecules ⁽⁶⁰⁾. For smaller, faster diffusing macromolecules, the tubes should be angled closer to the centre of rotation. Beckman Instruments have designed a near vertical tube rotor (NVT) for rapid isolation of plasmid DNA using cesium chloride/ethidium bromide gradients ⁽⁶⁷⁾.



Aston University

Content has been removed for copyright reasons

Figure 3.10. Separation in a fixed-angle rotor. A, the initial orientation of the particle-containing medium before centrifugation; B, as the rotor begins to move the liquid in the tube begins to reorientate; C, the particles sediment down the tube; and D, the tubes reorientates as gravity becomes stronger than the centrifugal force⁽⁶⁷⁾.

Swing-out rotors consist of removable centrifuge tubes that are held in buckets that swing out to an angle of 90° from the vertical under the influence of centrifugal force. The sedimentation of the particles is approximately parallel to the sides of the tube. The maximum distance of sedimentation of the particles is equal to the length of the centrifuge tube. The process of separation using a swing-out rotor is shown in Figure 3.11. When the rotor begins to rotate the buckets swing out to a horizontal position and this is usually achieved when the rotor attains speeds between 500 to 1 000 r.p.m.. With this type of rotor the centrifugal force is exerted along the axis of the tube. However, because the centrifugal force generated is a radial force, some of the particles are sedimented against the walls of the tube; this effect is described in 3.2.8. The rotor used in this research was a swing-out rotor manufactured by Beckman Instruments, High Wycombe, UK, and is described in detail in Chapter 7.

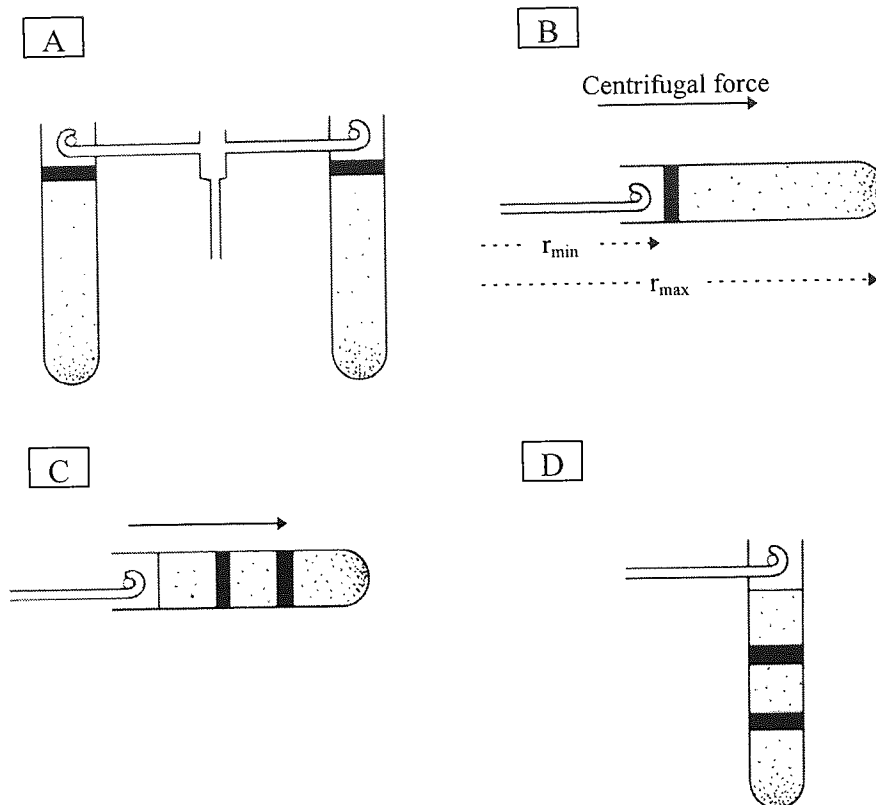


Figure 3.11. Separations in a swing-out rotor. At rest the buckets containing the centrifuge tubes hang vertically, A. As the rotor begins to move they move out so that they are perpendicular to the axis of rotation, B. During centrifugation the particles sediment down the tube, C. When the rotor stops the tubes return to the vertical position, D.

Zonal rotors were developed so that larger sample volumes can be processed. Zonal rotors are large bowl-shaped vessels with capacities of between 50 to 100 times that of a typical swing-out rotor system⁽⁸¹⁾. A photograph of a zonal rotor is shown in Figure 3.12a. The cylindrical bowl cavity is divided into four equal sector-shaped compartments by vanes attached to the bowl core. The rotor assembly is enclosed by a removable lid which is fitted with a rotating seal assembly. The rotating seal assembly allows fluid to be pumped into the bowl cavity whilst the rotor is spinning which is known as dynamic loading. Reorientation zonal rotors allow the rotor bowl to be loaded and unloaded whilst the rotor is at rest. The shape of the rotor core allows the smooth reorientation of the gradient medium to a vertical position when the rotor is spun. The reorientation zonal rotor is normally used for sedimenting fragile macromolecules which may be damaged by passage through a rotating seal assembly. In zonal rotors the particles sediment radially towards the outer wall and so

wall effects do not occur. Processing large volumes of medium induces high stresses on the rotor bowl so the zonal rotor is usually constructed from titanium alloys.

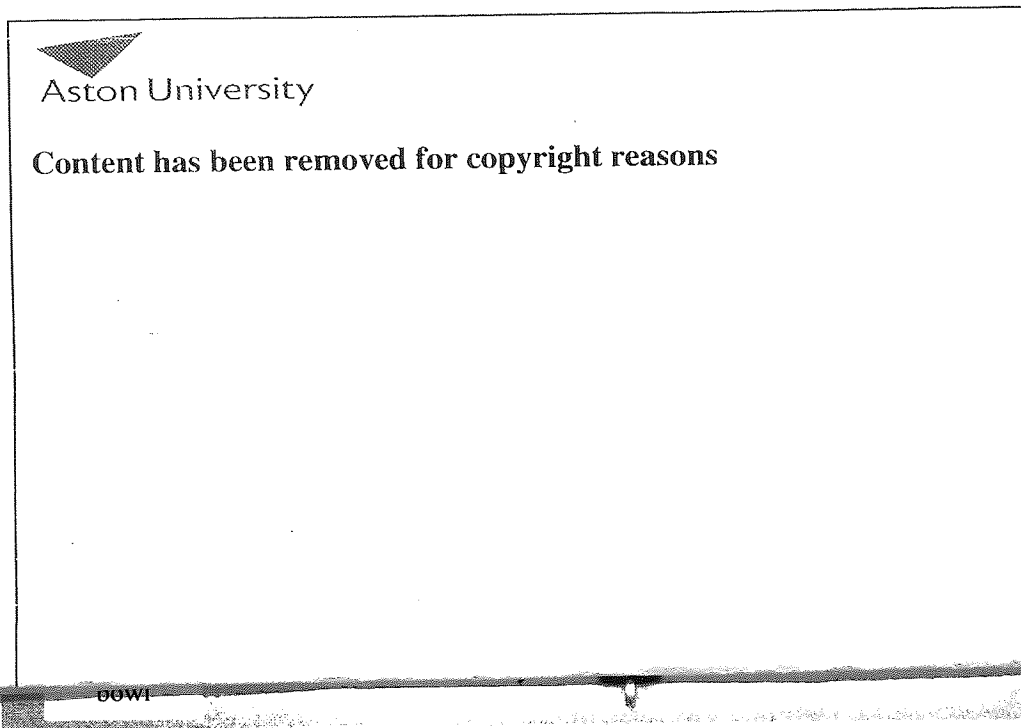


Figure 3.12a. Batch-type zonal rotor (Beckman Instruments) ⁽³⁾.

Figure 3.12b shows a diagrammatic representation of the operation of a batch-type zonal rotor, such as that shown in Figure 3.12a. Zonal rotors fitted with a special feed head allows them to be dynamically loaded or unloaded, as opposed to statically loaded and unloaded. If dynamically loaded, the rotor bowl is spun at $\sim 2\,000$ r.p.m and a discontinuous density gradient is fed to the rotor wall. The lower density layer is displaced towards the centre of the rotor by the incoming denser solutions (Figure 3.12b, diagram A). When the bowl is fully loaded with the density gradient, the particulate material to be separated is fed to the centre of the rotor and the rotor speed is then increased (Figure 3.12b, diagram B). Centrifugation proceeds until the desired separation of the particulate material has occurred (Figure 3.12b, diagram C) and then the rotor is decelerated to $\sim 2\,000$ r.p.m. A displacement fluid of greater density than that of the highest gradient density is pumped into the rotor wall. This displaces the gradient (lowest density first) through the feed head for collection.

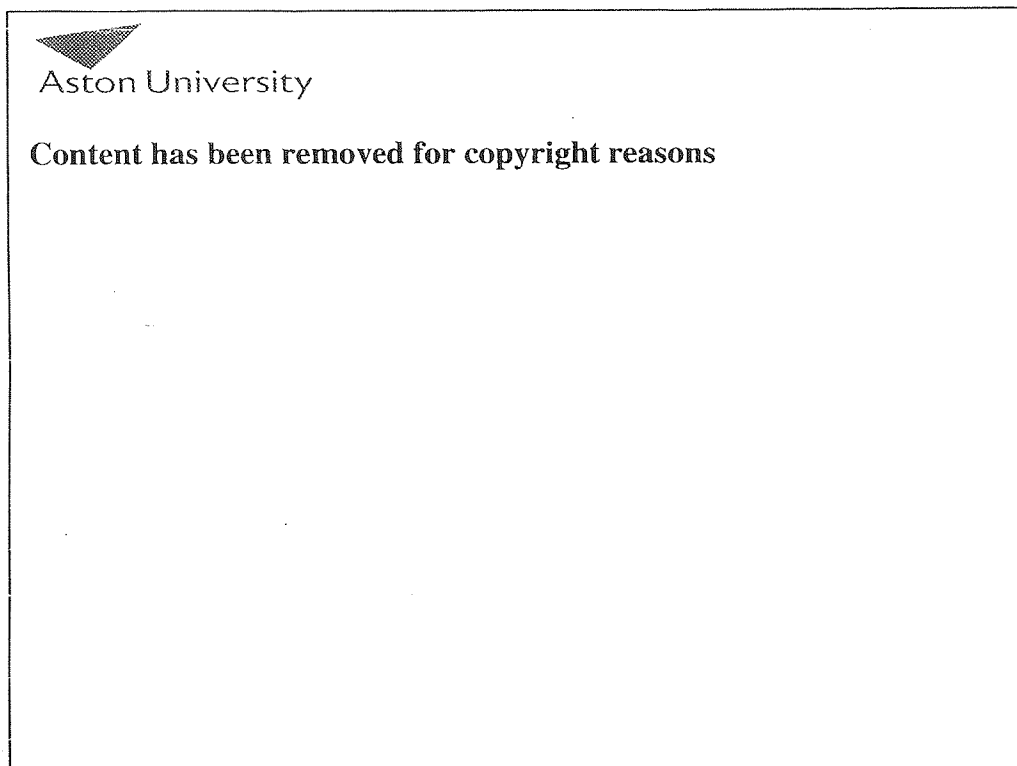


Figure 3.12b. Diagrammatic representation of the operation of a batch-type zonal rotor, the lettering is described in the text ⁽⁶⁶⁾.

Continuous flow zonal rotors have a similar design to that of the batch-type zonal rotors, shown in Figure 3.12a. In a continuous flow rotor the central core is much wider. Once the rotor has been loaded with a gradient medium a special feed head is attached which allows a continuous stream of sample to flow over the core surface and then out of the rotor. This type of rotor is mainly used for the harvesting and partial purification of bacteria and viruses from large volumes of medium ⁽⁸²⁾.

3.4 Normal rate separations

Normal rate separation is also known as differential pelleting, and is the most common and crudest method of centrifugal separation. In this type of separation the centrifuge or bowl is initially filled with a uniform mixture of medium containing different particle species. Under the influence of centrifugal force two distinct fractions are obtained; a pellet at the bottom of the tube containing fully sedimented particles and a supernatant solution containing unsedimented particles. The pellet contains a mixture of all the sedimented

particles and unsedimented particulate material that was initially present at the tube base. The supernatant liquid may contain particles that are predominantly found in the pellet and this is dependent on the centrifugation run time and the centrifugal forces applied. The process of normal rate separation is shown in Figure 3.13.

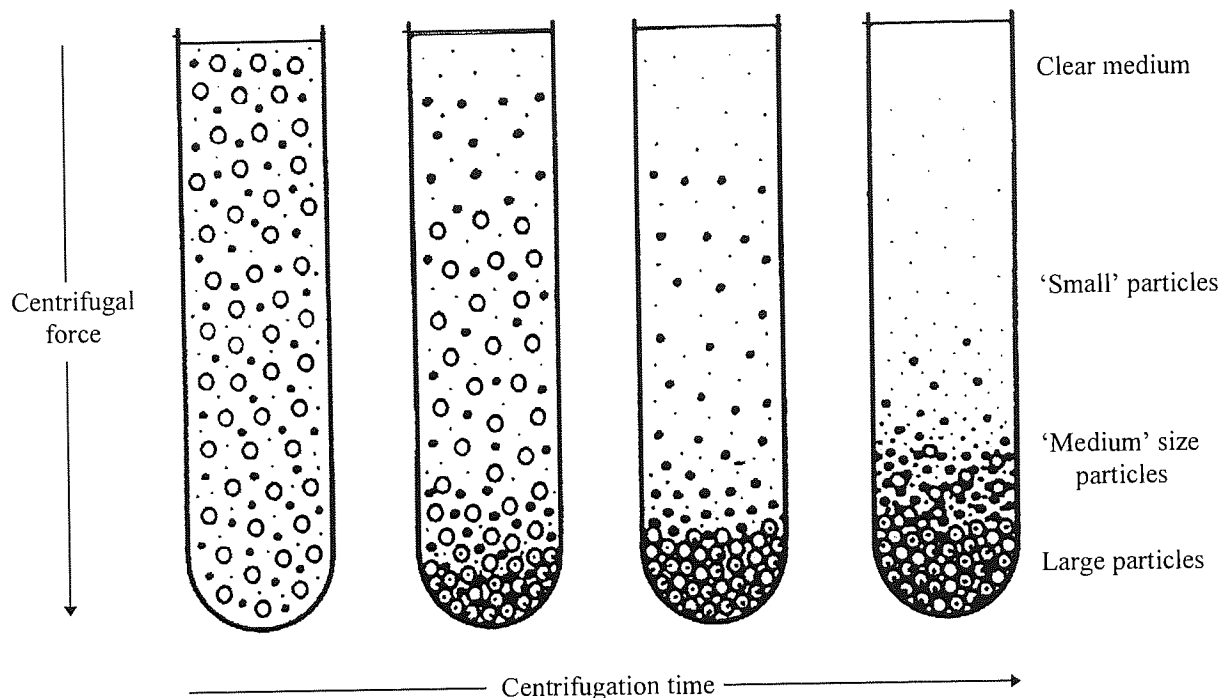


Figure 3.13. The normal rate separation, or differential pelleting.

The two fractions are separated by decanting the supernatant and this can be further purified by re-centrifugation at a higher rotation speed. The pellet can be re-centrifuged after re-suspension in fresh medium.

3.5 Centrifugation studies with soluble free β -galactosidase using a modified version of the normal rate separation technique

3.5.1 Introduction

Batch centrifugation studies were performed using the Beckman J2-MC high speed centrifuge fitted with a Beckman JS13.1 swing-out rotor which has a maximum rotation speed of 13 000 r.p.m. (26 122 g max), both of which are shown in Chapter 7. The enzymatic system studied was the hydrolysis of lactose by the enzyme β -galactosidase. The reaction system consisted of layering β -galactosidase from *Aspergillus oryzae*, Biolactase F, Quest Ltd, Cork, Ireland, on top of solutions of lactose monohydrate, the substrate, contained

within centrifuge tubes. The tubes were then centrifuged at various rotation speeds and stopped at various times; the tubes were then removed and fractions taken which related to a known position within the tube. The fractions collected were chemically quenched to prevent further enzymatic reaction and analysed using high performance liquid chromatography to determine the concentrations of the substrate and products formed. The distribution of the enzyme within the tubes was also determined using a protein assay. The aim of these experiments was to determine if, by varying the applied centrifugal force, the 'contact' time between the sedimenting enzyme and the substrate could be controlled. In principle, this would allow the formation of galacto-oligosaccharides, produced by the trans-galactosyl activity of β -galactosidase, to be controlled. All reactions were performed at 40°C which was the highest temperature attainable by the centrifuge. The experimental protocols used for these experiments are discussed in detail in Chapter 7.

3.5.2 Beckman J2-MC centrifuge temperature attainment and control

Experiments were performed to determine (a) at what range of rotation speeds the reaction temperature of 40°C could be achieved using the JS13.1 swing-out rotor, and (b) the accuracy to which this temperature could be maintained; experimental details are described in Chapter 7. The centrifuge is heated purely by the heat generated by friction as the rotor rotates. The heat generated at lower rotation speeds is insufficient to attain the maximum temperature of 40°C. The centrifuge is fitted with a refrigeration system which can cool the rotor if it exceeds the set temperature. Experiments showed that the rotor could attain a temperature of 40°C if the centrifuge was operated at rotation speeds ranging from 9 000 (12 520 g max) to 13 000 r.p.m. (26 122 g max). The accuracy to which an operational temperature of 40°C could be maintained was +/- 1°C.

3.5.3 Soluble free β -galactosidase centrifugation studies

The bioreaction system used was a modified version of the normal rate separation technique previously described in Section 3.4. The modification to this method was that the sedimenting material, the β -galactosidase, was not uniformly distributed throughout the medium, but was layered on top of the medium contained in the centrifuge tube. Also, the medium through which the enzyme sediments is also the substrate. Individual tubes were then centrifuged at rotation speeds of 9 000 (12 520 g max), 11 000 (18 703 g max) and

13 000 (26 122 g max) r.p.m. At each speed experiments were performed at various run times, 0, 30, 60, 90 and 120 minutes, so that the progression of the reaction could be monitored. For each experiment performed fractions were taken and the distribution of galacto-oligosaccharides within the centrifuge tube was determined. The experimental details are given in Chapter 7. The reaction system used is shown in Figure 3.14.

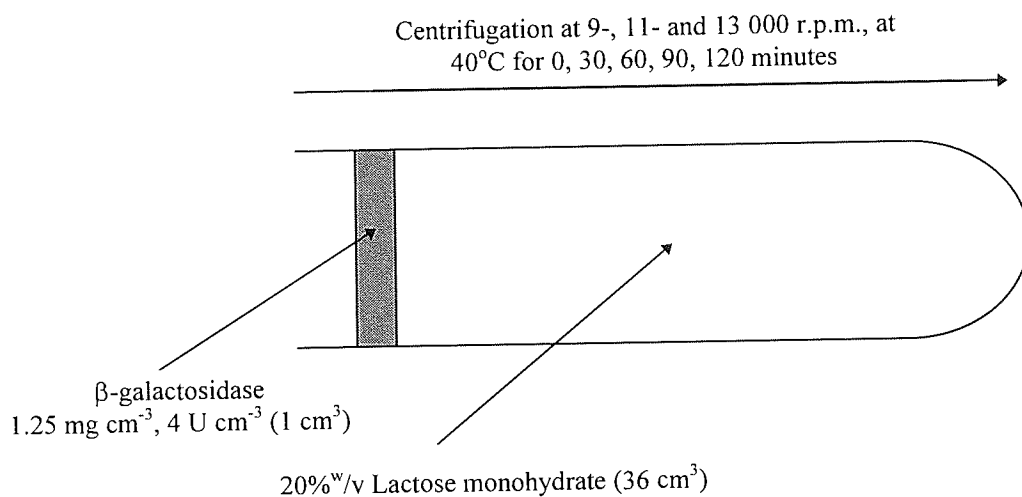


Figure 3.14. Reaction system used to determine galacto-oligosaccharide distribution profiles.

The protein distribution experiments used an identical reaction system to that shown in Figure 3.14, except that the enzyme concentration was increased from 1.25 mg cm^{-3} (4 U cm^{-3}) to 5 mg cm^{-3} (16 U cm^{-3}), so that the protein concentration was high enough to allow accurate determination by the protein assay used. As described in Section 3.2.9, the sample concentration loaded onto the medium should not exceed 10% of the medium concentration. In these experiments the maximum β -galactosidase concentration loaded was only 2.5% of the lactose monohydrate concentration. The results obtained for the galacto-oligosaccharide distribution profiles are shown in Figure 3.15, and the results obtained for the protein distribution profiles are shown in Figure 3.16.

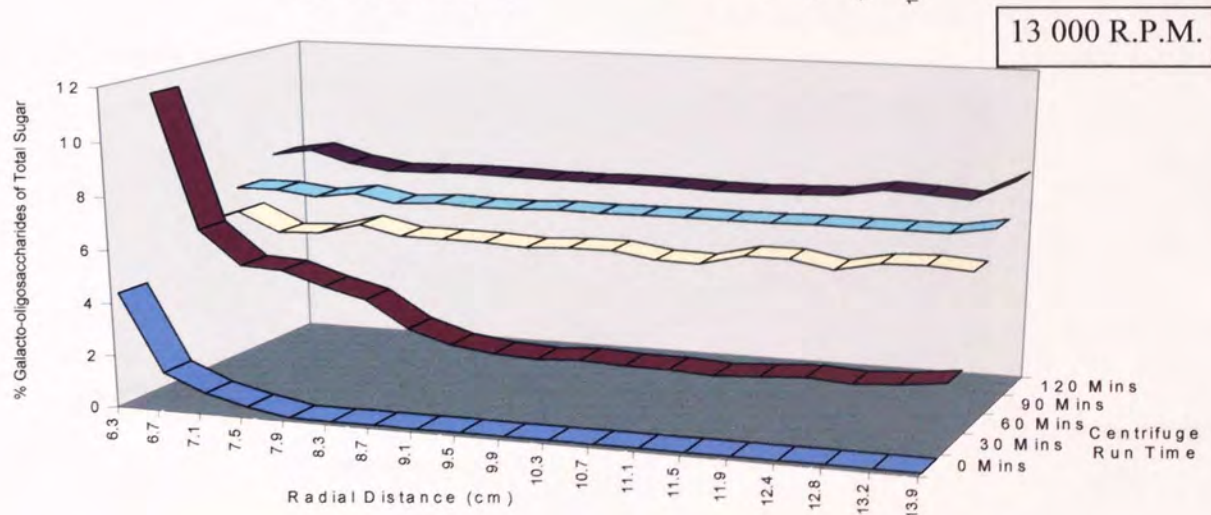
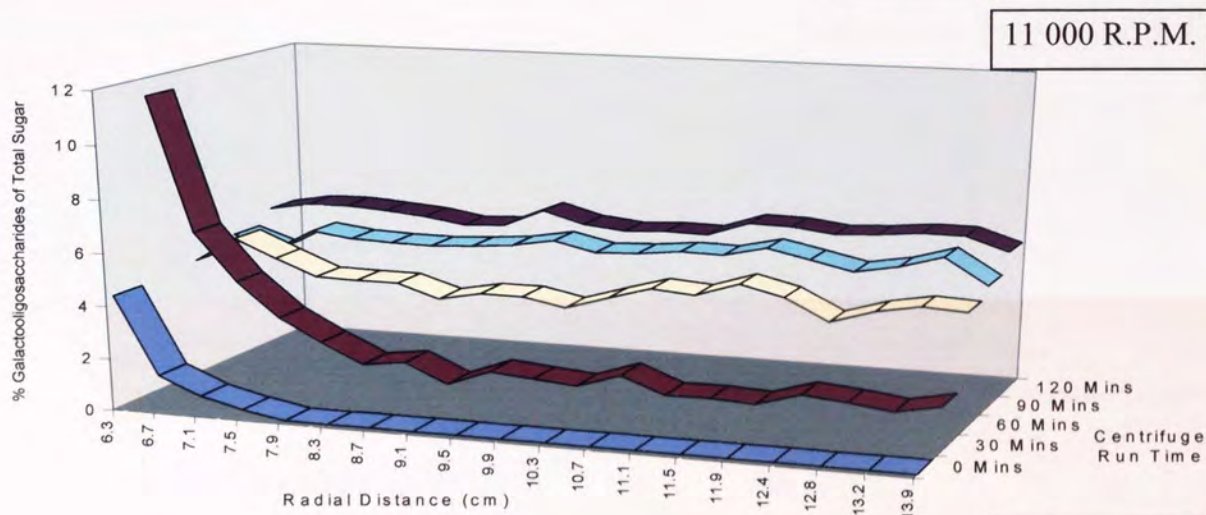
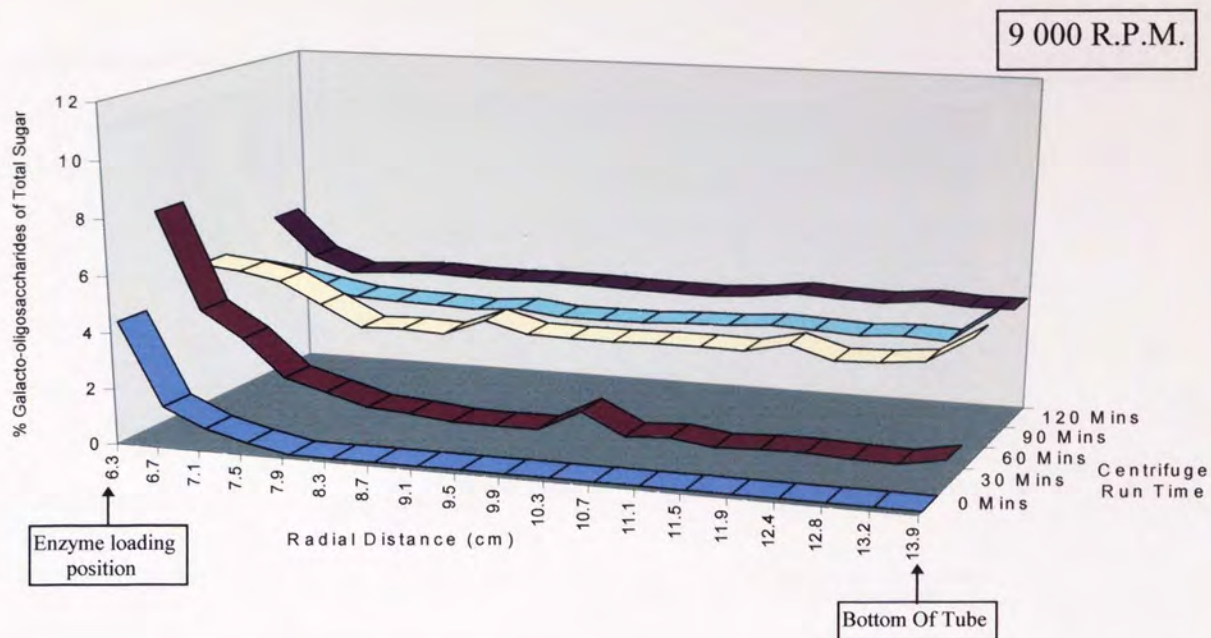


Figure 3.15. Galacto-oligosaccharide distribution profiles obtained for β -galactosidase (1.25 mg cm^{-3} , 4 U cm^{-3}) loaded on $20\% \text{ w/v}$ lactose monohydrate and centrifuged at 9-, 11- and 13 000 r.p.m. for 0, 30 60, 90 and 120 minutes, at 40° C .

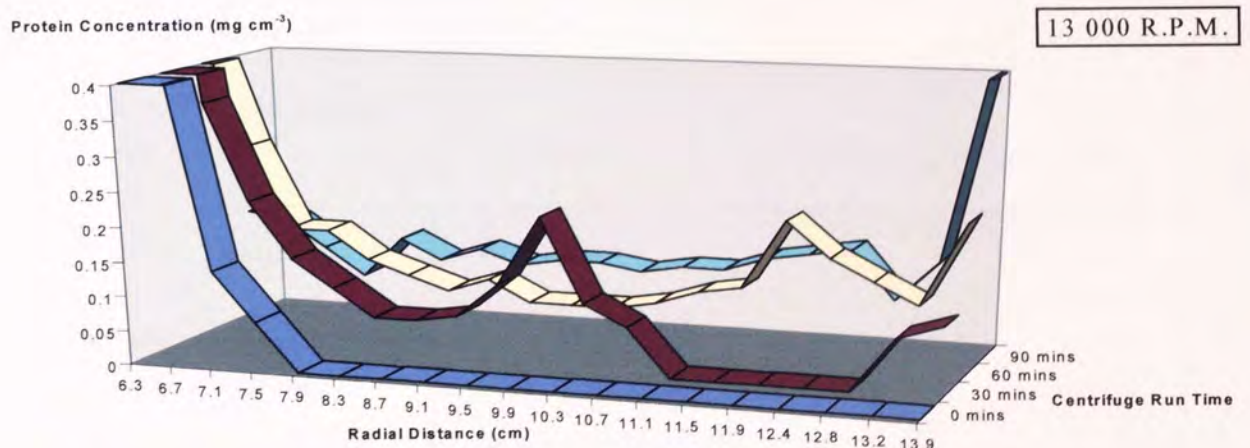
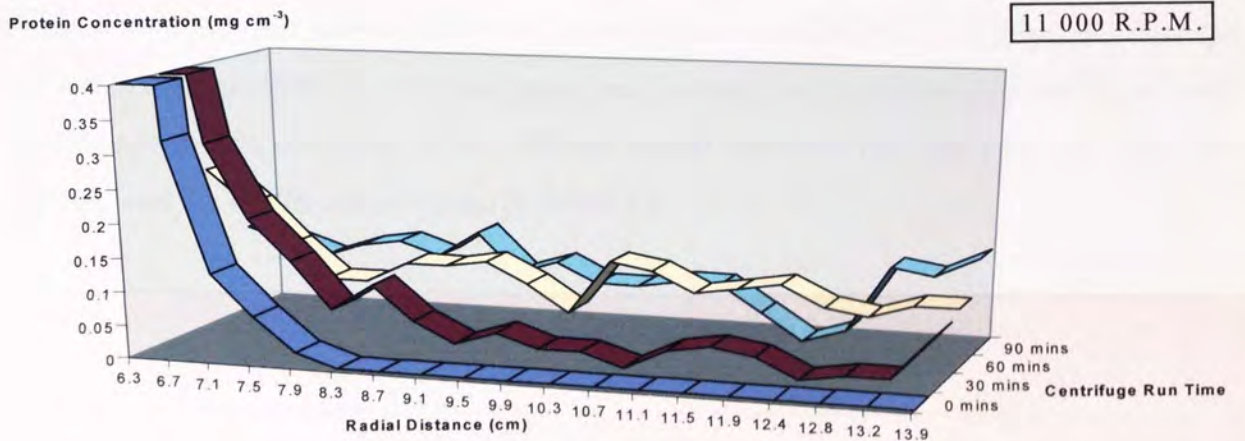
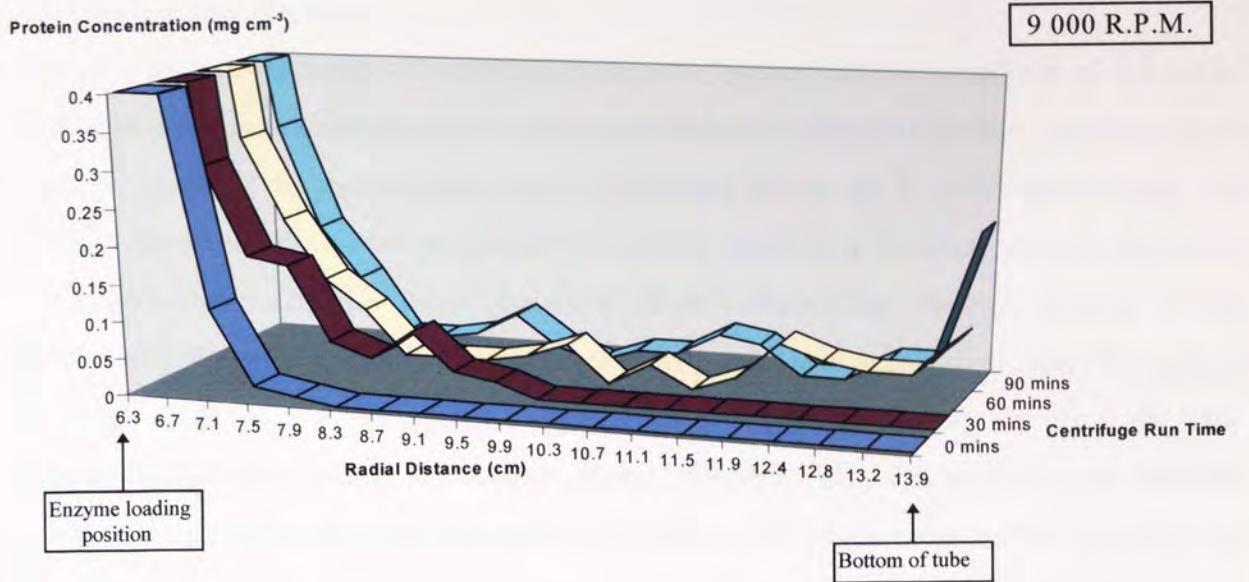


Figure 3.16. Protein sedimentation profiles of β -galactosidase (5 mg cm^{-3} , 16 U cm^{-3}) loaded on $20\% \text{ w/v}$ lactose monohydrate and centrifuged at 9-, 11- and 13 000 r.p.m. for 0, 30, 60, and 90 minutes, at 40°C .

3.5.4 Discussion of results

The galacto-oligosaccharide distribution profiles in Figure 3.15 show uniform distributions of the galacto-oligosaccharides at all speeds tested after 60 minutes run time. As the enzyme zone is subjected to increasingly higher centrifugal forces as it sediments through the medium the enzyme/substrate contact time would be expected to decrease, and the formation of galacto-oligosaccharides would be expected to reduce. The uniform increase in the profiles after 90 and 120 minutes would suggest that enzyme is evenly distributed throughout the tube contents. Also, against expectation the profiles show increasing galacto-oligosaccharide formation as the rotation speed increases. This can be correlated with the corresponding protein distribution profiles in Figure 3.16, which clearly show that more of the enzyme has moved from the loading position as the rotation speed increases. The protein profiles show that the enzyme does not sediment as a distinct band. To illustrate this, the % Galacto-oligosaccharide of Total Sugar and Protein Concentration (mg cm^{-3}) for each rotation speed were compared at two different Radial Distances (9.9 and 12.8 cm), after 120 minutes, and the results are presented in Table 3.4.

Radial Position	Rotation Speed (r.p.m.)		
	9 000	11 000	13 000
<u>9.9 cm</u>			
% Galacto-oligosaccharide of Total Sugar	5	6	8
Protein Concentration (mg cm^{-3})	0.10	0.17	0.20
<u>12.8 cm</u>			
% Galacto-oligosaccharide of Total Sugar	7	9	10
Protein Concentration (mg cm^{-3})	0.10	0.18	0.20

Table 3.4. Comparison of % Galacto-oligosaccharide of Total Sugar to Protein concentration obtained at Radial Positions of 9.9 and 12.8 cm, after centrifugation at 9 000, 11 000 and 13 000 r.p.m. (12 520, 18 703 and 26 122 g max respectively).

The results would seem to indicate that the reaction system is very unstable. It is likely that the movement of the enzyme from the loading position may be due to the effects of droplet sedimentation and swirling, and not due to true sedimentation. At all the rotation speeds, a considerable proportion of the protein remains at the loading position which indicates that the applied centrifugal forces are insufficient to produce sedimentation of the protein. Using a uniform medium concentration is inherently unstable because it provides no support to the enzyme as it sediments. The results obtained clearly show that the modified form of the normal rate separation method used is an unsuitable reaction system. The system ought to be improved by using a gradient, formed using lactose monohydrate; a gradient system should stabilise the enzyme zone as it sediments. Using a gradient should also minimise the effects of droplet sedimentation and swirling; this approach will help to confirm that the maximum rotation speed of 13 000 r.p.m. (26 122 g max) generates high enough centrifugal forces to sediment the enzyme. Experiments using a lactose monohydrate density gradient reaction system are detailed in Chapter 4.

4.0 RATE-ZONAL CENTRIFUGATION USING SOLUBLE β -GALACTOSIDASE

In this chapter, the theoretical principles upon which rate-zonal, or density gradient, centrifugation is based are discussed. The practical considerations of rate-zonal separation techniques are described. Centrifugal studies performed with soluble, free β -galactosidase, and using rate-zonal centrifugation are presented.

4.1 Introduction

Separations of particles in density gradients may be due to differences in size between the particles (rate-zonal centrifugation) or to differences in density between the particles (isopycnic centrifugation). With rate-zonal centrifugation the sample is layered as a narrow zone at the top of the gradient, but with isopycnic centrifugation the sample may be layered on the top or mixed within the gradient itself. An illustration of rate-zonal and isopycnic gradient centrifugation is shown in Figure 4.1.

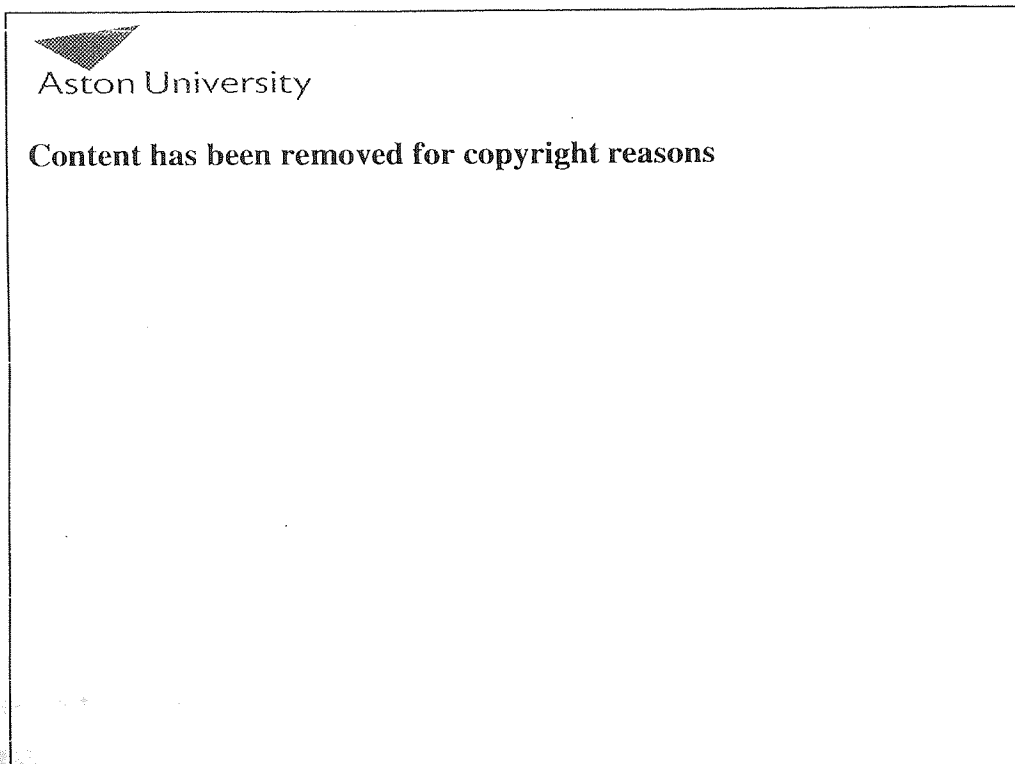


Figure 4.1. An illustration of rate-zonal and isopycnic gradient separation ⁽⁶⁵⁾.

Density gradient centrifugation involves using a supporting column of fluid whose density increases the further it is away from the centre of rotation. An isopycnic density gradient encompasses the whole range of densities of the particles present, whereas with rate-zonal operation the density of the sample particles must exceed the density at any specific point along the gradient medium. This research utilises the rate-zonal technique, whereby a density gradient is formed using the substrate, lactose monohydrate, and the enzyme, β -galactosidase, is layered on top of the gradient contained within a centrifuge tube prior to centrifugation. Under the influence of centrifugal force the enzyme sediments through the substrate gradient and is fully sedimented to the bottom of the tube, which effectively separates the enzyme from the majority of the tube contents. The general principle of the rate-zonal technique used in this research is shown in Figure 4.2.

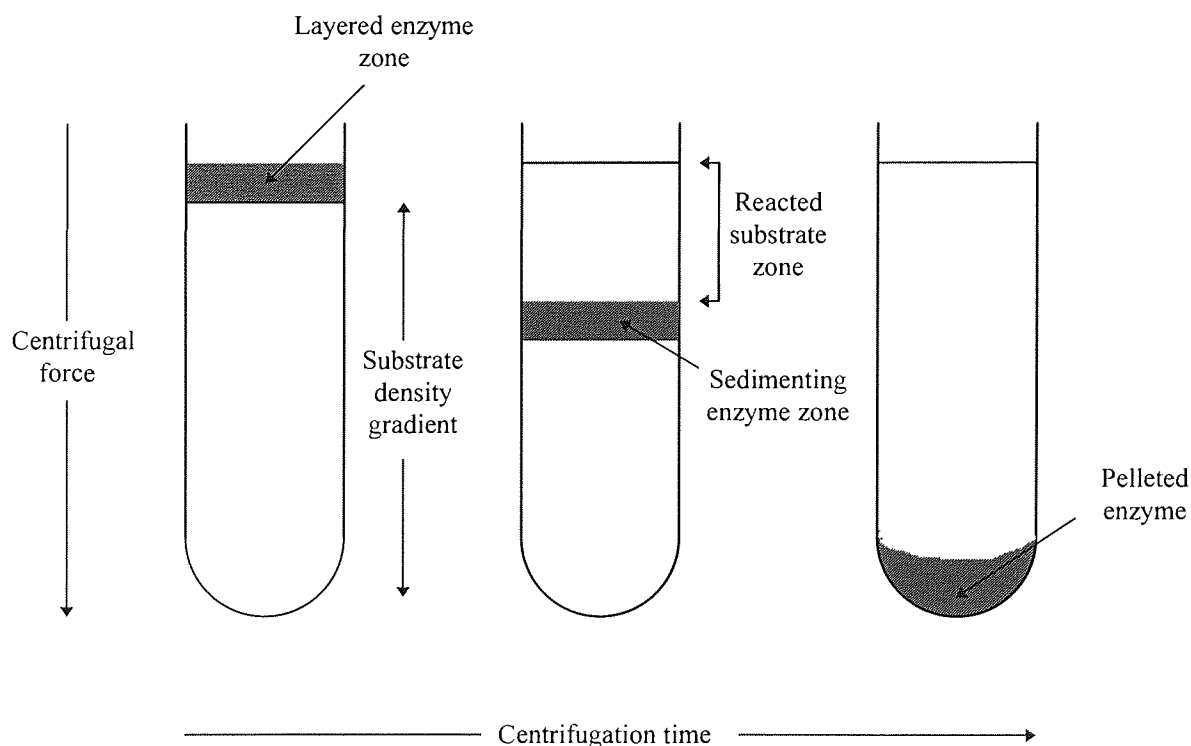


Figure 4.2. The general principles of the rate-zonal technique used in this research.

The rate-zonal technique was initially developed for preparative purposes, although the data obtained from such centrifugation allows the calculation of fairly accurate sedimentation coefficient values ⁽⁸³⁾. Separation is dependent upon differences in particle sedimentation rates, which is linked to the size, shape and the density of the various particle species, and

also to the density and viscosity of the medium. Rate-zonal centrifugation is used to separate particles ranging in size from macromolecules to cellular components and whole cells (57,65,83). In this research, the gradient was formed using lactose monohydrate which when reacted with β -galactosidase produces the monosaccharides, glucose and galactose, as well as galacto-oligosaccharides which are intermediate compounds consisting of up to 10 monosaccharide residues. The similar and very low sedimentation rates of these products relative to that of the substrate ensured that they remained at the position in the gradient where they were formed. The range of centrifugal forces applied was limited by the maximum operational speed of the rotor used; this would not allow the separation of the products formed.

4.2 Practical aspects of rate-zonal, or density gradient centrifugation

4.2.1 Density gradient media

The properties of an 'ideal' density gradient media can be listed as follows (65,66):

1. Its density range should allow separation of the particles of interest, without over-stressing the rotor.
2. It should be neither hyperosmotic nor hypoosmotic.
3. It should not affect the activity of the sample.
4. It should not interfere with any assay techniques used.
5. It should be inexpensive and readily available.
6. It should not be corrosive to the rotor.
7. It should not be flammable or toxic if aerosols are formed.

Ridge (84) states that the gradient material should be totally inert towards the sample material, although the reaction system used in this research requires the use of an interactive gradient material. The most commonly used gradient materials, with their applications and maximum densities at 20°C, are shown in Table 4.1 (65). The most popular gradient medium used is sucrose, which is readily soluble and covers the density range from 1.00 to 1.32 g cm⁻³. Sucrose is not suitable for the fractionation of living cells as even isotonic solutions can be deleterious or toxic. The disaccharide sugar lactose monohydrate, used as the gradient medium in this research, has very similar physical properties to that of sucrose and so is suitable as a gradient medium.



Aston University

Content has been removed for copyright reasons

Table 4.1. Commonly used gradient material, properties and uses ⁽⁶⁵⁾.

4.2.2 Density gradient preparation

Density gradients may be prepared in several ways depending on the type of gradient required and there are four main types of gradient: linear, convex, concave and step. Linear, convex and concave gradients are known as continuous, whereas step gradients are known as discontinuous. Examples of the different types of gradient profiles are shown in Figure 4.3. Discontinuous or step gradients are formed by layering solutions of increasing densities into a centrifuge tube, so that sharp interfaces are formed between the different solutions. The most popular method for producing discontinuous gradients is the under-layering technique, where the least dense solution is put into the tube first and successively denser solutions are introduced to the bottom of the tube to underlay the previous solution. The under-layering technique was used in this research and the basic principles of this technique are shown in Figure 4.4.; full experimental details are given in Chapter 7.

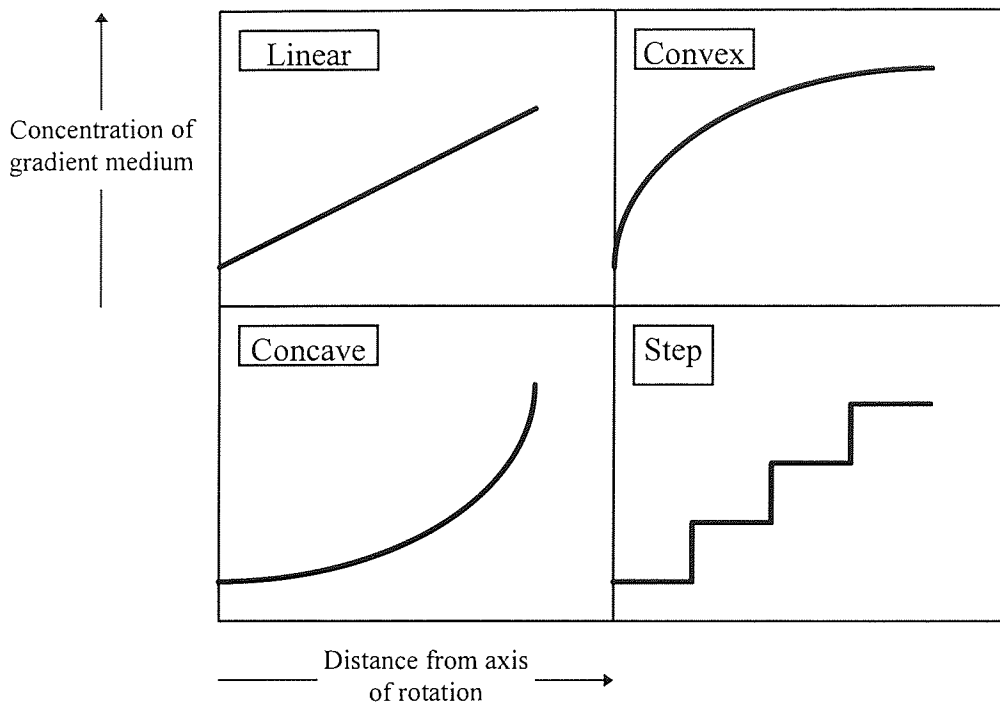


Figure 4.3. Examples of the different types of gradient profiles.

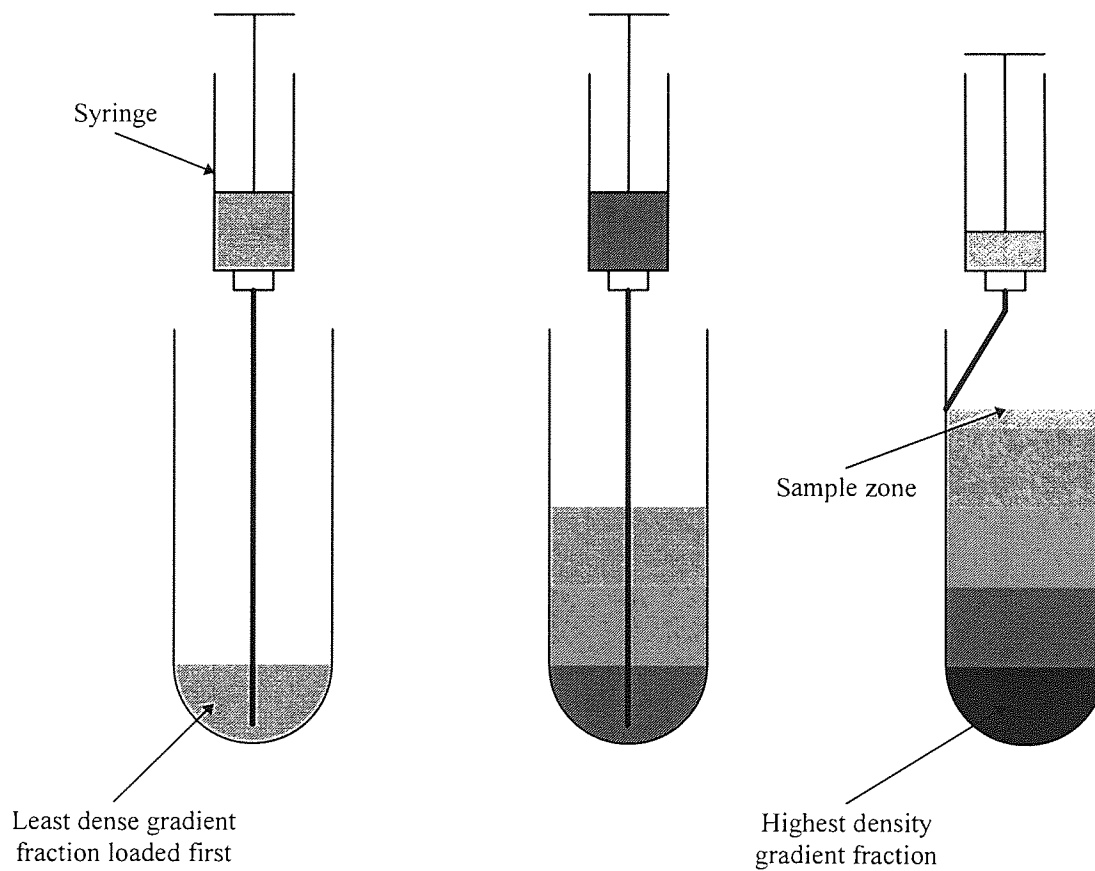


Figure 4.4. The under-layering density gradient technique.

The 'shape' of a gradient refers to its concentration profile, but concentration does not always have a linear relationship with either density or viscosity. The density gradient should be steep enough to provide support to the sedimenting zone during centrifugation. Linear gradients are most commonly used as they often produce the highest resolution of cellular components and proteins ⁽⁵⁹⁾. Convex gradients are used where maximum support is required at the top of the gradient where the sample is loaded, but does not have to be so steep further down the gradient if the sample components are adequately resolved. Concave gradients are mostly used for lipoprotein separation and discontinuous, or step, gradients are used for the separation of whole cells, cellular organelles and viruses ^(3,59).

A step gradient can be used to form a continuous gradient if the gradient solute is readily-diffusible. A step gradient consisting of only two solutions layered in a centrifuge tube will form a continuous, almost linear, gradient after standing for about 24 hours due to the diffusion of the solute ^(57,65). The diffusion process can be increased if more than two steps are used. The diffusion process can be further speeded up if the sealed centrifuge tube is laid horizontally which increases the surface area between the layers, and this allows a continuous gradient to form in about 1 hour ⁽⁶⁵⁾. An apparatus designed to produce a continuous gradient from a step gradient in about 1-2 minutes by rotating the centrifuge tube at a predetermined angle is shown in Figure 4.5.

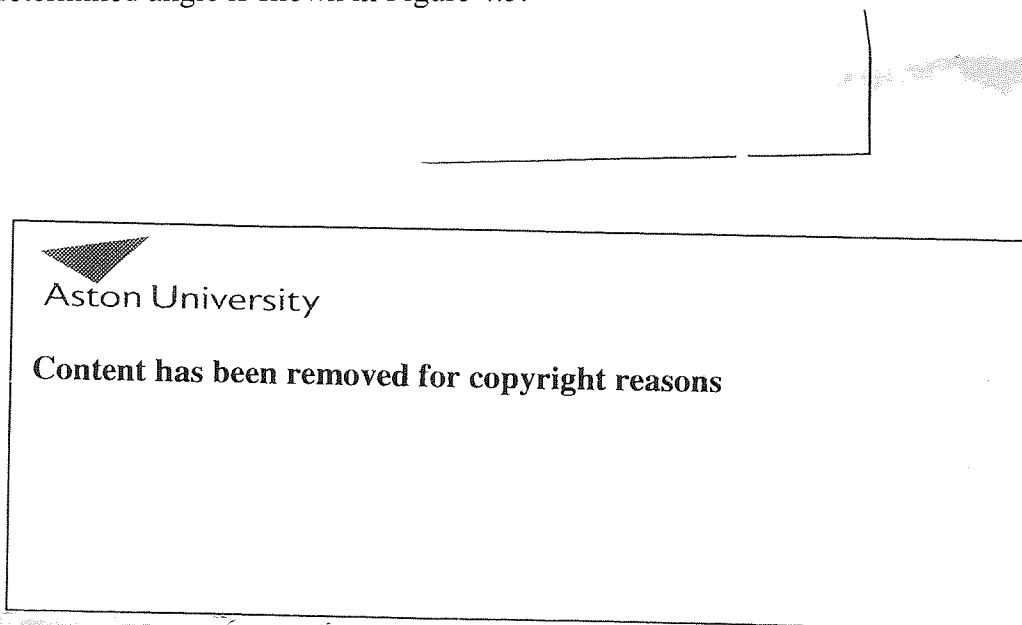


Figure 4.5. The Biocomp Gradient Master automatic continuous gradient former ⁽⁶⁶⁾.

Another method used to speed up the formation of a continuous gradient from a step gradient is to increase the temperature at which the step gradient is incubated. The rise in temperature increases the rate of diffusion of the gradient solute and reduces the time of formation. However, if the temperature is too high convection currents can be introduced, which will adversely affect the profile of the gradient. In this research, continuous gradients were prepared from step gradients at 40°C, and this incubation temperature was found not to adversely affect the gradient profile. Schumaker ⁽⁷⁴⁾ has calculated the time required for continuous gradient formation using the equation:

$$t_D = y^2 / 8D \quad \text{————— (4.1)}$$

where t_D = the time required for continuous gradient formation (seconds).

y = the distance between the initial sharp boundaries (cm).

D = the diffusion coefficient of the gradient solute at the gradient formation temperature ($\text{cm}^2 \text{sec}^{-1}$).

Once the gradient has been formed it will deteriorate due to diffusion. Fortuin ⁽⁸⁵⁾ has reported that the time that a linear gradient will remain stable can be defined as:

$$t_S = b^2 / 100D \quad \text{————— (4.2)}$$

where t_S = the time of stability (seconds).

b = the total gradient length (cm).

4.2.3 Sample loading and convection during rate-zonal centrifugation

Convection in a rate-zonal centrifugation may be defined as any form of mass transport by means other than by sedimentation and diffusion ⁽³⁾. The overloading of the gradient medium with sample material can lead to convection effects as well as 'sinking' of the

material into the gradient, which is known as density inversion. Before any centrifugation is undertaken the maximum sample capacity should be determined. Griffith ⁽⁵⁹⁾ has reported that gradients in swing-out rotors can support most protein samples provided that the ratio between the sample concentration and the starting gradient concentration is 1:10. Griffith also reported the maximum sample volume that can be loaded onto a gradient used in a swing-out rotor system and this value is 10% of the total gradient volume. These values are based on actual experimental data, rather than by theoretical calculations proposed by Svenssen et al ⁽⁸⁶⁾, Berman ⁽⁸⁷⁾ and Spragg and Rankin ⁽⁸⁸⁾, and so these experimentally determined limits have been used during this research. Applying these limits reduces the effects of density inversion and droplet sedimentation, which is described in Chapter 3.

4.2.4 Conditions during centrifugation

It is essential that the speed control and temperature control of the centrifuge is accurate to enable reliable and reproducible centrifugal experiments to be performed. The temperature attainment and control of the Beckman J2-MC centrifuge used in this research is reported in Chapter 3. It is beneficial to the stability of a gradient centrifugation experiment if the acceleration and deceleration periods are as slow as possible to minimise disturbance of the gradient medium and its contents. Ideally, the rotor should be accelerated to 500 r.p.m. as slowly as possible and decelerated from 500 r.p.m. as slowly as possible and this was achievable using the Beckman J2-MC centrifuge, which is programmed to do this automatically. The instrument should be correctly levelled and the rotor balanced to minimise vibration which can instigate droplet sedimentation, as described in Chapter 3.

4.2.5 Recovery of fractions from the gradient

In order to collect the whole gradient in a series of fractions, there are four different methods that can be used; these methods are shown in Figure 4.6. The oldest and simplest method is to pierce the bottom of the centrifuge tube and to collect volumes of the gradient as it drips from the bottom of the tube. This method can be expensive and certain centrifuge tube materials are not easily pierced or crack when pierced, leading to non-ideal leakage. Another method is to place a pipette tip at the top of the gradient and withdraw a fixed volume of liquid from the gradient whilst maintaining the pipette tip at the top of the falling gradient column. This method is simple but requires a high degree of practical ability to ensure that

the gradient is not disturbed, that air is not entrained into the fraction being taken, and that liquid is not removed from below the fraction being taken which would affect the resolution.

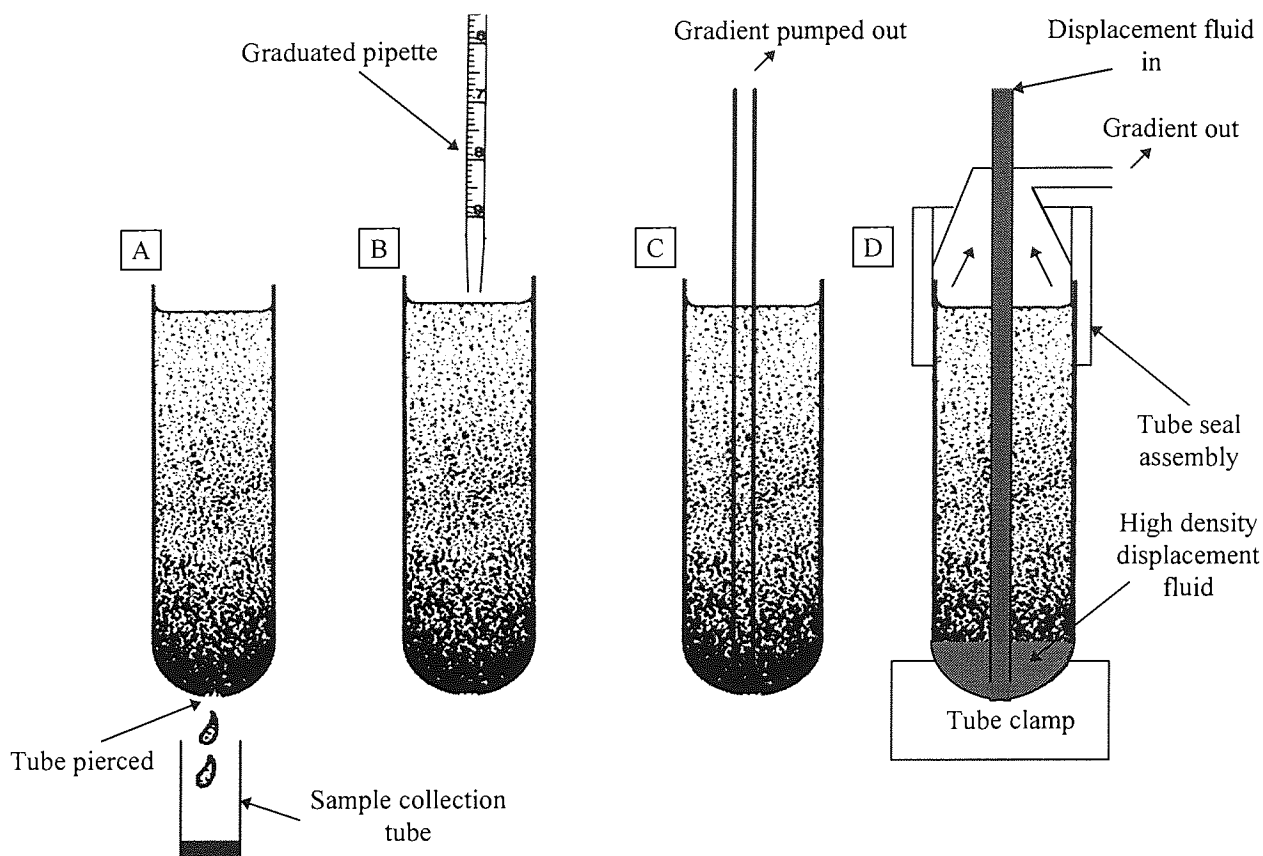


Figure 4.6. Methods for collecting density gradient fractions after centrifugation: A is the tube bottom piercing method; B is the withdrawal of the fractions from the top downwards using a graduated pipette; C is where fractions are removed by being pumped out; and D is the bottom displacement method using a dense liquid.

A pump can be used to remove the gradient via a narrow tube which is carefully lowered to the base of the tube. This method is not normally used because density inversion of the solution occurs during removal and there is a loss of fraction resolution as the liquid passes through the pump ⁽⁶⁵⁾. A technique commonly used is the bottom displacement method where a dense liquid, such as sucrose or fluorocarbons, are pumped to the bottom of the tube which upwardly displaces the gradient via a tapered cap and fractions are collected in collection tubes. In this research, the graduated pipette technique was preferred to the other methods because of its simplicity, after much practice, and the acceptable degree of resolution achieved.

4.2.6 Determining the density gradient profile

The profile of the gradient will be approximately known from the intended shape of the generated gradient. However, it is normal practice to determine the exact nature of the profile by measuring the density of the individual fractions. Accurate measurement of the density of the fractions is required for the calculation of sedimentation coefficients using Equation (3.14). The density of the fractions is normally measured using techniques such as pycnometry and refractive index measurement of the gradient solute concentration in the fractions, which can be converted to density using calibration graphs. In this research refractive index measurements were used to monitor the lactose monohydrate gradient profiles and this is described in detail in Chapter 7. Alternatively, density marker beads can be added to the gradient and these will band in the gradient at a position equal to their density. Density marker beads are available in a wide range of density values and each density value corresponds to a specific bead colour. The position of the beads can be correlated to their expected position if the gradient has successfully formed. Visual observations can be performed on the gradient to monitor the sharpness of the density interfaces if a step gradient is used, or to confirm the absence of interfaces if a continuous gradient is used. Ideally, transparent polycarbonate centrifuge tubes should be used for most centrifugal separations to allow visual monitoring of the separation process. Polycarbonate centrifuge tubes were used for all of the experiments performed during this research, details of which are given in Chapter 7.

4.2.7 Analytical determination of the fraction contents

This depends on the exact nature of the sample applied to the density gradient. Fractions can be analysed using a wide range of analytical techniques which include microscopy, UV/visible spectrophotometry, colorimetric assays, and various chromatographic methods including High Performance Liquid Chromatography (HPLC). The method used is dependent on the nature of the sample to be analysed as well as possible interference caused by the gradient solute used. In this research, a combination of HPLC and protein assay techniques have been used to analyse the fraction composition and these techniques are described in Chapter 7.

4.3 Centrifugation studies with soluble free β -galactosidase using the rate-zonal separation technique

4.3.1 Introduction and Experimental Programme

Chapter 3 describes modified normal-rate centrifugation experiments performed using free β -galactosidase, the reaction system being shown in Figure 3.14. Results presented in Figures 3.15 and 3.16 showed that the enzyme had become distributed throughout the single concentration lactose monohydrate solution contained within the centrifuge tube. This indicated that the enzyme was either non-ideally sedimenting through the substrate as a very broad band, or mixing was occurring due to the inherent instability of a single substrate concentration reaction system. Effects such as droplet sedimentation and mixing during centrifugation are associated with normal-rate separation techniques. The results clearly show that the enzyme movement from the loading position was due to these effects and not produced by the enzyme sedimenting under the influence of the applied centrifugal forces. The almost uniform distribution of the galacto-oligosaccharides, shown in Figure 3.15, confirms this conclusion. A more stable reaction environment was required that would minimise the effects of droplet sedimentation and mixing; the system that achieves this is rate-zonal, or density gradient, centrifugation. Such systems should confirm that the applied centrifugal force was sufficient to produce sedimentation of the enzyme.

Before any active enzyme reactions were performed, the formation and stability of the lactose monohydrate gradient was investigated. The continuous gradient formation time, t_D , for lactose monohydrate was determined both theoretically and practically. The time of stability of the gradient, t_S , was also determined theoretically and practically. The stability of the gradient during centrifugation at 40°C was investigated by comparison to identical gradients incubated in a waterbath at the same temperature. β -galactosidase was then loaded on top of the lactose monohydrate density gradient and centrifuged using the highest centrifugal forces attainable with the swing-out system used. The movement of the enzyme was monitored by protein assay and the gradient profile determined after varying centrifugation run times. Finally, β -galactosidase was layered within the gradient to increase the enzyme's radial position and increase the initial applied centrifugal forces.

4.3.2 Density and viscosity of lactose monohydrate solutions

The density and viscosity of aqueous lactose monohydrate solutions up to 40%^{w/v} were determined at 40°C, so that the physical properties of the gradient fractions taken after centrifugation could be characterised. Determination of the density and viscosity of individual fractions would also allow the calculation of sedimentation coefficients using Equation (3.13). The analytical procedures used to determine the density and viscosity of lactose monohydrate solutions are detailed in Chapter 7. The relationship of viscosity to lactose monohydrate concentration at 40°C is shown in Figure 4.7.

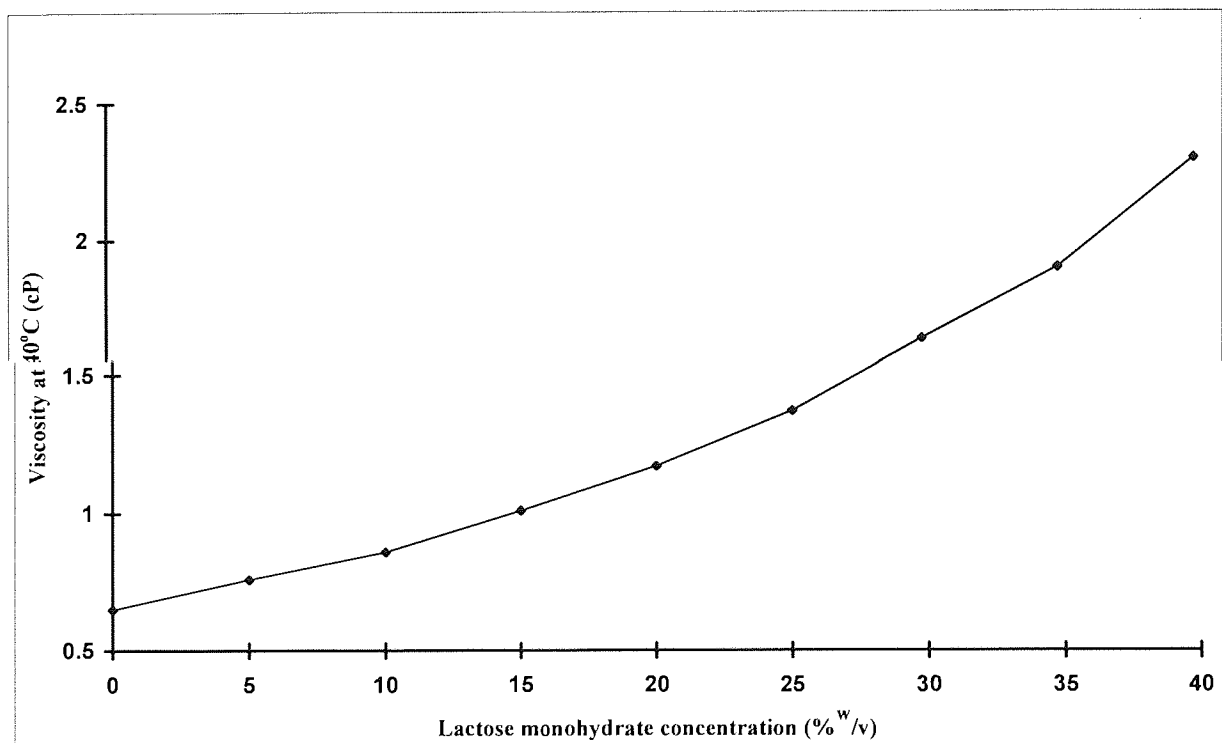


Figure 4.7. The relationship of viscosity to lactose monohydrate concentration at 40°C.

Figure 4.7 shows the non-linear relationship between viscosity and lactose monohydrate concentration. The relationship of density to lactose monohydrate concentration at 40°C is shown in Figure 4.8. Figure 4.8 shows that there is a linear relationship between density and lactose monohydrate concentration. By determining the total sugar content of the fractions collected after a reaction and taking these values to be lactose monohydrate, reasonably

accurate fraction density and viscosity values can be obtained by using the data presented in Figures 4.7 and 4.8.

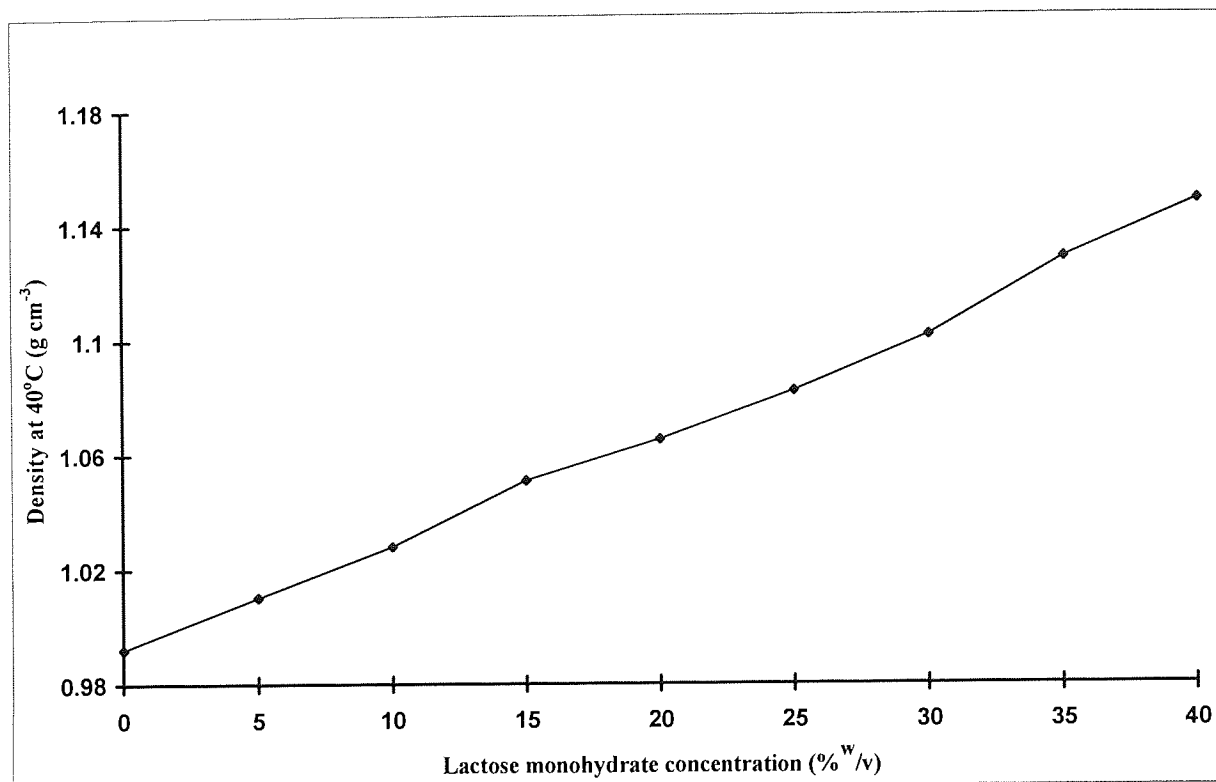


Figure 4.8. The relationship of density to lactose monohydrate concentration at 40°C.

4.3.3 Reaction system sedimentation coefficients

A knowledge of the sedimentation coefficients for the enzyme, substrate and products was required to ensure that the sedimenting enzyme was effectively separated from the reaction products allowing no further enzymatic reactions to take place in the reacted zone, as shown in Figure 4.2. The larger the sedimentation coefficient for the enzyme compared to the substrate and products the greater the separation. Providing that the centrifuge equipment used can generate high enough centrifugal forces, then the differences in the sedimentation coefficients can be exploited to produce an effective bioreaction and separation system.

4.3.3.1 β -Galactosidase sedimentation coefficient

A review of the literature revealed no instances of a sedimentation coefficient for free β -galactosidase, isolated from *Aspergillus oryzae*, being reported. Determination of the sedimentation coefficient was not possible because of the unavailability of an analytical ultracentrifuge. The operational limitations of the centrifugation equipment used in this research did not allow the sedimentation coefficient of free β -galactosidase to be estimated. However, Halsall⁽⁸⁹⁾ developed a series of empirical equations based on the Atassi-Ghandi relationship. This relationship links the sedimentation coefficients of proteins to their molecular weight and Halsall produced equations that extended the relationship to a wider range of molecular weights. If the molecular weight of a protein is known, then an estimate of its standard sedimentation coefficient can be calculated. β -Galactosidase from *Aspergillus oryzae* has a reported molecular weight of 90 000 daltons⁽³⁶⁾. For proteins with a molecular weight in the range of 1.7×10^4 to 4.9×10^7 the following equation is given:

$$S_{w,20} = 0.00242 M^{0.67} \quad \text{————— (4.3)}$$

where $S_{w,20}$ = the standard sedimentation coefficient (Svedbergs).
M = the molecular weight of the protein.

If the molecular weight for β -galactosidase is inserted into Equation (4.3), then a standard sedimentation coefficient of 5.05 Svedbergs is obtained. This value compares closely to an expected value based on the data presented in Table 3.2.

4.3.3.2 Carbohydrate sedimentation coefficients

This research has been concerned with the enzymatic activity of β -galactosidase on lactose monohydrate and the resulting products formed. In Chapter 2, it was shown that depending on the reaction conditions, the products formed were identified as galacto-oligosaccharides (di-, tri- and tetra-), glucose and galactose. A review of the literature revealed no instances of sedimentation studies being performed on these compounds or on lactose monohydrate

itself. However, sedimentation coefficients have been determined on similar compounds and this allows for the estimation of sedimentation coefficient values. The standard sedimentation coefficient ($S_{w,20}$) of sucrose, a disaccharide of glucose and fructose, was determined by LaBar and Baldwin⁽⁹⁰⁾ and found to be around 0.276 Svedbergs. This value can be used as an estimate for lactose monohydrate and for other disaccharides. Setford⁽³⁾ determined the standard sedimentation coefficient of fructose to be around 0.280 Svedbergs; this value can be used as an approximate one for glucose and galactose. The almost identical sedimentation coefficients reported for a monosaccharide and a disaccharide indicate that the sedimentation coefficients for galacto-oligosaccharides would be very similar to these values. For the purposes of this research, the standard sedimentation coefficient for galacto-oligosaccharides was estimated to be 0.276 Svedbergs, as this value is for a disaccharide which is the closest comparable compound for which sedimentation data are available.

4.3.3.3 Comparison of the reaction system sedimentation coefficients

In Section 4.3.3.1, the estimated standard sedimentation coefficient for β -galactosidase from *Aspergillus oryzae* was calculated to be 5.05 Svedbergs. In Section 4.3.3.2, the estimated values for lactose monohydrate, glucose, galactose and galacto-oligosaccharides were 0.276, 0.280, 0.280 and 0.276 Svedbergs respectively. Providing that high enough centrifugal forces can be generated, the differences in the enzyme sedimentation coefficient value compared to the substrate and reaction products values should allow effective separation of the enzyme from the reaction zone. However, the almost identical sedimentation coefficient values for the substrate and reaction products should prevent separation of these compounds.

4.3.4 The formation and stability of lactose monohydrate density gradients

Before any active enzyme reactions were performed, it was necessary to determine the formation time (t_D) and the stability time (t_S) for the lactose monohydrate density gradients used in this research. For these centrifugation experiments to be reproducible, the continuous profile of the density gradient should be fully formed and this should remain stable during the duration of the experiment.

4.3.4.1 The formation time (t_D) and the stability time (t_S) for a 10 to 40%^{w/v} lactose monohydrate continuous density gradient at 40°C

For the active enzyme centrifugation experiments performed at 40°C, a 10 to 40%^{w/v} lactose monohydrate continuous density gradient was used, and so the formation time and stability time for such a gradient was determined. A step gradient consisting of 10, 15, 20, 25, 30 and 40%^{w/v} lactose monohydrate solutions (6 cm³ of each concentration) was generated at 40°C using the under-layering technique, shown in Figure 4.4. Duplicate sets of centrifuge tubes filled with the step gradients were either incubated at 40°C in a waterbath or centrifuged at 13 000 r.p.m (26 122 g max) at 40°C for varying times. At 0, 30, 60, 90 and 180 minutes sets of tubes were removed from both the waterbath and the centrifuge. Fractions were taken from the tubes, and the lactose monohydrate gradient profile was determined by refractive index measurements of the fractions; full experimental details are given in Chapter 7. The results obtained for the waterbath incubated gradients are shown in Figure 4.9 and the results obtained for the centrifuged gradients are presented in Figure 4.10. A comparison of the two sets of results is shown in Figure 4.11.

The results presented in Figures 4.9, 4.10 and 4.11 clearly show that at 40°C the initial step profile forms a continuous gradient between 0 to 30 minutes, although slight degeneration occurs at the top of the gradient. The gradients maintain an acceptable continuous profile up to 180 minutes, but increasing degeneration of the top end of the gradient occurs after 30 minutes. The similarity of the waterbath incubated gradients to the centrifuged gradients demonstrated that the centrifugation process did not drastically affect the gradient stability. These results show that ideally the step gradient should be allowed to form a continuous gradient over a period of 30 minutes before an enzyme zone is layered on top of it, and that centrifugation experiments could be run for a further 150 minutes without significant degeneration of the gradient. These findings can be compared to calculated values for the gradient formation time (t_D) and the gradient stability time (t_S) using equations (4.1) and (4.2). After under-layering the density gradient solutions a sharp boundary between successive solutions was not visible. The theoretical distance between the sharp boundaries (y) was calculated to be 1.2 cm and the gradient length (b), measured immediately after under-layering at 40°C, was found to be 7.4 cm. The diffusion coefficient (D) for lactose monohydrate at 40°C was determined, by extrapolation of values obtained from the literature, to be $0.66 \times 10^5 \text{ cm}^2 \text{ sec}^{-1}$, details of which are shown in Figure 4.12.

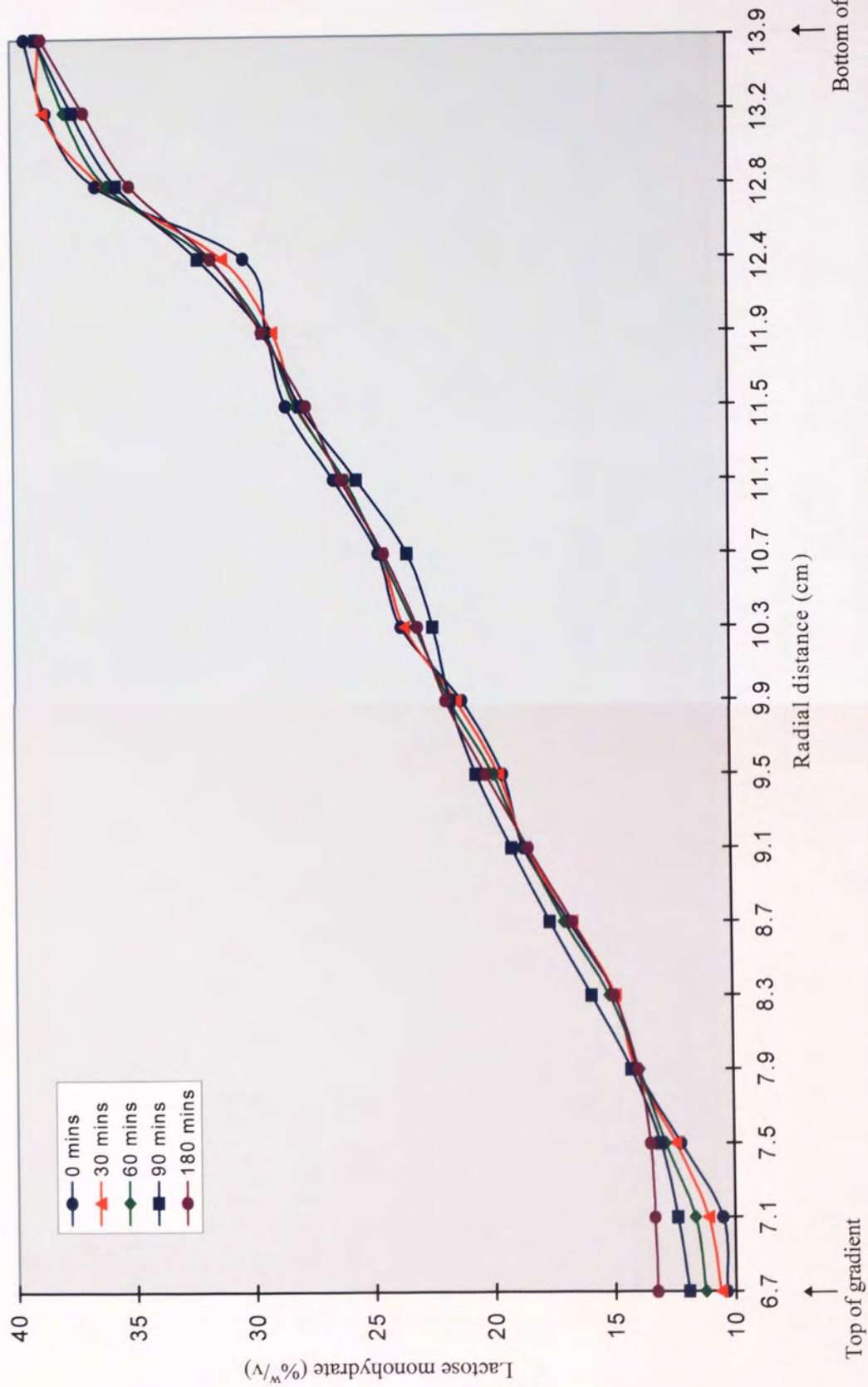


Figure 4.9. The profiles for an under-layered lactose monohydrate (10 to 40%^w/_v) step gradient incubated in a waterbath for 0, 30, 60, 90 and 180 minutes, at 40°C.

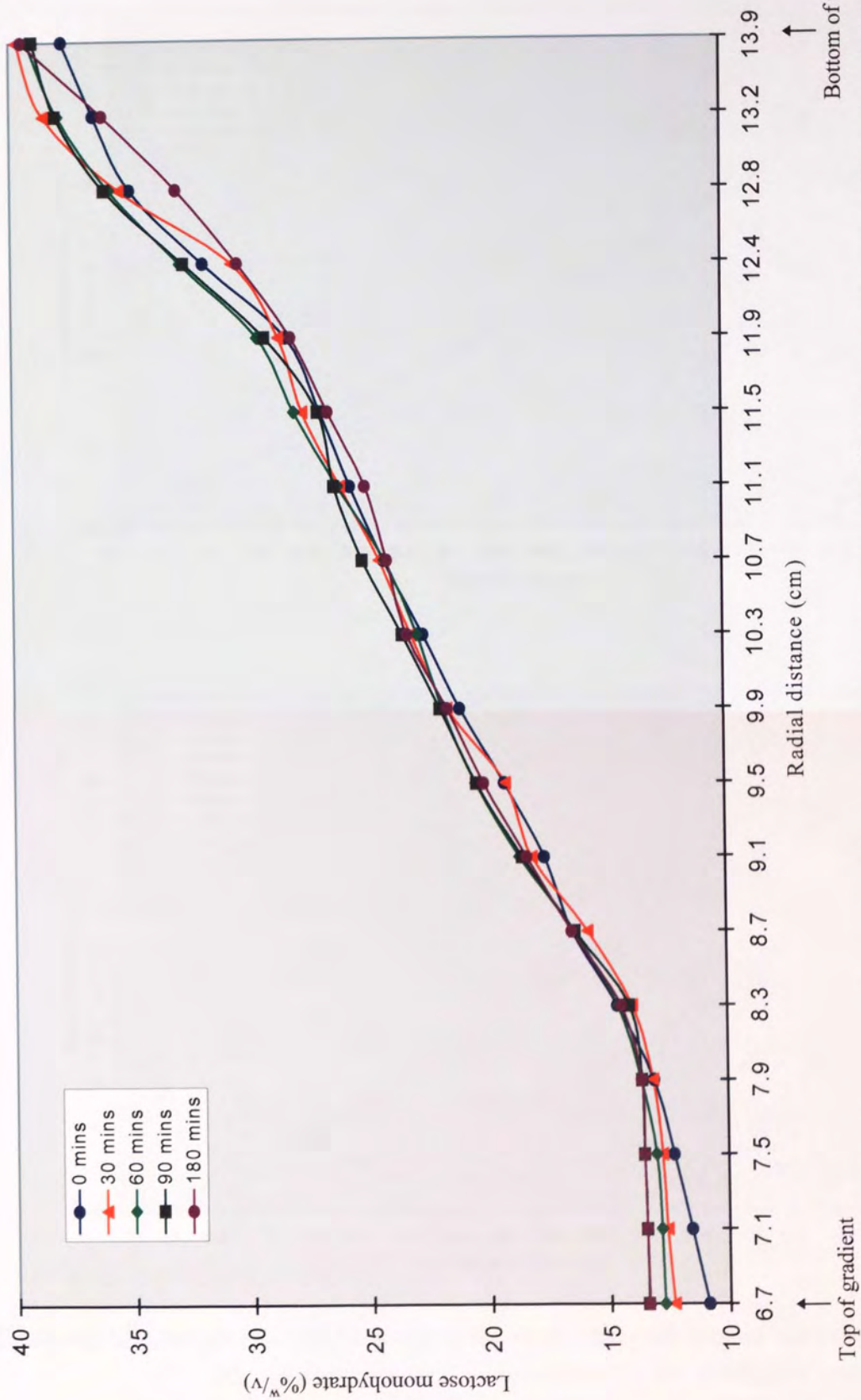


Figure 4.10. The profiles for an under-layered lactose monohydrate (10 to 40%^{w/v}) step gradient centrifuged at 13 000 r.p.m (26 122 g max) for 0, 30, 60, 90 and 180 minutes, at 40°C.

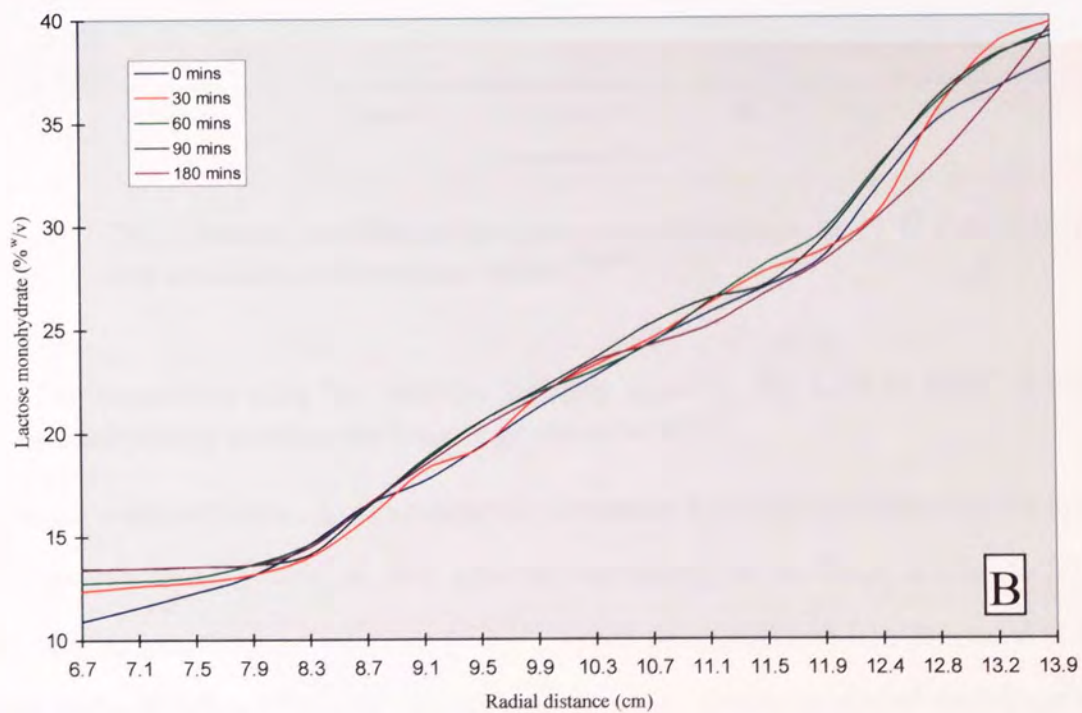
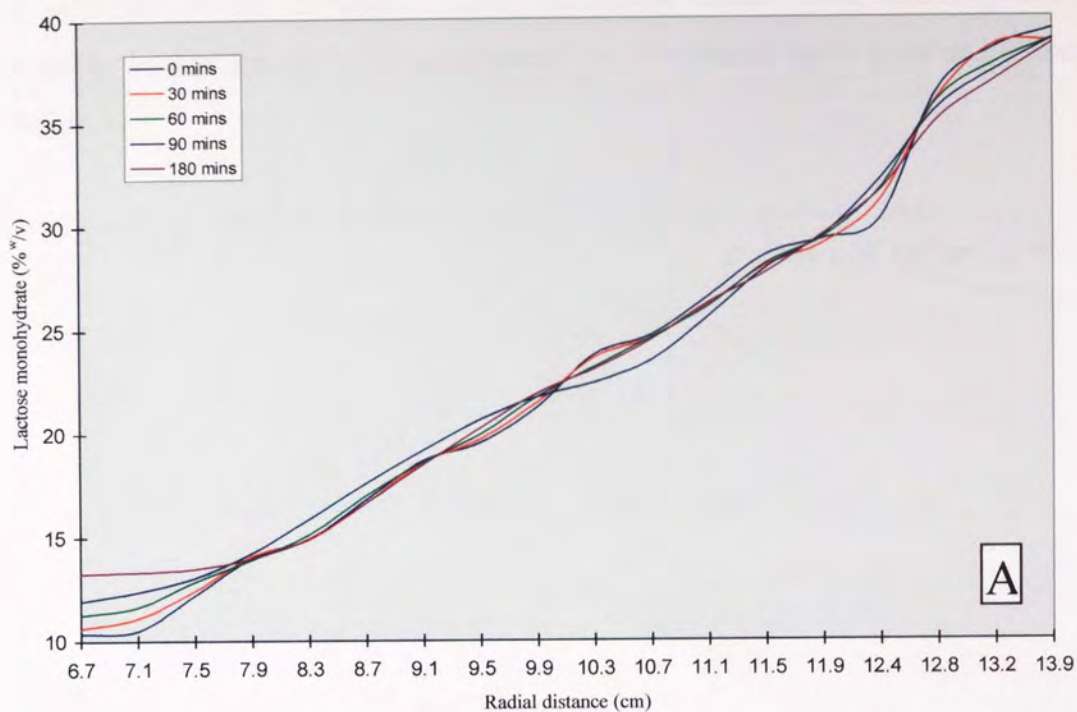


Figure 4.11. Comparison of the profiles for under-layered lactose monohydrate (10 to 40%^{w/v}) step gradients, A corresponds to gradients incubated in a waterbath for 0, 30, 60, 90 and 180 minutes, at 40°C (Figure 4.9), and B corresponds to gradients centrifuged at 13 000 r.p.m (26 122 g max) for 0, 30, 60, 90 and 180 minutes, at 40°C (Figure 4.10).

The gradient formation time (t_D) was calculated to be 8 hours and the gradient stability time (t_S) was calculated to be 23 hours. These calculated values differ radically from the experimentally determined value for t_D between 0 to 30 minutes and a t_S value between 30 to 60 minutes.

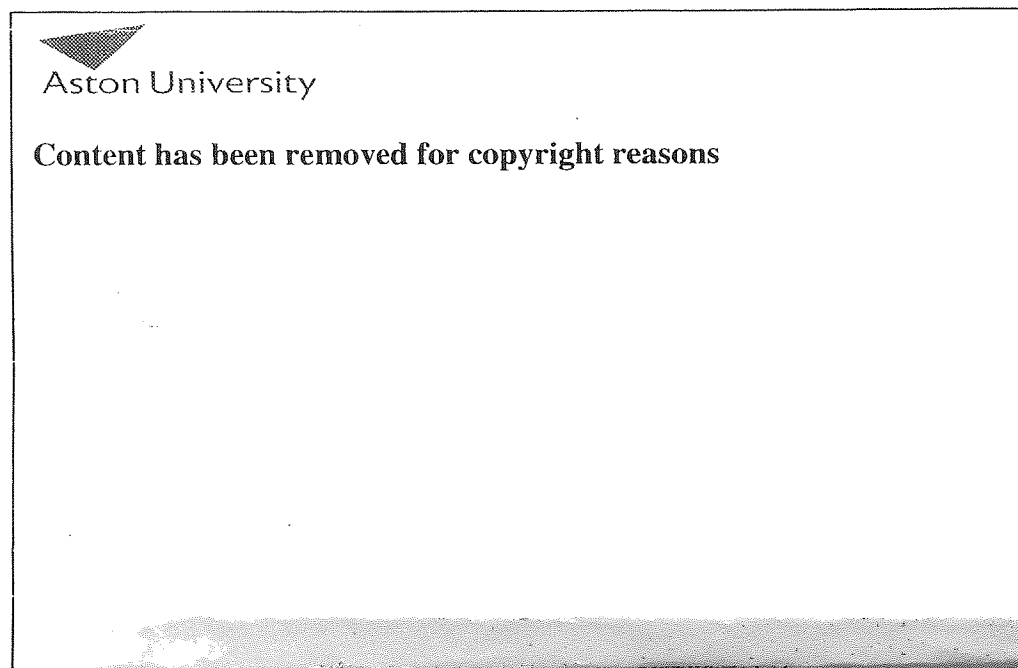


Figure 4.12 The diffusion coefficient for lactose monohydrate at 40°C determined by extrapolation of literature values ^(91,92).

4.3.4.2 The formation time (t_D) and the stability time (t_S) for a 20 to 40%^{w/v} lactose monohydrate continuous density gradient at 40°C

Experiments were performed to determine the formation time and stability time for a 20 to 40%^{w/v} lactose monohydrate. A step gradient consisting of 20, 22.5, 25, 27.5, 30 and 40%^{w/v} lactose monohydrate solutions (6 cm³ of each concentration) was generated at 40°C using the under-layering technique, shown in Figure 4.4. Duplicate sets of centrifuge tubes filled with the step gradients were centrifuged at 13 000 r.p.m at 40°C for varying times. At 0, 30, 60, 90 and 180 minutes sets of tubes were removed from the centrifuge. Fractions were taken from the tubes and the lactose monohydrate gradient profile was determined by refractive index measurements of the fractions; full experimental details are given in Chapter 7. The results obtained for the centrifuged gradients are presented in Figure 4.13.

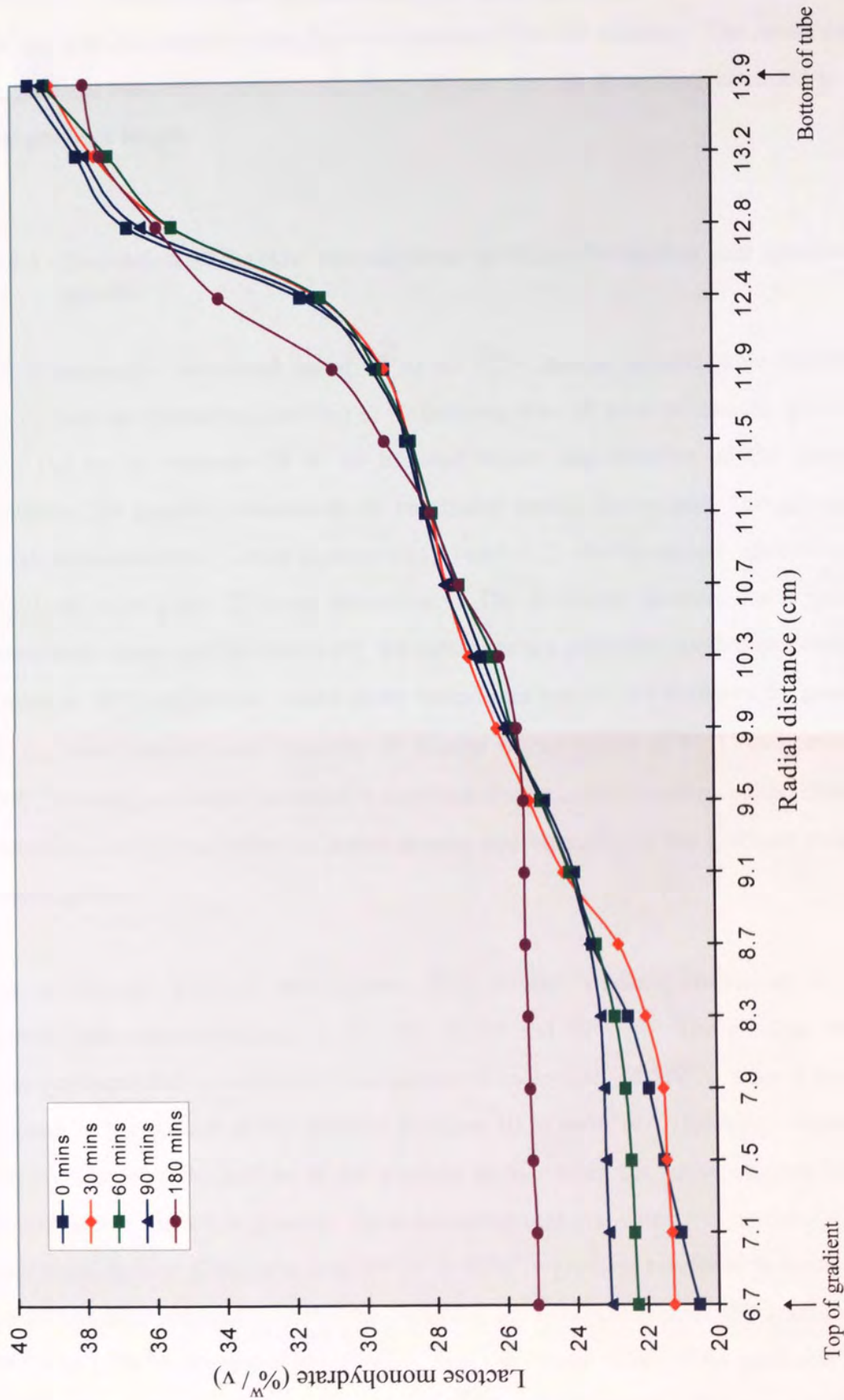


Figure 4.13. The profiles for an under-layered lactose monohydrate (20 to 40%^{w/v}) step gradient centrifuged at 13 000 r.p.m (26 122 g max) for 0, 30, 60, 90 and 180 minutes, at 40°C.

Figure 4.13 shows that the gradient formation time (t_D) occurred between 0 to 30 minutes and the gradient stability time (t_S) was between 30 to 60 minutes. The decay of the top of the gradient was very marked and after 180 minutes the decay had extended to half of the total gradient length.

4.3.4.3 Discussion of lactose monohydrate gradient formation and gradient stability results

The experiments performed using 10 to 40 %^w/v lactose monohydrate density gradients determined the formation time (t_D) to be between 0 to 30 minutes and the gradient stability time (t_S) to be between 30 to 60 minutes before degeneration of the gradient began. However, the gradient maintained an acceptable profile for at least 150 minutes after the initial formation time. Using Equations (4.1) and (4.2), the theoretical value of t_D and t_S was calculated to be 8 and 23 hours respectively. The difference between the experimental and theoretical values may be due to (a) the equations are generally applied to density gradients formed at 20°C and below, where sharp boundaries are formed between the gradient layers, (b) the lower density and viscosity of lactose monohydrate at 40°C compared to that at 20°C, allowing mixing of successive solutions during under-layering and no sharp boundary formation, and (c) the effect of lower density and viscosity on the gradient stability during centrifugation.

The continuous gradient was formed from a step gradient consisting of the lactose monohydrate concentrations, 10, 15, 20, 25, 30 and 40%^w/v. The gradient concentration steps corresponded to increases in the lactose monohydrate of 5%^w/v, except for the 10%^w/v increase at the bottom of the gradient between 30 to 40%^w/v. This larger incremental step was positioned at the bottom of the gradient so that when the active enzyme is centrifuged the maximum support is given to the sedimenting material when it is exposed to the highest centrifugal forces. Comparison of the 10 to 40%^w/v gradient results with those obtained for the 20 to 40%^w/v gradient showed that reducing the concentration of the gradient steps from 5%^w/v to 2.5%^w/v decreased the stability. Similar results obtained for gradients incubated in a waterbath at 40°C and those centrifuged at 13 000 r.p.m. (26 122 g max) at 40°C showed that the centrifugal process did not adversely affect the gradients, except for a slight loss of

stability at the top of the gradient. Based on these findings a 10 to 40%^{w/v} lactose monohydrate density gradient was used for the free β -galactosidase centrifugation studies.

4.3.5 Top-layering of soluble free β -galactosidase on a 10 to 40%^{w/v} lactose monohydrate continuous density gradient

Experiments performed on the lactose monohydrate density gradients showed that the 10 to 40%^{w/v} gradient would produce the most stable reaction environment for the active enzyme centrifugation experiments. Also, this concentration range would favour the formation of galacto-oligosaccharides. A 10 to 40%^{w/v} lactose monohydrate density gradient (6 x 6 cm³) was prepared at 40°C, as described in Chapter 7. β -Galactosidase (1 cm³ of 5 mg cm⁻³, 16 U cm⁻³) was layered on top of the gradient and centrifuged at 13 000 r.p.m (26 122 g max) for 0, 30, 90 and 180 minutes, at 40°C. At the completion of the run times the tubes were removed and fractions were taken. The movement of the enzyme was determined using the Bio-Rad protein assay, described in detail in Chapter 7, and the gradient profile was obtained by refractive index measurements of the fractions taken. It is assumed that the protein concentration determined is primarily due to β -galactosidase and the protein concentration is therefore referred to as β -galactosidase, although it is recognised that other contaminating enzymes and non-enzymatic proteins may contribute to the total protein concentration. The movement of β -galactosidase in the lactose monohydrate density gradient is shown in Figure 4.14.

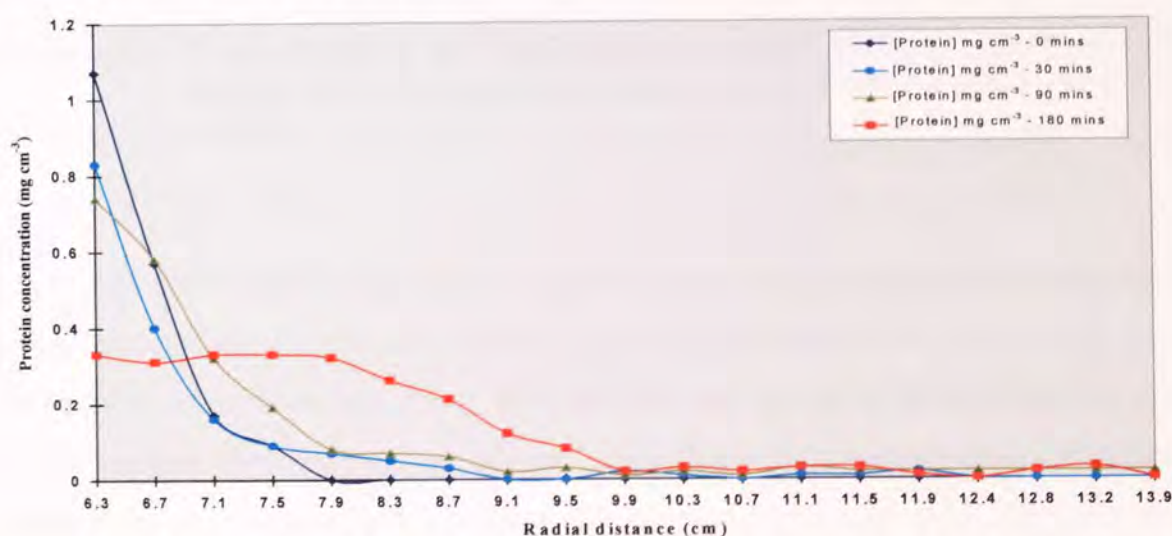


Figure 4.14. The movement of β -galactosidase (5 mg cm⁻³, 16 U cm⁻³) top-layered on a 10 to 40%^{w/v} lactose monohydrate density gradient and centrifuged at 13 000 r.p.m (26 122 g max) for 0, 30, 90, and 180 minutes, at 40°C.

Figure 4.14 shows that β -galactosidase moved from the top loading position and into the density gradient. As the centrifugation time increased the protein progressed further into the gradient. However, as clearly shown at 180 minutes the enzyme movement was as a very broad band and the band had a comparatively uniform plateau region extending back to the original loading position. Typically, a Gaussian-like profile would have been expected if the enzyme was sedimenting 'ideally'. A comparison of the protein profile at 180 minutes with the density gradient profile at 180 minutes is shown in Figure 4.15.

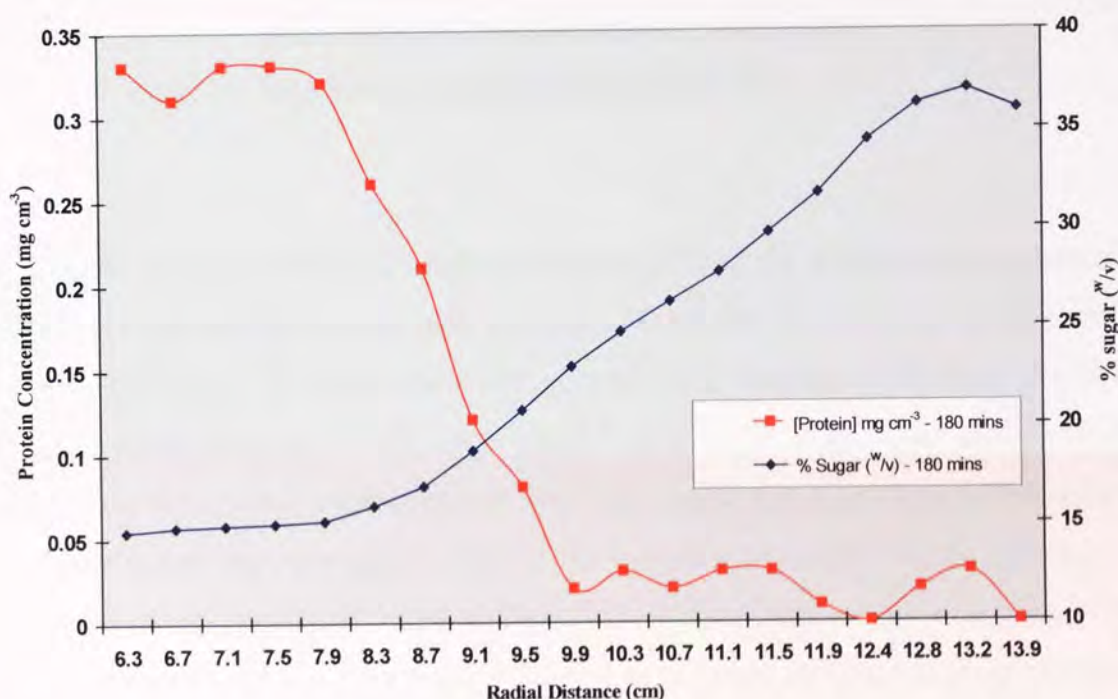


Figure 4.15. Comparison of the β -galactosidase profile with the density gradient profile after 180 minutes centrifugation at 13 000 r.p.m (26 122 g max), at 40°C.

Figure 4.15 shows that the flat plateau region obtained for β -galactosidase mirrors the flat region obtained for the density gradient. This clearly shows that the majority of the enzyme's movement was not due to sedimentation but caused by the degeneration of the density gradient after 180 minutes. A small proportion of the β -galactosidase did sediment ahead of this zone degeneration but this was probably due to droplet sedimentation or to the enzyme being 'carried' by contaminant particulate matter present originally in the top layer. It can be concluded from these results that the centrifugal forces applied to the top-layered

β -galactosidase solution at 13 000 r.p.m. (26 122 g max) was insufficient to sediment the enzyme faster than the degeneration of the lactose monohydrate density gradient. The range of centrifugal forces applied to the top-layered lactose monohydrate density gradients can be calculated using the following equation:

$$\text{RCF} = 11.12 r \left(\frac{\text{r.p.m.}}{1000} \right)^2 \quad \text{--- (4.4)}$$

where RCF = relative centrifugal force (g).

r = radial distance from the centre of rotation (cm).

r.p.m = the rotation speed (rotations per minute).

The distance from the centre of rotation to the middle of the top-layered β -galactosidase zone was 6.3 cm and the distance from the centre of rotation to the bottom of the centrifuge tube was 13.9 cm. If these values are inserted into Equation (4.4) then the relative centrifugal force range at 13 000 r.p.m was 11 840g to 26 122g. The centrifugal force applied to the top-layered β -galactosidase zone was insufficient to produce sedimentation of the enzyme faster than the degeneration of the lactose monohydrate density gradient. To increase the initial centrifugal forces applied to the enzyme zone, it must be placed further from the centre of rotation. This can be achieved by reducing the gradient length or layering the enzyme within the density gradient. Reducing the gradient length, whilst maintaining the concentration range, decreases the gradient stability time and adversely affects the gradient resolution. To maintain the gradient stability time and resolution, layering of the β -galactosidase within the lactose monohydrate density gradient was the preferred option.

4.3.6 Layering of soluble free β -galactosidase within a 10 to 40%^{w/v} lactose monohydrate density gradient

A 10 to 40%^{w/v} lactose monohydrate density gradient was prepared at 40°C as for the previous experiments, except that a 5 mg cm⁻³ (16 U cm⁻³) β -galactosidase solution (2 cm³), prepared using 17.5%^{w/v} lactose monohydrate, was under-layered between the 15%^{w/v} and 20%^{w/v} lactose monohydrate solutions during the preparation of the step gradient. Full

experimental details are given in Chapter 7. This increased the distance from the centre of rotation from 6.3 cm to 8.7 cm, which increased the initial relative centrifugal force applied from 11 840g to 16 350g. This corresponded to a 38% increase in the initial centrifugal force applied. The layered gradients were centrifuged at 13 000 r.p.m. for 0 and 180 minutes at 40°C. At the end of each experiment fractions were taken and analysed for protein and sugar content, so that the β -galactosidase distribution and the gradient profile could be determined. A comparison of the protein distributions within the centrifuge tubes after 0 and 180 minutes centrifugation at 13 000 r.p.m., at 40°C, is given in Figure 4.16. The protein content was assumed to be primarily β -galactosidase and the protein concentration is therefore referred to as β -galactosidase, but it is recognised that contaminating enzymes and non-enzymatic proteins may contribute to the protein content.

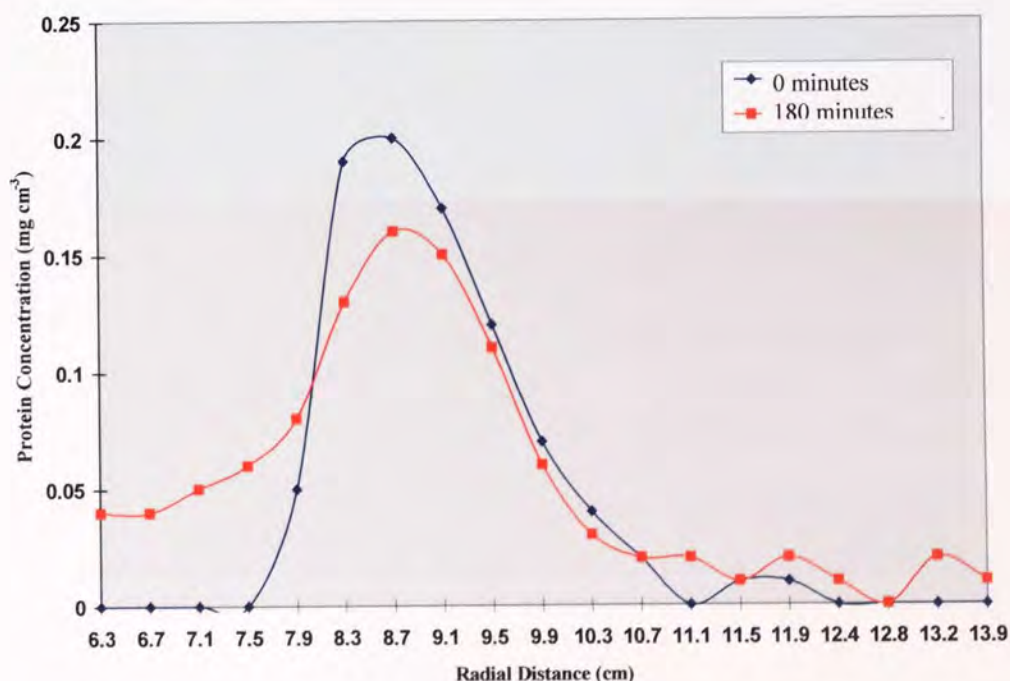


Figure 4.16. Comparison of the β -galactosidase distribution profiles for 10 to 40%^{w/v} lactose monohydrate density gradients layered with β -galactosidase (5 mg cm^{-3} , 16 U cm^{-3}) in 17.5%^{w/v} lactose monohydrate and centrifuged at 13 000 r.p.m. (26 122 g max) for 0 and 180 minutes, at 40°C.

Figure 4.16 clearly shows that the majority of the β -galactosidase layered into the gradient remained at the loading position even after centrifugation at 13 000 r.p.m. for 180 minutes. A small proportion of the enzyme did sediment to the bottom of the tube but this was

probably due to droplet sedimentation and also to the enzyme being 'carried' by its association with particulate matter in the enzyme solution. A significant amount of the enzyme moved backwards towards the top of the gradient and this was caused by the degradation of the gradient profile after 180 minutes. A comparison of the profiles for β -galactosidase and the density gradient after centrifugation at 13 000 r.p.m. for 180 minutes, at 40°C, is shown in Figure 4.17. Figure 4.17 shows a clear correlation between the backward movement of the enzyme and the degradation of the top of the gradient. When the uniform lactose monohydrate concentration at the top of the gradient reached the top of the layered enzyme zone it produced an unstable region, which allowed mixing of the enzyme within this unstable region. This is a similar effect to that reported with experiments performed using the modified normal rate technique, described in Chapter 3.

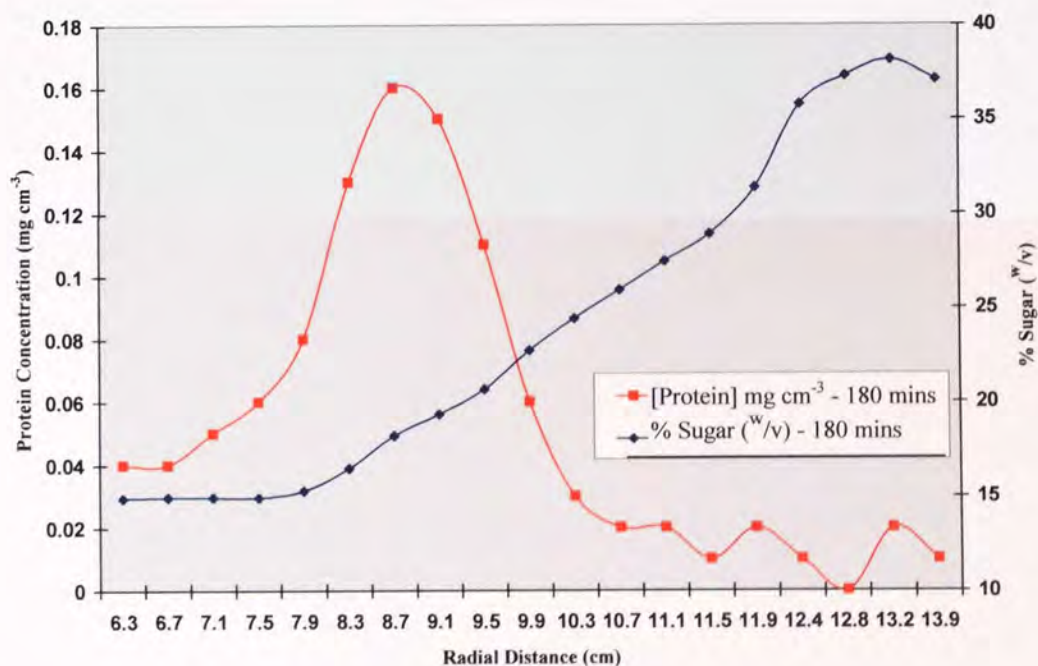


Figure 4.17 Comparison of β -galactosidase and density gradient distribution profiles after centrifugation at 13 000 r.p.m (26 122 g max) for 180 minutes, at 40°C.

4.3.7 Discussion of results

The results obtained from the experiments performed showed that the range of applied centrifugal forces used was insufficient to produce sedimentation of free β -galactosidase through a 10 to 40%^{w/v} lactose monohydrate density gradient at a rate that exceeded the

degradation of the gradient. To increase the sedimentation rate, either the individual size or the density of the enzyme particles must be increased, or the range of applied centrifugal forces needs to be increased. The applied centrifugal forces used were the maximum possible due to the limitations of the centrifuge and the rotor system used. Without upgrading the equipment used, the sedimentation of the enzyme can be increased by either immobilising the enzyme onto a 'carrier' material or by insolubilising the enzyme using a cross-linking agent. Both of these approaches effectively increase the size and the density of the enzyme particles and therefore increase the sedimentation rate. Increasing the sedimentation rate allows the enzyme to sediment through the density gradient without being affected by any degradation of the gradient. Immobilisation or insolubilisation also aid visualisation of the sedimenting enzyme and make recovery and re-use simpler. The preparation and use of immobilised and insolubilised β -galactosidase for rate-zonal centrifugation studies is presented in Chapter 5.

5.0 RATE-ZONAL CENTRIFUGATION USING IMMOBILISED AND INSOLUBILISED β -GALACTOSIDASE

In this chapter, the principles of enzyme immobilisation and insolubilisation are discussed. The practical considerations of both techniques are described. Centrifugal studies performed with immobilised and insolubilised β -galactosidase, and using rate-zonal centrifugation are presented.

5.1 Introduction

An immobilised enzyme is one which has been attached to, or enclosed by, an insoluble support medium, or carrier. Insolubilisation is where the enzyme molecules are chemically cross-linked to each other and form complexes that are insoluble in the liquid medium, and where the protein constitutes the bulk of the complex⁽⁹³⁾. There are four main methods for immobilising enzymes and these are; adsorption, covalent binding, entrapment, and membrane confinement. A diagrammatic representation of the main methods of enzyme immobilisation is shown in Figure 5.1.

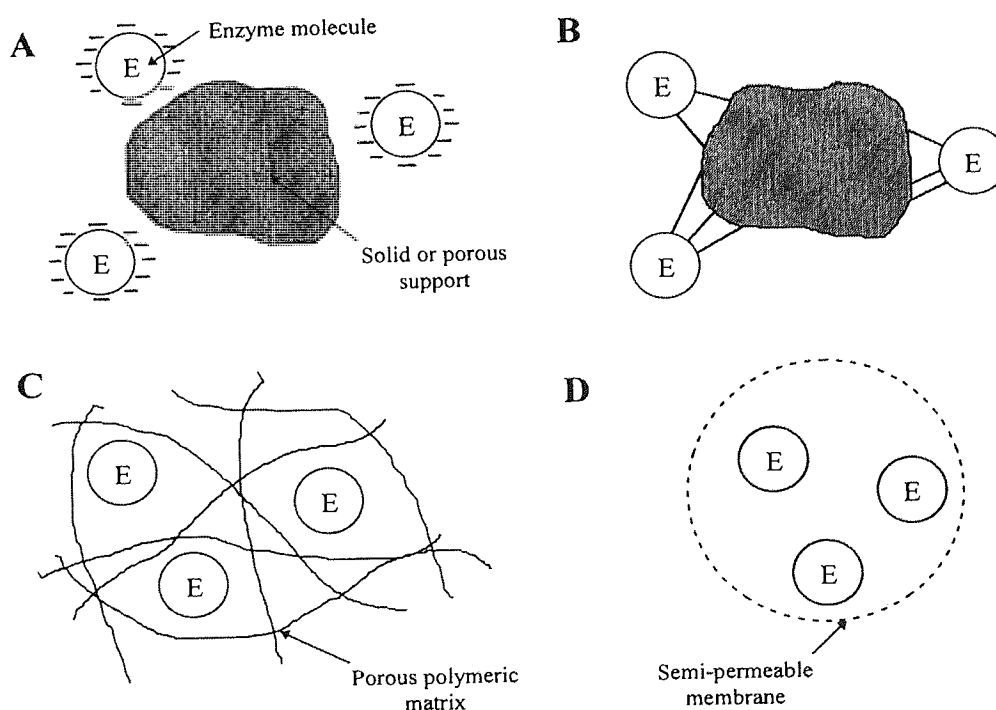


Figure 5.1. Different methods of enzyme immobilisation; A is adsorption, B is covalent binding, C is entrapment, and D is membrane confinement.

Insolubilisation of an enzyme is effected by using a chemical cross-linking agent and this is shown diagrammatically in Figure 5.2.

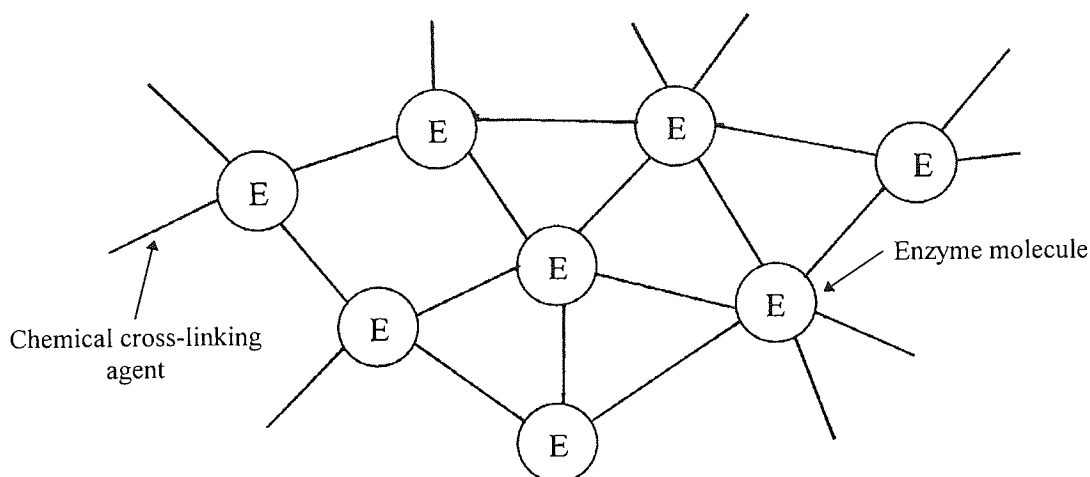


Figure 5.2. Enzyme insolubilisation using a chemical cross-linking agent.

Enzyme immobilisation or insolubilisation adds additional cost to an enzymatic reaction process and is only undertaken if the benefits exceed the extra expense. The main benefits include: easier separation of the enzyme from the reaction products, reduced downstream processing costs, recovery and re-use of the active enzyme, the reduction of the quantity of enzyme used, and a possible increase in the stability and activity of the enzyme^(48,93). The possible disadvantages of immobilisation and insolubilisation include: the process of immobilisation or insolubilisation may involve the use of highly toxic compounds, complex protocols may be required, the loss of enzyme activity and specificity, surface charge repulsion of the substrate from the immobilised/insolubilised enzyme's micro-environment, and a reduction in the enzyme activity due to internal and external diffusion effects.

Experimental results presented in Chapter 4 showed that the centrifugation equipment used was unable to generate sufficiently high centrifugal forces to effect the sedimentation of soluble free β -galactosidase before the degradation of the reaction environment occurred. According to Stokes' Law, represented by equation (3.3), the sedimentation rate of a particle is proportional to the square of its diameter and also proportional to the difference that exists

between the density of the particle and the density of the liquid medium. By using immobilisation or insolubilisation the sedimentation rate of an enzyme can be substantially increased due to the apparent increase in the size and density of the enzyme particles. Increasing the sedimentation rate of an enzyme allows it to be sedimented through a substrate using lower rotation speeds, and hence lower applied centrifugal forces. Reducing the rotation speed required to sediment the enzyme allows a low speed or high speed centrifuge to be used instead of a super-speed centrifuge or an ultracentrifuge. The cost of low speed or high speed centrifuges is significantly less than that of a super-speed centrifuge or an ultracentrifuge, the former can cost less than £10K compared to £20K+ for the latter. Applying lower centrifugal forces allows the rotor to be constructed from aluminium, instead of titanium which is required if very high centrifugal forces are used. A typical aluminium rotor costs approximately £4K compared to a titanium rotor which costs in the region of £14K. Immobilisation or insolubilisation of an enzyme also allows visualisation of the enzyme as it sediments through the substrate and aids in its recovery and re-use.

5.2 Methods of immobilisation and insolubilisation

In this section, the main methods used to immobilise or insolubilise enzymes are discussed and the advantages and disadvantages of each technique are reported.

5.2.1 Adsorption

In 1916, Nelson and Griffin were the first to immobilise an enzyme using the adsorption technique⁽⁹⁴⁾. They adsorbed the enzyme invertase on to activated charcoal without any significant loss in the enzyme activity. Adsorption is the simplest of the immobilisation techniques for producing a water-insoluble enzyme/support conjugate. It consists of mixing an aqueous solution of an enzyme with a surface-active adsorbent at a suitable pH, followed by washing the conjugate to remove any non-adsorbed enzyme^(93,94). The enzyme forms weak linkages to the adsorbent due to Van der Waals forces and hydrogen bonding. Van der Waals forces are produced due to the electron charge cloud around a molecule not being perfectly symmetrical. At any particular moment, there is more negative charge on one side of a molecule than on the other side, and therefore the molecule possesses an instantaneous electric dipole. This dipole induces dipoles in neighbouring molecules of an opposite charge and this produces a weak induced dipole-induced dipole attraction⁽⁵⁶⁾. This attraction is sufficient to weakly bind the enzyme to the support material.

Hydrogen bonding is produced when an hydrogen atom is attached to highly electronegative elements, such as N, O and F, and the shared pair of electrons in the covalent bond is drawn towards the electronegative atom. The hydrogen atom has no electrons, except for its share of the covalent bond which is drawn towards the electronegative atom. The hydrogen atom has no inner shell of electrons and the single proton in the nucleus is available to form a dipole-dipole attraction with an unshared pair of electrons on another electronegative atom⁽⁵⁶⁾. In an aqueous environment, hydrogen bonding allows strong intermolecular bonds to be formed between the enzyme and the support material. Table 5.1 lists support materials commonly used for immobilisation of enzymes by adsorption.

Support Material	Enzyme Immobilised
------------------	--------------------

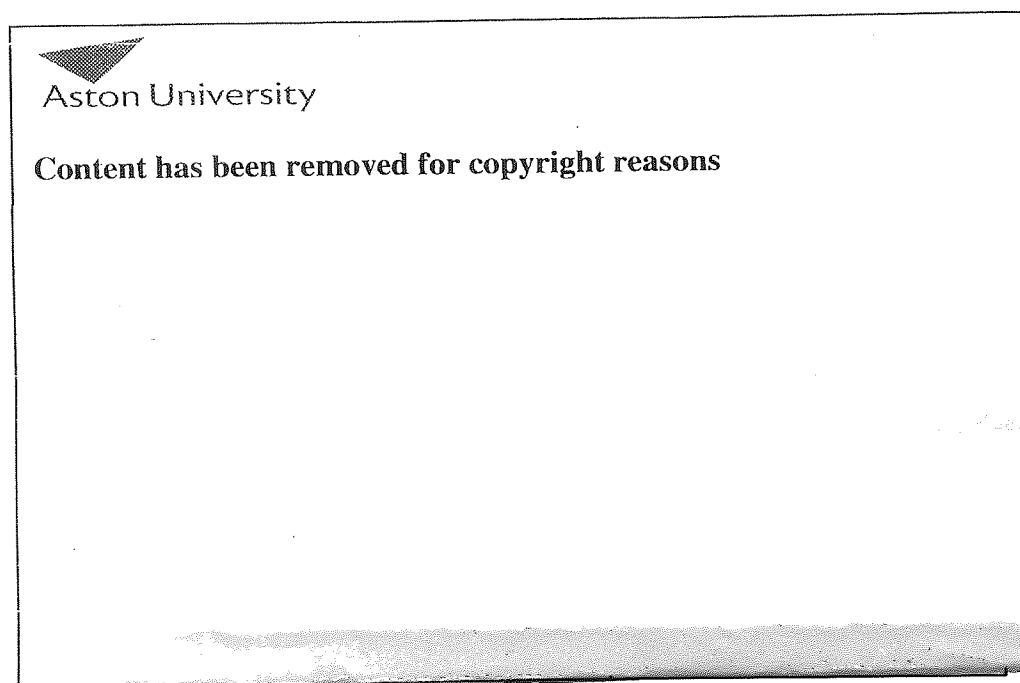


Table 5.1. Support materials commonly used for enzyme adsorption⁽⁹⁴⁾.

5.2.1.1 Activity of adsorbed enzymes

The activity of adsorbed enzymes can vary from low activity, to values very similar to that obtained for the soluble free enzyme⁽⁹³⁾. The enzyme loading on the support is affected by the pH at which adsorption takes place. The adsorption of β -fructofuranosidase (invertase)

to DEAE-Sephadex (diethylaminoethyl group $(-\text{OC}_2\text{H}_5\text{NH}(\text{C}_2\text{H}_5)_2)$ attached to cross-linked dextran), and CM-Sephadex, (carboxymethyl group $(-\text{OCH}_2\text{CO}_2^-)$ attached to cross-linked dextran), is an example of the pH dependence of enzyme adsorption. Table 5.2 shows the % binding of β -fructofuranosidase (400U cm^{-3}) to DEAE-Sephadex and CM-Sephadex (both 50mg) at various pH values ⁽¹⁹⁾.



Aston University

Content has been removed for copyright reasons

Table 5.2. The % binding of β -fructofuranosidase to DEAE-Sephadex and CM-Sephadex at varying pH ⁽¹⁹⁾.

Adsorption of an enzyme to a support material can produce loadings of up to 1g of enzyme per gram of support (1g g^{-1}) ^(19,93). A review of the literature showed that the activity of an adsorbed enzyme is dependent upon the support material used and by varying the support used improvements in the activity can be achieved.

5.2.1.2 Stability and reversibility of adsorption

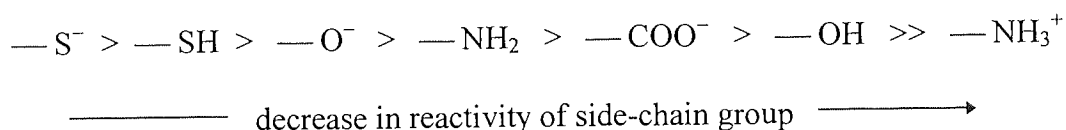
Depending on the specific enzyme and support material used the thermal stability of adsorbed enzyme can be increased, decreased, or remain unchanged. The storage stability of adsorbed enzymes varies depending upon the enzyme/support system used, but usually they are stable for several weeks if stored at 4°C ⁽⁹³⁾. Theoretically, the adsorption process can be reversed by changing the pH, ionic strength, or temperature of the enzyme/support environment. Reversibility of adsorption is not always possible and this is demonstrated by the irreversible binding of urease to kaolinite ^(93,95).

5.2.1.3 Advantages and disadvantages of immobilisation by adsorption

The main advantages of immobilisation using adsorption are: the simplicity, the extensive range of charged support materials, no toxic chemicals are required to effect immobilisation, and the immobilisation process does not usually produce inactivation of the enzyme. The disadvantages of this method include: the correct pH, ionic strength and temperature for successful adsorption must be determined; desorption of the enzyme can occur at high substrate concentrations or if physical changes in the reaction environment occur; there is no protection against microbial degradation; and contaminants may become adsorbed to the support.

5.2.2 Covalent binding

Covalent binding produces more permanent linkages between the enzyme and the support material compared to adsorption. The binding occurs due to the sharing of electrons between protein side-chain nucleophiles and nuclei on the surface of the support material. The propensity of the side-chain nucleophiles to form covalent bonds depends upon their state of protonation, or charged status and this is given by the following relationship:



The amino acid, lysine, is the most useful group for covalent linkage of an enzyme to an insoluble support, mainly due to its exposure on the enzyme's surface, its high reactivity, and the fact that it is rarely located in an enzyme's active site⁽¹⁹⁾. The formation of the covalent bonds between the enzyme and the support material should be performed under mild reaction conditions, which ensure that the majority of the activity is retained after immobilisation.

5.2.2.1 Covalent bond formation between enzymes and support materials

There are three main approaches used to covalently link enzymes to water-insoluble support materials and these are:

1. Linkage of the enzyme to a reactive polymer, where no activation of the support material is required.
2. Linkage of the enzyme to an activated polymer, where the polymer has been activated by chemical conversion of a functional group, and this is followed by the addition of the enzyme.
3. Formation of an activated polymer by chemical conversion of a functional group in the presence of the enzyme.

An example of a reactive polymer used as a support is maleic anhydride copolymer. This copolymer usually consists of maleic anhydride with ethylene or styrene. On the addition of an enzyme to the copolymer covalent bonds are formed between the maleic anhydride and amino acid groups on the enzyme's surface ⁽⁹⁴⁾; this process is shown in Figure 5.3. 1, 6 Diaminohexane is added to enhance the cross-linking of the polymer chains to produce a highly insoluble enzyme/support conjugate. This method has been successfully used to immobilise enzymes such as alcohol dehydrogenase, papain and trypsin ⁽⁹³⁾.

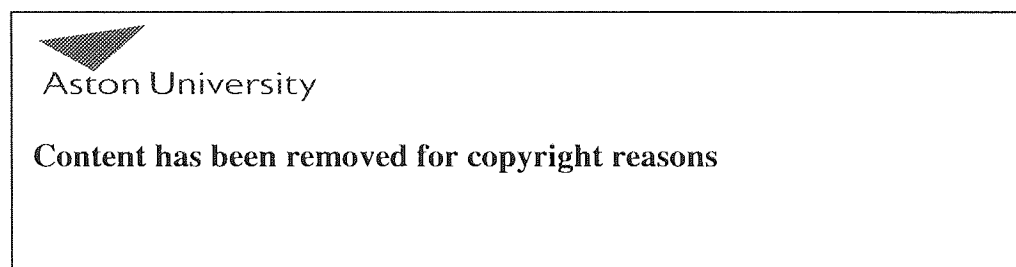


Figure 5.3. Enzyme immobilisation using maleic anhydride copolymer ⁽⁹⁴⁾.

The most common method used for immobilising an enzyme on a research-scale is the use of a chemically activated polymer support, which when prepared is mixed with the enzyme to produce covalent linkages. The support material most often used is Sepharose, poly (β -1,3-D-galactose- α -1,4-(3,6-anhydro)-L-galactose, which has been activated using cyanogen

bromide. The hydroxyl groups of Sepharose combine with the cyanogen bromide to yield the reactive cyclic imido-carbonate. This reacts with amino acid groups on the enzyme under slightly alkaline conditions (pH~9); the two-stage reaction system is shown in Figure 5.4. This method has been used successfully to immobilise enzymes such as β -amylase, β -galactosidase and trypsin ^(93,94,96,97,98).

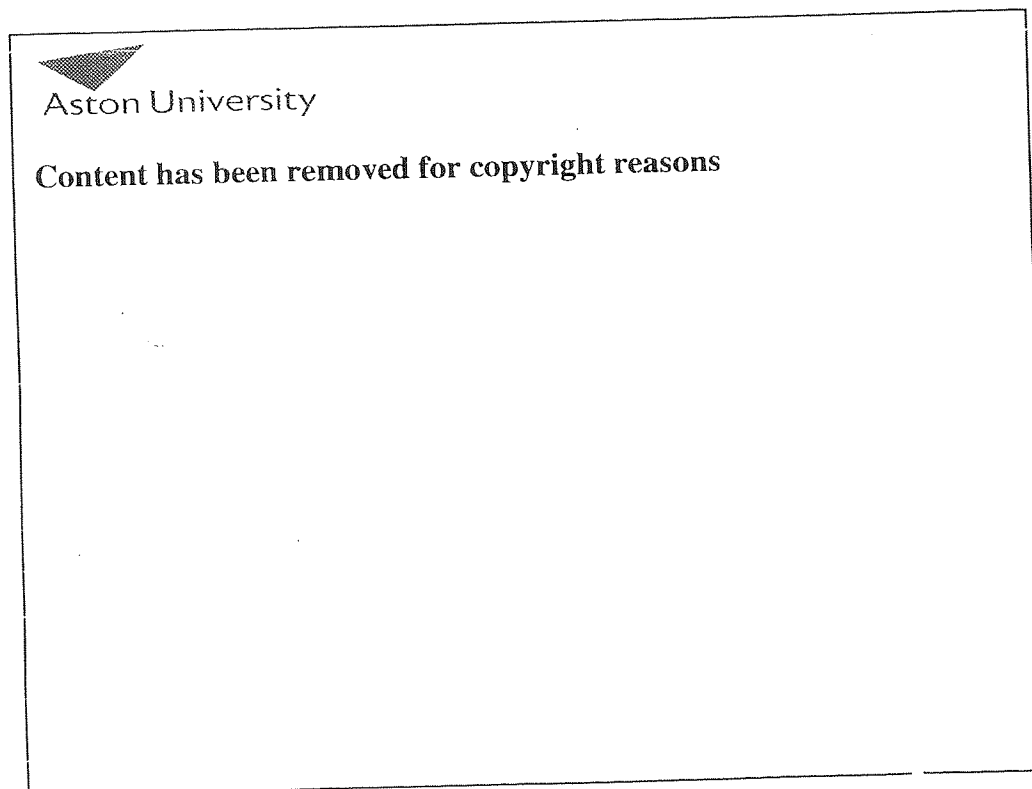
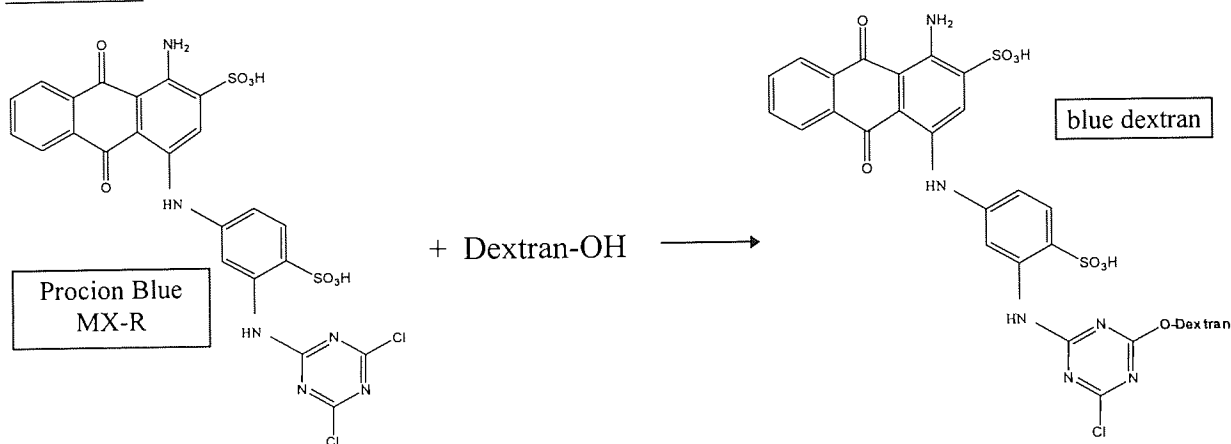


Figure 5.4. Enzyme immobilisation using cyanogen bromide activated Sepharose ⁽⁹³⁾.

Cyanogen bromide is a highly toxic compound and therefore Sepharose beads are normally purchased ready-activated, although this is very expensive. A less hazardous and cheaper method is the covalent linkage of an enzyme to a triazine dye activated support. Reactive triazine-based dyes, such as Cibacon Blue F3G-A and Procion Blue MX-R, have been extensively used in affinity chromatography to bind dehydrogenases and other enzymes ⁽⁹⁹⁾. The dye is bound to a support material by a triazine bond, which is formed by the reaction of

hydroxyl groups on the support with chloride groups on the dye. The enzyme binds to the immobilised dye by a coupling reactions between amino acid groups on the enzyme's surface, usually lysine, and the activated carbon of the triazine molecule^(93,99). Procion Blue MX-R, 1-amino-4-[3-(4,6-dichlorotriazin-2-ylamino)-4-sulfophenylamino]anthroquinone-2-sulfonic acid, binds to dextran to form blue dextran. Under suitable reaction conditions blue dextran is capable of forming covalent bonds with numerous enzymes, although the maximum loading is extremely variable⁽⁹⁹⁾. The activation of dextran by Procion Blue MX-R and the resulting enzyme coupling is shown in Figure 5.5.

Activation:



Coupling:

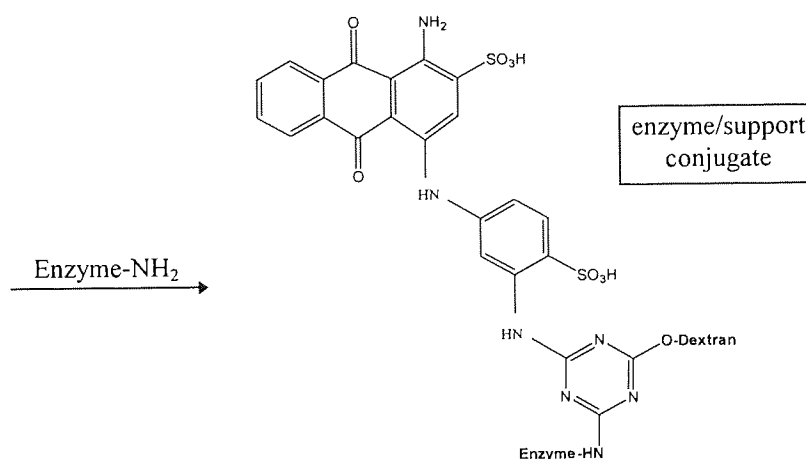


Figure 5.5. Enzyme immobilisation using Procion Blue MX-R activated dextran.

5.2.2.2 Activity of covalently bound enzymes

The activity of enzymes covalently bound to insoluble matrices can vary from low activity to values approaching that obtained for the free soluble enzyme ⁽⁹³⁾. Only small amounts of enzyme can be immobilised on to a support material using this technique; usually loadings of ~0.02g of enzyme per gram of support (0.02g g⁻¹) are produced, and this is substantially less than that produced using adsorption techniques ⁽¹⁹⁾.

5.2.2.3 Stability of covalently bound enzymes

Covalently bonded enzymes are extremely stable due to the strength of the binding between the enzyme and the support material, and very little leakage of the enzyme from the support occurs. Most covalently bound enzymes exhibit enhanced pH and thermal stabilities ⁽⁹³⁾. The storage stability varies depending on the particular enzyme/support used, but usually they are stable for several months if stored at temperatures between 0 to 5°C ⁽⁹³⁾.

5.2.2.4 Advantages and disadvantages of immobilisation using covalent binding

The main advantages of immobilisation using covalent binding are: the binding force between the enzyme and the support is extremely strong and there is very little enzyme leakage, diffusional effects are minimal, and the enzyme/support conjugate produces very few operational difficulties during use. The main disadvantages of this method include: the possible difficulty of preparation, the potential high cost of preparation, the selective applicability, and the potential for microbial degradation.

5.2.3 Entrapment

Enzyme molecules can be physically entrapped within the interstitial spaces of a polymerised gel lattice, or within a semi-permeable membrane. Entrapment of an enzyme within a semi-permeable membrane is also known as microencapsulation. Entrapment allows suitably sized substrate and product molecules to transfer across and within a gel matrix or membrane, whilst preventing the enzyme from permeating from these structures. The pore size of the gel can be controlled by the degree of cross-linking that is allowed to take place, and the degree of crosslinking is determined by the proportions of the reactants used. In

1963, Berfeld and Wan⁽¹⁰⁰⁾ were the first to successfully use the lattice entrapment method to immobilise the enzymes β -amylase, papain and trypsin within cross-linked polyacrylamide, and this is still the most widely used method for enzyme entrapment. Another entrapment method involves the use of high molecular weight dextran, which is a polymer predominantly of α ,-1,6 glucose monomeric units. High molecular weight dextran has been shown to form particles when in aqueous solution^(3,101). If this dextran is added to an enzyme-containing aqueous solution particles are formed that entrap the enzyme molecules. In 1964, Chang⁽¹⁰²⁾ developed an interfacial polymerisation method to microencapsulate urease within a nylon semi-permeable membrane. In 1970, Sessa and Weissman⁽¹⁰³⁾ developed a microencapsulation method using liposomes. Liposomes consist of amphipathic lipids, such as phosphatidyl choline and cholesterol, which can form membranes around water droplets containing soluble enzyme/s. A proportion of the enzyme remains within the aqueous phase contained within the membrane and the rest is incorporated into the membrane structure⁽⁴⁶⁾.

5.2.3.1 Methods for enzyme entrapment and microencapsulation

The most popular method used for the entrapment of enzymes is the use of polyacrylamide. An aqueous solution of acrylamide is mixed with N,N-methylene-bisacrylamide (BIS) in the presence of the enzyme, as well as with reaction initiators and accelerators. The reaction scheme is shown in Figure 5.6.

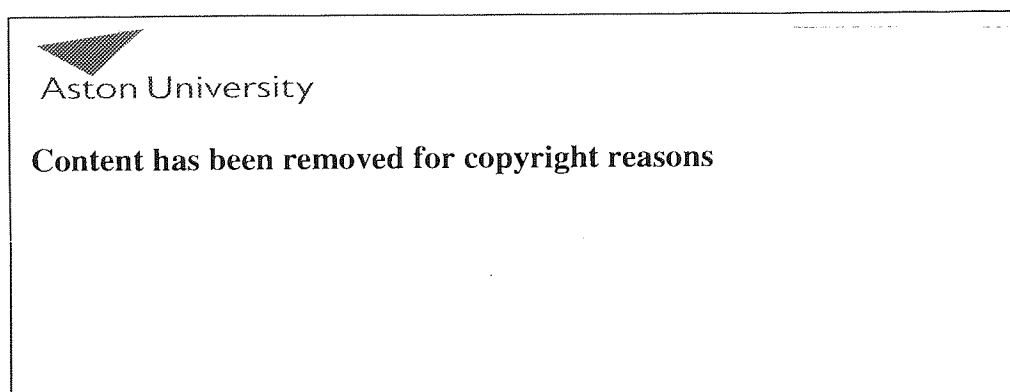


Figure 5.6. The reaction scheme for polyacrylamide formation (without stoichiometry)⁽⁴⁶⁾.

The lattice structure produced by the formation of polyacrylamide contains interstitial spaces which entrap enzyme molecules. The polyacrylamide entrapment method has been successfully used to immobilise a wide range of enzymes that includes aminoacylase, glucose oxidase, invertase, trypsin, and urease^(93,94). Dextran entrapment relies upon the property of high molecular weight dextran to form gel-like particles in aqueous solution. Dextran contains around 95% α 1-6 glucopyranose linkages and 5% α 1-3 glucopyranose linkages⁽³⁾. The α 1-6 linkages produce a linear monomeric chain, whilst α 1-3 linkages form branches from the linear chain^(3,101). The structure of dextran is shown in Figure 5.7.

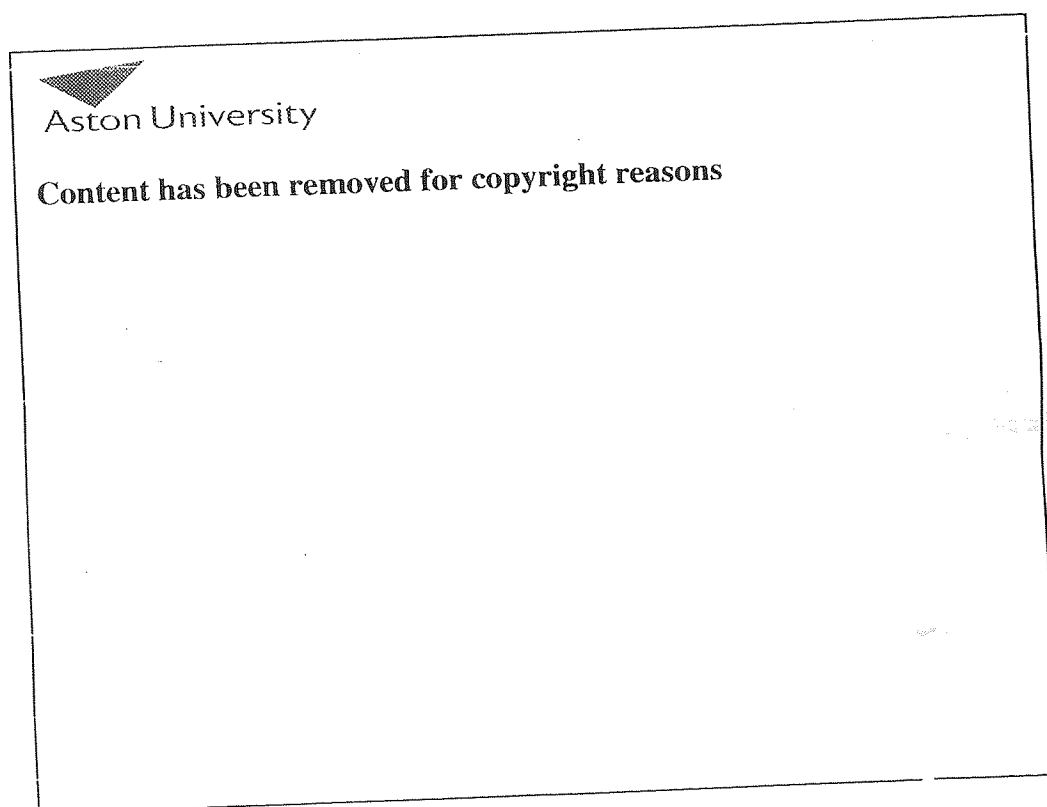


Figure 5.7. The chemical structure of dextran⁽³⁾.

High molecular weight dextran has a filamentous structure which when in aqueous solution undergoes hydrogen bonding between the C₃ hydroxyl groups. Intramolecular and

intermolecular hydrogen bonding produces dextran particles which can physically entrap enzyme molecules within the interstitial spaces; also hydrogen bonding between the dextran and the enzyme can occur. The entrapment of an enzyme within dextran particles has been demonstrated with the enzyme dextransucrase⁽³⁾.

The microencapsulation method developed by Chang⁽¹⁰²⁾ involves the formation of semi-permeable nylon membranes. An aqueous solution of both the enzyme and the hydrophilic monomer 1,6-diaminohexane is added to a chloroform/cyclohexane mixture. An emulsion is formed by vigorous stirring of the mixture, and to this is added the hydrophobic monomer sebacoyl chloride. Polymerisation of the monomers take place at the interface between the organic and aqueous solvents, and this produces spherical semi-permeable membranes containing the enzyme. Typically, the diameter of the nylon spheres range in size from 10 to 200 μm ^(46,93,94). A diagrammatic representation of enzyme-containing nylon microspheres is shown in Figure 5.8.

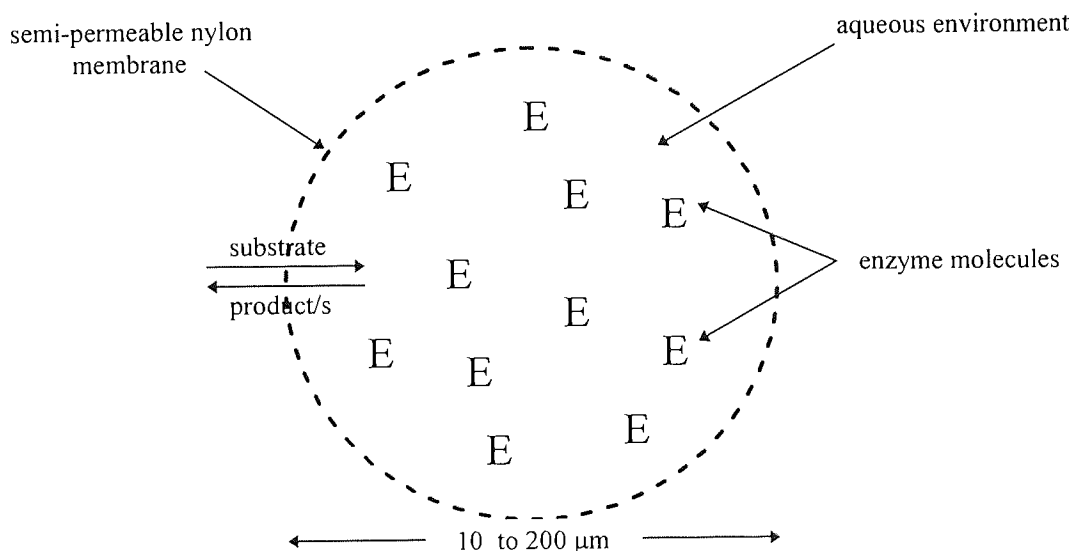


Figure 5.8. The microencapsulation of enzyme molecules in a semi-permeable nylon membrane.

The nylon microencapsulation method has been successfully used to immobilise the enzymes asparaginase, urease, and trypsin^(93,94).

Liposome membranes are made up of amphipathic lipids, such as phosphatidyl choline (lecithin), which are lipids that contain hydrophilic and hydrophobic regions. The hydrophilic region of the molecule is small in proportion to the hydrophobic region which contains long hydrocarbon chains. Liposomes are formed by dissolving the lipid in chloroform and using a rotary evaporator the chloroform is removed, leaving a uniformly thin film of lipid on the flask wall. An aqueous solution containing the enzyme is added to the flask and the lipid is dispersed by shaking. The lipid forms membranes around the enzyme-containing water droplets, with a small proportion of the enzyme becoming incorporated into the membrane ^(46,103). A diagrammatic representation of a liposome microencapsulated enzyme is shown in Figure 5.9

enzyme-containing



Figure 5.9. A diagrammatic representation of a liposome microencapsulated enzyme
(104)

5.2.3.2 Activity of entrapped and microencapsulated enzymes

The activity of lattice entrapped or microencapsulated enzymes is usually lower than that obtained for the soluble free enzymes, mainly due to external and internal diffusion effects. If the substrate molecular size exceeds the pore size/s of the lattice or membrane then the apparent enzyme activity will be zero. Also, if the product/s molecular size is too large they may be permanently trapped within the lattice structure or membrane, which would intensify the diffusional problems and further reduce the activity. Enzyme loadings are extremely

variable, but loadings approaching 1g of enzyme per gram of support (1g g^{-1}) have been reported ⁽¹⁹⁾.

5.2.3.3 Stability of entrapped and microencapsulated enzymes

Polyacrylamide lattice entrapped and microencapsulated enzymes generally demonstrate enhanced thermal stability, and may maintain appreciable activity for several months if stored between 0 to 5°C ⁽⁹³⁾.

5.2.3.4 Advantages and disadvantages of enzyme entrapment and microencapsulation methods

The advantages of immobilisation by entrapment are the wide applicability, and the protection from microbial degradation. The disadvantages are the preparation may be difficult, the binding force is weak, enzyme leakage occurs, and the problems of substrate/products diffusion. The advantages of membrane confinement of enzymes include: the preparation is simple, no enzyme leakage, the very wide applicability, and the protection against microbial degradation. Possible disadvantages of this method include the high cost of preparation, and the problems of substrate/product diffusion.

5.2.4 Insolubilisation

The insolubilisation of a soluble free enzyme is usually performed using a cross-linking agent such as glutaraldehyde. This was first performed by Quioco and Richards in 1964 who insolubilised carboxypeptidase A ⁽⁴⁶⁾. Glutaraldehyde contains two aldehyde groups which form linkages between free amino acids groups on the surface of enzyme molecules; the reaction scheme is shown in Figure 5.10. Lysine is the predominant amino acid that forms a chemical linkage with glutaraldehyde, but other amino acids such as tyrosine and cysteine are also involved. The degree of cross-linking can be controlled by the amount of glutaraldehyde that is present during the insolubilisation process. A high degree of cross-linking can produce interstitial spaces smaller than the molecular size of a substrate and this prevents the substrate diffusing to the active site, effectively preventing any catalytic activity.



Aston University

Content has been removed for copyright reasons

insoluble enzyme/glutaraldehyde conjugate

Figure 5.10. The reaction scheme for the insolubilisation of an enzyme using glutaraldehyde (pentane-1,5 dial) ⁽¹⁹⁾.

The rate and efficiency of insolubilisation is pH and temperature dependent and the optimum conditions vary for different enzymes. Examples of enzymes that have been insolubilised using glutaraldehyde include glucose oxidase, β -galactosidase, α -amylase, papain, and urease ^(93,94).

5.2.4.1 Activity of glutaraldehyde insolubilised enzymes

The activity of glutaraldehyde insolubilised enzymes varies depending upon the type of enzyme and the insolubilisation conditions used. Activities can range from zero to that obtained for the free soluble enzyme. The most important factor is the concentration of glutaraldehyde used for insolubilisation ⁽⁹³⁾: the higher the concentration, the greater the degree of cross-linking, along with an increase in diffusional problems. Also, if high concentrations of glutaraldehyde are used, the enzyme's active site may become blocked or undergo conformational changes, which leads to a reduction in activity. From the literature, most insolubilisation is performed using glutaraldehyde solutions ranging from 1 to 2.5%^{w/v} and this allows the retention of enzyme activity ^(105,106,107,108).

5.2.4.2 Stability of glutaraldehyde insolubilised enzymes

With a number of enzymes the insolubilisation process produces enhanced thermal stability by maintaining the enzyme's structure at higher than optimal temperatures ⁽⁹³⁾. The cross-linked structure can in some cases enhance the pH stability by resisting major conformational changes associated with shifts in pH ^(19,93). Glutaraldehyde insolubilised catalase, pepsin and papain have been reported to retain up to 80% of their initial activity after storage for several months at 4°C ^(93,105,106).

5.2.4.3 Advantages and disadvantages of glutaraldehyde insolubilisation

The main advantages of this method are: the insolubilisation process is simple, the process is reproducible, the process is effective for a wide range of enzymes, and the cost of glutaraldehyde is comparatively low. The main disadvantages include the optimal reaction conditions for insolubilisation must be determined, the high toxicity of glutaraldehyde, the formation of insoluble aggregates which require mechanical dispersion, and the variability of the insoluble particle size.

5.3 Centrifugation studies with immobilised and insolubilised β -galactosidase using the rate-zonal separation technique

5.3.1 Introduction

Chapter 4 described rate-zonal centrifugation experiments performed using soluble free β -galactosidase, and results presented in Figures 4.14, 4.15 and 4.16 showed that the maximum attainable rotation speed of 13 000 r.p.m. (26 122 g max) was insufficient to effect sedimentation of the free enzyme. According to Stokes' Law, represented by equation (3.3), the sedimentation rate of a particle can be increased by increasing the size or density of the particle. As previously described in this chapter, immobilisation or insolubilisation of an enzyme can be used to increase both the apparent size and density of the enzyme particles. Using the rate-zonal centrifugation technique a stable reaction environment promoting the sedimentation of the immobilised or insolubilised enzyme as a distinct band is possible.

In this chapter, various immobilisation techniques are evaluated, to determine their suitability to produce the sedimentation of β -galactosidase through a lactose monohydrate density

gradient, performed at rotation speeds up to 13 000 r.p.m. (26 122 g max). Setford ⁽³⁾ described the entrapment of dextransucrase by high molecular weight dextran particles. Dextran particles immobilise an enzyme by a combination of physical entrapment within the interstitial spaces and adsorption to the dextran chains. Centrifugation experiments were performed using blue dextran (Mwt ~2 000 000) to visualise the movement of high molecular weight dextran through a lactose monohydrate density gradient, and to determine the molecular weight of dextran required to produce particles of sufficient size and density to act as a carrier for β -galactosidase. Rate-zonal centrifugation experiments were performed using β -galactosidase immobilised using industrial-grade dextran (Mwt 5×10^6 - 40×10^6).

The immobilisation of β -galactosidase using covalent binding was investigated and various support materials were evaluated. Blue dextran consists of dextran (Mwt ~2 000 000) covalently bound to a triazine dye. Experiments were performed to link Procion Blue MX-R dye to industrial-grade dextran particles, and to then link β -galactosidase to these activated particles. The effectiveness of this immobilisation process was determined and evaluated as a possible support for β -galactosidase during rate-zonal centrifugation. Amberlite resin beads were evaluated as a possible support material, allowing covalent linkage of β -galactosidase using cyanogen bromide.

The insolubilisation of β -galactosidase using glutaraldehyde was performed and the production of a particulate product suitable for rate-zonal centrifugation was investigated. Rate-zonal centrifugation experiments were performed at various rotation speeds using insolubilised β -galactosidase of varying activities, and the galacto-oligosaccharides profile within the lactose monohydrate density gradients was determined.

5.3.2 Rate-zonal centrifugation studies using blue dextran

Rate-zonal centrifugation experiments were performed using 1%^{w/v} blue dextran (Mwt ~2 000 000). This concentration was used because at higher values the dextran solution has a consistency similar to wallpaper paste, which would have presented loading problems. Lactose monohydrate density gradients (10-40%^{w/v}, 36 cm³) were prepared at 40°C as described in detail in Chapter 7, and these were top-layered with 1%^{w/v} blue dextran solution

(1cm³). The top-layered gradients were centrifuged at 13 000 r.p.m. (26 122 g max) for 0, 30, 60, 90 and 180 minutes, at 40°C. At the termination of a run, the centrifuge tube was removed and photographed to allow the comparison of the positions of the blue dextran after different centrifugation times. Blue dextran top-layered density gradients were centrifuged at 13 000 r.p.m. for 0 and 180 minutes and fractions taken were analysed using a uv/visible spectrophotometer, to allow a more precise comparison of the movement of blue dextran to the gradient profile. Control gradients top-layered with water (1 cm³) were centrifuged for 0, 30, 60, 90 and 180 minutes to enable changes in the gradient profile to be determined by refractive index measurement of the gradient fractions. Figure 5.11 shows the movement of blue dextran after centrifugation at 13 000 r.p.m (26 122 g max) for 0, 30, 60, 90 and 180 minutes, at 40°C. A comparison of the position of the blue dextran with the corresponding lactose monohydrate gradient profile at 0, 30, 60, 90 and 180 minutes is shown in Figures 5.11a, 5.11b, 5.11c, 5.11d and 5.11e. A comparison of the movement of blue dextran after centrifugation for 0 and 180 minutes, monitored by absorbance measurements at 617.6 nm, to the lactose density gradient profiles is presented in Figure 5.11f.

The photographs presented in Figure 5.11 show the movement of the blue dextran from the initial loading position (0 minutes). During centrifugation at 13 000 r.p.m., the blue dextran does not sediment as a narrow discrete band, but broadening does occur. Broadening of the band slowly occurs (from the initial loading position), until after 180 minutes a comparatively uniformly coloured band extending approximately half the length of the lactose monohydrate density gradient was produced. By comparing the lactose monohydrate density gradient profiles to the position of the blue dextran, as shown in Figures 5.11a, 5.11b, 5.11c, 5.11d, 5.11e and 5.11f, the movement is shown to correspond closely to the progressive degeneration of the gradient profile. These results show that the maximum attainable rotation speed of 13 000 r.p.m. (26 122 g max) used was insufficient to produce sedimentation of the blue dextran (Mwt ~2 000 000) at a rate faster than the degradation in the profile of the lactose monohydrate gradient. Using dextran with molecular weights higher than 2 000 000 would produce particles of increased size and density compared to those obtained for blue dextran, and this would increase the particle sedimentation rate.

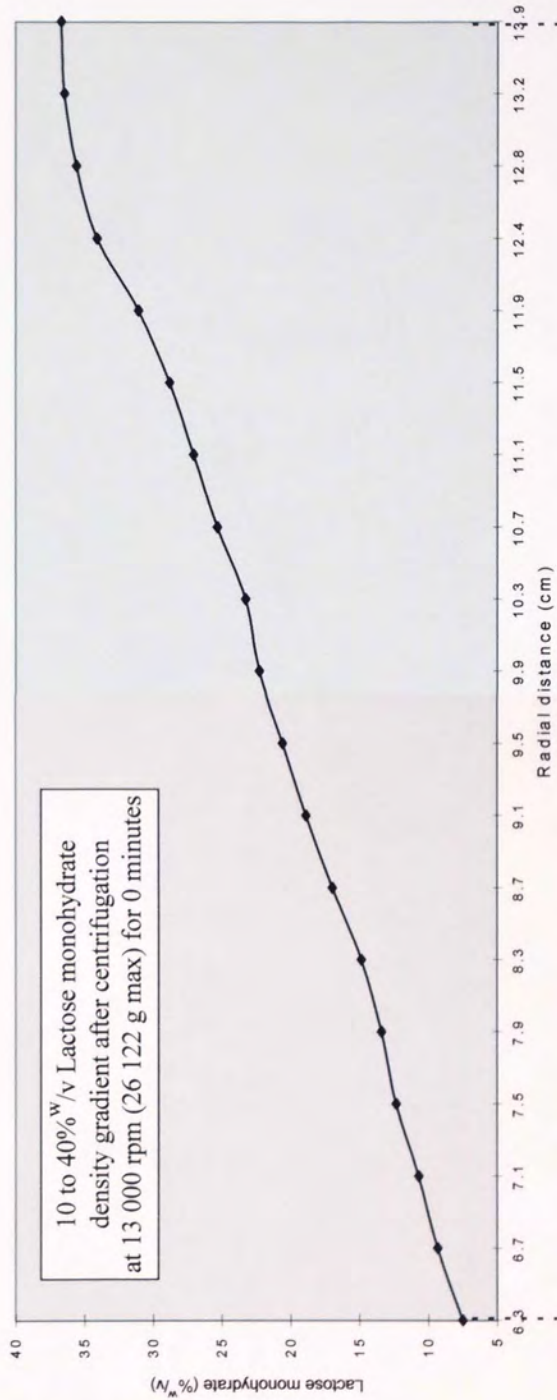


Figure 5.11a. A comparison of the position of blue dextran with the corresponding lactose monohydrate density gradient after centrifugation at 13 000 r.p.m. (26 122 g max) for 0 minutes, at 40°C.

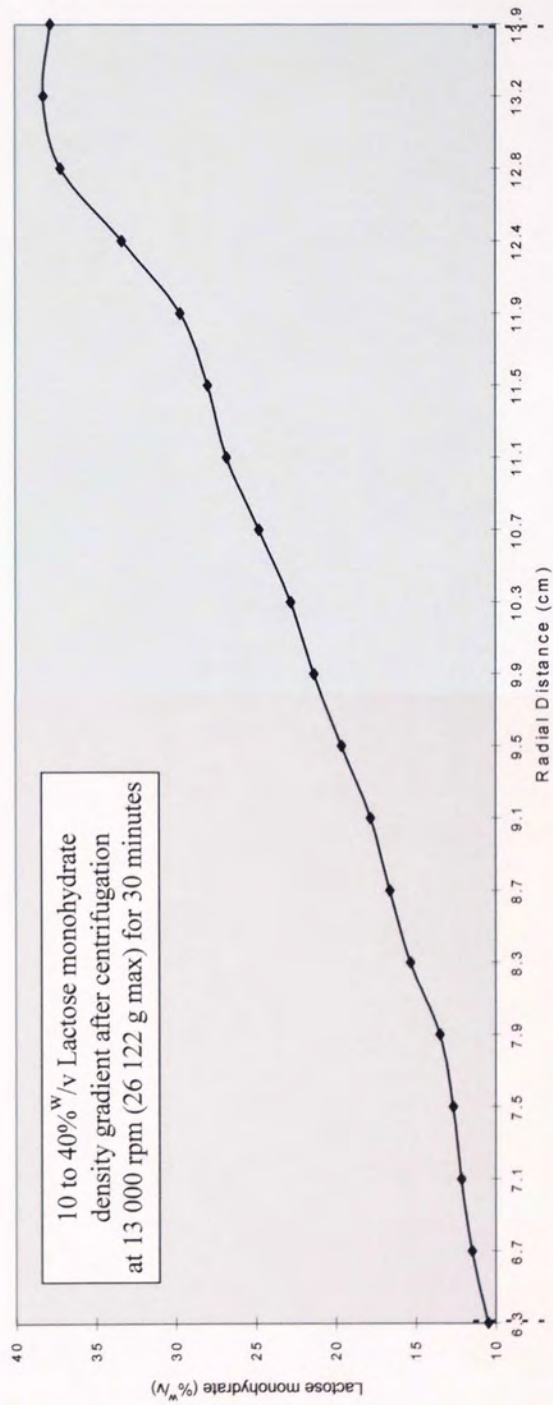


Figure 5.11b. A comparison of the position of blue dextran with the corresponding lactose monohydrate density gradient after centrifugation at 13 000 r.p.m. (26 122 g max) for 30 minutes, at 40°C.

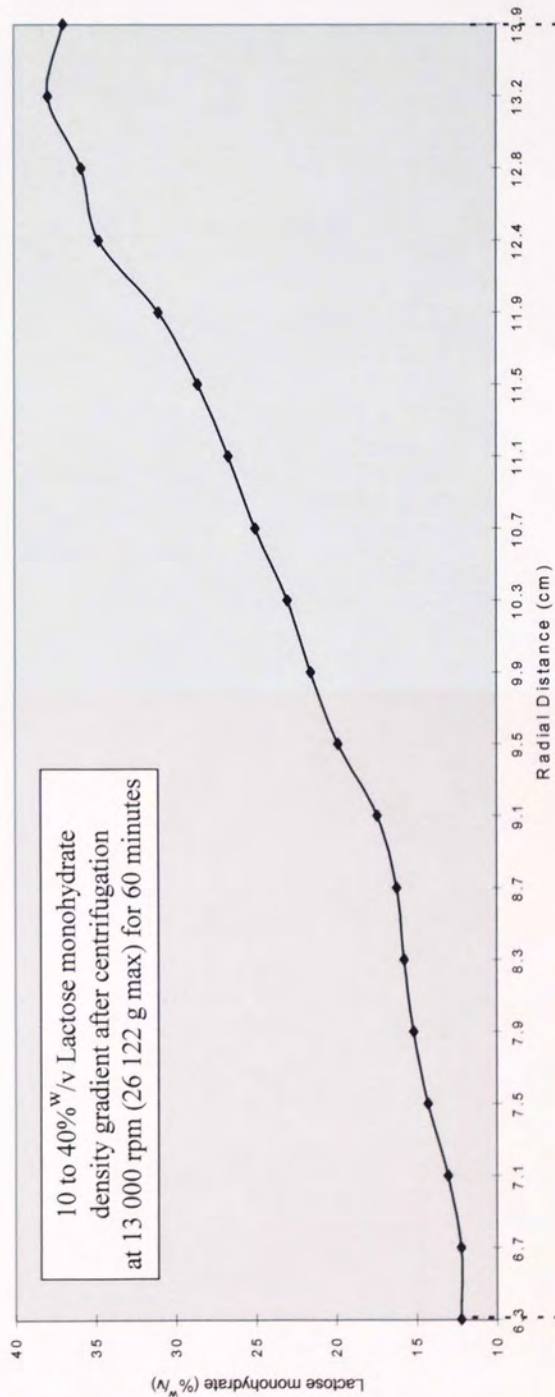


Figure 5.11c. A comparison of the position of blue dextran with the corresponding lactose monohydrate density gradient after centrifugation at 13 000 r.p.m. (26 122 g max) for 60 minutes, at 40°C.

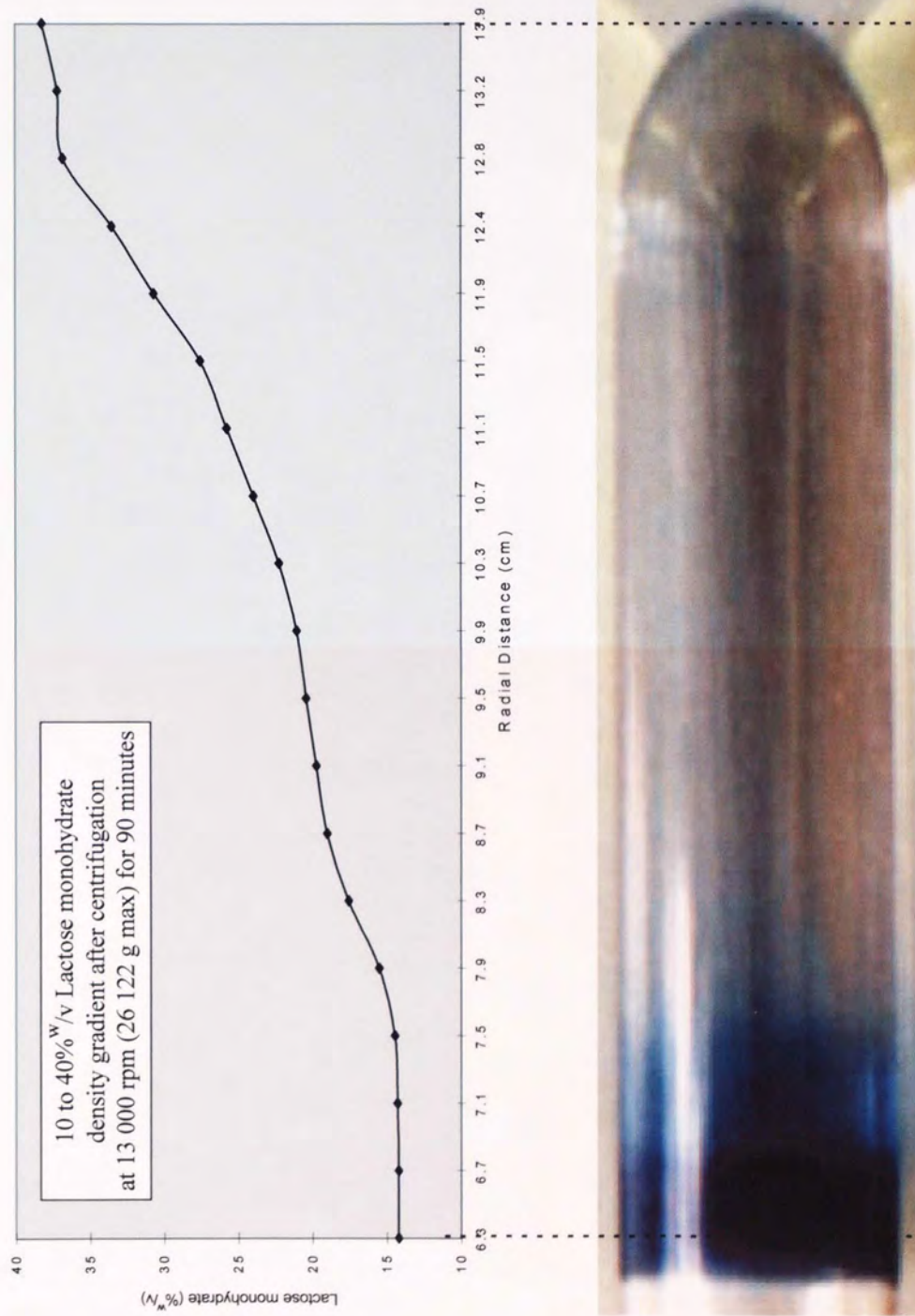


Figure 5.11d. A comparison of the position of blue dextran with the corresponding lactose monohydrate density gradient after centrifugation at 13 000 r.p.m. (26 122 g max) for 90 minutes, at 40°C.

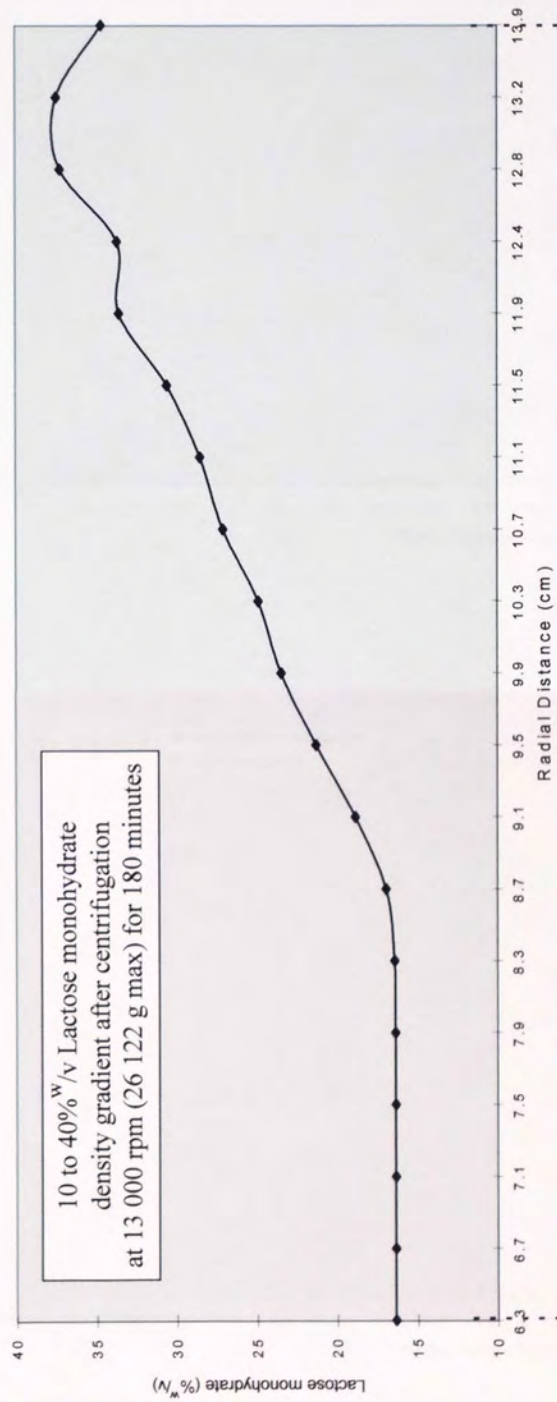


Figure 5.11e. A comparison of the position of blue dextran with the corresponding lactose monohydrate density gradient after centrifugation at 13 000 r.p.m. (26 122 g max) for 180 minutes, at 40°C.

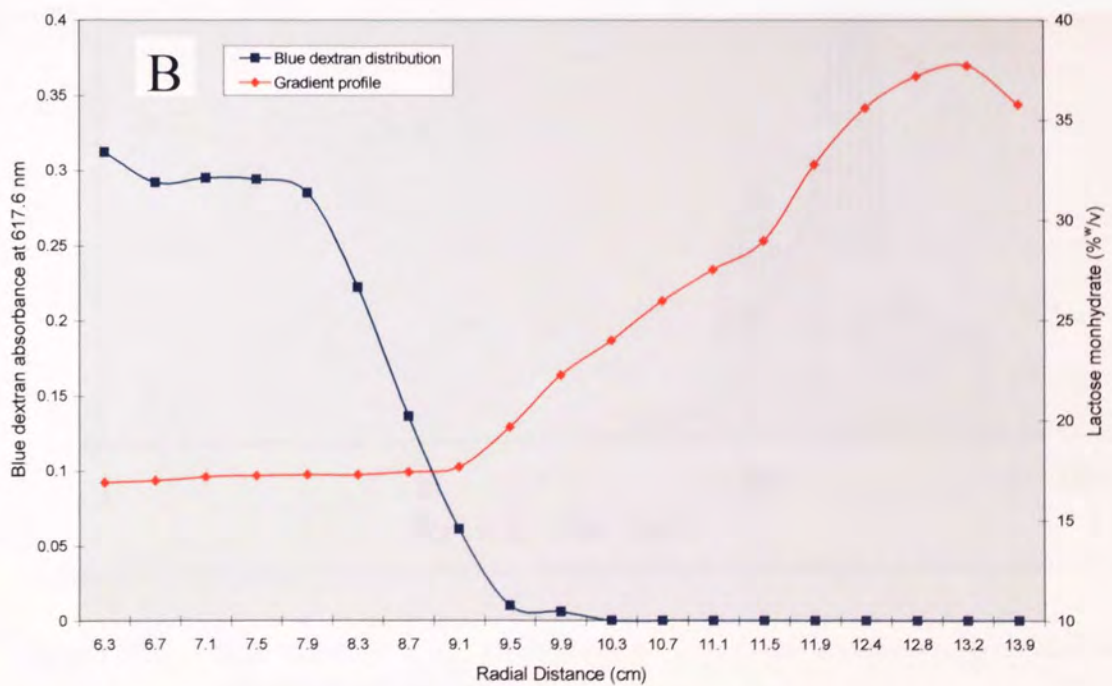
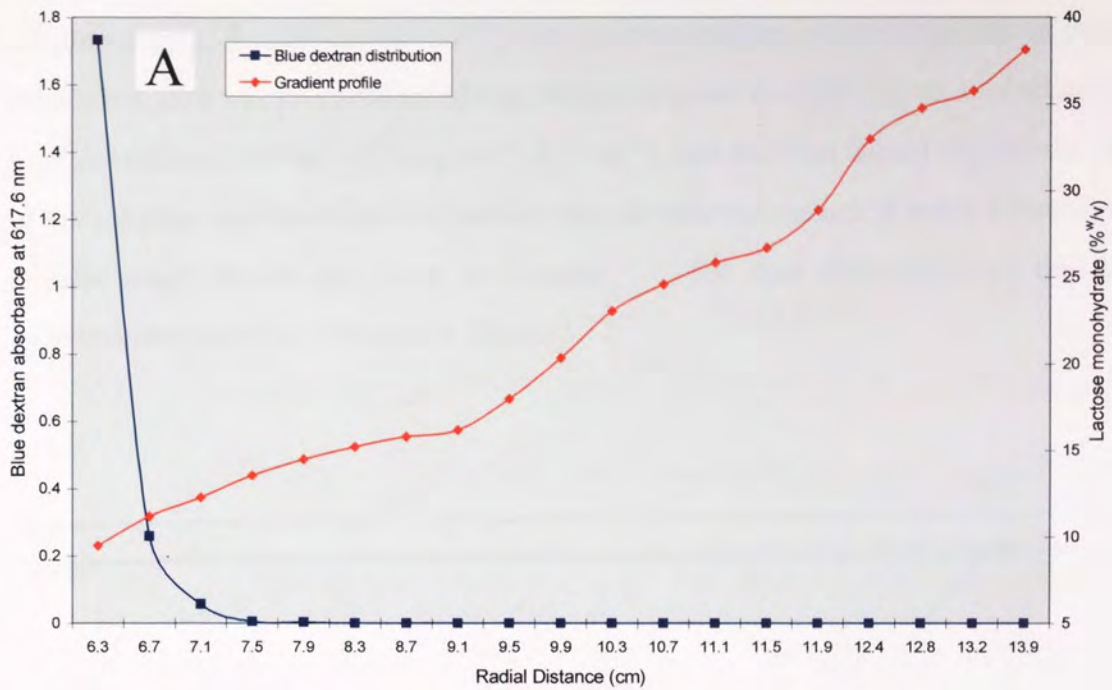


Figure 5.11f. A comparison of the movement of 1%^{w/v} blue dextran (1 cm³) to the corresponding 10-40%^{w/v} lactose monohydrate density gradient profile (36 cm³), during centrifugation at 13 000 r.p.m. (26 122 g max) for 0 and 180 minutes, at 40°C. A is at 0 minutes and B is at 180 minutes. Blue dextran movement monitored by absorbance measurements at 617.6 nm of the gradient fractions.

5.3.3 Rate-zonal centrifugation studies using dextran entrapped β -galactosidase.

Rate-zonal experiments were performed using industrial-grade dextran with a molecular weight range of 5×10^6 to 40×10^6 . An aqueous solution containing dextran immobilised β -galactosidase was prepared by adding industrial-grade dextran (1g) to a solution containing β -galactosidase (100 cm^3 of 5 mg cm^{-3} , 6 U cm^{-3}), and this was stirred vigorously. A sample of the solution was taken and the particle size distribution measured using a laser droplet and particle sizer; details are given in Chapter 7. The size distribution of the dextran/ β -galactosidase particles is shown in Figure 5.12.

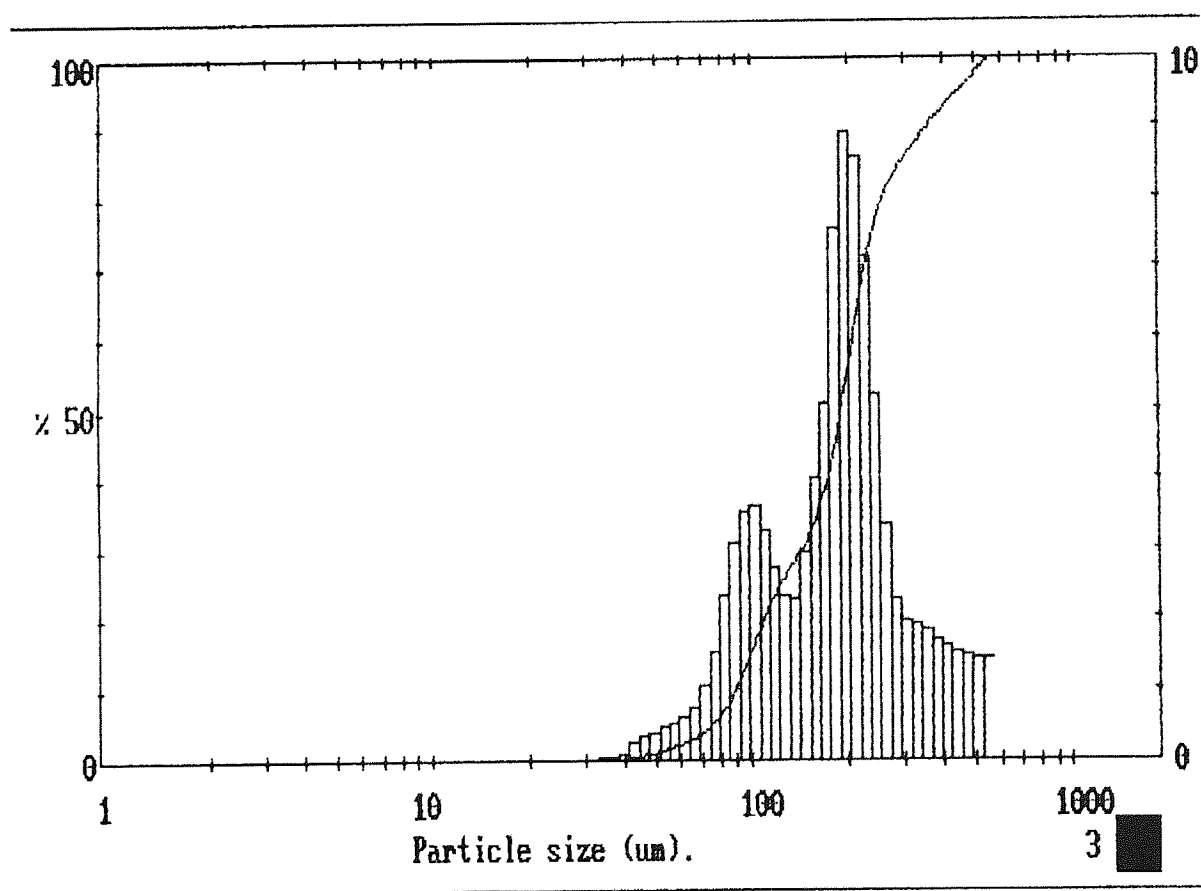


Figure 5.12. The particle size distribution for β -galactosidase immobilised using industrial-grade dextran.

Lactose monohydrate density gradients (10-40%^{w/v}, 36 cm^3) were prepared at 40°C as described in detail in Chapter 7, and these were top-layered with the industrial-grade dextran/ β -galactosidase suspension (1 cm^3). The top-layered gradients were centrifuged at

13 000 r.p.m. (26 122 g max) for 0 and 30 minutes, at 40°C. At the termination of a run the centrifuge tube was removed and photographed; also fractions were taken and analysed by HPLC. The HPLC results were used to determine the galacto-oligosaccharide distribution profile within the gradient and to identify the position of the dextran particles within the gradient. Control experiments were performed using lactose monohydrate density gradients (10-40%^{w/v}, 36 cm³) top-layered with a solution of free soluble β -galactosidase (5mg cm⁻³, 16 U cm⁻³, 1 cm³). Photographs showing the position of the dextran particles after 0 and 30 minutes centrifugation at 13 000 r.p.m.(26 122 g max), at 40°C, is shown in Figure 5.13.

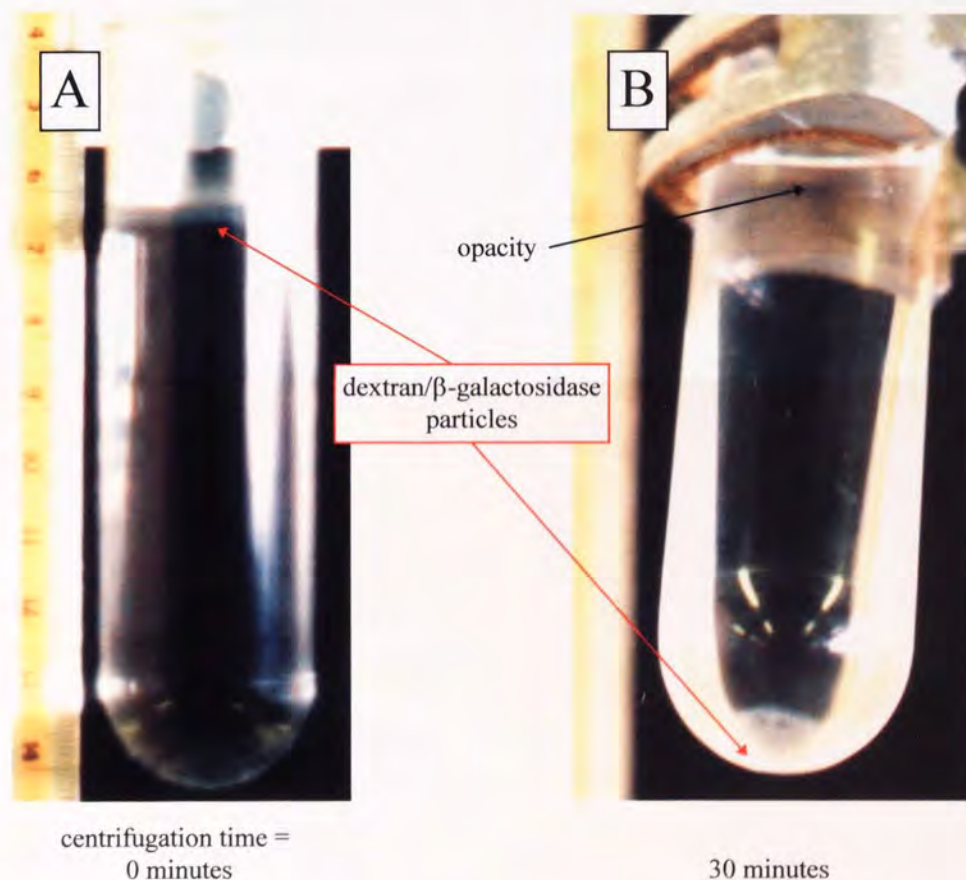


Figure 5.13. Lactose monohydrate density gradients (10-40%^{w/v}, 36 cm³) top-layered with a solution of industrial-grade dextran/ β -galactosidase particles (1 cm³ of bulk solution, equivalent to 5mg cm⁻³ (16 U cm⁻³) β -galactosidase and 10 mg cm⁻³ of industrial-grade dextran) and centrifuged at 13 000 r.p.m (26 122 g max) for 0, and 30 minutes, at 40°C. A is after 0 minutes and B is after 30 minutes.

Figure 5.13 shows that after 30 minutes centrifugation at 13 000 r.p.m. a proportion of the industrial dextran/ β -galactosidase particles had reached the bottom of the centrifuge tube,

whilst the opacity at the top of the gradient indicated that a considerable amount did not sediment to the bottom of the tube. To confirm that dextran immobilised β -galactosidase had sedimented, a comparison was made between the HPLC analysis of the fractions obtained for the dextran/ β -galactosidase and the soluble free enzyme reactions. A comparison of the chromatograms obtained for the bottom fraction of the density gradients after centrifugation at 13 000 r.p.m. for 30 minutes, at 40°C, is shown in Figure 5.14.

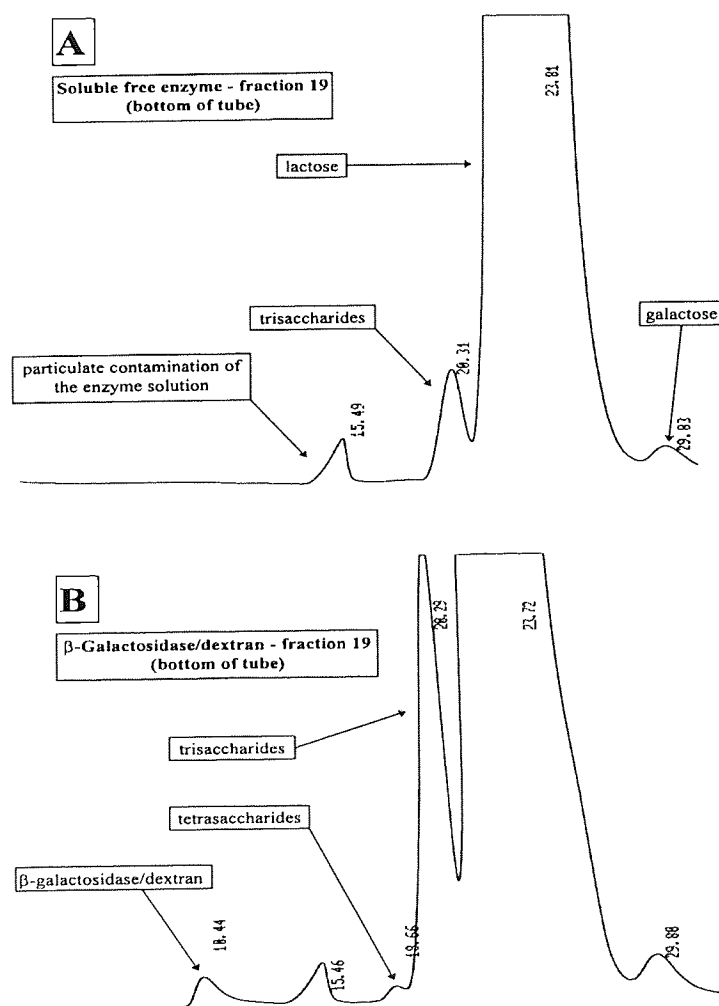


Figure 5.14 A comparison of the chromatograms obtained for the bottom fraction of the β -galactosidase/dextran and the soluble free β -galactosidase centrifugation experiments, performed at 13 000 r.p.m. (26 122 g max) for 30 minutes, at 40°C. A is for top-layered soluble free β -galactosidase (5mg cm^{-3} , 16 U cm^{-3} , 1 cm^3) and B is for top-layered β -galactosidase/dextran conjugate (1 cm^3 of bulk solution, equivalent to 5mg cm^{-3} (16 U cm^{-3}) of β -galactosidase and 10 mg cm^{-3} of industrial-grade dextran).

From the HPLC results obtained, the galacto-oligosaccharide distribution profile for the industrial-grade dextran/ β -galactosidase was compared to the dextran distribution profile and the results are presented in Figure 5.15.

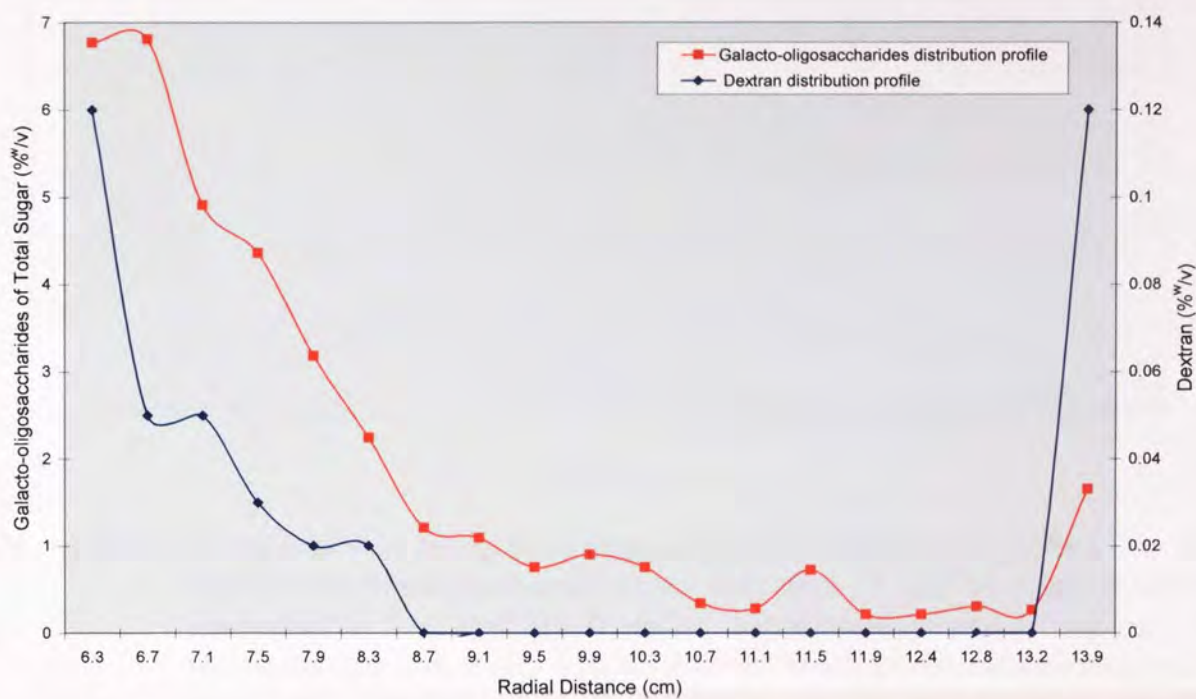


Figure 5.15. Comparison of the galacto-oligosaccharide distribution profile with the dextran distribution profile for top-layered β -galactosidase/dextran conjugate (1 cm^3 of bulk, solution equivalent to 5 mg cm^{-3} (16 U cm^{-3}) β -galactosidase and 10 mg cm^{-3} of industrial-grade dextran) loaded on to a 10-40%^{w/v} lactose monohydrate density gradient and centrifuged at 13 000 r.p.m. (26 122 g max) for 30 minutes, at 40°C.

Figure 5.15 shows that only the particles produced by the highest molecular weight fraction of the industrial-grade dextran (approaching a Mwt of $\sim 40\,000\,000$) were of sufficient size and density to completely sediment. A considerable amount of the lower molecular weight fraction (Mwt $\sim 5\,000\,000$) remained at the initial loading position, whilst higher molecular weight fractions sedimented away from the initial loading position, as demonstrated by the peaks on the distribution profile. The shape of the distribution profiles can be seen to closely mirror one another, which would indicate an association between the enzyme and the support material. A comparison of the galacto-oligosaccharide profiles for the β -galactosidase/dextran conjugate and for the soluble free β -galactosidase is shown in Figure 5.16.

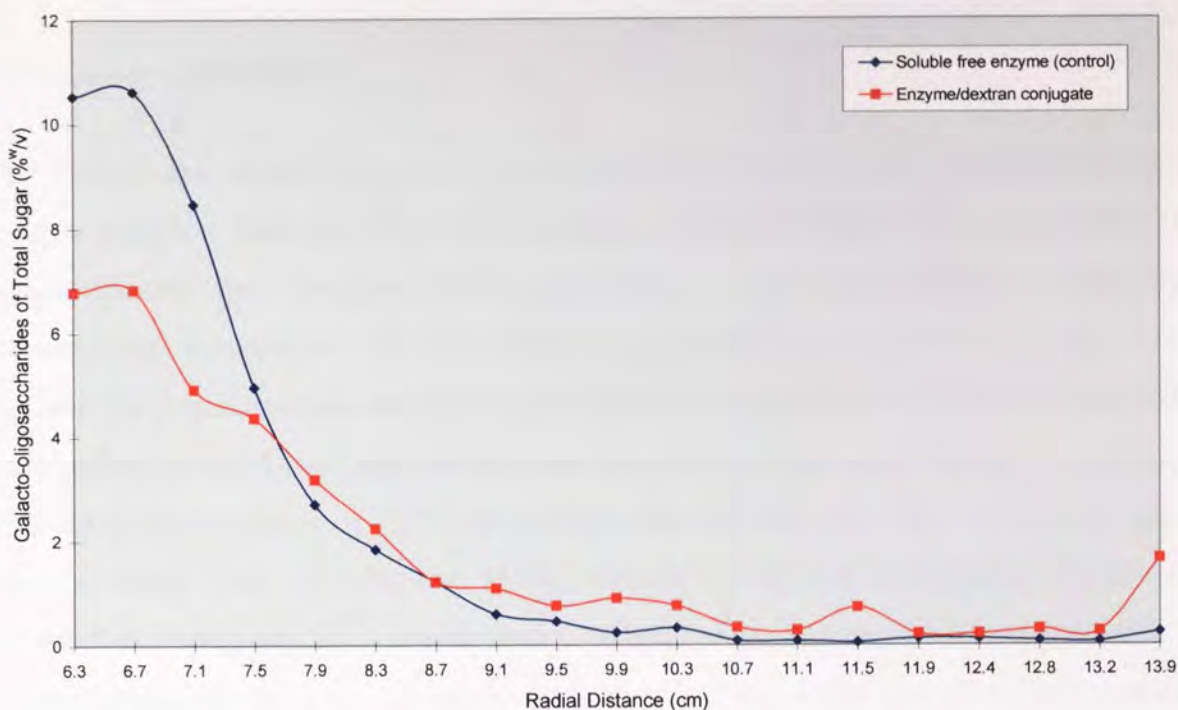


Figure 5.16. Comparison of the galacto-oligosaccharide distribution profiles for the top-layered β -galactosidase/dextran conjugate (1 cm^3 of bulk, solution equivalent to 5 mg cm^{-3} (16 U cm^{-3}) (β -galactosidase and 10 mg cm^{-3} of industrial-grade dextran) and the soluble free β -galactosidase (5 mg cm^{-3} , 16 U cm^{-3}), loaded on to a 10-40%^{w/v} lactose monohydrate density gradient and centrifuged at 13 000 r.p.m. (26 122 g max) for 30 minutes, at 40°C.

Figure 5.16 shows that the sedimenting β -galactosidase/dextran produced only slightly more galacto-oligosaccharides than that obtained for the soluble free enzyme (control), as shown at radial distances between 7.9 to 13.9 cm. This indicates that the activity of the fully sedimented β -galactosidase/dextran particles was comparatively low and/or the sedimentation rate was very high, reducing the contact time between the immobilised enzyme and the substrate at any given position within the gradient. At radial distances between 6.3 to 13.9 cm, the β -galactosidase/dextran system produced less galacto-oligosaccharides, which would suggest that the immobilisation process produced a decrease in the enzyme activity, probably caused by diffusional problems. An alternative immobilisation strategy is to covalently link the enzyme to the pre-formed high molecular weight dextran particles, producing strong surface immobilisation rather than entrapment within the particle, and reduce the diffusional effects.

5.3.4 Rate-zonal centrifugation studies using β -galactosidase covalently linked to industrial-grade dextran

The triazine dye method was used to covalently link β -galactosidase to industrial-grade dextran particles, following the reaction scheme shown in Figure 5.5 (see p.152). The dichlorotriazine dye, Procion MX-R, was used, as this was readily available and comparatively inexpensive. Procion MX-R is an intense blue coloured dye, which when linked to the β -galactosidase/dextran would aid in the use and recovery of the conjugate. The experimental protocol used was based on that described by Dean and Watson⁽⁹⁹⁾. Briefly, a buffered aqueous solution of 1%^{w/v} industrial-dextran (70 cm³, pH 5.2) was prepared, and to this was added 1 cm³ of a Procion MX-R solution (10 mg cm⁻³), producing triazine dye activated dextran particles. The activated particles were recovered and re-suspended in buffered water (20 cm³, pH 5.2), which was then added to a 10 mg cm⁻³ (32 U cm⁻³) solution of β -galactosidase (60 cm³, pH 5.2). After incubation, the particles were recovered and re-suspended in buffered water (10 cm³). Lactose monohydrate density gradients (10-40%^{w/v}, 36 cm³) were prepared and these were top-layered with the triazine linked industrial-grade dextran/ β -galactosidase solution (1 cm³). The top-layered gradients were centrifuged at 9 000 and 13 000 r.p.m. (12 520 g max and 26 122 g max respectively) for 0 and 30 minutes, at 40°C. At the termination of a run the centrifuge tube was removed and photographed; also fractions were taken and analysed by HPLC. The HPLC results were used to determine the galacto-oligosaccharide distribution profile within each gradient. The photographs taken after 0 and 30 minutes centrifugation at 9 000 r.p.m are shown in Figure 5.17. A comparison of the galacto-oligosaccharide distributions obtained for gradients centrifuged at 9 000 and 13 000 r.p.m., for 30 minutes, is presented in Figure 5.18.

Figure 5.17 shows that at 9 000 r.p.m. (12 520 g max), the lowest speed at which an operational temperature of 40°C can be attained, full sedimentation of the triazine linked β -galactosidase/dextran conjugate is achieved. The distribution profiles presented in Figure 5.18 show that very little galacto-oligosaccharide was produced, indicating that the β -galactosidase activity was very low. The galacto-oligosaccharide produced was far less than that achieved for the physically entrapped β -galactosidase/dextran conjugate, results of which are presented in Figure 5.16

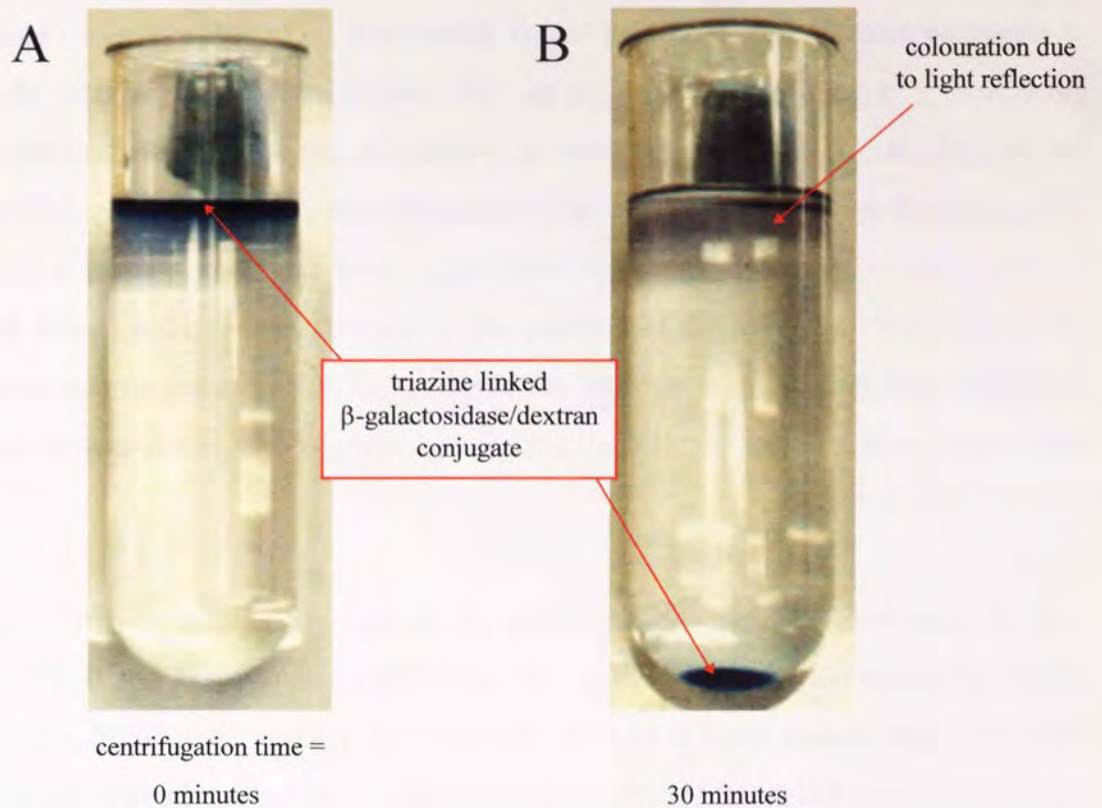


Figure 5.17. Lactose monohydrate density gradients (10-40%^{w/v}, 36 cm³) top-layered with a solution of triazine linked β -galactosidase/dextran particles (1 cm³) and centrifuged at 9 000 r.p.m (12 520 g max) for 0, and 30 minutes, at 40°C. A is after 0 minutes and B is after 30 minutes.

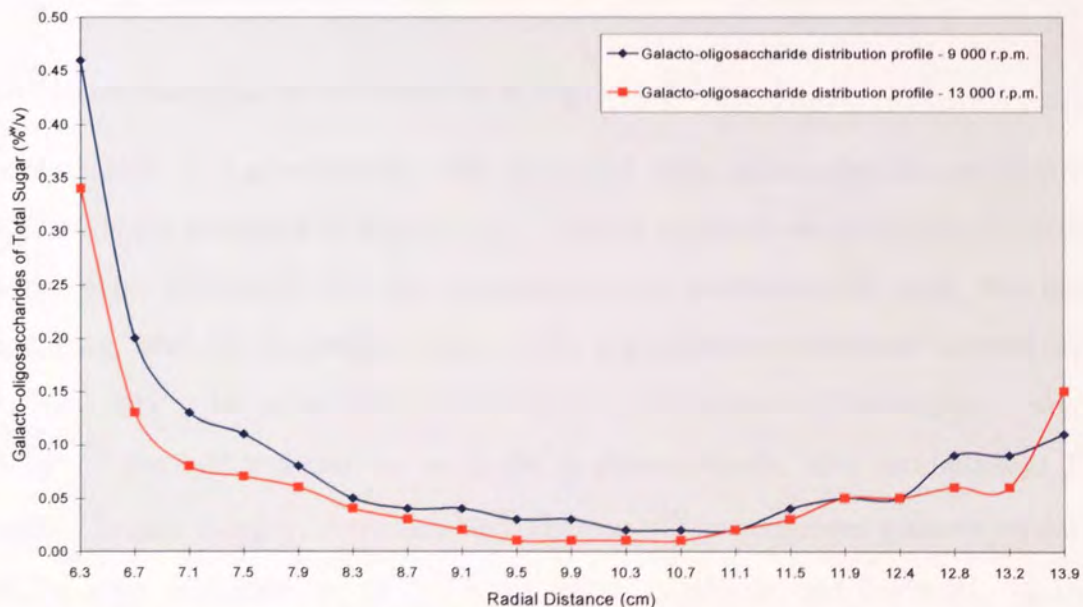


Figure 5.18. Comparison of the galacto-oligosaccharide distribution profiles for the top-layered triazine linked β -galactosidase/dextran particles (1 cm³), loaded on to a 10-40%^{w/v} lactose monohydrate density gradient and centrifuged at 9 000 (12 520 g max) and 13 000 r.p.m. (26 122 g max) for 30 minutes, at 40°C.

Activity assays were performed on the triazine linked β -galactosidase/dextran conjugate to determine the enzyme loading, and a value of 3 mg per g of dextran (3 mg g^{-1}), or 0.03 mg cm^{-3} was obtained. This loading is extremely poor compared to 20 mg g^{-1} usually obtained by covalent linkage, and explains why the galacto-oligosaccharide formation is so low. The β -galactosidase loading may have been higher than that calculated, due to a proportion of the enzyme being bound, but inactivated by the position of the linkages. Variation of the triazine experimental protocol did not increase the enzyme loading, and this method of immobilisation was found to be unsuitable for β -galactosidase isolated from *Aspergillus oryzae*.

Figure 5.18 shows the slight difference in the galacto-oligosaccharide distribution profiles obtained at 9 000 and 13 000 r.p.m., indicating that, at the lower rotation speed, the longer the contact time between the enzyme and substrate resulted in more galacto-oligosaccharide being produced. This gives the first indication that by varying the applied centrifugal fields, the formation of galacto-oligosaccharides can be controlled. To increase the activity of the sedimenting enzyme and produce higher yields of galacto-oligosaccharides, insolubilisation of the enzyme using glutaraldehyde was pursued.

5.3.5 Glutaraldehyde insolubilisation of β -galactosidase

Insolubilisation of β -galactosidase was performed using glutaraldehyde, as shown by the reaction scheme presented in Figure 5.10. Various methods are described in the literature and the main differences are the concentration of glutaraldehyde used, the incubation temperature, and the incubation time. The experimental conditions depend upon the particular enzyme being insolubilised and on the concentration of the enzyme. Schejter and Bar-Eli⁽¹⁰⁵⁾ insolubilised catalase using 4%^{v/v} glutaraldehyde, after incubation at 20°C for 2 hours. Broun, Selegny, Avrameas and Thomas⁽¹⁰⁶⁾ insolubilised glucose oxidase using 2.5%^{v/v}, after incubation at 37°C for 12 hours. Quioco and Richards insolubilised carboxypeptidase-A using 1%^{v/v} glutaraldehyde, after incubation at 20°C for 12 hours⁽⁴⁶⁾. No papers were found describing the glutaraldehyde insolubilisation of β -galactosidase, isolated from *Aspergillus oryzae*. Experiments were performed to determine the optimal reaction conditions to produce glutaraldehyde insolubilisation of β -galactosidase, whilst

retaining an acceptable level of enzyme activity. The optimal conditions for the insolubilisation of β -galactosidase isolated from *Aspergillus oryzae* were found to be as follows; incubation of β -galactosidase solution (10 mg cm^{-3} (32 U cm^{-3}), 20 cm^3 , pH 5.2) with 4%^{v/v} glutaraldehyde (10 cm^3 , equivalent to 1.33%^{v/v}), at 25°C for 18 hours. Full experimental details of the insolubilisation process and preparation of the top-layering solution are described in Chapter 7. The insolubilised β -galactosidase was re-dispersed in buffered water (pH 5.2), and using a laser particle sizer the size distribution was measured; the results are shown in Figure 5.19.

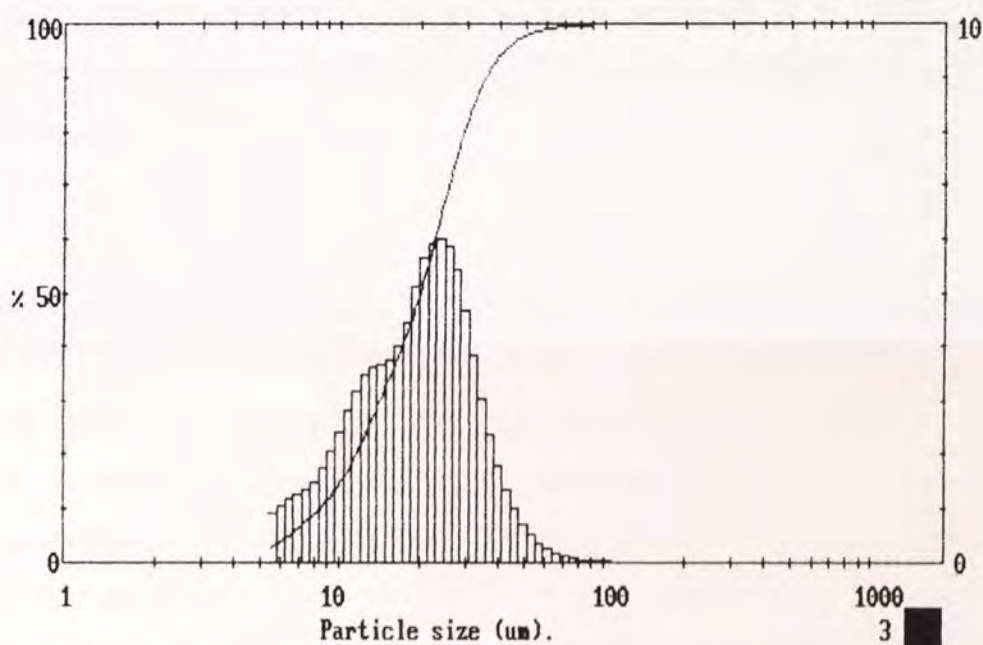


Figure 5.19. The particle size distribution for glutaraldehyde insolubilised β -galactosidase.

5.3.5.1 Determination of the density of glutaraldehyde insolubilised β -galactosidase

The density of the insolubilised β -galactosidase was determined at 40°C , using a cesium chloride density gradient. Buffered cesium chloride solutions (5-50%^{w/w}, pH 5.2) were used to produce a continuous density gradient (36 cm^3), on which the insolubilised β -galactosidase (1 cm^3), equivalent in activity to 6 mg cm^{-3} (19.2 U cm^{-3}) of soluble free β -galactosidase, was top-layered. The gradient was centrifuged at 12 000 r.p.m. ($22\,258 \text{ g max}$) for 30 minutes, at 40°C . After centrifugation, a photograph showing the position of the

insolubilised enzyme was taken. A control cesium chloride gradient top-layered with water (1 cm^3) was centrifuged and fractions were taken to assign a density value to a specific point within the gradient. Measurement of the position of the insolubilised enzyme was made and the density was determined, as shown in Figure 5.20. The glutaraldehyde insolubilised β -galactosidase was found to have a density of 1.38 g cm^{-3} . This value greatly exceeds the density range of the lactose monohydrate gradients used. Therefore, it can be concluded that the insolubilised enzyme will fully sediment to the bottom of the centrifuge tube and that the standard sedimentation coefficient ($S_{20,w}$) is extremely high. The high $S_{20,w}$ value means that the contact time between the insolubilised enzyme and the substrate at any given point in the gradient will be short, producing a low conversion of lactose monohydrate and a low yield of galacto-oligosaccharides. However, insolubilised β -galactosidase with a very high activity could be produced, which would increase both the substrate conversion and the product yield.

5.3.5.2 Estimation of the standard sedimentation coefficient ($S_{20,w}$) for glutaraldehyde insolubilised β -galactosidase

Usually, an analytical ultracentrifuge would be used to estimate the standard sedimentation coefficient ($S_{20,w}$) of an enzyme. An analytical ultracentrifuge was not available, and so an improvised method was developed to allow a crude estimation of the standard sedimentation coefficient for the glutaraldehyde insolubilised β -galactosidase to be calculated. Lactose monohydrate density gradients ($10\text{-}40\% \text{ w/v}$, 36 cm^3) were top-layered with the insolubilised β -galactosidase (1 cm^3) and centrifuged at $9\,000 \text{ r.p.m.}$ ($12\,520 \text{ g max}$) for varying times, at 40°C . After each centrifugation time, the centrifuge tube was removed and photographed. The photographs were used to estimate the radial position of the centre of the sedimenting enzyme band after various times, and this is shown in Figure 5.21. The experimental data obtained for the insolubilised β -galactosidase was inserted into Equation (3.14) and an estimated standard sedimentation coefficient ($S_{20,w}$) value of $79\,860\text{S}$ was calculated. This is an extremely high sedimentation rate and corresponds to that obtained for sub-cellular particles, such as plasma membranes, mitochondria, plastids and nuclei⁽⁵⁹⁾. The high value results from a combination of the large size and the high density of the particles. Calculations based on extrapolation of Equation (4.3), shows that a protein having an $S_{20,w}$

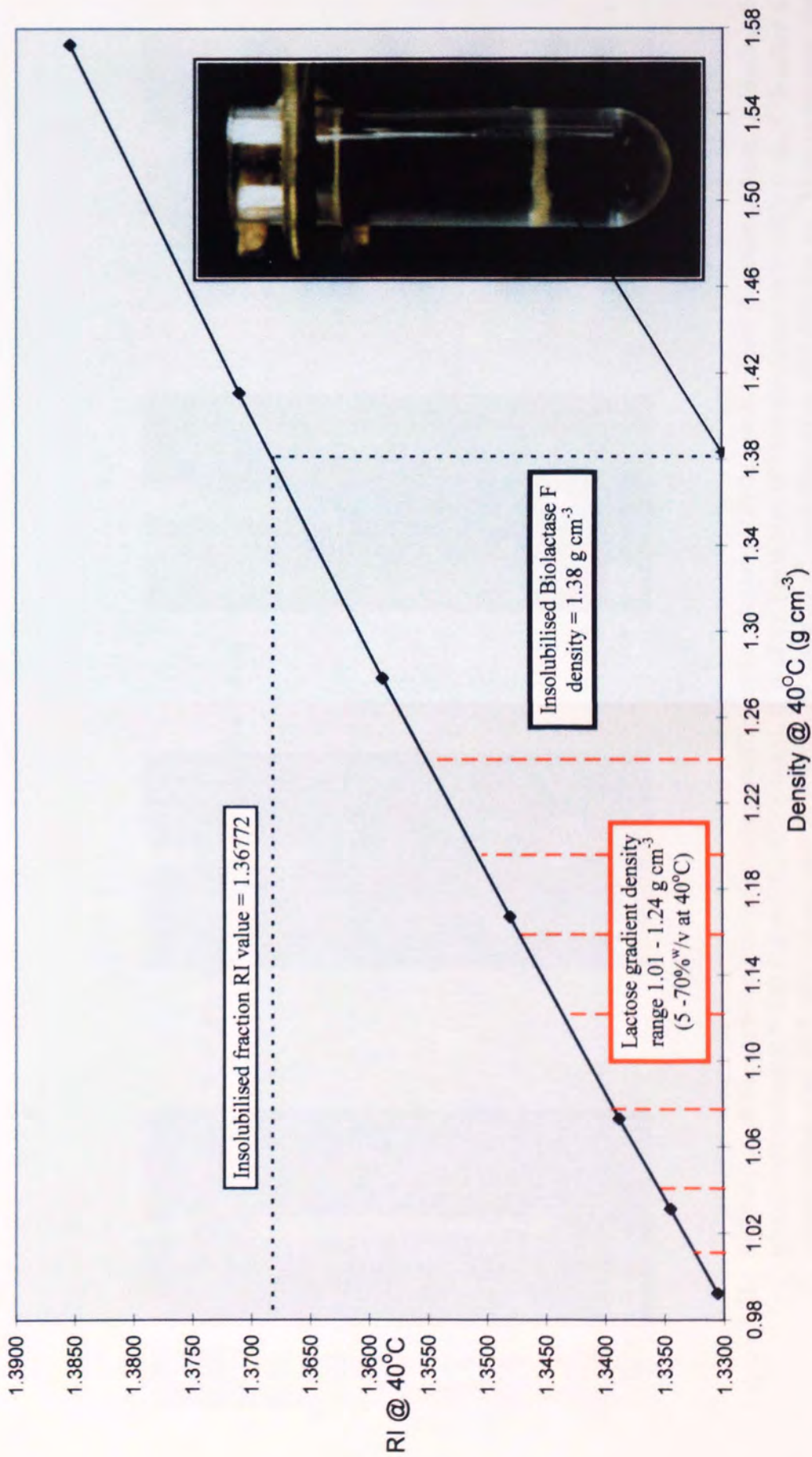


Figure 5.20. Determination of the density of glutaraldehyde insolubilised β -galactosidase using a cesium chloride density gradient (5-50%^{w/w}) centrifuged at 12 000 r.p.m (22 258 g max) for 30 minutes, at 40°C.

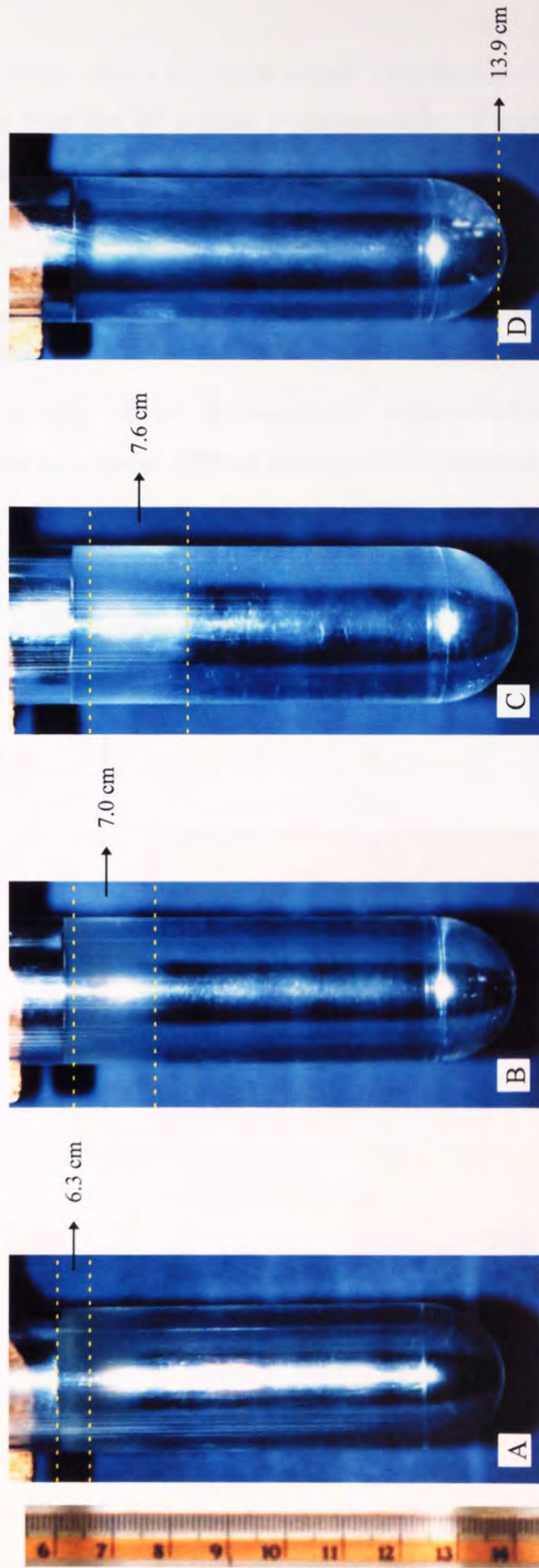


Figure 5.21. Estimation of the standard sedimentation coefficient for glutaraldehyde insolubilised β -galactosidase. A is after 0 minutes of centrifugation at 9 000 r.p.m. (12 520 g max), B is after 2 minutes of centrifugation at 9 000 r.p.m., C is after 4 minutes of centrifugation at 9 000 r.p.m., and D is after 15 minutes of centrifugation at 9 000 r.p.m. Measurements were taken from the actual tubes to eliminate errors due to photographic distortion and light reflection.

of 79 860S would have a molecular weight equivalent to $\sim 20 \times 10^7$, which is about 2 000 times larger than that of soluble β -galactosidase. Figure 5.21 shows that the enzyme sediments in a broad band and this is due to the wide particle size distribution of the insolubilised enzyme, as shown in Figure 5.19.

5.3.5.3 Reproducibility of the glutaraldehyde insolubilisation process, the weight equivalent and the storage stability of insolubilised β -galactosidase

The reproducibility of the glutaraldehyde insolubilisation process was monitored by comparing the activities of different batches of the cross-linked β -galactosidase. The activity could be varied by altering the final re-dispersion volume. The reproducibility of the cross-linked β -galactosidase re-dispersed in buffered water (10 cm^3 , pH 5.2) is shown in Table 5.3.

Cross-linked β -galactosidase activity (U cm^{-3}) (re-dispersion volume = 10 cm^3)	
28.1	
29.8	
27.8	
28.5	
29.7	
31.3	
31.4	
28.8	
30.9	
30.3	
33.6	Average = 29.9
28.6	$\sigma = 1.66$

Table 5.3. Reproducibility of the β -galactosidase insolubilisation process.

The results presented in Table 5.3 shows that the insolubilisation process was capable of producing insolubilised β -galactosidase of reproducible activity. The activity values obtained were compared to the activity of soluble free β -galactosidase (1.25 mg cm^{-3} , 4 U

cm^{-3}) and this gave an equivalent concentration of 7 mg cm^{-3} (22.4 U cm^{-3}). Solutions of the insolubilised β -galactosidase were dried to constant weight at room temperature. Known equivalent concentrations of the soluble free β -galactosidase (based on activity) were similarly dried. The dry weights were compared and it was found that:

$$1 \text{ mg of soluble free } \beta\text{-galactosidase} = 3.14 \text{ mg of insolubilised } \beta\text{-galactosidase}$$

Insolubilised β -galactosidase solution stored at $\sim 20^\circ\text{C}$ for 7 days showed a 12.7% loss of activity, compared to a 17.4% loss of activity for soluble free β -galactosidase stored under the same conditions. The higher retained activity was probably due to the increased resistance to denaturation and microbial degradation afforded to the insolubilised enzyme particles.

5.3.6 Rate-zonal centrifugation studies using glutaraldehyde insolubilised β -galactosidase

Rate-zonal centrifugation studies were performed using the insolubilised β -galactosidase. All of the insolubilised β -galactosidase concentrations stated in these rate-zonal centrifugal studies are the soluble free enzyme equivalent, based on enzymatic activity. This was used to allow comparison of these results with the stirred-batch reaction data presented in Chapter 2. To calculate the actual concentration of the insolubilised β -galactosidase (enzyme + cross-linking agent) the values must be multiplied by 3.14, for example 1.25 mg cm^{-3} soluble free β -galactosidase equivalent corresponds to an actual insolubilised β -galactosidase concentration of 3.93 mg cm^{-3} . Firstly, experiments were performed to confirm the findings presented in Figure 5.21, that the insolubilised β -galactosidase, top-layered on a lactose monohydrate density gradient ($10\text{-}40\% \text{ w/v}$), is fully sedimented when centrifuged at 9 000 r.p.m. for 30 minutes, at 40°C . A rotation speed of 9 000 r.p.m. was the minimum speed used to perform centrifugal experiments, as this is the lowest speed at which the centrifuge can maintain a reaction temperature of 40°C . Achieving complete sedimentation of the insolubilised material at this speed removes the requirement to chemically quench the gradient fractions taken and validates the term bioreaction and separation in a single

integrated process. The experiments were performed using insolubilised β -galactosidase (soluble free β -galactosidase equivalent of 12 mg cm^{-3} , 38.4 U cm^{-3}) centrifuged for 0 minutes and for 30 minutes. The protein distribution profiles were determined by measuring the absorbance at 280 nm of the gradient fractions; the results are presented in Figure 5.22. The results show that the insolubilised β -galactosidase is fully sedimented, except for any that may have adhered to the centrifuge tube during sample loading and that due to wall effects. Using Equation (3.41), the proportion of the particles that would have been expected to collide with, and possibly adhere to the tube walls, was calculated to be 6.7%. This value does not include collisions resulting from possible electrostatic interactions between the particles and the walls. A proportion of the fully sedimented material was not recovered due to adhesion to the bottom of the tube, produced by the pelleting. Although these findings indicated that chemical quenching of the gradient fractions was not required, it was continued to maintain comparability of results with the stirred-batch reactions described in Chapter 2.

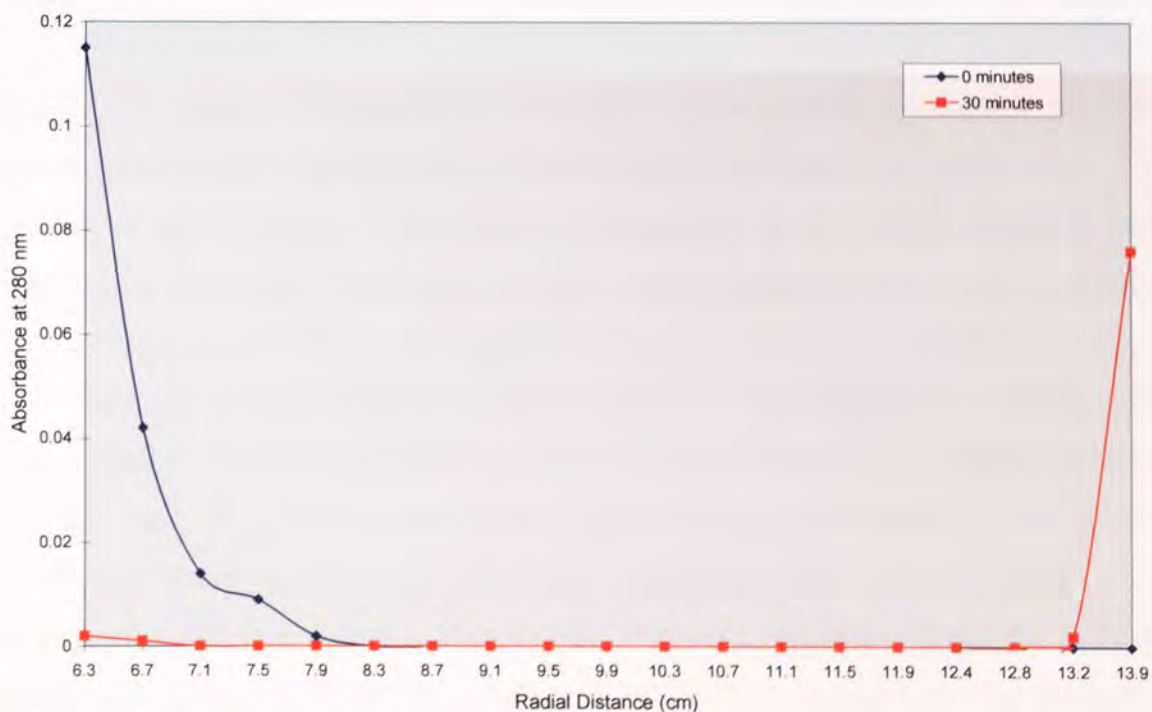


Figure 5.22. The protein distribution profiles for insolubilised β -galactosidase (12 mg cm^{-3} , 38.4 U cm^{-3} , 1 cm^3) top-layered on to a lactose monohydrate density gradient ($10\text{-}40\% \text{ w/v}$, 36 cm^3) and centrifuged at 9 000 r.p.m. ($12\,520 \text{ g max}$) for 0 and 30 minutes, at 40°C . Relative protein concentration determined by absorbance measurement at 280 nm.

Lactose monohydrate density gradients (10-40%^{w/v}, 36 cm³) were prepared and these were top-layered with varying concentrations of insolubilised β -galactosidase, equivalent in activity to that of the soluble free β -galactosidase concentrations of 1.25, 6, (2x) 6 (pulsing), and 12 mg cm⁻³ (4, 19.2, (2x) 19.2 and 38.4 U cm⁻³ respectively). The top-layered gradients were centrifuged at 9-, 11- and 13 000 r.p.m. (12 520, 18 703 and 26 122 g max respectively) for 30 minutes, at 40°C. At the end of a run, the centrifuge tube was removed and fractions were recovered. These were chemically quenched, as for all previous experiments and analysed by HPLC. The HPLC results were used to determine both the galacto-oligosaccharide distribution within each gradient and the corresponding % lactose monohydrate conversion distribution profile.

The pulsing experiment consisted of top-layering insoluble β -galactosidase (6 mg cm⁻³, 19.2 U cm⁻³, 1 cm³) on to the gradients and centrifuging as described above. At the termination of a run a further solution of insolubilised β -galactosidase (6 mg cm⁻³, 19.2 U cm⁻³, 1 cm³) was top-layered on to the gradient and re-centrifuged for a further 30 minutes.

Figure 5.23a shows a comparison of the galacto-oligosaccharide distribution profiles for varying insolubilised β -galactosidase concentrations centrifuged at 9 000 r.p.m. for 30 minutes, at 40°C. Figure 5.23b shows a comparison of the corresponding % lactose monohydrate conversion distribution profiles, obtained using the same reaction conditions. Figures 5.24a and 5.24b show the results obtained at 11 000 r.p.m. and Figures 5.25a and 5.25b show the results obtained at 13 000 r.p.m.. A comparison of both the galacto-oligosaccharide distribution profiles and the % lactose conversion profiles obtained for 1.25 mg cm⁻³ (4 U cm⁻³) insolubilised β -galactosidase, top-layered on to a lactose monohydrate density gradient (10-40%^{w/v}) and centrifuged at 9-, 11- and 13 000 r.p.m. for 30 minutes at 40°C, is shown in Figure 5.26. Similarly, the data obtained for 6, (2x) 6 - pulsing and 12 mg cm⁻³ (19.2, (2x) 19.2 and 38.4 U cm⁻³ respectively) are presented in Figures 5.27, 5.28 and 5.29 respectively.

5.3.6.1 Reproducibility of insolubilised β -galactosidase rate-zonal centrifugation experiments

The insolubilised β -galactosidase rate-zonal centrifugation experiments were performed in duplicate and the mean of the results was plotted. The reproducibility of the results can be

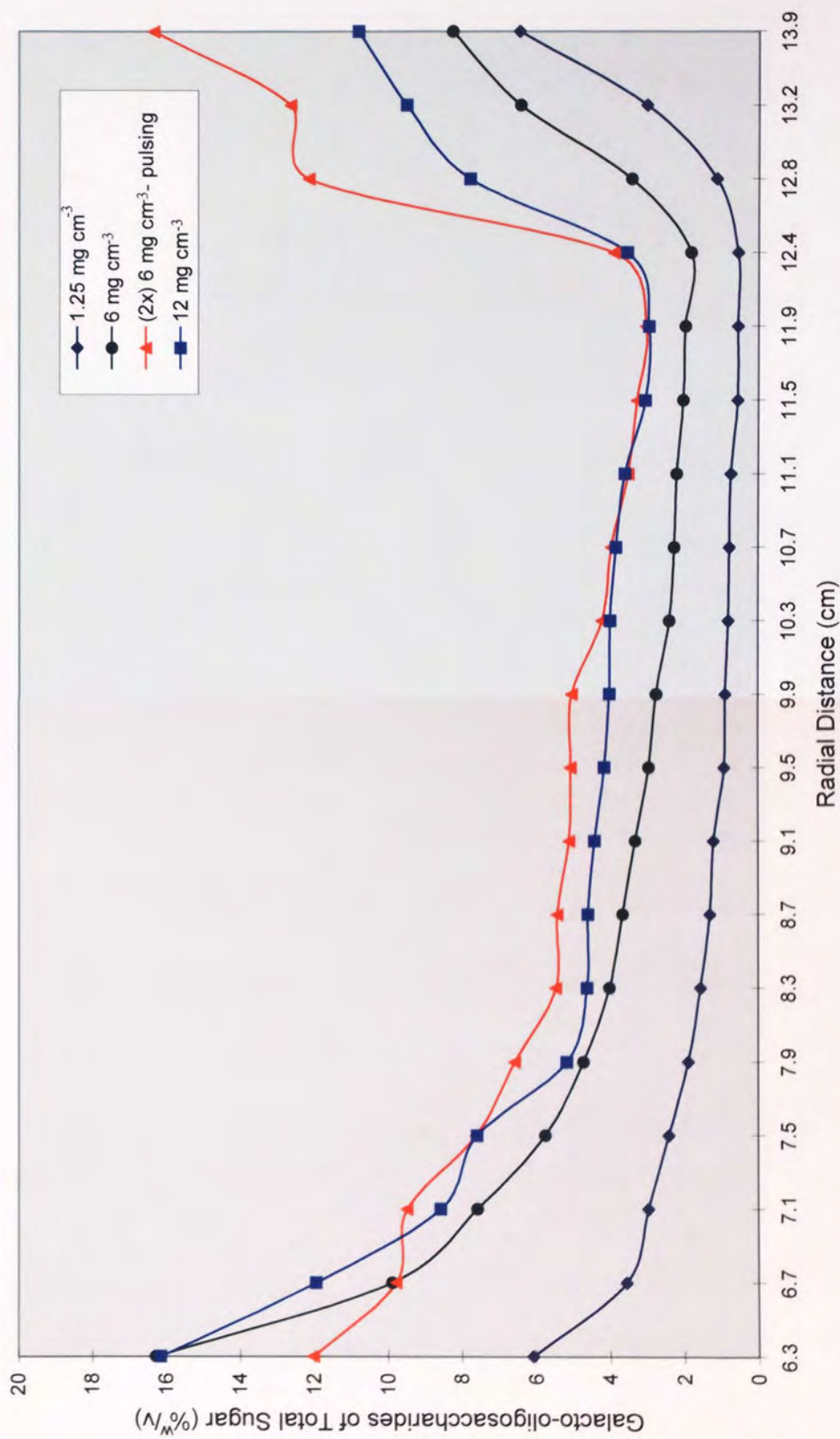


Figure 5.23a. Galacto-oligosaccharide distribution profiles for insolubilised β -galactosidase concentrations of 1.25, 6, (2x) 6 - pulsing and 12 mg cm⁻³ (4, 19.2, (2x) 19.2 and 38.4 U cm⁻³ respectively) top-layered on to lactose monohydrate density gradients (10-40%^{w/v}) and centrifuged at 9 000 r.p.m. (12 520 g max) for 30 minutes, at 40°C.

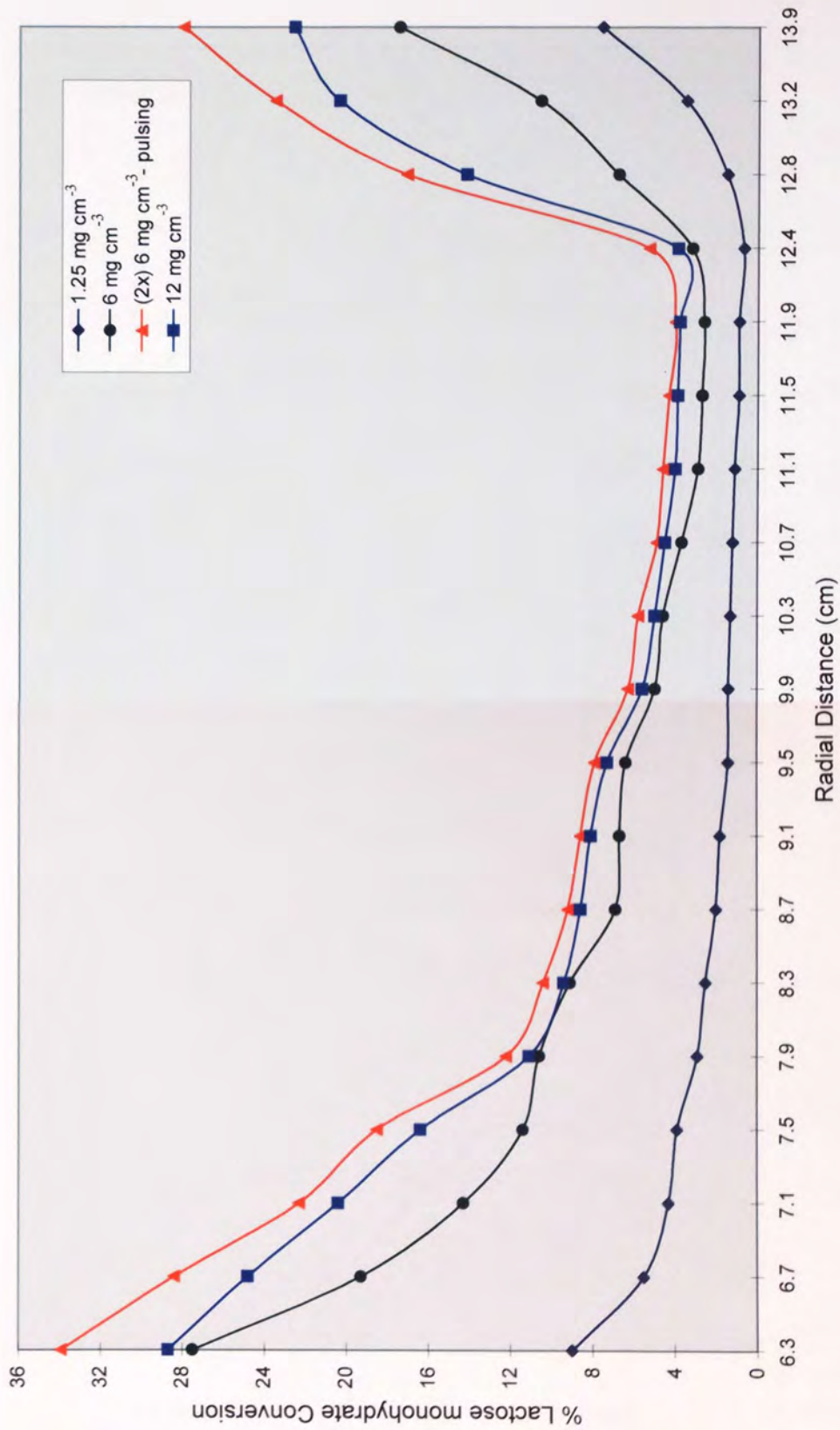


Figure 5.23b. % Lactose monohydrate conversion profiles for insolubilised β -galactosidase concentrations of 1.25, 6, (2x) 6 - pulsing and 12 mg cm⁻³ (4, 19.2, (2x) 19.2 and 38.4 U cm⁻³ respectively) top-layered on to lactose monohydrate density gradients (10-40%^{w/v}) and centrifuged at 9 000 r.p.m. (12 520 g max) for 30 minutes, at 40°C.

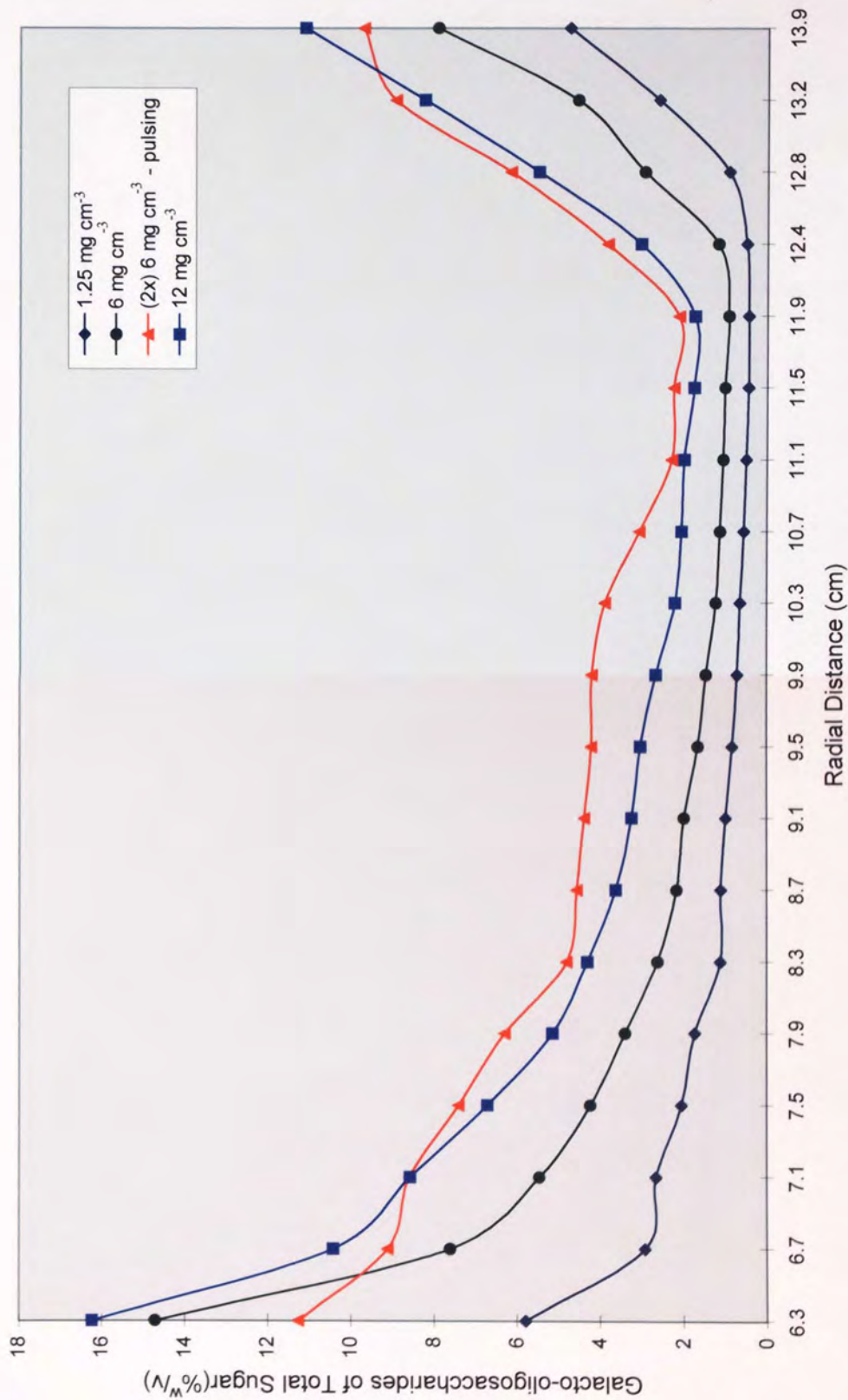


Figure 5.24a. Galacto-oligosaccharide distribution profiles for insolubilised β -galactosidase concentrations of 1.25, 6, (2x) 6 - pulsing and 12 mg cm⁻³ (4, 19.2, (2x) 19.2 and 38.4 U cm⁻³ respectively) top-layered on lactose monohydrate density gradients (10-40% w/v) and centrifuged at 11 000 r.p.m. (18 703 g max) for 30 minutes, at 40°C.

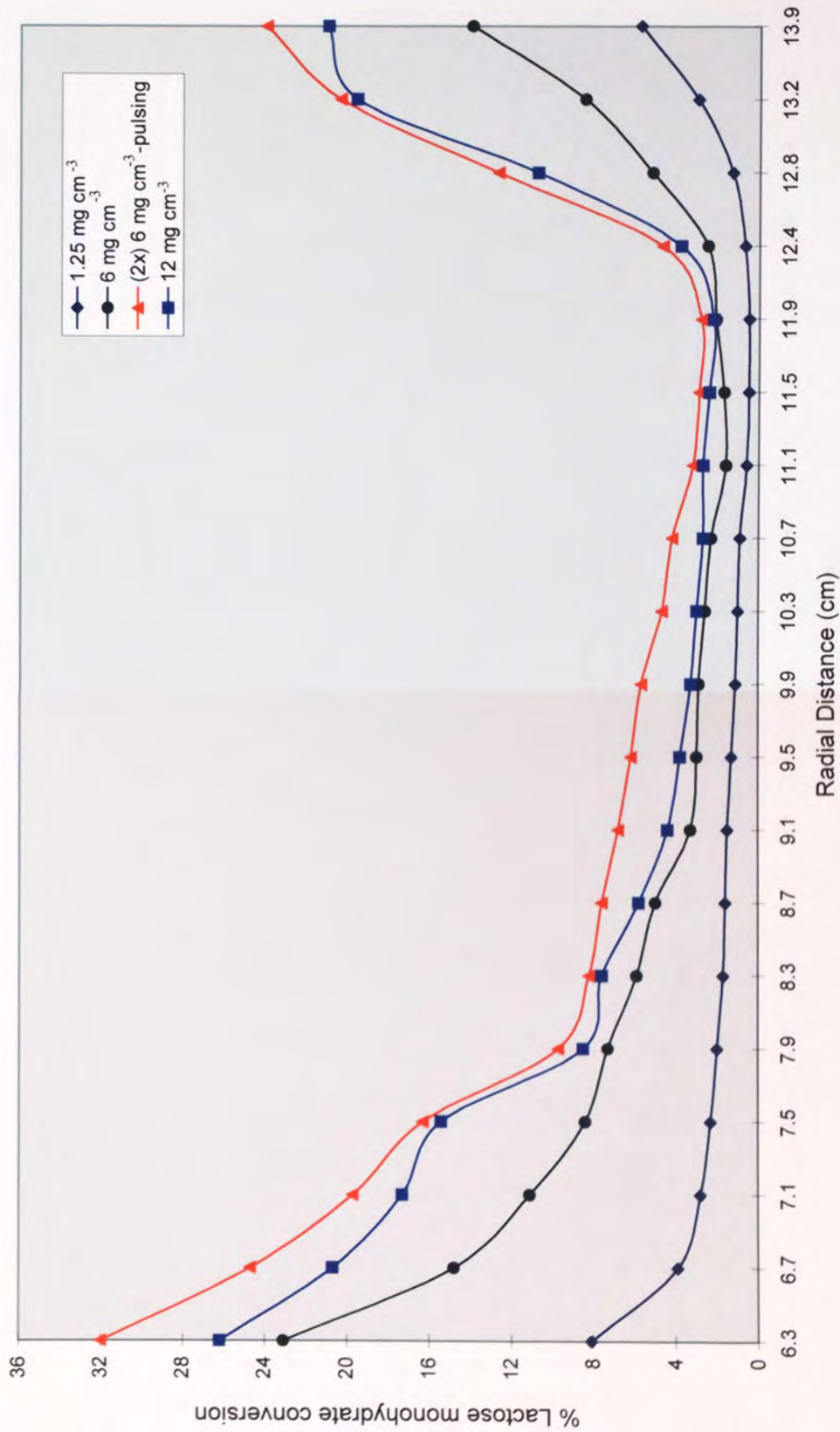


Figure 5.24b. % Lactose monohydrate conversion profiles for insolubilised β -galactosidase concentrations of 1.25, 6, (2x) 6 - pulsing and 12 mg cm⁻³ (4, 19.2, (2x) 19.2 and 38.4 U cm⁻³ respectively) top-layered on lactose monohydrate density gradients (10-40%^{w/v}) and centrifuged at 11 000 r.p.m. (18 703 g max) for 30 minutes, at 40°C.

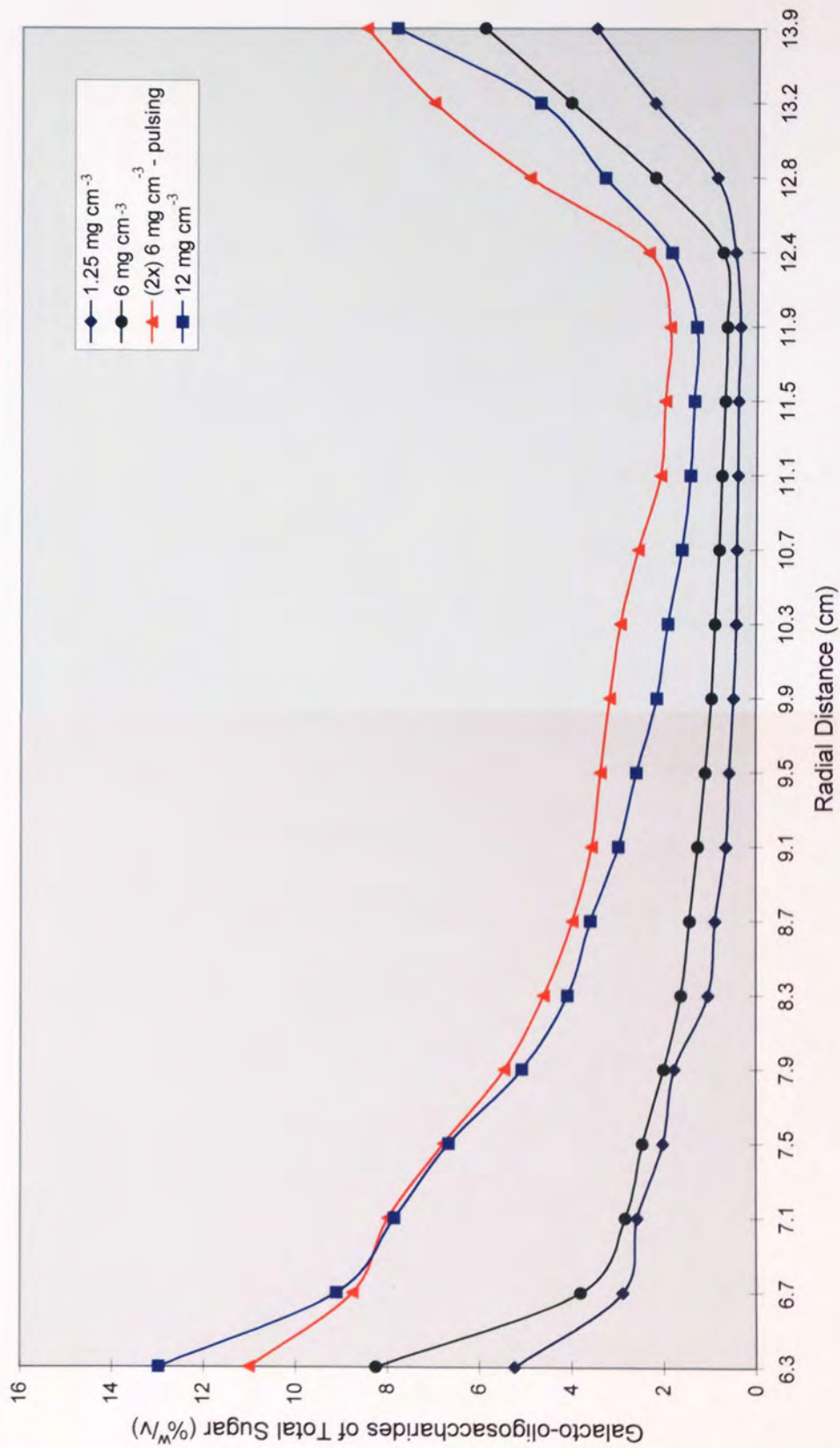


Figure 5.25a. Galacto-oligosaccharide distribution profiles for insolubilised β -galactosidase concentrations of 1.25, 6, (2x) 6 - pulsing and 12 mg cm⁻³ (4, 19.2, (2x) 19.2 and 38.4 U cm⁻³ respectively) top-layered on to lactose monohydrate density gradients (10-40%^{w/v}) and centrifuged at 13 000 r.p.m. (26 122 g max) for 30 minutes, at 40°C.

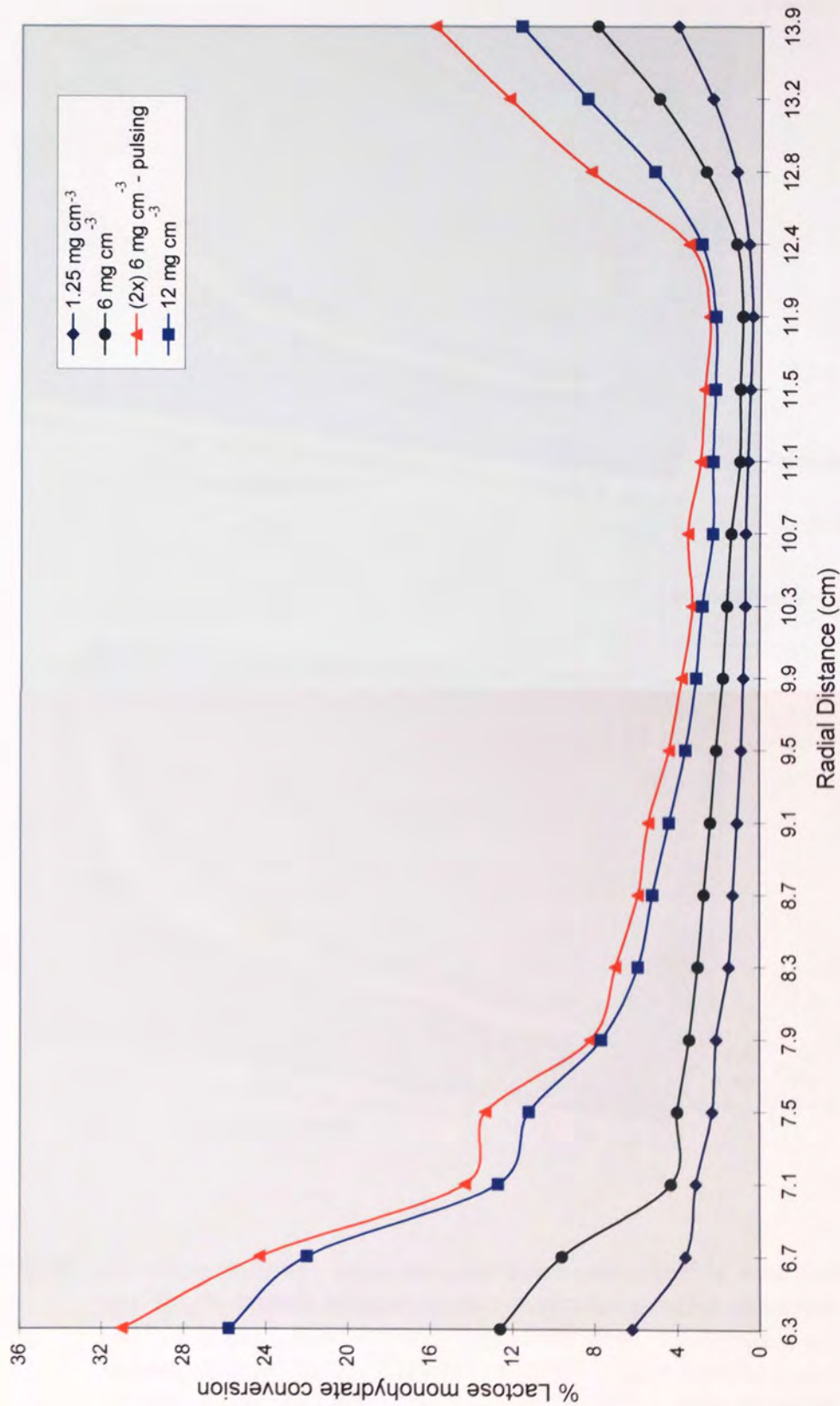


Figure 5.25b. % Lactose monohydrate conversion profiles for insolubilised β -galactosidase concentrations of 1.25, 6, (2x) 6 - pulsing and 12 mg cm⁻³ (4, 19.2, (2x) 19.2 and 38.4 U cm⁻³ respectively) top-layered on to lactose monohydrate density gradients (10-40%^{w/v}) and centrifuged at 13 000 r.p.m. (26 122 g max) for 30 minutes, at 40°C.

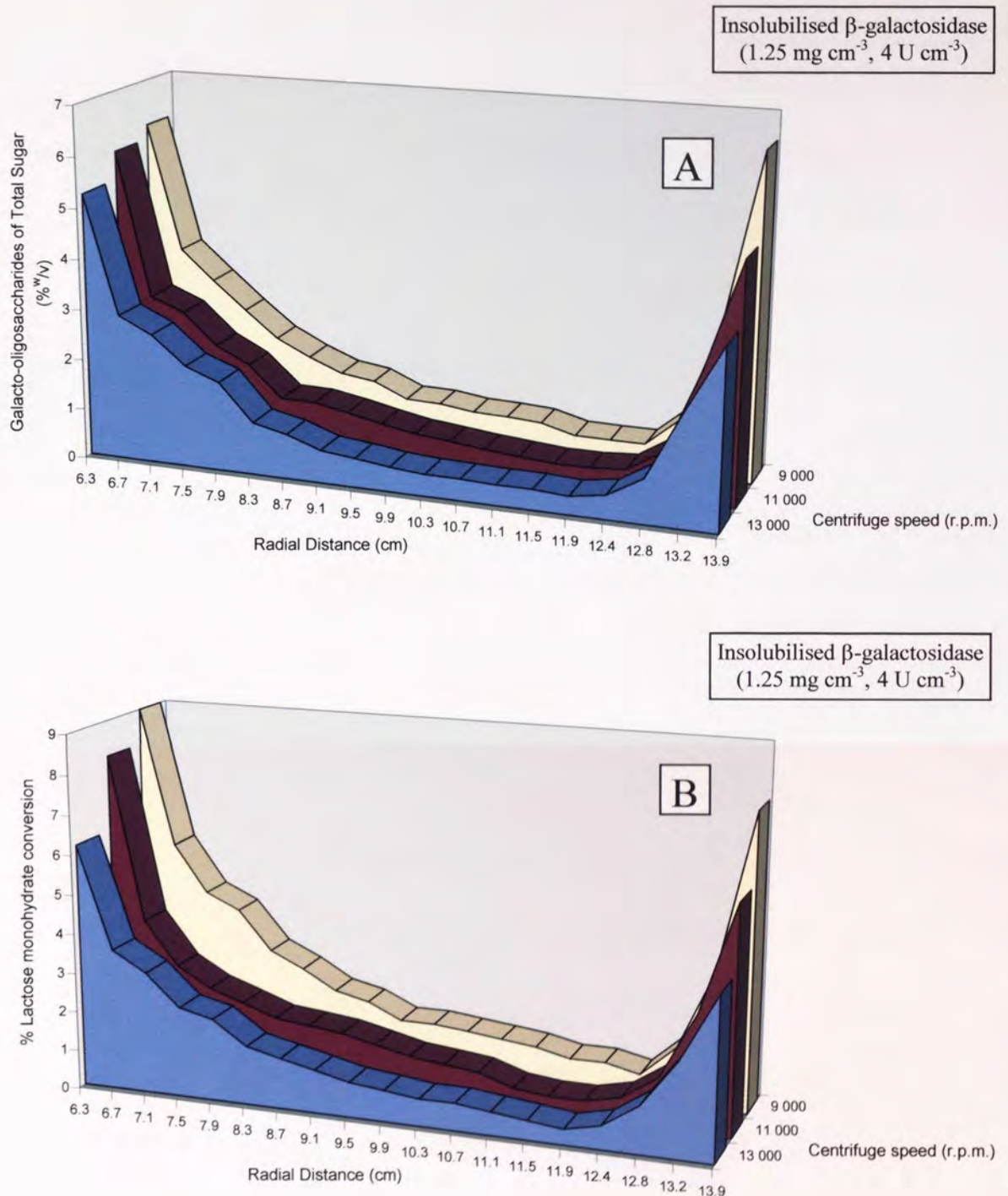


Figure 5.26. A comparison of both the galacto-oligosaccharide distribution profiles and the % lactose monohydrate conversion profiles obtained for 1.25 mg cm^{-3} (4 U cm^{-3}) insolubilised β -galactosidase, top-layered on to a lactose monohydrate density gradient ($10\text{-}40\% \text{ w/v}$) and centrifuged at 9-, 11- and 13 000 r.p.m. (12 520, 18 703 and 26 122 g max respectively) for 30 minutes at 40°C . A is the galacto-oligosaccharide distribution profiles and B is the % Lactose monohydrate conversion profiles.

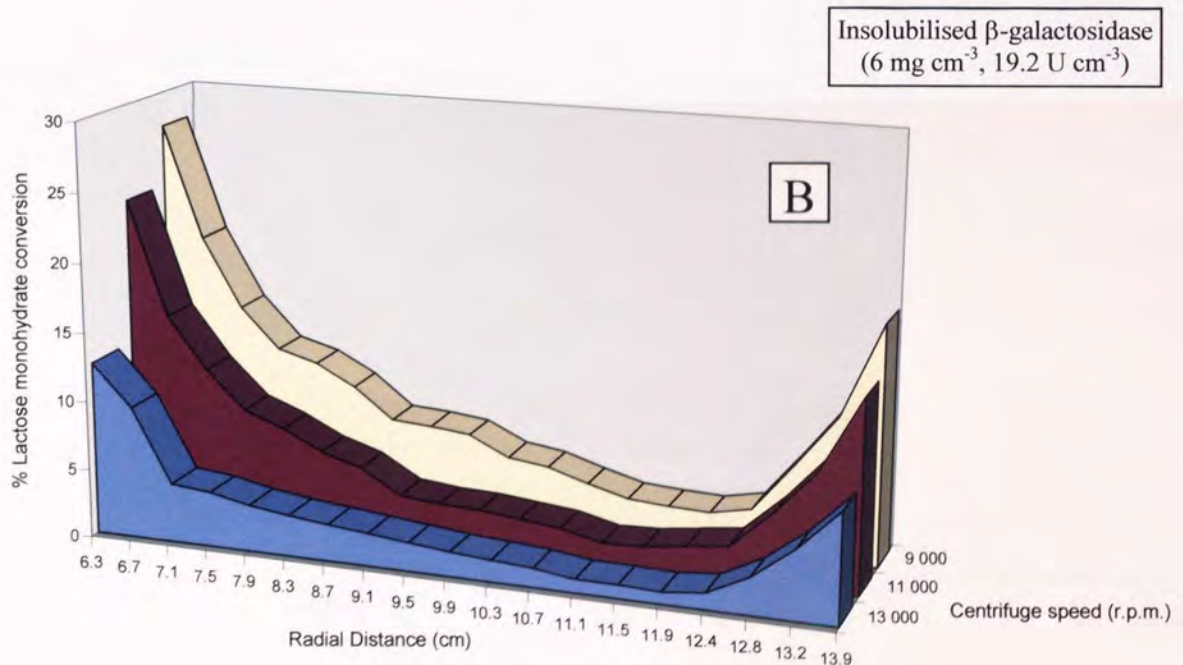
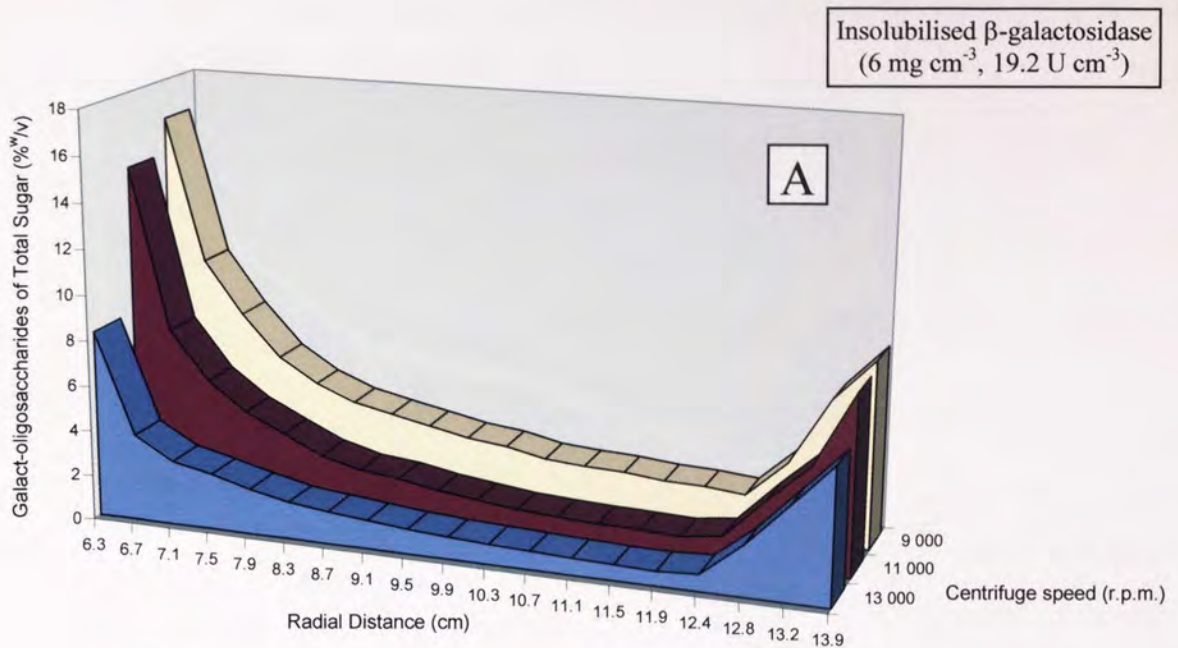


Figure 5.27. A comparison of both the galacto-oligosaccharide distribution profiles and the % lactose monohydrate conversion profiles obtained for 6 mg cm⁻³ (19.2 U cm⁻³) insolubilised β -galactosidase, top-layered on to a lactose monohydrate density gradient (10-40% w/v) and centrifuged at 9-, 11- and 13 000 r.p.m. (12 520, 18 703 and 26 122 g max respectively) for 30 minutes at 40°C. A is the galacto-oligosaccharide distribution profiles and B is the % Lactose monohydrate conversion profiles.

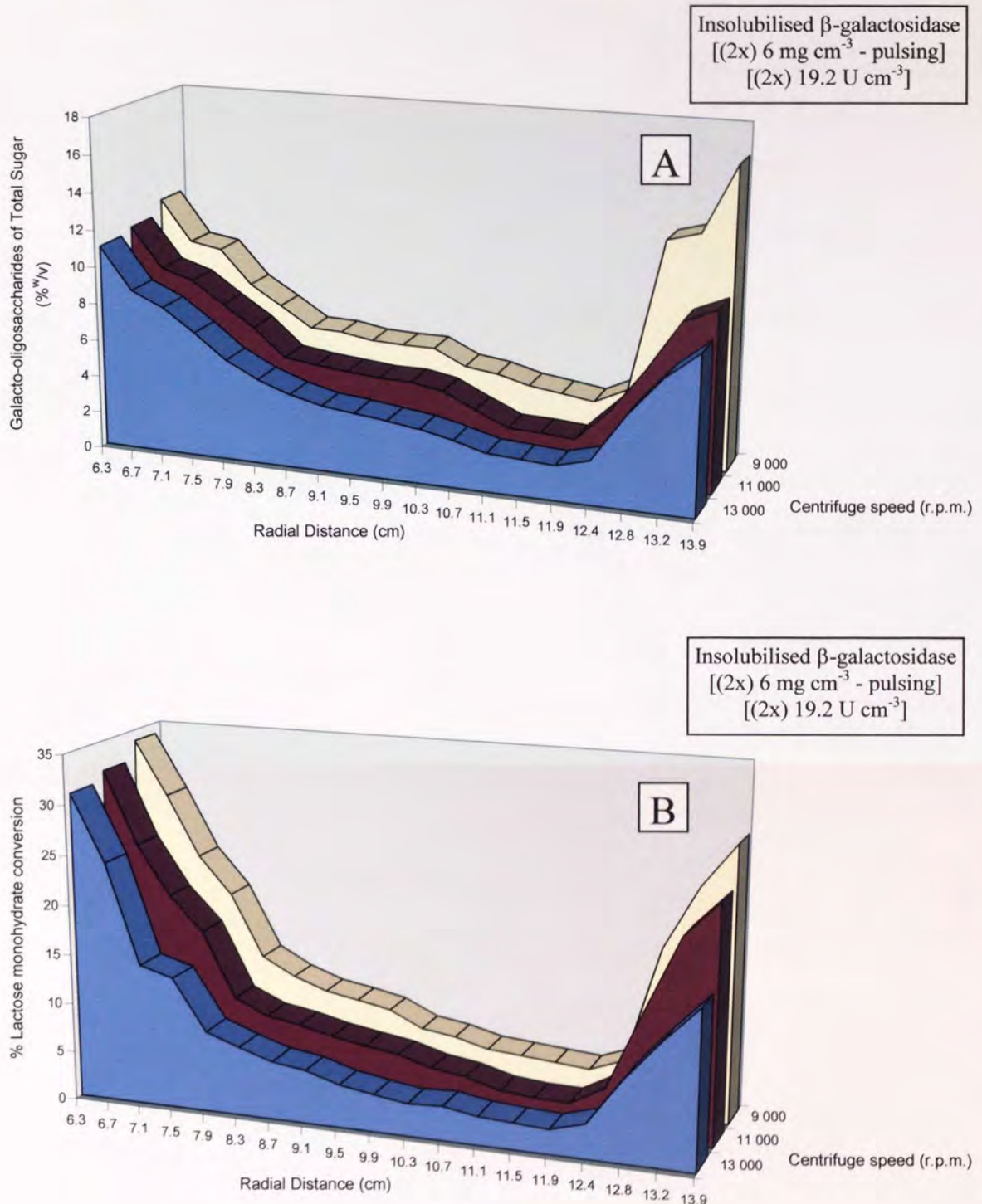


Figure 5.28. A comparison of both the galacto-oligosaccharide distribution profiles and the % lactose monohydrate conversion profiles obtained for (2x) 6 mg cm^{-3} ((2x) 19.2 U cm^{-3}) (pulsing) insolubilised β -galactosidase, top-layered on to a lactose monohydrate density gradient (10-40% w/v) and centrifuged at 9-, 11- and 13 000 r.p.m. (12 520, 18 703 and 26 122 g max respectively) for 30 minutes at 40°C . A is the galacto-oligosaccharide distribution profiles and B is the % Lactose monohydrate conversion profiles.

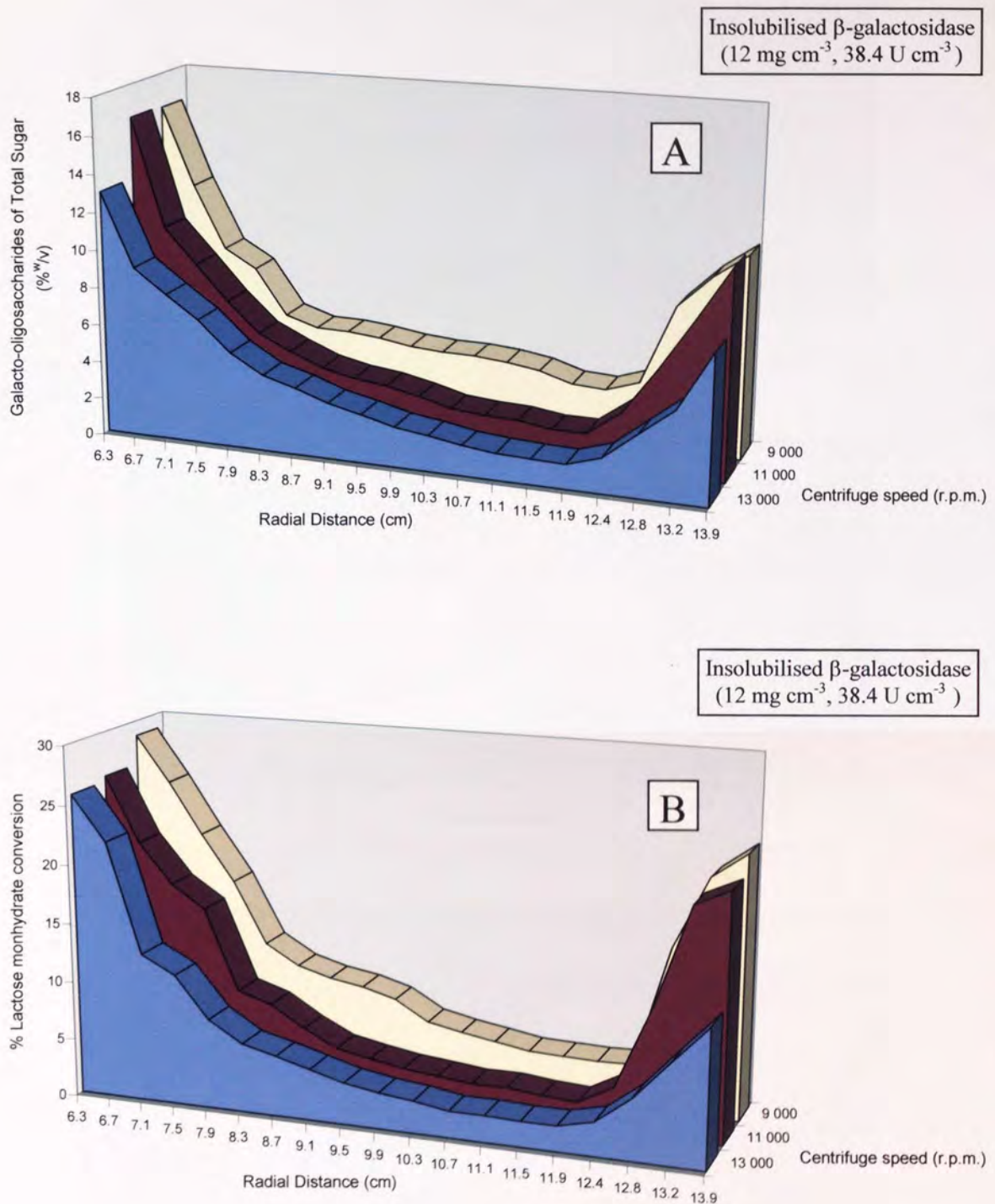


Figure 5.29. A comparison of both the galacto-oligosaccharide distribution profiles and the % lactose monohydrate conversion profiles obtained for 12 mg cm^{-3} (38.4 U cm^{-3}) insolubilised β -galactosidase, top-layered on to a lactose monohydrate density gradient ($10\text{-}40\% \text{ w/v}$) and centrifuged at 9-, 11- and 13 000 r.p.m. ($12\ 520$, $18\ 703$ and $26\ 122 \text{ g max}$ respectively) for 30 minutes at 40°C . A is the galacto-oligosaccharide distribution profiles and B is the % Lactose monohydrate conversion profiles.

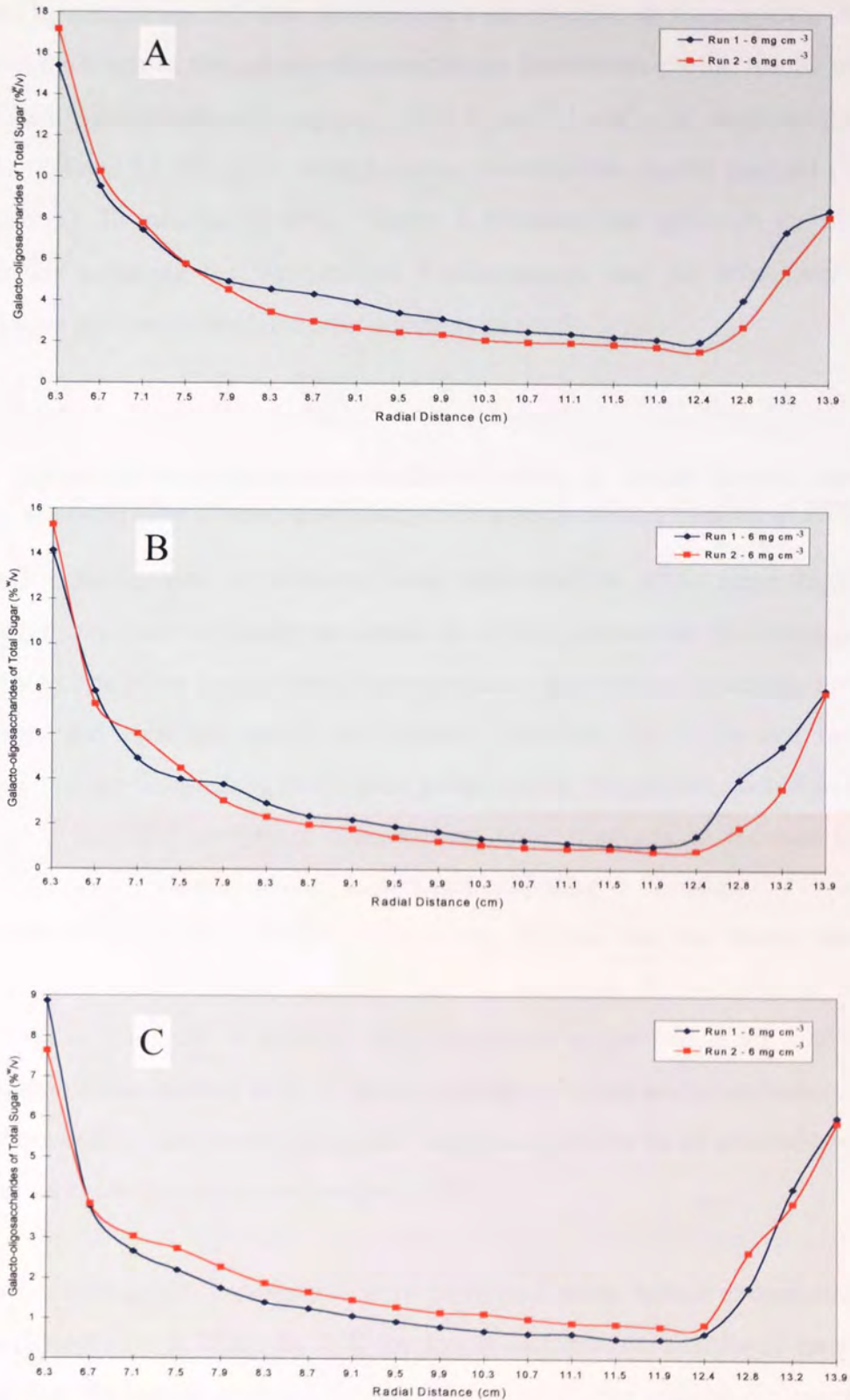


Figure 5.30. A comparison of the galacto-oligosaccharide distribution profile results obtained for duplicate experiments using insolubilised β -galactosidase (6 mg cm^{-3} (19.2 U cm^{-3}), 1 cm^3), for reactions performed at 9-, 11- and 13 000 r.p.m. (12 520, 18 703 and 26 122 g max respectively) using a lactose monohydrate density gradient ($10\text{-}40\% \text{ w/v}$) centrifuged for 30 minutes at 40°C . A is at 9-, B is at 11- and C is at 13 000 r.p.m..

illustrated by comparison of data obtained for a set of duplicate experiments. Figure 5.30 shows a comparison of the galacto-oligosaccharide distribution profile results obtained for insolubilised β -galactosidase (6 mg cm^{-3} , 19.2 U cm^{-3} , 1 cm^3), for reactions performed at 9 000, 11 000 and 13 000 r.p.m. using a lactose monohydrate density gradient (10-40%^{w/v}) centrifuged for 30 minutes at 40°C. Figure 5.30 shows that although the experimental protocols for preparing the insolubilised β -galactosidase and the subsequent rate-zonal centrifugation are complicated, the reproducibility of results is good.

5.3.6.2. Rate-zonal centrifugation experiments using (a) higher lactose monohydrate concentration density gradients and (b) performing reactions at 25°C.

Rate-zonal centrifugation experiments were performed at 40°C using higher lactose monohydrate concentration density gradients (40-70%^{w/v}) in an attempt to decrease the high sedimentation rate of the insolubilised β -galactosidase. In this way, the contact time between the enzyme and substrate should be increased and both the % lactose monohydrate conversion and the galacto-oligosaccharide yields within the gradient should be improved. Using higher lactose monohydrate concentration range produces an increase in both the density and viscosity profiles of the gradient and, according to Equation (3.14), reduces the particle sedimentation rate. In fact, experiments showed that the lactose monohydrate density gradient was extremely unstable due to the rapid precipitation of the lactose monohydrate as it fell out of solution; this was caused by the maximum solubility of the lactose monohydrate in water at 40°C being exceeded. Consequently, increasing the lactose monohydrate density gradient concentration range was found to be an unsuitable method for increasing substrate conversion and product yields.

Rate-zonal centrifugation experiments were performed using lactose monohydrate density gradients (10-40%^{w/v}) at 25°C. At 25°C the density and viscosity profiles of the gradient are increased, but the lactose monohydrate stays in solution long enough for reactions to be performed. Also, reducing the reaction temperature allowed the centrifuge to be operated at lower rotation speeds (range 2 000 to 13 000 r.p.m. (618 and 26 122 g max respectively)), whilst maintaining a reaction temperature of 25°C. This approach produced both lower galacto-oligosaccharide yields and % lactose monohydrate conversions because of a marked

reduction in the insolubilised β -galactosidase activity. A comparison of Galacto-oligosaccharide of Total Sugar (%^{w/v}) obtained at 25°C using a rotation speed of 2 000 r.p.m. with that obtained at 40°C using a rotation speed of 9 000 r.p.m is shown in Figure 5.31. The results presented in Figure 5.31 were obtained using an insolubilised enzyme concentration of 6 mg cm⁻³ (19.2 U cm⁻³) and a 10-40%^{w/v} lactose monohydrate gradient.

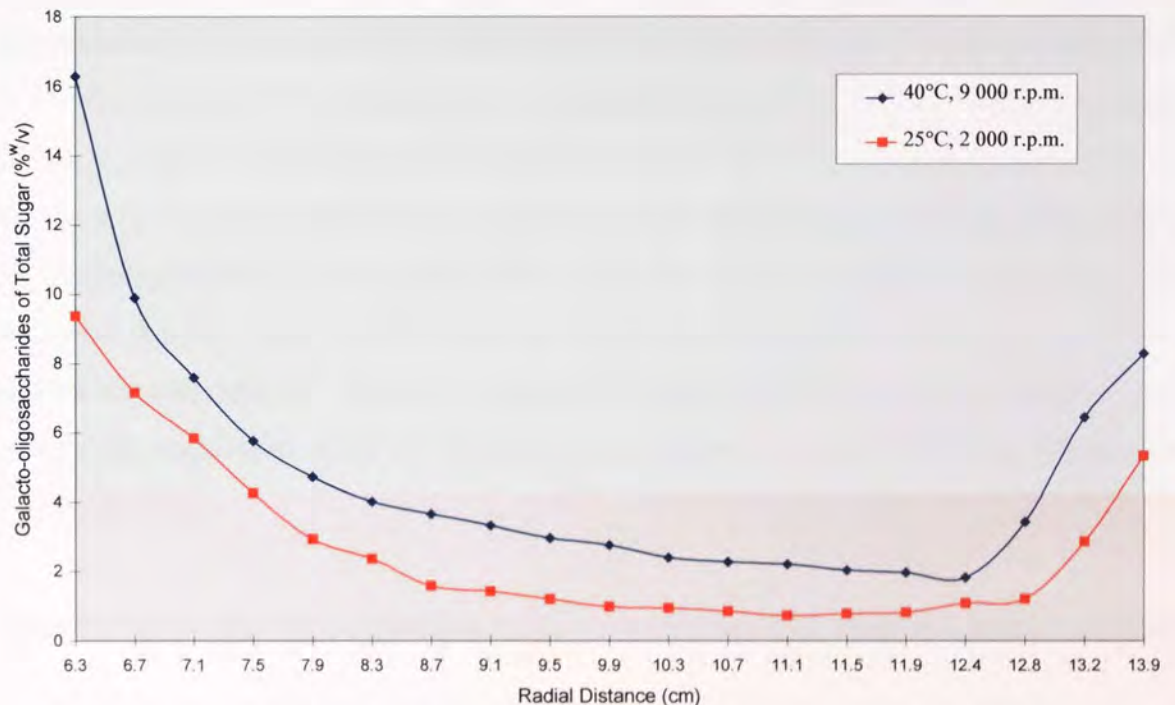


Figure 5.31. Comparison of Galacto-oligosaccharide of Total Sugar (%^{w/v}) results for centrifugation reactions performed using (a) 6 mg cm⁻³ (19.2 U cm⁻³) insolubilised β -galactosidase from *Aspergillus oryzae* layered onto a 10 to 40%^{w/v} lactose monohydrate gradient and centrifuged at 2 000 r.p.m. (618 g max) for 30 minutes at 25 °C, and (b) 6 mg cm⁻³ (19.2 U cm⁻³) insolubilised β -galactosidase from *Aspergillus oryzae* layered onto a 10 to 40%^{w/v} lactose monohydrate gradient and centrifuged at 9 000 r.p.m. (12 520 g max) for 30 minutes at 40 °C.

Figure 5.31 shows that although the sedimentation rate of the insolubilised enzyme would have been reduced by performing the centrifugation reaction at 2 000 r.p.m., the reaction temperature of 25°C lowered the enzyme's activity, and consequently reduced the galacto-

oligosaccharide yield. Similar trends to those presented in Figure 5.31 were obtained for the % Lactose monohydrate conversion results.

5.3.6.3 Discussion of results

The results presented in Figures 5.23a, 5.23b, 5.24a, 5.24b, 5.25a and 5.25b show that the % lactose conversions and the galacto-oligosaccharide yields were controlled by varying both the applied centrifugal fields (rotation speed) and the concentration of insolubilised β -galactosidase top-layered onto the lactose monohydrate density gradient. The highest % lactose conversions and galacto-oligosaccharide yields were obtained using a rotation speed of 9 000 r.p.m. (12 520 g max) and by pulsing the insolubilised β -galactosidase through a lactose monohydrate gradient, at a reaction temperature of 40°C. Of the rotation speeds used 9 000 r.p.m. was the lowest and this would have allowed the longest 'contact time' between the enzyme/substrate at any given point along the lactose monohydrate gradient. This increased 'contact time' would allow for higher lactose conversion and greater yield of galacto-oligosaccharide. Table 5.4 shows a comparison of the results obtained for % galacto-oligosaccharide yield at various rotation speeds and using different insolubilised enzyme loadings.

Galacto-oligosaccharide of Total Sugar (%^{w/v}) results taken at a Radial Distance of 10.3 cm

Rotation Speed (r.p.m.)	Insolubilised Enzyme Loading (mg cm ⁻³)			
	1.25	6	12	12 (2 x 6)
9 000	1.2	2.6	4.5	5.5
11 000	0.6	1.3	2.3	4.5
13 000	0.5	0.8	2.0	3.4

Table 5.4. Comparison of the results obtained for Galacto-oligosaccharide of Total Sugar (%^{w/v}) at various rotation speeds and using different insolubilised enzyme loadings. The reactions were performed using a 10-40%^{w/v} lactose monohydrate gradient centrifuged for 30 minutes at 40°C.

Table 5.5 shows a comparison of the results obtained for % Lactose Monohydrate Conversion at various rotation speeds and using different insolubilised enzyme loadings.

% Lactose Monohydrate Conversion results taken at a Radial Distance of 10.3 cm

Rotation Speed (r.p.m.)	Insolubilised Enzyme Loading (mg cm^{-3})			
	1.25	6	12	12 (2 x 6)
9 000	2.1	5.0	6.2	8.3
11 000	1.7	2.5	3.0	5.5
13 000	1.0	1.5	3.0	3.9

Table 5.5. Comparison of the results obtained for % Lactose Monohydrate Conversion at various rotation speeds and using different insolubilised enzyme loadings. The reactions were performed using a 10-40%^{w/v} lactose monohydrate gradient centrifuged for 30 minutes at 40°C.

Reducing the reaction temperature from 40°C to 25°C in an attempt to increase the 'contact time' produced lower galacto-oligosaccharide yields and decreased % lactose monohydrate conversion due to the reduction in the enzyme's activity.

Pulsing the insolubilised β -galactosidase ($2 \times 6 \text{ mg cm}^{-3}$ ($2 \times 19.2 \text{ U cm}^{-3}$)), as opposed to a single high concentration loading (12 mg cm^{-3} (38.4 U cm^{-3})), probably produced higher galacto-oligosaccharide yields because the gradient was effectively 'pre-seeded' with galactose and galacto-oligosaccharides ready for trans-galactosylation. West ⁽⁷⁾ performed stirred fed-batch reactions and found that higher lactose conversion and greater galacto-oligosaccharide yields were produced when the enzyme was added incrementally. Tables 5.4 and 5.5 show a comparison of results obtained for a single 12 mg cm^{-3} insolubilised enzyme loading and two 6 mg cm^{-3} pulses.

The slope in the profiles is produced by the decreasing contact time between the enzyme and the substrate as the applied centrifugal field increases. The increase towards the bottom of the gradients was probably caused by back-diffusion of galacto-oligosaccharides, formed by the action of the pelleted insolubilised β -galactosidase on localised lactose monohydrate. Data presented in Figure 5.21 indicates that the insolubilised β -galactosidase had been pelleted for ~15 minutes before the reactions were terminated.

The composition of the lactose monohydrate gradient was determined by the limit of solubility of the sugar at 40°C. Experiments showed that gradients prepared using lactose monohydrate above 40%^w/v were unstable and rapidly degraded due to the precipitation of the sugar. Decreasing the lactose monohydrate gradient range from 10-40%^w/v to 20-40%^w/v was found to reduce the stability because of the reduction in the dynamic density range of the gradient.

6.0 CONCLUSIONS, INTEGRATING DISCUSSION AND RECOMMENDATIONS FOR FURTHER WORK

In this Chapter, the main conclusions from this project are summarised. An integrating discussion includes (a) a comparison of stirred-batch and centrifugation reactions using soluble and insolubilised β -galactosidase, (b) a discussion of the novel immobilised and insolubilised enzyme centrifugation reaction system developed, (c) the use of a novel insolubilised enzyme pulsing technique developed in this project, and (d) the applicability of the centrifugal reaction system used to industry. This Chapter concludes with a list of recommendations for further work.

6.1 Conclusions

In this section, the main conclusions from this research project are summarised.

6.1.1 Stirred-batch reactions performed using soluble free and glutaraldehyde insolubilised β -galactosidase from *Aspergillus oryzae*

The results obtained from the stirred-batch reactions performed using soluble free β -galactosidase, performed at 25°C, 40°C and 55°C can be summarised as follows:

1. Maximum galacto-oligosaccharide yields are achieved at lactose monohydrate conversions between 40-55%.
2. The higher the initial lactose monohydrate concentration the greater the yield of galacto-oligosaccharide.
3. Similar maximum galacto-oligosaccharide yields were obtained at 25°C, 40°C and 55°C (see Table 2.3).
4. The galacto-oligosaccharides formed consist predominantly of galactose.
5. The highest galacto-oligosaccharide detected was a tetrasaccharide.
6. The higher the degree of polymerisation of the galacto-oligosaccharide the lower the yield (tri- > tetra-).

A comparison of both the % Galacto-oligosaccharides of Total Sugar and the % Lactose Monohydrate Conversion for soluble β -galactosidase and glutaraldehyde insolubilised β -galactosidase, for stirred-batch reactions performed at 40°C shows:

1. The rate of lactose monohydrate conversion is slower for the insolubilised β -galactosidase.
2. For a given % Lactose Monohydrate Conversion the % Galacto-oligosaccharides of Total Sugar is slightly lower for the insolubilised β -galactosidase.
3. The insolubilisation process does not greatly affect the hydrolytic and trans-galactosyl activity of β -galactosidase from *Aspergillus oryzae* (Biolactase F).

A preliminary mathematical model for estimating lactose monohydrate conversion, based on Michaelis-Menten kinetics with competitive inhibition, was found to show divergence between theoretical and experimental results. This was due to the omission of certain factors which include (a) the trans-galactosyl activity of β -galactosidase, (b) the mutarotation of galactose, (c) the increased formation of galacto-oligosaccharides at higher initial lactose monohydrate concentrations, (d) competition for the enzyme's active site between lactose monohydrate and the galacto-oligosaccharides formed and (e) the effects of diffusion and partition on the kinetic parameters of insolubilised β -galactosidase.

Particles of glutaraldehyde insolubilised β -galactosidase were found to have no obvious porous structure and were comparatively spherical in shape. The high water content of the particles would indicate that they may exist in the form of an hydrogel, which is a water-rich colloidal system where the particle structure consists of chemically-linked colloidal particles.

6.1.2 Normal -Rate centrifugation studies using soluble β -galactosidase

Experiments performed with soluble free β -galactosidase using a modified normal-rate centrifugation technique produced the following findings: (a) the normal-rate centrifugation system is too unstable for performing enzyme sedimentation experiments, (b) the centrifuge used was unable to generate sufficiently high centrifugal fields to effect sedimentation of the enzyme, and (c) performing the reactions at 40°C increased the system's instability.

6.1.3 Rate-Zonal centrifugation studies using soluble β -galactosidase

Experiments performed with soluble free β -galactosidase using a rate-zonal centrifugation technique produced the following findings: (a) the use of a lactose monohydrate density

gradient stabilised the reaction system, and (b) the centrifuge used was unable to generate sufficiently high centrifugal fields to effect sedimentation of the enzyme through the substrate gradient medium.

6.1.4 Rate-Zonal centrifugation studies using immobilised and insolubilised β -galactosidase

Various methods were used to immobilise and insolubilise β -galactosidase. This led to an increase in the apparent sedimentation rate of the enzyme, allowing the enzyme to sediment through a 10-40%^{w/v} lactose monohydrate gradient using the range of centrifugal fields attainable. Dextran entrapment of the enzyme allowed the dextran/enzyme conjugate to fully sediment through the gradient, although the % Lactose Monohydrate Conversion and % Galacto-oligosaccharide formed was low. Covalent bonding of β -galactosidase to dextran particles produced low enzyme loadings, and consequently low values of % Lactose Monohydrate Conversion and % Galacto-oligosaccharide of Total Sugar were obtained from centrifugation experiments.

Methods for insolubilisation of β -galactosidase using glutaraldehyde were developed that produced particles which retained high enzymatic activity. Suspensions of the insolubilised particles were fully sedimented through the lactose monohydrate gradient and produced higher values for % Lactose Monohydrate Conversion and % Galacto-oligosaccharide of Total Sugar than had been previously achieved. It was found that by pulsing the insolubilised enzyme through the substrate higher values for % Lactose Monohydrate Conversion and % Galacto-oligosaccharide of Total Sugar could be achieved, compared to that obtained using a single enzyme loading equivalent in activity.

It was found that by varying the applied centrifugal fields and the concentration of the insolubilised enzyme used the formation of galacto-oligosaccharide could be controlled. The higher the applied centrifugal fields the lower the yield of galacto-oligosaccharide. The highest galacto-oligosaccharide yield was obtained using two insolubilised enzyme pulses, each equivalent to 6 mg cm⁻³ (19.2 U cm⁻³), sedimented through a 10-40%^{w/v} lactose monohydrate gradient centrifuged at 9 000 r.p.m. (12 520 g max) for 30 minutes, at 40°C.

6.2 Integrating discussion

This section compares the stirred-batch and centrifugation reactions performed. A discussion of the novel immobilised and insolubilised enzyme centrifugation reaction system developed in this research and the use of a novel insolubilised enzyme pulsing technique. Also, the applicability of this centrifugal reaction system to industry is commented upon.

6.2.1. A comparison of stirred-batch and centrifugation reactions performed

The high sedimentation rate of the insolubilised β -galactosidase produced short 'contact times' between the enzyme and the substrate as it sedimented through the lactose monohydrate gradient. Also, as the insolubilised β -galactosidase sediments through the gradient the substrate concentration that it encounters is constantly changing. This makes it difficult to compare directly the stirred-batch and centrifugation results. However, using gradient profile data a specific lactose monohydrate concentration can be assigned to a position within the profile; the % Lactose Monohydrate Conversion and % Galacto-oligosaccharide of Total Sugar obtained at this position can thus be determined. Comparative figures can be obtained for the stirred-batch system using data obtained for the equivalent lactose monohydrate concentration and % lactose conversion. The % Galacto-oligosaccharide of Total Sugar values can then be compared for any significant differences that may have been produced by the different reaction methods. The only comparison possible is for an enzyme concentration of 1.25 mg cm^{-3} (4 U cm^{-3}), as this was the concentration used for the stirred-batch reactions. The results obtained are shown in Table 6.1. Centrifugation data used was taken from reactions performed at 9 000 r.p.m at 40°C .

The results presented in Table 6.1 show that for an equivalent % Lactose Monohydrate Conversion the corresponding % Galacto-oligosaccharide of Total Sugar values for soluble/insoluble stirred-batch and centrifugation reactions are similar. Due the very high sedimentation rate of the insolubilised β -galactosidase only low % Lactose Monohydrate Conversion values can be compared and the results obtained may not be mirrored at higher lactose monohydrate conversion. However, the results indicate that the insolubilisation process and the application of centrifugal fields does not adversely affect the enzyme's trans-galactosyl activity.

% Lactose monohydrate concentration (gradient and stirred-batch)	% Lactose monohydrate conversion value	% Galacto-oligosaccharide of Total Sugar		
		Stirred-batch (soluble)	Stirred-batch (insoluble)	Centrifuge (insoluble)
15	3.0	1.0	1.0	1.8
20	2.0	0.8	0.6	1.0
25	1.5	0.7	0.4	0.9

Table 6.1. Comparison of equivalent % Galacto-oligosaccharide of Total Sugar values for stirred-batch and centrifugation reactions performed using a soluble/insolubilised enzyme concentration of 1.25 mg cm^{-3} (4 U cm^{-3}), at 40°C . Centrifuge data was taken from reactions performed at 9 000 r.p.m. ($12\ 520 \text{ g max}$) for 30 minutes, at 40°C using a 10-40%^{w/v} lactose monohydrate gradient.

6.2.2 A novel immobilised and insolubilised enzyme centrifugation reaction system

This research has produced a novel immobilised and insolubilised centrifugation reaction system which has not previously been reported in the literature. However, researchers have reported increased enzyme sedimentation rates due to substrate/enzyme complexes being formed during a centrifugal reaction ^(2,3). Centrifugation reactions performed using glutaraldehyde insolubilised β -galactosidase were found to produce the highest yields of galacto-oligosaccharides. The size and density of the insolubilised particles resulted in a very high sedimentation rate and consequently short enzyme/substrate 'contact time'. The sedimentation rate could be reduced by reducing the particle size or by immobilising the enzyme onto a material of lower density and smaller particle size, and this would increase the enzyme/substrate 'contact time'. Using nylon microspheres or liposomes as a 'carrier' for the enzyme may significantly reduce the sedimentation rate.

The stirred-batch reactions performed using both soluble and insolubilised β -galactosidase required chemical quenching of the reaction to eliminate enzyme activity. During the centrifugation reaction the insolubilised enzyme is fully sedimented and is effectively separated from the reaction products. Quenching of the centrifuge samples was only performed to allow comparison with the stirred-batch results. Separation of the active enzyme allows for recovery and re-use of the enzyme and removes the requirement for the

enzyme to be removed during downstream processing. Immobilisation/insolubilisation allows visualisation of the enzyme and this aids in the removal of the enzyme.

6.2.3 Pulsing of insolubilised β -galactosidase

Centrifugation experiments performed using pulses of insolubilised β -galactosidase produced higher yields of galacto-oligosaccharide compared to a single enzyme loading of equivalent activity. Pulsing of the enzyme may be continued until the desired product profile is achieved or until the gradient degenerates. The development of a continuous system would allow the recovery and recycling of each enzyme pulse. This novel approach could be applied to multi-enzyme sequential synthesis products.

6.2.4 The applicability of the centrifugal reaction system used to industry

Currently, the use of the centrifuge in industry is mainly limited to product recovery in the downstream process. Also, the industrial centrifuges described in Chapter 3 are not suitable for performing the type of reaction employed in this research. The rate-zonal system used in this research can be applied to zonal rotors (see Figure 3.12) which have a capacity of ~ 2 litres. These rotors are designed to be used at rotation speeds in excess of 20 000 r.p.m. and so are constructed from titanium to withstand the dynamic forces. Using an immobilised/insolubilised enzyme reduces the rotation speeds required to sediment the enzyme and this would reduce the dynamic forces, and allow cheaper materials (such as aluminium) to be used to construct larger capacity zonal rotors. This type of reaction system would only be cost effective for high value/low volume products, prepared using high cost enzymes.

6.3 Recommendations for further work

The following are recommendations for further work:

1. Immobilisation of β -galactosidase onto a lower density material with a smaller particle size to reduce the sedimentation rate. Possible materials may be sub-micron nylon spheres or liposomes (see Chapter 5).
2. Perform enzyme pulsing experiments to determine if the use of more pulses of lower activity will increase yields further.

3. Scale-up of the process using a zonal rotor to confirm the results obtained using the centrifuge tube batch system used in this research.
4. Introduce a suitable organic solvent to the gradient to determine if this enhances the trans-galactosyl activity of β -galactosidase and improves galacto-oligosaccharide yields.
5. Identify other suitable enzymatic reaction systems suitable for immobilisation and investigation using the centrifuge as a bioreactor. Polymer forming reactions would be most suitable as the density gradient could be used to separate products of differing sedimentation rates and density.
6. Controlled hydrolysis of polysaccharides, such as the hydrolysis of dextran by dextranase. Produce a dextran density gradient and sediment immobilised or insolubilised dextranase through the gradient using different applied centrifugal fields ⁽¹⁰⁹⁾.
7. Pulsing of different enzymes to produce sequential multi-enzyme products.
8. Perform a more detailed study of galacto-oligosaccharide formation and use this data to derive a mathematical model for their production.

7.0 MATERIALS AND EXPERIMENTAL METHODS

In this Chapter, the materials used during this research are listed and the experimental methods performed are described in detail.

7.1 Materials

The materials used in this research project are listed in Table 7.1.

Product	Specification/Grade	Supplier
Amberlite resin CG-400 (Cl form) (cross-linked polystyrene)	Chromatographic grade, 100-200 mesh (75-125 μ m)	Merck, Poole, Dorset, UK.
Bio-Rad protein assay reagent	Standard assay	Bio-Rad Limited, Hemel Hempstead, Herts, UK.
Blue dextran 2000	Mwt ~ 2 000 000	Amersham PharmaciaBiotech, Little Chalfont, Bucks, UK.
Bovine serum albumin (BSA)	Fraction V (96%)	Sigma-Aldrich, Poole, Dorset, UK.
Buffer powders	pH4 and pH7	Merck, Poole, Dorset, UK.
Calcium nitrate	Standard laboratory reagent (SLR)	Fisher Scientific, Loughborough, Leics, UK.
Cesium chloride	Purum	Fluka, Gillingham, Dorset, UK.
Dextran (from <i>Leuconostoc mesenteroides</i> B-512)	Industrial-grade, Mwt 5×10^6 to 40×10^6	Sigma-Aldrich, Poole, Dorset, UK.
Galactose	Standard laboratory reagent (SLR)	Fisher Scientific, Loughborough, Leics, UK.
β -Galactosidase from <i>Aspergillus oryzae</i>	Biolactase F (Food-grade)	Biocon Biochemicals Limited, Cork, Ireland.
Glucose	General purpose reagent (GPR)	Merck, Poole, Dorset, UK.
Glutaraldehyde (50% ^v /v)	Standard laboratory reagent (SLR)	Fisher Scientific, Loughborough, Leics, UK.
Hydrochloric acid	General purpose reagent (GPR)	Merck, Poole, Dorset, UK.
Lactose monohydrate	'Analar' grade	Merck, Poole, Dorset, UK.
Procion blue MX-R	Standard grade	Fluka, Gillingham, Dorset, UK.
Sodium acetate, anhydrous	Standard laboratory reagent (SLR)	Fisher Scientific, Loughborough, Leics, UK.
Sodium carbonate	Standard laboratory reagent (SLR)	Fisher Scientific, Loughborough, Leics, UK.
Sodium chloride	Standard laboratory reagent (SLR)	Fisher Scientific, Loughborough, Leics, UK.
Sodium hydroxide	Standard laboratory reagent (SLR)	Fisher Scientific, Loughborough, Leics, UK.
Urea	Microselect	Fluka, Gillingham, Dorset, UK.
Water	HPLC-grade	Fisher Scientific, Loughborough, Leics, UK.

Table 7.1. The materials used in this research project.

7.2 Experimental methods

In this Section, the experimental methods and analytical techniques used during this research are described in detail.

7.2.1 Stirred-batch reactions using soluble β -galactosidase from *Aspergillus oryzae* (Biolactase F)

Stirred-batch reactions were performed using soluble β -galactosidase from *Aspergillus oryzae* (Biolactase F) and the results obtained are presented in Chapter 2.

7.2.1.1 Preparation of soluble β -galactosidase from *Aspergillus oryzae* (Biolactase F) solutions

A bulk solution of the β -galactosidase from *Aspergillus oryzae* (Biocon Biochemicals Limited, Cork, Ireland) was prepared by grinding 1.565g of the enzyme in 20 cm³ of degassed HPLC-grade water (Fisher Scientific, Leics, UK) in a 100 cm³ glass beaker, using a glass stirring rod. The grinding was continued until a thin paste was formed. A further 60 cm³ of degassed HPLC-grade water was added in three 20 cm³ aliquots and after each addition the solution was mixed using a magnetic stirrer and stirrer bar. This solution was transferred to a 100 cm³ glass volumetric flask (grade A) and the volume adjusted to 100 cm³ using degassed HPLC-grade water. This solution was placed in a clean 100 cm³ glass beaker and the pH of the solution was adjusted to 5.2 (+/- 0.1) using 5%^{v/v} hydrochloric acid. The hydrochloric acid solution was prepared from concentrated hydrochloric acid (Merck, Dorset, UK) diluted using degassed HPLC-grade water. To the pH adjusted enzyme solution 1 cm³ of 0.05M sodium acetate buffer (Fisher Scientific, Leics. UK) was added.

The solution was then decanted into two 50 cm³ polycarbonate centrifuge tubes and centrifuged at 3 500 r.p.m. for 20 minutes at 20°C, using a Beckman J2-MC centrifuge fitted with a JS13.1 swing-out rotor (Beckman Instruments, High Wycombe, UK). After centrifugation, the slightly coloured but clear solution was decanted into a clean 100 cm³ glass beaker, whilst leaving the insoluble material pelleted at the bottom of the centrifuge tube. The bulk enzyme solution was then assayed to determine the β -galactosidase activity, which allowed the activities of successive bulk solutions to be monitored.

7.2.1.2 The measurement of β -galactosidase activity

The activity of β -galactosidase from *Aspergillus oryzae* was determined by incubating the enzyme with lactose monohydrate and measuring the rate of lactose monohydrate conversion. β -Galactosidase activity was calculated in terms of units per cm^3 (U cm^{-3}) and 1 unit (U) is defined as the amount of enzyme which converts 1 μmole of lactose monohydrate in 1 minute at the stated conditions of pH and temperature.

A solution of 1%^{w/v} lactose monohydrate (Merck, Dorset, UK) was prepared using degassed HPLC-grade water and 2 cm^3 was pipetted into a glass test tube. The test tube was then placed into a waterbath and attemperated at the stated reaction temperature. A 1 cm^3 aliquot of enzyme solution to be tested was diluted with 9 cm^3 of degassed HPLC-grade water, giving a dilution factor of 10x. This solution was then attemperated at the same temperature as the lactose monohydrate solution. A 2 cm^3 aliquot of the attemperated diluted enzyme solution was added to the test tube containing the 1%^{w/v} lactose monohydrate solution (2 cm^3). The solutions were mixed using a vortex mixer, whilst simultaneously starting a timer and incubated at the desired reaction temperature for exactly 5 minutes. After 5 minutes, the reaction was quenched using 2 cm^3 of 0.05M sodium hydroxide solution and 1 cm^3 of degassed HPLC-grade water was then added. The resulting solution was analysed by HPLC (see 3.2.1.7) and the μmoles of lactose monohydrate converted calculated by reference to a 1%^{w/v} lactose monohydrate standard. The β -galactosidase activity was then calculated in terms of U cm^{-3} , taking dilution factors into account.

7.2.1.3 Preparation of lactose monohydrate solutions

The stirred-batch reactions performed used a total reaction volume of 250 cm^3 , which initially consisted of a mixture of; 200 cm^3 of a lactose monohydrate solution, 30 cm^3 of degassed HPLC-grade water and 20 cm^3 of the bulk β -galactosidase solution (see 7.2.1.1). Based on a lactose monohydrate solution volume of 200 cm^3 , sufficient lactose monohydrate was dissolved and made up to 200 cm^3 to give the desired initial substrate concentration when diluted to 250 cm^3 . For example, 25g of lactose monohydrate was dissolved in, and made up to 200 cm^3 in a glass volumetric flask (grade A). This gave a 12.5%^{w/v} lactose monohydrate solution, which when diluted to 250 cm^3 at the start of a stirred-batch reaction experiment produced a substrate concentration of 10%^{w/v}. When preparing lactose

monohydrate solutions $>15\%^{w/v}$ heating was required to completely dissolve the sugar and these solutions were allowed to cool before being made up to 200 cm^3 in a volumetric flask.

7.2.1.4 Preparation of degassed HPLC-grade water

Degassed water used in this research was prepared by heating HPLC-grade water (Fisher Scientific, Leics, UK) in a glass beaker to 100°C and cooling to 20°C before being used to prepare solutions in volumetric glassware.

7.2.1.5 Stirred-batch reactions using soluble β -galactosidase from *Aspergillus oryzae*

Stirred-batch reactions were performed using various initial lactose monohydrate concentrations (5, 10, 15, 20, 25, 30 and $40\%^{w/v}$) and incubated with β -galactosidase from *Aspergillus oryzae* at a concentration of 1.25 mg cm^{-3} , at 25°C , 40°C and 55°C . The apparatus used to perform the reactions is shown in Figure 7.1. The total reaction volume was 250 cm^3 and this consisted initially of; 200 cm^3 of lactose monohydrate solution at a suitable concentration (see 7.2.1.3), 20 cm^3 of bulk β -galactosidase solution (see 7.2.1.1), and 30 cm^3 of degassed HPLC-grade water (see 7.2.1.4).

The lactose monohydrate solution and the degassed HPLC-grade water were placed in a glass three-necked round bottomed flask (500 cm^3) and incubated in a Grant W14 waterbath (Grant Instruments, Royston, Herts, UK) at the desired reaction temperature. A glass volumetric flask (20 cm^3) containing the bulk β -galactosidase was placed in the same waterbath and allowed to attemperate. Through the centre socket a polypropylene 2-blade swivel impellor (Fisher Scientific, Leics, UK) was inserted. The impellor had a length of 350mm and a shaft diameter of 8mm, with a minimum blade diameter of 25mm and a maximum diameter of 60mm. The stirrer was attached to a Citenco variable control overhead stirrer (Citenco Limited, Boreham Wood, Herts, UK). A digital optical tachometer (R.S Components Limited, Saltley, West Midlands) was used to set the rotation speed of the impellor to 200 r.p.m., the speed used for all the reactions performed.

At the start of a stirred-batch reaction the bulk β -galactosidase solution was poured into the reaction flask through one of the side sockets, which gave an enzyme concentration of 1.25

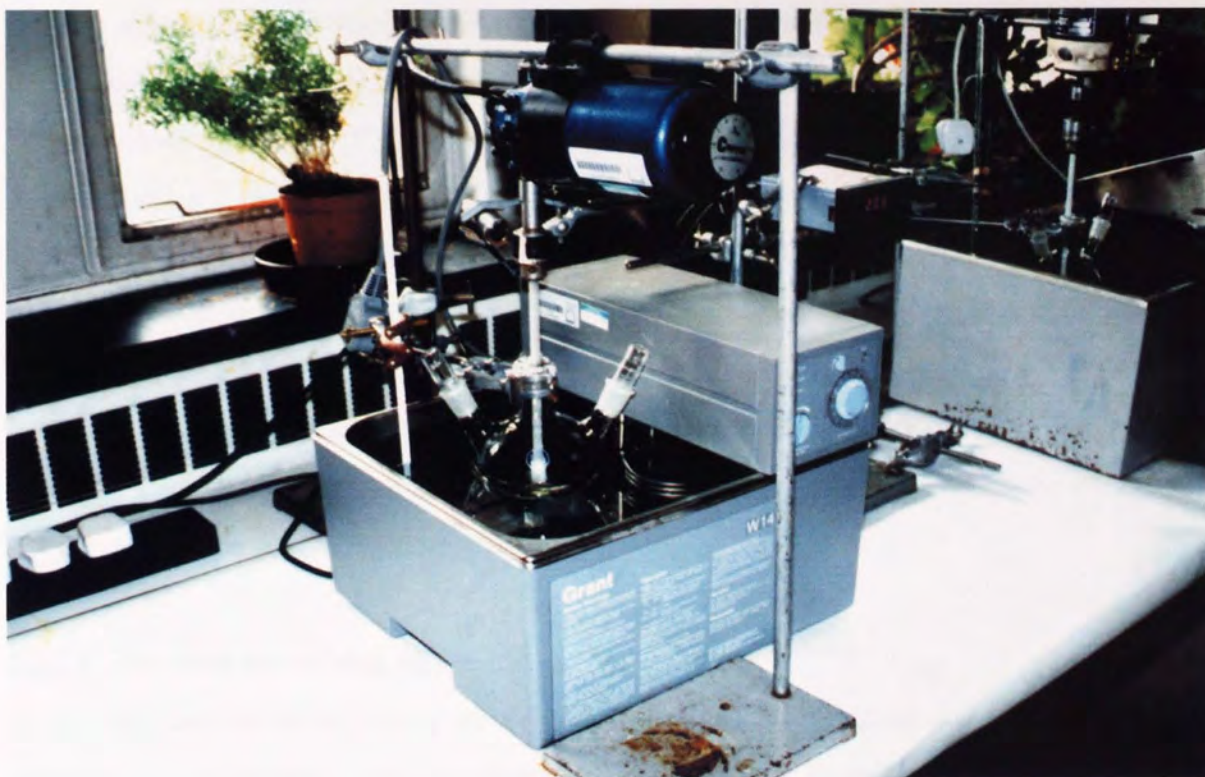


Figure 7.1. The apparatus used to perform stirred-batch reactions.

mg cm³ (4 U cm⁻³) within the reaction volume. Simultaneously with the addition of the enzyme solution a timer was started and a 2 cm³ sample was taken using a Gilson Pipetman P5000 variable volume pipette (Anachem Limited, Luton, Beds, UK), fitted with a 2.5 cm³ polypropylene pipette tip (Fisher Scientific, Leics, UK). The sample was expelled into a test tube containing 2 cm³ of 0.05M sodium hydroxide and this was mixed using a vortex mixer. The sodium hydroxide was used to instantaneously quench the reaction (see 7.2.1.6) and prevent any further enzymatic activity. At 1 minute intervals further samples were taken up to a total of 30 minutes and similarly quenched. Stirred-batch reactions performed at 40°C were also run for a total of 330 minutes, with samples taken every 10 minutes. Stirred-batch reactions were performed in duplicate. Each sample generated was analysed by HPLC (see 7.2.1.7) and the sugar profile determined.

7.2.1.6 Reaction quenching efficiency

To prevent samples taken during stirred-batch reactions from undergoing further enzymatic reaction prior to analysis, it was necessary to instantaneously quench the reaction. Shieh⁽⁴³⁾ and Taddei⁽⁵³⁾ working with β -galactosidase from *Aspergillus oryzae* used boiling as a means of quenching samples taken from chromatographic columns. Their samples were placed in a boiling waterbath for 3 minutes to eliminate all enzymatic activity. However, boiling the samples would not have instantaneously quenched the reaction due to the period of time required to heat the samples to >85°C to denature the enzyme. In this research, samples were taken every 1 minute and required instantaneous reaction quenching, so that an accurate reaction sugar profile against time could be determined. For this reason, an alkali quenching method previously used by West⁽⁷⁾ was preferred.

West⁽⁷⁾ evaluated the use of 0.05M sodium hydroxide to quench reaction samples containing β -galactosidase from *Aspergillus oryzae*. West found that equivolumes of sample and 0.05M sodium hydroxide produced a mixture with a pH between 12-13, far outside the pH range for enzymatic activity. It was also found that alkali quenched samples frozen, thawed, and left at room temperature for 16 hours prior to analysis, gave identical degrees of lactose conversion as found for duplicate quenched samples analysed immediately after collection. This showed that the alkali quenching had eliminated all enzymatic activity and that storage of samples containing alkali did not affect the sugar profiles. An additional advantage to this method was that the total sample volume was increased, which provided

sufficient sample for the HPLC autosampler glass vials (1.5 cm³ capacity), syringes and filters to be flushed with sample prior to their use. The advantages discussed meant that the alkali quenching method was used in this research.

7.2.1.7 HPLC analysis of stirred-batch reaction samples

The quenched stirred-batch reaction samples produced were analysed by high performance liquid chromatography (HPLC) using the apparatus shown in Figure 7.2.

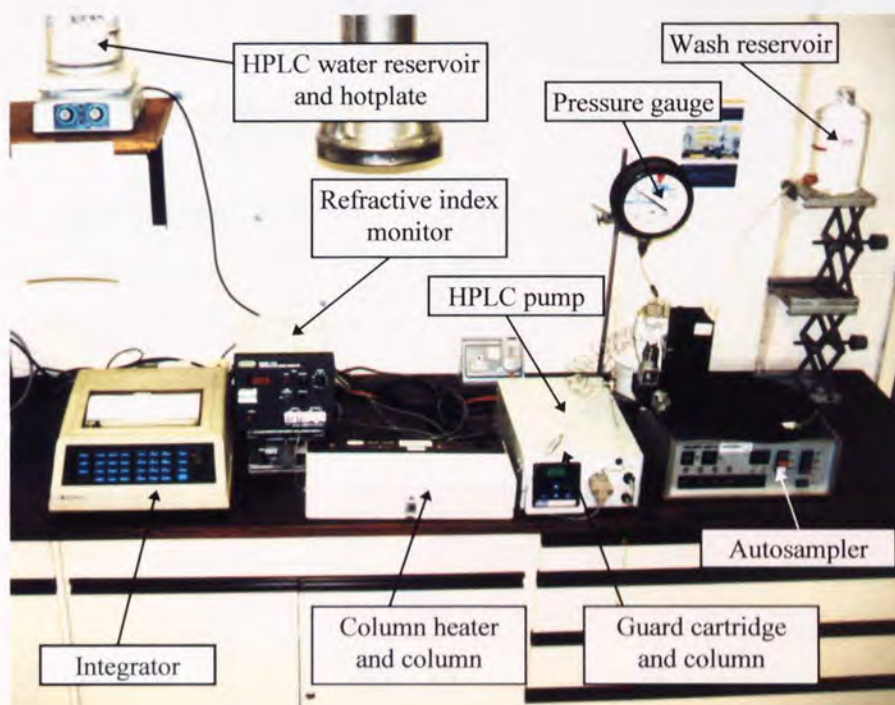


Figure 7.2. The high performance liquid chromatograph (HPLC) used to analyse samples.

The HPLC system shown in Figure 7.2 consisted of; a Bio-Rad Model 1250426 Column Heater (Bio-Rad Limited, Hemel Hempstead, Herts, UK) fitted with a Bio-Rad Aminex[®] HPX-87C Carbohydrate Column (300mm x 7.8mm), an Alltech Model 301 HPLC Pump (Alltech Limited, Carnforth, UK), Bio-Rad Model 1755 Refractive Index Monitor, a Talbot Model ASI-4 Autosampler (Talbot Scientific, Alderley Edge, UK), a Lichrospher[®] 100 Diol 5mm Cartridge and Column (Merck, Poole, Dorset, UK), a Fisher Stirring Hotplate (Fisher Scientific, Leics, UK), and a Spectra-Physics Model SP4270 Computing Integrator (Thermoelectron Limited, Stone, Staffs, UK).

Each sample to be analysed was transferred to a 10 cm³ sterile polypropylene Plastpak[®] luer slip syringe (Fisher Scientific, Leics, UK) fitted with a 13mm 0.45µm PVDF syringe filter (Whatman International Limited, Maidstone, Kent, UK) and the sample was filtered into a 1.5 cm³ capacity glass autosampler vial (Fisher Scientific, Leics, UK). The vials containing the filtered samples were placed on the autosampler carousel (60 vial capacity) along with 1%^{w/v} standards of lactose monohydrate, glucose and galactose, which were diluted with 0.05M sodium hydroxide (1:1) as for the samples. In the absence of an oligosaccharide standard, the lactose monohydrate standard was used to quantify oligosaccharides detected in the product mixture, which is common practice in the literature ^(7,23,30,43,51). The HPLC was operated using the following conditions:

- column temperature - 85°C
- mobile phase - water
- mobile phase flowrate - 0.5 cm³ min⁻¹

A typical chromatogram obtained for a reaction sample is shown in Figure 7.3.

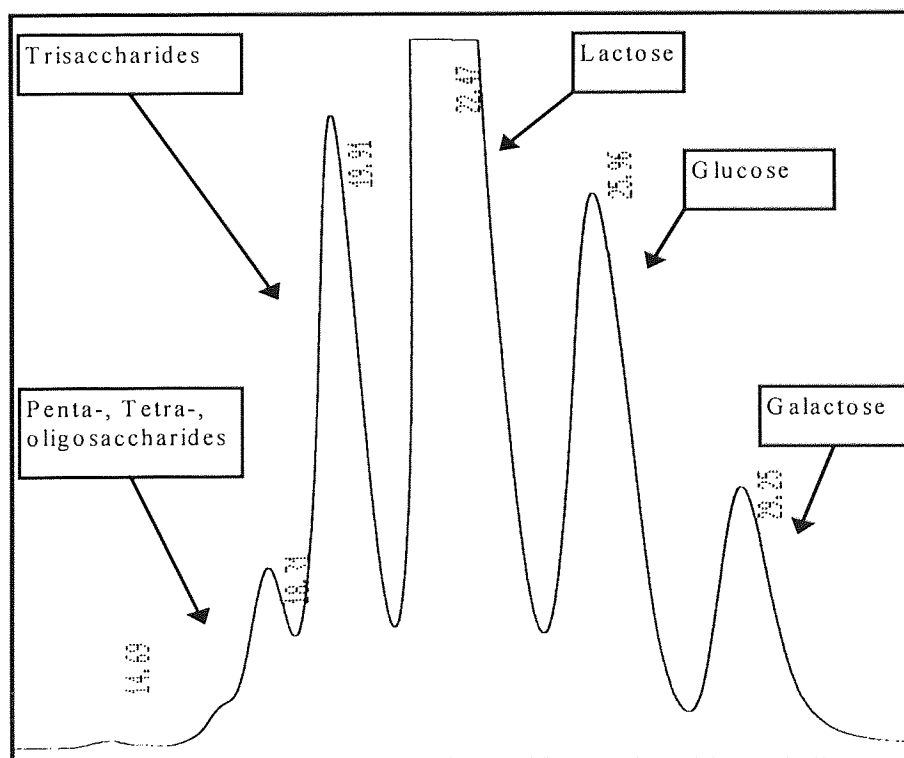


Figure 7.3. A typical chromatogram obtained of products formed during hydrolysis of lactose monohydrate by β -galactosidase from *Aspergillus oryzae*.

The chromatographic data obtained for each stirred-batch reaction performed was entered into an Excel spreadsheet and the sugar profile for each sample was calculated. Examples of the type of spreadsheets produced are shown in Appendix A-1.

7.2.2 Stirred-batch reactions using glutaraldehyde insolubilised β -galactosidase from *Aspergillus oryzae* (Biolactase F)

Stirred-batch reactions were performed using glutaraldehyde insolubilised β -galactosidase from *Aspergillus oryzae* (Biolactase F) and the results obtained are presented in Chapter 2.

7.2.2.1 Preparation of glutaraldehyde insolubilised β -galactosidase from *Aspergillus oryzae* (Biolactase F)

A diagrammatic representation of the insolubilisation procedure is presented in Appendix A-3. The procedure used was divided into three stages and these were:

- 1.) Soluble enzyme preparation.
- 2.) Glutaraldehyde cross-linking of enzyme.
- 3.) Final solution preparation.

The soluble enzyme preparation involved the removal of insoluble material and temperature labile contaminating enzymes from the soluble β -galactosidase solution, which produced a 'clean' enzyme solution for glutaraldehyde cross-linking.

Experiments were performed that optimised the reaction conditions required to cross-link the enzyme. These experiments were based on the work performed by other researchers^(11,12,13,14), although no methods were found in the literature specifically for the glutaraldehyde insolubilisation of β -galactosidase from *Aspergillus oryzae*. The experiments showed that the insolubilisation process was dependent on; the concentration of the 'clean' enzyme concentration, the concentration of the glutaraldehyde used, the pH, the incubation temperature, and the duration of the incubation. After suitable incubation of the 'clean' β -galactosidase with glutaraldehyde, insolubilisation of the enzyme was produced and this is shown in Figure 7.4.

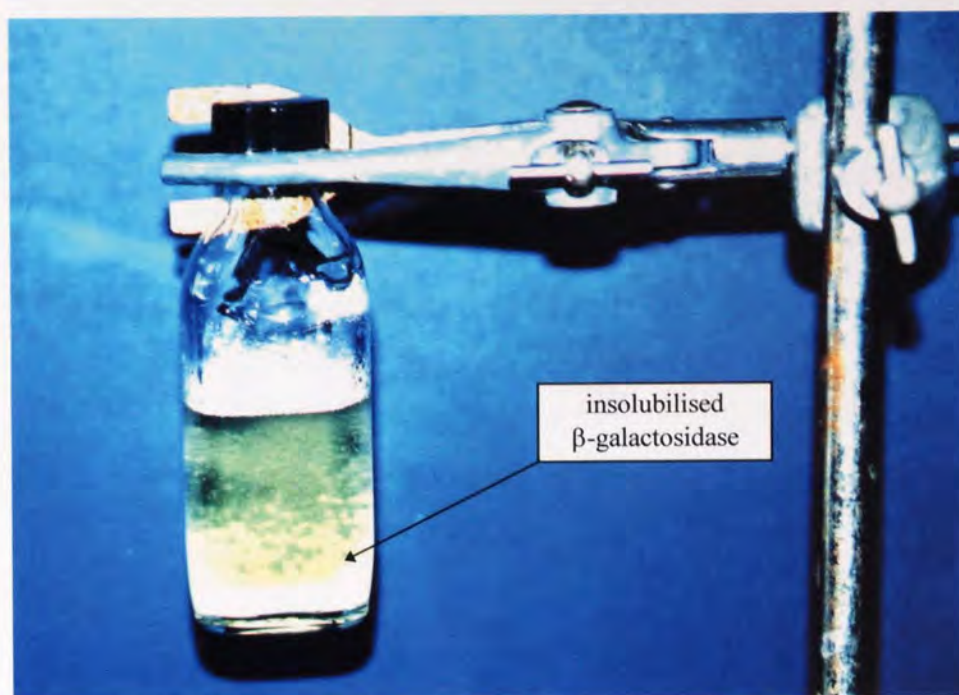
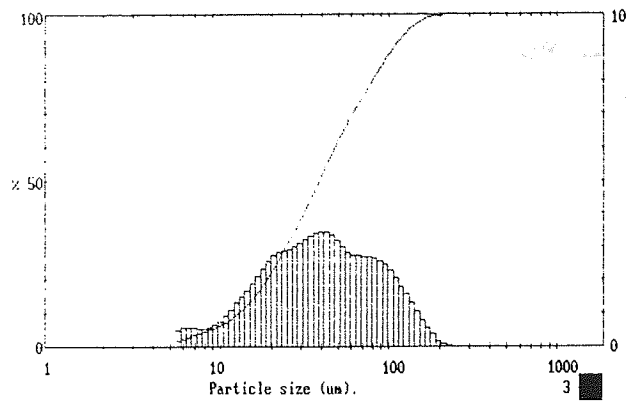
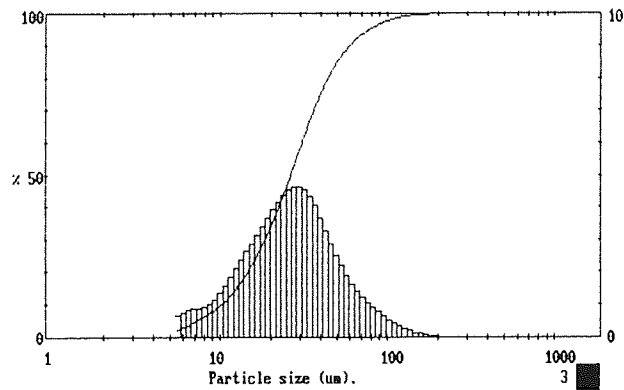


Figure 7.4. The formation of glutaraldehyde insolubilised β -galactosidase from *Aspergillus oryzae*.

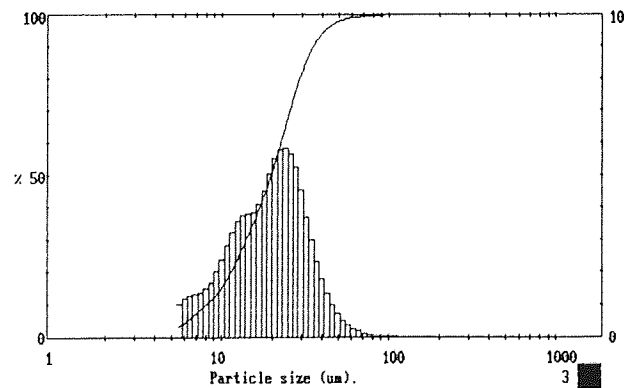
The preparation of the cross-linked enzyme for use in stirred-batch reactions and centrifugation experiments involved the grinding of the material shown in Figure 7.4, to form a suspension containing discrete cross-linked enzyme particles. This suspension was transferred to a test tube and mixed using a vortex mixer. To produce the narrowest particle size distribution, the suspension was allowed to settle for various times (0, 10, 20 and 30 minutes) to allow the largest particles to fully sediment. The particle size distribution of the suspended material was measured using the Malvern Model 2600c Laser Particle Sizer (Malvern Instruments, Worcester, UK) after the various settling times and the results obtained are presented in Figure 7.5. The results show that the narrowest particle size distribution was obtained after a settling time of 30 minutes. A settling time of 30 minutes was used for all of the insolubilised enzyme produced. Figure 7.6 shows the insolubilised enzyme suspension after a settling time of 30 minutes. The unsedimented suspension was removed and the fully sedimented material was discarded. An activity assay was performed on the enzyme suspension to determine the β -galactosidase activity (see 7.2.1.2). A solution of soluble β -galactosidase from *Aspergillus oryzae* (1.25 mg cm^{-3} , 4 U cm^{-3}) was also assayed at the same time, so that the insolubilised enzyme activity could be related to the soluble enzyme concentration.



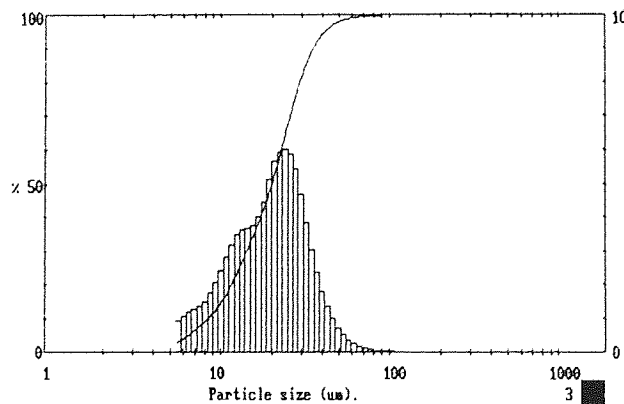
Cross-linked enzyme,
mixed, 0 minutes
settling time



Cross-linked enzyme,
after 10 minutes
settling time



Cross-linked enzyme,
after 20 minutes
settling time



Cross-linked enzyme,
after 30 minutes
settling time

Figure 7.5. The effect of settling time on the narrowing of insolubilised β -galactosidase particle size distribution.

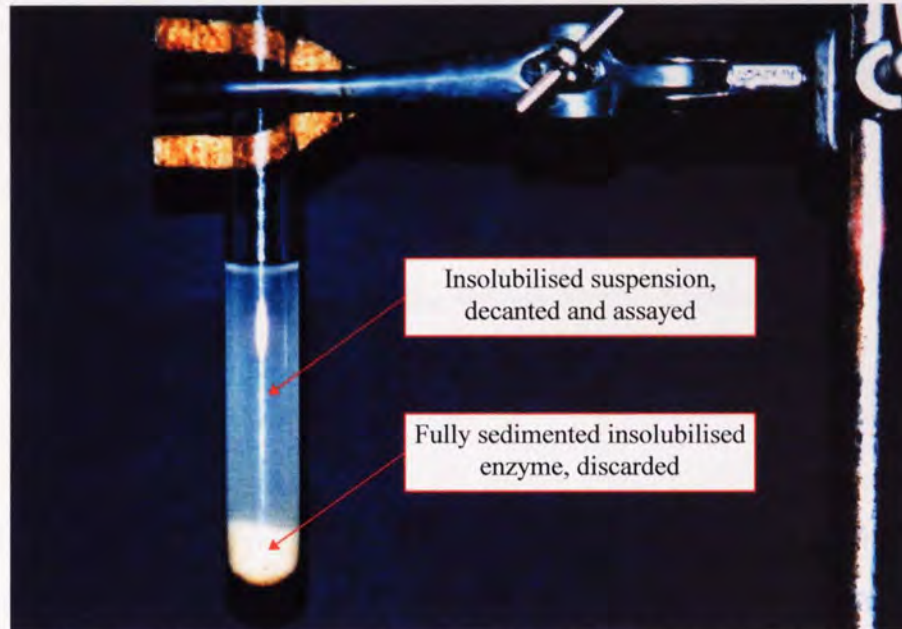


Figure 7.6. Insolubilised β -galactosidase from *Aspergillus oryzae* after 30 minutes settling time.

7.2.2.2 Stirred-batch reactions using insolubilised β -galactosidase from *Aspergillus oryzae*

Stirred-batch reactions were performed using various initial lactose monohydrate concentrations (5, 10, 15, 20, 25, 30 and 40%^{w/v}) and incubated with insolubilised β -galactosidase from *Aspergillus oryzae* at a concentration equivalent to 1.25 mg cm⁻³ (4 U cm⁻³) of the soluble enzyme, at 25°C and 40°C. The apparatus used to perform the reactions is shown in Figure 7.1, except that a 250 cm³ three necked round bottomed flask was used. The total reaction volume was 100 cm³ and this consisted initially of; sufficient volume of insolubilised β -galactosidase suspension to give an equivalent concentration to 1.25 mg cm⁻³ (4 U cm⁻³) of the soluble enzyme, and the remaining volume up to 100 cm³ of a suitable lactose monohydrate solution to give the desired overall substrate concentration. The reaction volume was lower than that used for the soluble stirred-batch reactions (250 cm³) due to the difficulty in producing sufficient insolubilised enzyme. The sample volume was reduced to 1 cm³ and samples were taken at 1 minutes intervals for a period of 30 minutes. The samples were quenched with 1 cm³ of 0.05M sodium hydroxide solution and were analysed by HPLC, as described in 7.2.1.7.

7.2.3 Rate-zonal batch centrifugation reactions

Rate-zonal centrifugation reactions were performed using soluble and insolubilised β -galactosidase from *Aspergillus oryzae* (Biolactase F) and the results obtained are presented in Chapter 4 and 5.

7.2.3.1 Preparation of linear lactose monohydrate density gradients

Linear lactose monohydrate density gradients were prepared using the under-layering gradient technique described in 4.2.2 and Figure 4.4. The gradients were hand-formed rather than by using an automatic continuous gradient former, such as that shown in Figure 4.5. To produce a linear density gradient ranging from 10%^{w/v} to 40%^{w/v} lactose monohydrate the following solutions were required; 10, 15, 20, 25, 30 and 40%^{w/v} lactose monohydrate. The main experiments presented in Chapters 4 and 5 were performed at 40°C and so the formation of a gradient at this temperature will be described.

Solutions of lactose monohydrate (100 cm³) at the concentrations described above were prepared using degassed HPLC-grade water (see 7.2.1.4). Degassed water was essential to prevent bubble formation within the gradient during a reaction. The solutions were incubated in a waterbath at 40°C, for at least 15 minutes to allow the solutions to attemperate. The batch centrifuge reactions were performed in duplicate and so two 50 cm³ polycarbonate centrifuge tubes (Beckman Instruments, High Wycombe, UK) were placed in a waterbath at 40°C, with the tubes submerged to within 1 cm of the top of the tube. An example of the centrifuge tubes used is shown in Figure 7.7.

The tubes were allowed to attemperate, so that expansion or contraction did not occur during the under-layering process. Using a 10 cm³ sterile polypropylene Plastpak[®] luer slip syringe fitted with a 18 gauge stainless steel needle (12 cm) 8cm³ of 10%^{w/v} lactose monohydrate solution was withdrawn from its volumetric flask (100 cm³). The syringe needle had been purpose made by cutting a 18 gauge needle with a length of 20 cm (Fisher Scientific, Leics, UK) to 12 cm and grinding a flat profile on the needle tip. This was done to allow the needle to locate flush with the tube bottom and to reduce the turbulence produced during loading. Air was expelled from the syringe by expelling 2 cm³ of the lactose monohydrate solution and the tip of the needle was then placed at the bottom of the tube. The solution was expelled over a period of ~30 seconds (12 cm³ min⁻¹) and the needle was removed with

minimal disruption to the layer. The process was repeated with the next highest lactose monohydrate concentration, and a new syringe and needle was used. This was repeated until all of the solutions had been under-layered ($6 \times 6\text{cm}^3$). The under-layering technique is shown in Figure 7.8, with the tube removed from the waterbath to allow the process to be photographed.

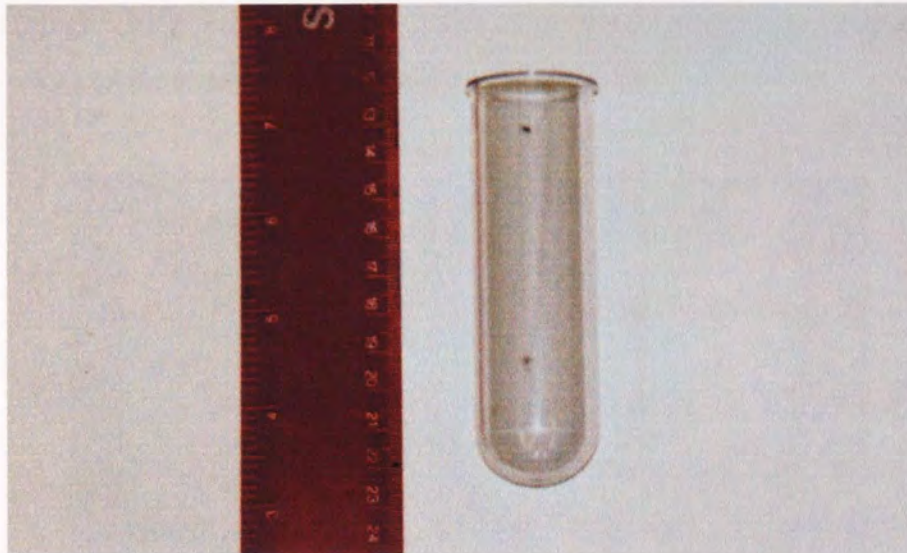


Figure 7.7. Beckman polycarbonate centrifuge tubes (50 cm^3).

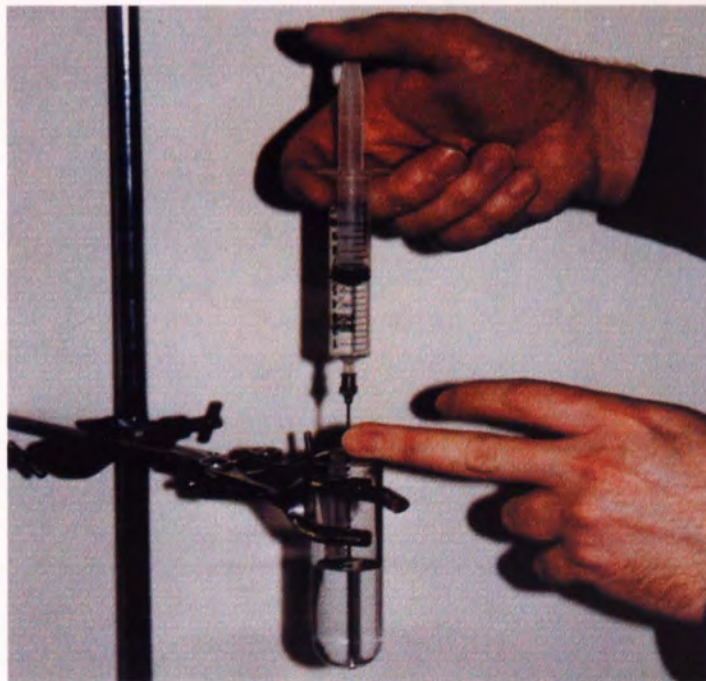


Figure 7.8. The under-layering of lactose monohydrate solutions.

The centrifuge tubes were then incubated at 40°C for 30 minutes to allow a linear density gradient to form (see 4.3.4).

7.2.3.2 Rate-zonal batch centrifugation reactions performed using soluble and insolubilised β -galactosidase from *Aspergillus oryzae* (Biolactase F)

Rate-zonal centrifugation experiments were performed using the Beckman J2-MC High Speed Centrifuge fitted with a JS13.1 Swing-out Rotor (Beckman Instruments, High Wycombe, UK) and these are shown in Figures 7.9 and 7.10.



Figure 7.9. Beckman J2-MC High Speed Centrifuge.



Figure 7.10. Beckman JS13.1 Swing-out Rotor.

Prior to a centrifugation experiment being performed the centrifuge and empty rotor was operated at 40°C for 30 minutes. This was to pre-warm the centrifuge and rotor to prevent convection currents disrupting the density gradients during the initial stages of an experiment. Attenuated centrifuge tubes containing the lactose monohydrate density gradients were placed into the pre-warmed JS13.1 swing-out rotor, and using a 1 cm³ sterile polypropylene Plastpak[®] luer slip syringe fitted with a 22 gauge stainless steel needle (3 cm) 1 cm³ of pre-warmed enzyme solution was layered on top of the gradient. The enzyme solution/suspension was prepared as described in either 7.2.1.1 or 7.2.2.1 depending on whether soluble or insolubilised β -galactosidase was used, and the enzyme activity was adjusted to the desired value. The centrifuge was operated at the desired rotation speed for the required length of time. Enzyme pulsing experiments were performed by layering 1 cm³ of the insolubilised enzyme (soluble enzyme equivalent of 6 mg cm⁻³ (19.2 U cm⁻³)) on top of a 10-40%^{w/v} lactose monohydrate density gradient and this was centrifuged at the desired rotation speed, at 40°C. After 30 minutes, the centrifuge was stopped and a second 1 cm³ of the insolubilised enzyme was layered on top of the gradient and this was then centrifuged at the same speed for a further 30 minutes.

At the end of a run, the centrifuge tubes were removed and using a Class A Bibby E-Mil[®] borosilicate blow-out type glass pipette (Fisher Scientific, Leics, UK) 2 cm³ fractions were removed by maintaining the pipette tip just below the meniscus surface, as the gradient level drops (see Figure 4.6, method B). Each fraction taken was immediately quenched with 2 cm³ of 0.05M sodium hydroxide and the fractions were analysed by HPLC, as described in 7.2.1.7. The HPLC data was entered into an Excel spreadsheet to determine the sugar profile of each sample.

7.2.3.3 Further experimental methods

The concentration profile of lactose monohydrate density gradients was determined by measuring the refractive index of sequential samples taken against the values obtained for standard lactose monohydrate solutions. The refractive index measurements were made using an Index Instruments Model GPX-37 Automatic Refractometer (Index Instruments, Huntingdon, Cambs, UK). The density of lactose monohydrate solutions was measured using a Parr Model DMA 60 Density Meter (Parr Scientific, Raynes Park, London) and using a 10cm³ glass density bottle (Fisher Scientific, Leics, UK). Viscosity was measured using a Cannon-Fenske No 50 and No 100 U-tube glass viscometer (Fisher Scientific, Leics, UK).

Protein assays were performed using the Bio-Rad protein assay reagent (Bio-Rad, Herts, UK), which consists of an acidic solution containing Coomassie Brilliant Blue G-250 dye. The assay involved mixing 0.1 cm³ of test sample with 5 cm³ of diluted assay reagent (1:4) and incubating at ambient temperature for 10 minutes. The absorbance of each sample was measured at 595nm using a Perkin Elmer Model Lamda 12 UV/Visible Spectrophotometer (Perkin-Elmer, Cambs, UK) using polystyrene cuvettes with a pathlength of 10mm and a volume of 1.6 cm³ (Fisher Scientific, Leics, UK). The protein concentration (mg cm⁻³) was determined by comparison to the absorbance values obtained from standard solutions of Bovine Serum Albumin Fraction V (Sigma-Aldrich, Dorset, UK).

The particle size distributions presented in 5.12 and 7.5 were obtained using a Malvern Instruments Model 2600c Droplet and Particle Sizer (Malvern Instruments, Worcester, UK). Approximately 0.5 cm³ of the insolubilised β -galactosidase suspension was placed in an stirred optical cell located on the instruments optical bed. The laser beam passing through the cell is diffracted by the particles and the diffraction pattern produced is used to calculate the particle size distribution.

REFERENCES

- 1 Cohen, R., Giraud, B. and Messiah, A., 1967, Theory and Practice of the Analytical Centrifugation of an Active Substrate-Enzyme Complex. *Biopolymers*, **5**: 203-225.
- 2 Palmer, T., 1995, *Understanding Enzymes*. Fourth edition, Prentice Hall/Ellis Horwood Publishers (Hertfordshire, UK).
- 3 Setford, S. J., 1992, Combined Bioreaction and Separation in Centrifugal Fields. PhD Thesis, Aston University.
- 4 Parts, A.G., and Elbing, E., 1975, The Polymerisation of Acetonitrile in Centrifugal Fields. Paper presented at American Chemical Society Meeting, Philadelphia. *Polym. Prepr.*: **16**, 211-216.
- 5 Carenza, M., Tavan, M., and Palma, G., 1979, Radiation Induced Bulk Polymerisation Of Vinyl Chloride under Centrifugation. *J. Polym. Sci.*: **17**, 2087-2091.
- 6 Setford, S.J., Barker, P.E., and Ganetsos, G., 1994, Combined Bioreaction and Separation in Centrifugal Fields. *Bioseparation*, **4**: 117-126.
- 7 West, C.M., 1997, Bioreaction and Separation in Preparative Batch Chromatographic Columns, The Hydrolysis of Lactose to Yield Glucose, Galactose and Oligosaccharides. PhD Thesis, Aston University.
- 8 Crittenden, R.G., and Playne, M.J., 1996, Production, Properties and Applications of Food-grade Oligosaccharides. *Trends in Food Science and Technology*, **7**: 353-361.
- 9 Tanaka, Y., Kagamishi, A., Kiuchi, A., and Horiuchi, T., 1975, Purification and Properties of β -Galactosidase from *Aspergillus oryzae*. *J. Biochem.*, **77**: 241-247.
- 10 Wierzbicki, L.E., and Kosikowski, F.V., 1972, Formation of Oligosaccharides During β -Galactosidase action on Lactose. *J. Dairy. Sci.*, Vol **56**: No 11, 1400-1404.
- 11 Wallenfells, K., 1951, Enzymatische Synthese von Oligosacchariden aus Disacchariden. *Die Naturwissenschaften*, **38**: 306-307.
- 12 Aronson, M., 1952, Transgalactosidation During Lactose Hydrolysis. *Arch. Biochem. Biophys.*, **39**: 370-378.
- 13 Roberts, H.R., and McFarren, E.F., 1953, The Chromatographic Observation of Oligosaccharides Formed During the Lactase Hydrolysis of Lactose. *J. Dairy. Sci.*, **36**: 620-632.
- 14 Roberts, H.R., and Pettinati, J.D., 1957, Concentration Effects in the Enzymatic Conversion of Lactose to Oligosaccharides. *Journal of Agricultural and Food Chemistry*, Vol **5**: No 2, 130-134.

- 15 Pazur, J.H., Tipton, C.L., Budovich, T., and Marsh, J.M., 1958, Structural Characterisation of Products of Enzymatic Disproportionation of Lactose. *J. Am. Chem. Soc.*, **80**:119-121.
- 16 Toba, T., Tomita, Y., Itoh, T., and Adachi, S., 1985, Characterisation of Oligosaccharides formed During the Hydrolysis of Lactose. *Food Chem.*, **16**: 147.
- 17 Matsumoto, K., Kobayashi, Y., Ueyama, S., Watanabe, T., Tanaka, R., Kan, T., Kuroda, A., and Sumihara, Y., 1993, Galacto-oligosaccharides. *Japanese Technology Reviews*, Vol **3**: Part 2, 90-106.
- 18 Tang, S.T., and Silva, E.M., 1995, Novel Products and New Technologies for Use of a Familiar Carbohydrate, Milk Lactose. *Am. J. Dairy. Sci.*, **78**: 2541-2562.
- 19 Chaplin, M.F., and Bucke, C., 1992, *Enzyme Technology*. Second Edition, Cambridge University Press (Cambridge, UK).
- 20 Toba, T., Watanabe, A., and Adachi, S., 1982, Allolactose and 6-O- β -Galactopyranosyl-D-Galactose in Commercial Yoghurt. *J. Dairy. Sci.*, **65**: 702-706.
- 21 Flaschel, E., Raetz, E., and Renken, A., 1982, The Kinetics of Lactose Hydrolysis for the β -Galactosidase from *Aspergillus niger*. *Biotechnology and Bioengineering*, **24**, 2499-2518.
- 22 Betschart, H.F., and Prenosil, J.E., 1984, High Performance Liquid Chromatographic Analysis of the Products of Enzymatic Lactose Hydrolysis. *Journal of Chromatography*, **299**: 498-502.
- 23 Jeon, I.J., and Mantha, V.R., 1985, High Performance Liquid Chromatography Analysis of Oligosaccharides Formed During β -Galactosidase Action on Lactose. *J. Dairy. Sci.*, **68**: 589-593.
- 24 Van Den Broek, A.W.M.H., 1993, Functional Food the Japanese Approach. *International Food Ingredients*, Vol **1**: Part 2, 4-9.
- 25 Hasler, C.M., 1998, A New Look at an Ancient Concept. *Chemistry and Industry*, No 3, February, 84-89.
- 26 Ito, M., Deguchi, Y., Miyamori, A., Matsumoto, K., Kikuchi, H., Matsumoto, K., Kobayashi, Y., Yajima, T., and Kan, T., 1990, Effects of Administration of Galacto-oligosaccharides on the Human Faecal Microflora, Stool Weight and Abdominal Sensation. *Microbial Ecology in Health and Disease*, **3**: 285-292.
- 27 Iwasaki, K., Nakajima, M., and Nakao, S., 1996, Galacto-oligosaccharide Production From Lactose by an Enzymic Batch Reaction Using β -Galactosidase. *Process Biochemistry*, Vol **31**: No 1, 69-76.

- 28 Tomomatsu, H., 1994, Health Effects of Oligosaccharides. *Food Technology*, Volume **October**: 61-65.
- 29 Ito, M., Kimura, M., Deguchi, Y., Miyamori-Watabe, A., Yajima, T., and Kan, T., 1993, Effects of Transgalactosylated Disaccharides on the Human Intestinal Microflora and Their Metabolism. *J. Nutr. Sci. Vitaminol.*, **39**: 279-288.
- 30 Yang, S.T., and Tang, I.C., 1988, Lactose Hydrolysis and Oligosaccharide Formation Catalyzed by β -Galactosidase. *Annals of the New York Academy of Sciences*, **542**: 417-422.
- 31 Prenosil, J.E., Stuker, E., and Bourne, J.R., 1987, Formation of Oligosaccharides During Enzymatic Lactose Hydrolysis and Their Importance in a Whey Hydrolysis Process: Part 1: State of the Art. *Biotechnology and Bioengineering*, **30**:1019-1025.
- 32 Prenosil, J.E., Stuker, E., and Bourne, J.R., 1987, Formation of Oligosaccharides During Enzymatic Lactose Hydrolysis and Their Importance in a Whey Hydrolysis Process: Part 2: Experimental. *Biotechnology and Bioengineering*, **30**:1026-1031.
- 33 Honsha, K.K.Y., 1987, Method for Producing Galacto-oligosaccharide. European Patent Application, Application Number 87311051.4.
- 34 Shang-Tian, Y., and Okos, M.R., 1989, Effects of Temperature on Lactose Hydrolysis by Immobilised β -Galactosidase in Plug-Flow Reactor. *Biotechnology and Bioengineering*, **33**: 873-885.
- 35 Patil, D.R., Rethwisch, D.G., and Dordick, J.S., 1991, Enzymatic Synthesis of a Sucrose-containing Linear Polyester in Nearly Anhydrous Media. *Biotechnology and Bioengineering*, **37**: 639-646.
- 36 Gekas, V., and Lopez-Leiva., 1985, Hydrolysis of Lactose: A Literature Review. *Process Biochemistry*, Volume **February**: 2-12.
- 37 Bergmeyer, H.U., 1974, *Methods of Enzymatic Analysis: Volume 1*. Second English Edition, Academic Press (New York, U.S.A).
- 38 Richmond, M.L., Gray, J.I., and Stine, C.M., 1981, Beta-Galactosidase: Review of Recent Research Related To Technological Application, Nutritional Concern and Immobilisation. *J. Dairy. Sci.* **64**: 1759-1771.
- 39 Wallenfels, K., and Malhotra, O.P., 1960, *The Enzymes*. Volume **4**, Second Edition, Edited by Boyer, P.D. Academic Press (New York, U.S.A).
- 40 Wallenfels, K., and Weils, R., 1972, *The Enzymes*. Volume **7**, Third Edition, Edited by Boyer, P.D. Academic Press (New York, U.S.A).
- 41 Shukla, T.P., 1975, Beta-Galactosidase Technology: A Solution to the Lactose Problem. *CRC Critical Reviews in Food Technology*, January: 325-356.

- 42 Friend, B.A., and Shahani, K.M., 1982, Characterisation and Evaluation of *Aspergillus oryzae* Lactase Coupled to a Regenerable Support. *Biotechnology and Bioengineering*, **24**: 329-345.
- 43 Shieh, M.T., 1994, Combined Bioreaction and Separation in a Simulated Counter-current Chromatographic Bioreactor-separator System. PhD Thesis, Aston University.
- 44 Gould, R.F., 1971, Carbohydrates in Solution. Based on a symposium held by the American Chemical Society, Washington, D.C. (14-15 September). Published by the the American Chemical Society, Washington, D.C..
- 45 Engel, P.C., 1977, Enzyme Kinetics. Published by Chapman and Hall (London).
- 46 Palmer, T., 1995, Understanding Enzymes. Fourth Edition, Prentice Hall/Ellis Horwood Publishers (Herts, UK).
- 47 Cornish-Bowden, A., 1979, Fundamentals of Enzyme Kinetics. Published by Butterworths (London).
- 48 Trevan, M.D., 1980, Immobilised Enzymes - An Introduction and Applications in Biotechnology. John Wiley and Sons Limited Publishers (Chichester, UK).
- 49 Greenberg, N.A., and Mahoney, R.R., 1981, Immobilisation of Lactase (β -Galactosidase) for Use in Dairy Processing: A Review. *Process Biochemistry*, Volume **Feb/March**: 2-8.
- 50 Playne, M.J., and Crittenden, R., 1996, Commercially Available Oligosaccharides. *Bulletin of the IDF*, **313**: 10-22.
- 51 Taddej, L.E.M., 1994, Bioreaction and Separation in Batch Chromatographic Columns. PhD Thesis, Aston University.
- 52 Begum, R., Canuto, C., Hussain, I., and Petrou, T., 2000, Personal Communication.
- 53 Shultz, A. R., 1994, Enzyme Kinetics - From Diastase to Multi-enzyme Systems. Published by Cambridge University Press (Cambridge, UK).
- 54 Weetall, H.H., Havewala, N.B., Pitcher, W.H., Detar, C.C., Vann, W.P., and Yaverbaum., S., 1974, The preparation of Immobilised Lactase and its Use in the Enzymatic Hydrolysis of Whey. *Biotechnology and Bioengineering*, **16**: 295-313.
- 55 Zaborsky, O.R., 1974, Immobilised Enzymes. Third Edition, published by CRC press (Cleveland, Ohio, USA).
- 56 Freemantle, M., 1995, Chemistry in Action. Second Edition, published by Macmillan Press limited (Hampshire, UK).

- 57 Wilson, K., and Goulding, K.H., 1988, A Biologist's Guide to Principles and Techniques of Practical Biochemistry. Third Edition, published by Hodder and Stoughton (London).
- 58 Bowen, T.J., 1970, An Introduction to Ultracentrifugation. Published by John Wiley and Sons (London).
- 59 Griffiths, O.M., 1986, Techniques of Preparative, Zonal, and Continuous Flow Ultracentrifugation. Fifth Edition, Published by Beckman Instruments (Palo Alto, California, U.S.A).
- 60 Hsu-Wen, H., 1981, Separations by Centrifugal Phenomena. Techniques of Chemistry, Volume 16, Published by John Wiley and Sons (London).
- 61 Bershad, B.C., Chaffiotte, R.M., and Leung, W.F., 1990, Making Centrifugation Work for You. Chemical Engineering, August 1990, 84-89.
- 62 Perry, R.H., and Green, D., 1984, Perry's Chemical Engineers' Handbook. Sixth Edition, Published by McGraw-Hill (Berks, UK).
- 63 Datar, R., 1984, Centrifugal and Membrane Filtration Methods in Biochemical Separation. Filtration and Separation, November/ December, 403-406.
- 64 Ongley, E.D., and Thomas, R.L., 1989, Dewatering Suspended Solids by Continuous-Flow Centrifugation: Practical Considerations. Hydrological Processes, 3: 255-260. Published by John Wiley and Sons (London).
- 65 Rickwood, D., 1992, Preparative Centrifugation: A practical Approach. Published by Oxford University Press (Oxford, UK).
- 66 Ford, T.C., and Graham, J.M., 1991, An Introduction to Centrifugation. Published by Bios Scientific (Oxford, UK).
- 67 Rickwood, D., Ford, T.C., and Steensgaard, J., 1994, Centrifugation: Essential Data. Published by John Wiley and Sons (London).
- 68 Svedberg, T., and Pederson, K.O., 1940, The ultracentrifuge. Published by Oxford University Press (Oxford, UK).
- 69 McCall, J.S., and Potter, B.J., 1973, Ultracentrifugation. Published by Baillere Tindall (London).
- 70 Martin, R.G., and Ames, B.N., 1961, A Method for Determining the Sedimentation Behaviour of Enzymes. J. Biol. Chem, 236: 1372-1379.
- 71 Noll, H., 1969, Techniques in Protein Biosynthesis. Volume 2, Published by Academic Press (London).

- 72 McCarty, K.S., and Vollmar, R.T., 1974, Improved Computer Program Data for the Resolution and Fractionation of Macromolecules by Isokinetic Sucrose Density Gradient Sedimentation. *Anal. Biochem*, **61**: 165-183.
- 73 Monsan, P., and Lopez, A., 1981, On the Production of Dextran by Free and Immobilised Dextranase. *Biotech. Bioeng.*, **23**: 2027-2037.
- 74 Schumaker, V.N., 1967, Zone Centrifugation. *Advan. Biol. Med. Phys.*, **11**: 245-339.
- 75 Pickels, E.G., 1943, Sedimentation in the Angle Centrifuge. *J. Gen. Phys.*, **26**: 341-365.
- 76 de Duve, C., Berthet, J., and Beaufay, H., 1959, Gradient Centrifugation of Cell Particles: Theory and Applications. *Progr. Biophys. Chem.*, **9**: 326-369.
- 77 Brakke, M.K., 1964, Wall Effects during Density Gradient Centrifugation of Southern Bean Mosaic Viruses. *Advan. Virus Res.*, **7**: 193-224.
- 78 Coulson, J.M., and Richardson, J.F., 1999, *Chemical Engineering: Volume 2, Particle Technology and Separation Processes*. Fourth Edition, Published by Butterworth Heinemann (Oxford, UK).
- 79 Rousselet Technical Brochure 2C2, Multipurpose Batch Centrifuges with Removable Filtration Bag for Products with High Value. Rousselet (UK), Beds, UK.
- 80 Chervenka, C.H., 1973, A Manual of Methods for the Analytical Ultracentrifuge. Library of Congress Number 72-81833, Beckman Instruments (California, U.S.A).
- 81 Anderson, N.G., 1966, The Development of Zonal Centrifuges. *Natl. Cancer Inst. Monogr.* **21**: 9-39.
- 82 Continuous Flow Centrifugation, Beckman Applications Data Number DS-595B, Beckman Instruments (California, U.S.A).
- 83 Birnie, G.D., and Rickwood, D., 1978, *Centrifugal Separations in Molecular and Cell Biology*. Published by Butterworth and Co. (London).
- 84 Ridge, D., 1978, *Practical Aspects of Rate Zonal Centrifugation in Molecular and Cell Biology*. Published by Butterworth and Co. (London).
- 85 Fortuin, J.M.H., 1960, Theory and Application of Two Supplementary Methods for Constructing Density Gradient Columns. *J. Polym. Sci.*, **44**: 505-515.
- 86 Svensson, H., Hagdahl, L., and Lerner, K.D., 1957, Zone Electrophoresis in a Density Gradient. Stability Conditions and Separation of Serum Proteins. *Science Tools*, **4**: 1-10.
- 87 Berman, A.S., 1966, Theory of Centrifugation. *Natl. Cancer Inst. Monogr.*, **21**: 41-76.

- 88 Spragg, S.P., and Rankin, C.T., 1967, The Capacity of Zones in Density Gradient Centrifugation. *Biochim. Biophys. Acta.*, **141**: 164-173.
- 89 Halsall, H.B., 1967, Atassi-Ghandi Sedimentation Coefficient and Molecular Weight Determination. *Nature*, **215**: 880-881.
- 90 LaBar, F.E., and Baldwin, R.L., 1963, The Sedimentation Coefficient of Sucrose. *J. Am. Chem. Soc.*, **85**: 3105-3108.
- 91 Washburn, E.W., 1929, International Critical Tables of Numerical Data, Physics, Chemistry and Technology. Volume 3, Published by McGraw-Hill Book Company (New York).
- 92 Coulson, J.M., and Richardson, J.F., 1985, Chemical Engineering: Volume 1, Fluid Flow, Heat Transfer and Mass Transfer. Third Edition (Third Revision), Published by Butterworth Heinemann (Oxford, UK).
- 93 Zaborsky, O.R., 1974, Immobilised Enzymes. Third Edition, Published by CRC Press (Ohio, U.S.A.).
- 94 Chibata, I., 1978, Immobilised Enzymes, Research and Development. Published by John Wiley and Sons (London).
- 95 Sundaram, P.V., and Crook, E.M., 1971, Preparation and Properties of Solid-Supported Urease. *Can. J. Biochem.*, **49**: 1388.
- 96 Porath, J., Axen, R., and Ernback, S., 1967, Chemical Coupling of Proteins to Agarose. *Nature*, **215**: 1491-1492.
- 97 Porath, J., Axen, R., and Ernback, S., 1967, Chemical Coupling of Peptides and Proteins to Polysaccharides by Means of Cyanogen Halides. *Nature*, **214**: 1302-1304.
- 98 Porath, J., and Ernback, S., 1971, Chemical Fixation of Enzymes to Cyanogen Halide activated Polysaccharide Carriers. *Eur. J. Biochem.*, **18**: 351-354.
- 99 Dean, P.D.G., and Watson, D.H., 1979, Protein Purification Using Immobilised Triazine Dyes. *Journal of Chromatography*, **165**: 301-319.
- 100 Berfield, P., and Wan, J., 1963, Antigens and Enzymes Made Insoluble By Entrapping Them Into Lattices of Synthetic Polymers. *Science*, **142**: 678-685.
- 101 Bovey, F.A., 1959, Enzyme Polymerisation, Molecular Weight and Branching During the Formation of Dextran. *J. Polym. Sci.*, **35**: 167-183.
- 102 Chang, T.M.S., 1964, Semi-permeable Microcapsules. *Science*, **146**: 524-525.
- 103 Sessa, G., and Weissmann, G., 1970, Incorporation of Lysozyme into Liposomes. *Journal of Biological Chemistry*, Number 13, **245**: 3295-3301.

- 104 Keeton, W.T., and Gould, J.L., 1986, Biological Science. Fourth Edition, Published by W. W. Norton and Company (London).
- 105 Schelter, A., and Bar-Eli, A., 1970, Preparation and Properties of Crosslinked Water-Insoluble Catalase. Archives of Biochemistry and Biophysics, **136**: 325-330.
- 106 Broun, G., Selegny, E., Avrameas, S., and Thomas, D., 1969, Enzymatically Active Membranes: Some Properties of Cellophane Membranes Supporting Cross-linked Enzymes. Biochim. Biophys. Acta, **185**: 260-262.
- 107 Jansen, E.F., Tomimatsu, Y., and Olson, A.C., 1971, Cross-linking of α -Chymotrypsin and Other Proteins by Reaction with Glutaraldehyde. Archives of Biochemistry and Biophysics, **144**: 394-400.
- 108 Jansen, E.F., and Olson, A.C., 1969, Properties and Enzymatic Activities of Papain Insolubilised with Glutaraldehyde. Archives of Biochemistry and Biophysics, **129**: 221-227.
- 109 Rastall, R., 2001, Personal Communication.

Appendix A-1

(Examples of soluble and insolubilised stirred-batch reaction Excel spreadsheets)

All the key experimental data is available on disk.

Soluble β -galactosidase stirred-batch reaction Excel spreadsheets

5% Lactose monohydrate

Time (mins)	1%*/v lactose peak area 2475544	1%*/v Oligo* peak area 2475544	1%*/v Glucose peak area 1955569	1%*/v Galactose peak area 2472434	% Lactose (*/v)	% Lactose Conversion	% Oligo (††-tet)-(*†v)	% OTS (††-tet)	% Glucose (*/v)	% GluTS (*/v)	% Galactose (*/v)	% GalTS	Mass Balance
0	12363123	0	0	0	4.99	0.00	0.00	0.00	0.00	0.00	0.00	0.00	4.99
1	10328722	695954	1078428	0	4.17	16.46	0.28	5.62	0.55	11.02	0.00	0.00	5.00
2	9084995	884441	1163136	618781	3.41	31.77	0.36	7.75	0.59	12.90	0.00	5.43	4.61
3	8435365	1042699	1585966	940816	3.67	26.52	0.42	7.97	0.81	15.35	0.25	7.20	5.28
4	8053895	1124083	1947515	1232910	3.00	39.86	0.45	9.17	1.00	20.11	0.38	10.07	4.95
5	7433168	1100745	2175225	1455960	3.25	34.86	0.44	8.24	1.11	20.60	0.59	10.91	5.40
6	7076761	1078156	2433063	1721208	2.86	42.76	0.44	8.32	1.24	23.76	0.70	13.30	5.23
7	6774517	1028538	2705059	2078714	2.74	45.20	0.42	7.73	1.38	25.73	0.84	15.64	5.38
8	6282738	829199	2697802	2009210	2.54	49.18	0.38	7.35	1.38	27.02	0.81	15.92	5.11
9	6178663	884835	3037131	2543277	2.50	50.02	0.36	6.58	1.55	28.57	1.03	18.93	5.43
10	5693979	803009	3075463	2681272	2.30	53.94	0.32	6.14	1.57	29.77	1.08	20.53	5.28
11	5554794	768219	3252091	2937482	2.24	55.07	0.31	5.74	1.66	30.76	1.19	21.98	5.40
12	5320084	705660	3363990	3120646	2.15	56.97	0.29	5.26	1.72	31.75	1.26	23.30	5.42
13	5046997	651653	3410713	3242763	2.04	59.18	0.26	4.91	1.74	32.55	1.31	24.48	5.36
14	4881558	615810	3511947	3404370	1.97	60.52	0.25	4.61	1.80	33.29	1.38	25.63	5.39
15	4673253	579284	3626388	3544504	1.89	62.20	0.23	4.33	1.85	34.27	1.43	26.50	5.41
16	4482618	535239	3725217	3718224	1.81	63.74	0.22	3.98	1.90	35.04	1.50	27.67	5.44
17	4400668	486408	3807713	3857311	1.78	64.40	0.20	3.58	1.95	35.52	1.56	28.46	5.48
18	4086242	360378	3761662	3889407	1.65	66.95	0.15	2.75	1.92	36.34	1.57	29.72	5.29
19	3946382	341032	3817747	4004349	1.59	68.06	0.14	2.60	1.95	36.80	1.62	30.54	5.30
20	3671466	313786	3850003	4171821	1.56	68.69	0.13	2.37	1.97	36.82	1.69	31.56	5.35

Soluble Bilelectase F. Stirred-Batch Reaction

Date - 21/5/1995
 [lactose monohydrate] - 5%*/v
 Soluble [Bilelectase F] - 1.25 mg cm⁻³
 Temperature - 40°C
 Run Time - 0-20 minutes
 Reaction volume - 250 cm³
 Sample volume - 2 cm³
 Stirrer speed - 200 rpm
 Quench - 0.05M sodium hydroxide (2 cm³)

Abbreviations:
 %OTS - % Oligosaccharides of Total Sugar
 %GluTS - % Glucose of Total Sugar
 %GalTS - % Galactose of Total Sugar
 (††-tet) - trisaccharides+tetrascaccharides
 Oligo - oligosaccharides

* - lactose peak area used for oligo value.

10% Lactose monohydrate

Time (mins)	1% ^{w/v} lactose peak area 2081663		1% ^{w/v} oligo ₂ peak area 2081663		1% ^{w/v} glucose peak area 2170522		1% ^{w/v} galactose peak area 2067055		Mass Balance	
	Lactose peak area	% Lactose	Oligo peak area (tri+tet)	% Oligo (tri+tet)	Glucose peak area	% Glucose	Galactose peak area	% Galactose	% GalTS	9.75
0	20286380	9.75	0	0.00	0	0	0	0	0	9.75
1	18042450	8.67	1135872	0.55	0	0	0	0	0.00	9.21
2	16569070	7.96	1585655	0.76	0	0	0	0	0.00	8.72
3	14613613	7.02	1973557	0.95	0	0.00	0	0	0.00	9.15
4	14230107	6.84	2210157	1.06	2555845	1.18	841566	0.41	4.33	9.41
5	12959952	6.23	2569573	1.23	2400968	1.11	1021047	0.49	5.34	9.25
6	12599098	6.05	2708672	1.30	2821667	1.30	1179939	0.57	6.12	9.33
7	12054110	5.79	2682138	1.29	3055116	1.41	1302447	0.63	6.83	9.22
8	12017682	5.77	2816477	1.35	3284905	1.51	1499555	0.73	7.64	9.50
9	11195261	5.38	2740099	1.32	3580677	1.65	1573989	0.76	8.31	9.16
10	11139996	5.35	2700567	1.30	3701112	1.71	1751506	0.85	9.06	9.35
11	10487537	5.04	2827321	1.26	4033081	1.86	1815977	0.88	9.76	9.00
12	10229659	4.91	2566910	1.23	3949348	1.82	1958720	0.95	10.55	8.98
13	10370377	4.88	2670482	1.28	4093257	1.89	2138673	1.03	11.08	9.34
14	9821439	4.72	2505344	1.20	4426431	2.04	2207750	1.07	11.82	9.04
15	969629	4.66	2428392	1.17	4440896	2.05	2320101	1.12	12.36	9.08
16	9376530	4.50	2385932	1.15	4634001	2.13	2392672	1.16	12.86	9.00
17	9239227	4.43	2298213	1.10	4755594	2.19	2498457	1.21	13.51	8.96
18	8920229	4.29	2271310	1.09	4781306	2.20	2574458	1.25	14.08	8.84
19	8777258	4.22	2228061	1.07	4825201	2.22	2660677	1.29	14.57	8.83
20	8773143	4.21	2184791	1.05	4904895	2.26	2802180	1.36	15.14	8.95

Soluble Biotactase F. Stirred-Batch Reaction

Date - 22/5/1996
 (lactose monohydrate) - 10%^{w/v}
 Soluble (Biotactase F) - 1.25 mg cm³
 Run Time - 0-20 minutes
 Temperature - 40°C
 Reaction volume - 250 cm³
 Sample volume - 2 cm³
 Stirrer speed - 200 rpm
 Quench - 0.05M sodium hydroxide (2 cm³) + water (1 cm³)

Abbreviations:

%OTS - % Oligosaccharides of Total Sugar
 %GluTS - % Glucose of Total Sugar
 %GalTS - % Galactose of Total Sugar
 (tri+tet) - trisaccharides+tetrasaccharides
 Oligo - oligosaccharides

* - lactose peak area used for oligo value.

15% Lactose monohydrate

Time (mins)	1% ^{v/v} lactose peak area 2081653	1% ^{v/v} Oligo* peak area 2081653	1% ^{v/v} Glucose peak area 2170522	1% ^{v/v} Galactose peak area 2087055	Mass Balance
	Lactose peak area	Oligo peak area (tr+tet)	Glucose peak area	Galactose peak area	
	% Lactose (w/v)	% Oligo (tr+tet):(w/v)	% Glucose (w/v)	% Galactose (w/v)	% GalTS
	% Lactose Conversion	% OTS (tr+tet):(w/v)	% GluTS	% GalTS	% GalTS
0	14.60	0.00	0.00	0.00	0.00
1	12.21	0.72	0.00	0.00	0.00
2	11.87	1.17	0.71	0.00	0.00
3	11.50	1.75	1.54	0.00	0.00
4	11.02	1.95	1.42	0.39	0.38
5	10.56	2.18	1.64	0.50	0.50
6	9.95	2.26	1.76	0.58	0.58
7	9.65	2.39	1.90	0.66	0.66
8	9.37	2.43	2.06	0.74	0.74
9	9.09	2.47	2.16	0.81	0.81
10	8.67	2.59	2.31	0.92	0.92
11	8.46	2.57	2.39	0.96	0.96
12	8.27	2.58	2.47	1.02	1.02
13	8.12	2.59	2.58	1.07	1.07
14	7.92	2.57	2.61	1.13	1.13
15	7.87	2.57	2.71	1.18	1.18
16	7.62	2.56	2.76	1.25	1.25
17	7.45	2.54	2.82	1.28	1.28
18	7.41	2.51	2.85	1.32	1.32
19	7.31	2.53	2.94	1.37	1.37
20	7.17	2.49	2.99	1.43	1.43
21	7.03	2.47	3.02	1.45	1.45
22	6.90	2.46	3.09	1.50	1.50
23	6.79	2.45	3.15	1.56	1.56
24	6.79	2.40	3.16	1.58	1.58
25	6.64	2.40	3.23	1.61	1.61
26	6.52	2.34	3.23	1.65	1.65
27	6.52	2.31	3.26	1.68	1.68
28	6.51	2.31	3.32	1.73	1.73
29	6.41	2.31	3.38	1.76	1.76
30	6.41	2.27	3.40	1.79	1.79

Soluble Biotinase F Stirred-Batch Reaction

Date - 22/5/1996
 [lactose monohydrate] - 15%^{v/v}
 Soluble [Biotinase F] - 1.25 mg cm³
 Temperature - 40°C
 Run Time - 0-30 minutes
 Reaction volume - 250 cm³
 Sample volume - 2 cm³
 Stirrer speed - 200 rpm
 Quench - 0.05M sodium hydroxide (2 cm³) + water (1 cm³)

Abbreviations:
 %OTS - % Oligosaccharides of Total Sugar
 %GluTS - % Glucose of Total Sugar
 %GalTS - % Galactose of Total Sugar
 (tr+tet) - trisaccharides+tetrasaccharides
 Oligo - oligosaccharides

* - lactose peak area used for oligo value.

20% Lactose monohydrate

Time (mins)	Lactose peak area	% Lactose (%)	% Lactose Conversion	Oligo peak area (tritet)	% Oligo (tritet)(%)	% OTS (tritet)	Glucose peak area	% Glucose (%)	% GluTS	Galactose peak area	% Galactose (%)	% GalTS	Mass Balance
0	68095448	21.36	0.00	345861	0.11	0.51	0	0.00	0.00	0	0.00	0.00	21.47
1	61316039	19.23	9.96	3722377	1.17	5.72	0	0.00	0.00	0	0.00	0.00	20.40
2	54017950	16.94	20.67	5586507	1.75	9.07	0	0.00	3.26	0	0.00	0.00	19.33
3	52865447	16.52	22.66	7480254	2.35	11.62	5324236	1.15	5.67	889626	0.20	0.99	20.22
4	49205186	15.43	27.74	8414822	2.64	13.42	5324236	1.34	6.83	1120730	0.25	1.29	19.67
5	46429232	14.56	31.82	9315083	2.92	15.12	6081978	1.53	7.94	1336981	0.30	1.56	19.32
6	45310186	14.21	33.46	10039817	3.15	16.20	6821601	1.72	8.85	1591200	0.36	1.85	19.44
7	44048575	13.82	35.31	10682014	3.35	17.22	7430031	1.87	9.63	1857739	0.42	2.16	19.46
8	41852590	13.13	38.54	11060951	3.47	18.26	7737500	1.95	10.27	2006242	0.45	2.38	19.00
9	40029374	12.56	41.22	11158651	3.50	18.83	8064845	2.03	10.94	2201662	0.50	2.68	18.59
10	38468803	12.07	43.51	11267036	3.53	19.34	8475042	2.14	11.70	2354085	0.53	2.91	18.27
11	37131231	11.65	45.47	11347199	3.56	19.82	8880587	2.19	12.19	2478285	0.56	3.12	17.96
12	36513657	12.08	43.44	12440196	3.90	20.48	9616592	2.43	12.73	2870526	0.65	3.40	19.06
13	36051085	11.31	47.06	11928639	3.74	20.65	9539619	2.41	13.28	2923201	0.66	3.65	18.12
14	35303729	11.07	48.16	12135410	3.81	21.05	9957578	2.51	13.89	3054813	0.69	3.82	18.08
15	34059045	10.68	49.98	11975760	3.76	21.25	10011972	2.53	14.29	3139425	0.71	4.01	17.67
16	32807589	10.23	52.11	11729469	3.68	21.47	9961374	2.51	14.66	3186797	0.72	4.20	17.14
17	32148420	10.08	52.79	11804241	3.70	21.63	10216619	2.58	15.06	3334412	0.75	4.40	17.12
18	32198291	10.10	52.72	11851454	3.75	21.66	10574879	2.67	15.41	3520034	0.80	4.59	17.31
19	31019497	9.73	54.45	11819555	3.71	21.87	10691743	2.70	15.91	3619537	0.82	4.82	16.85
20	30500397	9.57	55.21	11778633	3.69	21.52	11126386	2.81	16.35	4859934	1.10	6.40	17.17
21	30213263	9.48	55.63	11594796	3.64	21.22	11473123	2.89	16.88	5011252	1.13	6.61	17.14
22	29847260	9.36	56.17	11547769	3.62	21.20	11549627	2.91	17.05	5245899	1.19	6.84	17.08
23	29189072	9.16	57.14	11703973	3.67	21.63	11676568	2.95	17.35	5324890	1.20	7.09	16.98
24	28866463	9.05	57.61	11547789	3.62	21.41	11890378	3.00	17.73	5497939	1.24	7.34	16.92
25	28710997	9.01	57.84	11703973	3.67	21.60	11883242	3.02	17.79	5725435	1.29	7.61	16.89
26	28066583	8.80	58.78	11521535	3.61	21.57	12007989	3.03	18.07	5804491	1.31	7.83	16.76
27	27633715	8.67	59.42	11491429	3.60	21.59	12271118	3.10	18.54	5881862	1.33	7.98	16.70
28	27063329	8.49	60.26	11295822	3.54	21.48	12324801	3.11	18.84	6002987	1.36	8.22	16.50
29	26714726	8.38	60.77	11200882	3.51	21.42	12405169	3.13	19.07	6123157	1.38	8.43	16.41
30	26787925	8.68	59.35	11528315	3.62	21.25	12954230	3.27	19.21	6408506	1.45	8.51	17.01

Soluble Biotinase F. Stirred-Batch Reaction

Date - 29/4/1996
 [lactose monohydrate] - 20% %v
 Soluble [Biotinase F] - 1.25 mg cm⁻³
 Temperature - 40°C
 Run Time - 0-30 minutes
 Reaction volume - 250 cm³
 Sample volume - 2 cm³
 Stirrer speed - 200 rpm
 Quench - 0.05M sodium hydroxide (2 cm³) + water (2 cm³)

Abbreviations:
 %OTS - % Oligosaccharides of Total Sugar
 %GluTS - % Glucose of Total Sugar
 %GalTS - % Galactose of Total Sugar
 (tritet) - trisaccharides+tetrasaccharides
 Oligo - oligosaccharides

* - lactose peak area used for oligo value.

25% Lactose monohydrate

Time (mins)	1% w/v lactose peak area		1% w/v Oligo* peak area		1% w/v Glucose peak area		1% w/v Galactose peak area		Mass Balance
	Lactose peak area	% Lactose (w/v)	Oligo peak area (tri+tet)	% Oligo (tri+tet, (w/v)	Glucose peak area	% Glucose (w/v)	Galactose peak area	% Galactose (w/v)	
0	61559297	24.03	328805	0.13	0	0.00	0	0.00	24.16
1	55125421	21.52	3100841	1.21	1928986	0.72	3314223	0.13	0.55
2	19171111	20.28	4940664	1.93	3128660	1.16	523541	0.20	23.58
3	50774949	19.82	6687244	2.61	4253312	1.58	760094	0.30	24.31
4	47680455	18.61	7927282	3.09	4888126	1.85	979954	0.38	23.93
5	46216220	18.04	8944437	3.49	5608228	2.09	1182980	0.46	24.08
6	45121185	17.61	9761183	3.81	6169712	2.30	1373694	0.54	24.25
7	44231653	16.09	10553187	4.12	6818410	2.54	1558980	0.61	24.53
8	41230838	16.09	10475903	4.09	7033359	2.62	2002301	0.78	23.58
9	41842769	16.33	11576825	4.52	7828926	2.91	2171325	0.85	24.61
10	40516225	15.81	11781973	4.60	8104774	3.02	2321973	0.91	24.34
11	39450390	15.40	12120168	4.73	8481913	3.16	2515735	0.98	24.27
12	36643866	14.30	11750718	4.59	8275378	3.08	2542266	0.99	22.96
13	38920889	15.19	12837024	5.01	9320326	3.47	2920208	1.14	24.81
14	37791156	14.75	12795134	4.99	9352256	3.47	2992344	1.17	24.38
15	37613911	14.68	13311880	5.20	9773003	3.64	3206399	1.25	24.77
16	35038470	13.67	12652982	4.94	9531194	3.55	3203582	1.25	23.41
17	33833228	13.21	13573365	5.30	10345932	3.85	3545120	1.39	23.74
18	31717577	12.38	12003594	4.89	9320193	3.47	3254778	1.27	21.81
19	34713970	13.55	13277215	5.18	10448014	3.89	3697165	1.44	24.07
20	35399597	13.62	13990393	5.46	11018804	4.10	3958120	1.55	24.93
21	34870677	13.61	13877293	5.42	11152480	4.15	4059919	1.59	24.77
22	34130952	13.32	13682733	5.42	11340627	4.22	4210821	1.65	24.61
23	33954271	13.25	13825040	5.43	11346455	4.30	4324903	1.69	24.68
24	34553078	13.49	14463988	5.65	11965824	4.45	4547885	1.78	25.36
25	34671781	13.53	14463988	5.65	12329382	4.59	4760279	1.86	25.63
26	34209329	13.35	14616085	5.70	12414420	4.62	4849922	1.90	25.57
27	33062805	12.90	14765596	5.76	12368732	4.60	4879010	1.91	25.18
28	32548115	12.70	14378269	5.61	12255293	4.56	4896649	1.91	24.79
29	32167361	12.56	13900242	5.43	12480085	4.65	5055314	1.98	24.60
30	31831043	12.42	14137503	5.52	12564878	4.68	5128657	2.00	24.62

Soluble Biotinase F Stirred-Batch Reaction

Date - 21/5/1996

[lactose monohydrate] - 25% w/v

Soluble [Biotinase F] - 1.25 mg cm³

Temperature - 40°C

Run Time - 0-30 minutes

Reaction volume - 250 cm³

Sample volume - 2 cm³

Stirrer speed - 200 rpm

Quench - 0.05M sodium hydroxide (2 cm³) + water (2 cm³)

Abbreviations:

%OTS - % Oligosaccharides of Total Sugar

%GlUTS - % Glucose of Total Sugar

%GalTS - % Galactose of Total Sugar

(tri+tet) - trisaccharides+tetrasaccharides

Oligo - oligosaccharides

* - lactose peak area used for oligo value.

Insolubilised β -galactosidase stirred-batch reaction Excel spreadsheets

5% Lactose monohydrate

Time (mins)	1% ¹³ C lactose peak area 4709141	% Lactose (°/v)	% Lactose Conversion	1% ¹³ C Oligo ⁰ peak area 4709141	% Oligo (tr+tet)(°/v)	% OTS (tr+tet)(°/v)	1% ¹³ C Glucose peak area 4273471	% Glucose (°/v)	% GluTS	1% ¹³ C Galactose peak area 4609425	% Galactose (°/v)	% GalTS	Mass Balance
0	25367065	5.39	1.90	214507	0.05	0.83	0	0.00	0.00	270548	0.06	1.07	5.49
1	23903393	5.08	4.54	664416	0.14	2.65	0	0.00	0.00	462808	0.10	1.69	5.32
2	21227812	4.34	15.81	927016	0.20	3.81	2050972	0.48	9.30	642625	0.14	2.70	5.16
3	20460866	4.51	19.58	1172555	0.25	4.44	2734629	0.84	11.42	960655	0.21	3.72	5.61
4	18298037	3.86	23.35	1204068	0.26	5.08	2921080	0.68	13.68	1087106	0.24	4.89	5.03
5	18164140	3.89	25.65	1324786	0.28	5.38	3107532	0.73	13.91	1530524	0.33	6.35	5.23
6	17026372	3.62	27.87	1337180	0.28	5.66	3169683	0.74	14.80	1711119	0.37	7.41	5.01
7	16349958	3.47	29.44	1352490	0.29	5.84	3200759	0.75	15.22	1901169	0.41	8.38	4.92
8	16153469	3.43	30.83	1553146	0.33	6.65	3231834	0.76	15.23	2042121	0.44	8.83	4.96
9	15937536	3.38	34.37	1564588	0.33	6.44	3743523	0.88	16.99	2598862	0.56	10.93	5.16
10	14939932	3.17	34.38	1474976	0.31	6.48	3785643	0.89	18.32	2135064	0.46	9.58	4.83
11	14283277	3.03	36.95	1505822	0.32	6.65	3779616	0.88	18.39	2642485	0.50	11.92	4.81
12	14334811	3.04	38.64	1527579	0.32	6.54	4227074	0.99	19.94	2782820	0.87	12.17	4.96
13	13979303	2.87	40.36	1587677	0.34	6.82	4470020	1.05	21.02	2873269	0.62	12.52	4.88
14	13205635	2.80	42.02	1604528	0.34	7.04	4503572	1.05	21.79	2941479	0.64	13.19	4.84
15	13138607	2.79	43.38	1650478	0.35	7.11	4718118	1.10	22.40	3150143	0.68	13.87	4.93
16	12796302	2.72	44.89	1649875	0.35	7.11	4906540	1.15	23.29	3294569	0.71	14.50	4.93
17	121452917	2.58	45.91	1558349	0.33	6.94	4944136	1.16	24.25	3238880	0.70	14.73	4.77
18	11482310	2.44	46.87	1486832	0.32	6.88	4901464	1.15	24.99	3174683	0.69	15.01	4.66
19	11419642	2.42	47.91	1512281	0.32	6.90	5006501	1.17	25.17	3399681	0.74	15.84	4.59
20	11126997	2.36	49.40	1486746	0.31	6.72	4856124	1.16	25.32	3458407	0.75	16.38	4.58
21	1092764	2.36	49.40	1496775	0.32	6.83	5128630	1.20	25.78	3601658	0.78	16.79	4.65
22	10896764	2.31	50.14	1481812	0.31	6.78	5178751	1.21	26.12	3687627	0.80	17.24	4.84
23	10518040	2.23	52.59	1527910	0.32	6.89	5479419	1.28	27.22	4014236	0.87	18.49	4.71
24	10021608	2.13	53.55	1356569	0.29	6.29	5514407	1.29	28.16	4035249	0.88	19.11	4.68
25	9642958	2.09	54.81	1334015	0.26	6.13	6000469	1.40	30.36	3906013	0.85	18.32	4.62
26	9775401	2.08	54.64	1216837	0.26	5.65	5951526	1.39	30.43	3917462	0.85	18.57	4.59
27	9729098	2.07	55.47	1225132	0.26	5.61	6149662	1.44	31.02	4031423	0.87	18.85	4.64
28	9720997	2.06	55.65	1214430	0.26	5.54	6150873	1.44	30.92	4116048	0.89	19.19	4.65
29	8791610	1.87	57.76	1310240	0.28	6.30	6085331	1.42	32.22	3919721	0.85	19.24	4.42
30	8689891	1.85	60.11	1270558	0.27	5.83	6650072	1.56	33.64	4398867	0.95	20.63	4.63

Glutaraldehyde Cross-linked Biotinase F. Stirred-Batch Reaction

Date - 16/3/1999
 [lactose monohydrate] - 5%¹³C
 Cross-linked [Biotinase F] - 1.25 mg cm⁻³ (free-enzyme equivalent)
 Temperature - 40°C
 Run Time - 0-30 minutes
 Reaction volume - 100 cm³
 Sample volume - 1 cm³
 Stirrer speed - 200 rpm
 Quench - 0.05M sodium hydroxide (1 cm³)

Abbreviations:
 %OTS - % Oligosaccharides of Total Sugar
 %GluTS - % Glucose of Total Sugar
 %GalTS - % Galactose of Total Sugar
 (tr+te) - trisaccharides+tetrasaccharides
 Oligo - oligosaccharides

* - lactose peak area used for oligo value.

10% Lactose monohydrate

Time (mins)	1% ¹⁴ C lactose peak area 4709141	1% ¹⁴ C oligo [*] peak area 4709141	1% ¹⁴ C Glucose peak area 4273471	1% ¹⁴ C Galactose peak area 4609425	Mass Balance
	Lactose peak area	Oligo peak area (tri+tet)	Glucose peak area	Galactose peak area	
	% Lactose (%)	% Oligo (tri+tet)(%)	% Glucose (%)	% Galactose (%)	% GalTTS (%)
	Conversion	% OTS (tri+tet)(%)	% GluTS	% GalTS	
	1.23	1.23	0	0	0
	5.68	4.83	0	0	0.85
1	52391915	653656	0	460684	11.80
2	44122853	3493072	3285827	1068956	11.11
3	42254000	4648421	4400023	1773750	11.37
4	40469487	5274476	5171170	2156597	11.38
5	39062733	5727494	5844908	2492579	11.42
6	37371960	5937723	6332278	3075447	11.35
7	38068498	6376094	7002113	3630778	11.87
8	34156716	6097657	6982458	3754382	11.00
9	33471815	6227067	7330977	4107558	11.04
10	32036686	6158652	7594764	4381837	10.84
11	32603734	6480580	8277800	4925041	11.30
12	31100937	6286484	8416573	5256755	11.05
13	31481573	6532475	8955839	5566283	11.38
14	29766604	6276853	8914269	5649952	10.97
15	29525665	6539345	8684038	5116646	11.16
16	27195992	6117485	8361986	5074398	10.87
17	28012462	6400272	9048302	5499217	10.13
18	26266742	5958658	8700714	5329156	10.04
19	27099343	6289987	9302309	5620870	10.53
20	29675989	6929899	10491211	6420997	11.89
21	27774272	6517972	10047354	6393967	12.59
22	27690413	6567502	10271049	6411628	12.57
23	25889885	6133990	9875023	6431605	11.07
24	27802315	6587373	10328524	6940861	13.25
25	26245228	6210426	10560044	6922696	13.84
26	25165949	5980601	9963052	6209596	13.84
27	25258112	5938437	10471172	7024918	13.11
28	23139975	5475745	9873924	6677329	14.38
29	23853677	5655902	10378832	7042885	14.73
30	27225465	5683719	10833275	6938399	14.95
					13.58

Glutaraldehyde Cross-linked Biotactase F Stirred-Batch Reaction

Date - 16/3/1999
 [lactose monohydrate] - 10% w/v
 Cross-linked [Biotactase F] - 1.25 mg cm³ (free-enzyme equivalent)
 Temperature - 40°C
 Run Time - 0-30 minutes
 Reaction volume - 100 cm³
 Sample volume - 1 cm³
 Stirrer speed - 200 rpm
 Quench - 0.05M sodium hydroxide (1 cm³)

Abbreviations:

%OTS - % Oligosaccharides of Total Sugar
 %GluTS - % Glucose of Total Sugar
 %GalTS - % Galactose of Total Sugar
 (tri+tet) - trisaccharides+tetrasaccharides
 Oligo - oligosaccharides

* - lactose peak area used for oligo value.

15% Lactose monohydrate

Time (mins)	1% ¹⁴ C lactose peak area 2608423	1% ¹⁴ C Oligo* peak area 2608423	1% ¹⁴ C Glucose peak area 2550151	1% ¹⁴ C Galactose peak area 2689676	Mass Balance
	% Lactose (n/n)	% Oligo (n/n+tel)	% Glucose (n/n)	% Galactose (n/n)	
0	42480200	551351	0	0	16.50
1	40850048	2269082	0	336926	16.87
2	35664435	3706154	2996508	949136	16.70
3	33466193	4557315	3847149	1328901	16.58
4	32350574	5235400	4622335	1652631	16.81
5	28946203	5280299	4895796	1817566	15.72
6	28693568	5796650	5597531	2197237	18.23
7	27752391	5969452	5979072	2440888	16.18
8	26552264	6087100	6289498	2601525	15.90
9	24827687	6007854	6622598	2838309	15.90
10	22404324	5574987	7794565	3948155	14.7
11	23868777	6061544	8426785	4187436	14.89
12	22898755	5931306	8759065	3907968	9.76
13	22000585	5877656	9046968	4012943	16.02
14	21468555	5824161	8984767	4187436	15.75
15	22074145	5764271	9220794	4499209	10.83
16	21353566	5703961	9244458	4674390	11.73
17	20524372	5450067	9639291	4965037	15.74
18	19797040	5629460	9850691	5197335	12.14
19	18683211	5505821	9826820	5254377	15.92
20	19587269	5450500	9864193	5479747	12.56
21	19185056	5275	9864193	5254377	15.70
22	18488042	5147733	10100035	5254377	15.63
23	18198913	5147733	10100035	5254377	15.73
24	18189456	5057044	10147260	6041449	14.28
25	17699410	5081452	10458439	6104134	15.57
26	17850068	4896725	10460734	6244864	14.93
27	17390603	5055433	10983410	6393310	15.85
28	18188539	5055433	10983410	6562688	15.28
29				6618171	15.41
30				6838622	15.16
				6816450	15.44
				7227544	16.74
					15.91

Glutaraldehyde Cross-linked Biotinase F Stirred-Batch Reaction

Date - 8/4/1999
 Lactose monohydrate) - 15% ¹⁴C
 Cross-linked [Biotinase F] - 1.25 mg cm⁻³ (free-enzyme equivalent)
 Temperature - 40°C
 Run Time - 0-30 minutes
 Reaction volume - 100 cm³
 Sample volume - 1cm³
 Stirrer speed - 200 rpm
 Quench - 0.05M sodium hydroxide (2 cm³) + water (1cm³)

Abbreviations:
 %OTS - % Oligosaccharides of Total Sugar
 %GLUTS - % Glucose of Total Sugar
 %GalTS - % Galactose of Total Sugar
 (n+tel) - trisaccharides+tetrasaccharides
 Oligo - oligosaccharides

* - lactose peak area used for oligo value.

20% Lactose monohydrate

Time (mins)	1% ^{v/v} lactose peak area 2739854	1% ^{v/v} oligo* peak area 2739854	1% ^{v/v} Glucose peak area 2633456	1% ^{v/v} Galactose peak area 2761317	Mass Balance
0	58784087	907565	12785	131993	21.84
1	53336604	3186799	1530586	401557	22.08
2	52176272	5348113	2589469	874663	22.30
3	49534196	6776713	3475378	1230077	22.32
4	46818716	7616807	4169298	1471258	21.98
5	44985793	8429704	4757330	1757225	21.94
6	43040640	8641755	5205422	2000213	21.84
7	41704908	9333783	5761972	2220297	21.82
8	40610461	9656808	6219436	2577040	21.64
9	39366824	9783306	6554791	2681404	21.40
10	37564233	10229436	6862698	3010673	21.14
11	36965184	10424387	7226921	3184589	21.19
12	38229561	11246579	8115346	3655335	22.48
13	37309616	11270937	8222117	3780229	22.22
14	36429012	11257427	8521388	3940671	22.07
15	36227223	11480032	8835130	4145011	22.76
16	36422187	11811301	9364447	4500397	22.30
17	35522406	11603669	9790803	4775734	22.63
18	35374695	11714495	9790803	4775734	21.75
19	33715497	11240449	9573781	4708832	7.84
20	34157188	11929596	10127551	5007640	8.10
21	34462941	11810552	10484813	5268869	8.36
22	34345772	11969313	10877893	5403662	8.57
23	32960995	11479548	10587152	5622835	8.81
24	32973771	11699387	10889641	5620069	9.06
25	31871986	11400553	11585677	6040790	9.28
26	33279257	11891955	10782464	5889138	9.47
27	31200092	11320322	11073784	5889138	9.76
28	30091351	10889950	10938482	5837665	9.94
29	31519886	11604066	11803667	6311416	10.16
30	30219709	11132986	11335130	5835532	9.82

Glutaraldehyde Cross-linked Biotactase F. Stirred-Batch Reaction

Date - 30/03/1999
 [lactose monohydrate] - 20%^{v/v}
 Cross-linked [Biotactase F] - 1.25 mg cm³ (free-enzyme equivalent)
 Temperature - 40°C
 Run Time - 0-30 minutes
 Reaction volume - 100 cm³
 Sample volume - 1 cm³
 Stirrer speed - 200 rpm
 Quench - 0.05M sodium hydroxide (2 cm³) + water (1 cm³)

Abbreviations:
 %OTS - % Oligosaccharides of Total Sugar
 %GlUTS - % Glucose of Total Sugar
 %GalTTS - % Galactose of Total Sugar
 (tri-tet) - trisaccharides+tetrascacharides
 Oligo - oligosaccharides

* - lactose peak area used for oligo value.

25% Lactose monohydrate

Time (mins)	1% % Lactose peak area 2261511	% Lactose (%)	% Lactose Conversion	1% % Oligo* peak area 2261511	% Oligo (tri+tet)-(%)	1% % Glucose peak area 2188230	% Glucose (%)	% GluTS	1% % Galactose peak area 2242542	% Galactose (%)	% GalTS	Mass Balance
0	55363331	24.48	1.69	898664	0.40	0	0.00	0.00	52921	0.02	0.09	24.90
1	54160395	23.95	10.00	3697771	1.72	1669662	0.76	2.87	390063	0.17	0.65	26.61
2	49696414	14.96	10.00	5495951	2.43	2492635	1.14	4.41	664333	0.30	1.15	25.84
3	46349450	20.49	19.76	6925406	3.06	3382952	1.55	6.05	984858	0.44	1.72	25.54
4	43429323	22.66	22.66	7565130	3.35	3629048	1.75	7.05	1191475	0.63	2.14	24.83
5	43801360	19.20	26.83	9240155	4.09	4887619	2.28	8.61	1650070	0.74	2.78	26.47
6	40273369	17.81	29.16	9428775	4.17	5166758	2.36	9.39	1793418	0.80	3.18	25.14
7	36961966	16.35	31.17	9294422	4.11	5344277	2.44	10.28	1911678	0.85	3.59	23.78
8	36416515	16.10	33.35	9859964	4.36	5975811	2.73	11.30	2169694	0.97	4.00	24.18
9	33961932	15.02	34.78	9607600	4.25	6023893	2.75	11.96	2259539	1.01	4.38	23.03
10	33200855	14.68	36.87	10199861	4.51	6461105	2.95	12.70	2490650	1.11	4.78	23.25
11	33663861	14.89	37.89	10617002	4.69	6952287	3.18	13.26	2711478	1.21	5.05	23.97
12	32221581	14.25	39.16	10517671	4.65	7096919	3.24	13.85	2864007	1.28	5.45	23.42
13	32601392	14.42	40.52	11152614	4.93	7692185	3.52	14.50	3079909	1.37	5.67	24.24
14	31577414	13.96	41.13	10885689	4.81	7824809	3.52	14.82	3197822	1.43	6.01	23.72
15	30631987	13.54	41.95	10683351	4.72	7925351	3.62	15.52	3236337	1.44	6.18	23.33
16	29900733	13.22	43.01	10730988	4.75	8117169	3.71	15.99	3414730	1.52	6.56	23.20
17	29926626	13.23	43.51	10624843	4.79	8349912	3.82	16.29	3569140	1.59	6.78	23.43
18	29042541	12.84	44.66	10876060	4.81	8545814	3.91	16.83	3694379	1.65	7.10	23.20
19	29169788	12.90	45.00	10887575	4.81	8789637	4.02	17.13	3865002	1.72	7.35	23.45
20	29133821	12.88	45.59	10946327	4.84	9093178	4.21	17.55	4032450	1.80	7.59	23.68
21	27636227	12.66	46.09	10962047	4.85	9205753	4.21	17.92	3958577	1.77	7.52	23.48
22	28624107	12.22	47.02	10618467	4.70	9297609	4.25	18.42	4265755	1.90	8.25	23.07
23	28707612	12.69	47.82	11487133	5.08	9955686	4.55	18.70	4497894	2.01	8.24	24.33
24	27114325	11.99	48.36	10935534	4.84	9576431	4.38	18.85	4517496	2.01	8.68	23.22
25	27814512	12.21	48.98	11295136	4.99	10114570	4.62	19.31	4720790	2.11	8.80	23.93
26	27706840	12.25	49.64	11569065	5.12	10440899	4.77	19.61	4904729	2.19	8.99	24.33
27	27306712	12.07	50.21	11549449	5.11	10471300	4.79	19.73	5126009	2.29	9.42	24.25
28	28266183	12.50	50.42	11995346	5.30	10952620	5.01	19.86	5383131	2.40	9.52	25.21
29	27361475	12.10	50.96	11688814	5.17	10862879	4.96	20.12	5468488	2.44	9.88	24.67
30	26535335	11.73	51.43	11407639	5.04	10773780	4.92	20.38	5505369	2.45	10.16	24.16

Glutinaldehyde Cross-linked Biotectase F Stirred-Batch Reaction

Date -13/4/1999
 [lactose monohydrate] - 25% %
 Cross-linked [Biotectase F] - 1.25 mg cm³ (free-enzyme equivalent)
 Temperature - 40°C
 Run Time - 0-30 minutes
 Reaction volume - 100 cm³
 Sample volume - 1 cm³
 Stirrer speed - 200 rpm
 Quench - 0.05M sodium hydroxide (2 cm³) + water (2 cm³)

Abbreviations:
 %OTS - % Oligosaccharides of Total Sugar
 %GluTS - % Glucose of Total Sugar
 %GalTS - % Galactose of Total Sugar
 (tri+tet) - trisaccharides+tetrasaccharides
 Oligo - oligosaccharides

* - lactose peak area used for oligo value.

30% Lactose monohydrate

Time (mins)	1% ^{w/v} Lactose peak area 3371366		1% ^{w/v} Oligo ⁺ peak area 3371366		1% ^{w/v} Glucose peak area 3165585		1% ^{w/v} Galactose peak area 3390635		Mass Balance
	Lactose peak area	% Lactose (°w/v)	Oligo peak area (tri+tet)	% Oligo (tri+tet)(°w/v)	Glucose peak area	% Glucose (°w/v)	Galactose peak area	% Galactose (°w/v)	
0	9657014	28.76	1170747	0.35	1.19	0.00	183560	0.05	28.16
1	94894860	28.15	4230740	1.25	4.25	0.00	501288	0.15	28.55
2	87768093	26.03	6807317	2.09	6.90	0.93	992425	0.29	29.27
3	84411595	25.04	8742939	2.59	8.84	1.33	1262570	0.37	29.34
4	80058727	23.75	10195312	3.02	10.48	1.62	1523748	0.45	28.84
5	82332033	24.42	12355880	3.66	11.93	2.03	2031067	0.60	30.72
6	76020437	22.55	12760659	3.79	13.02	2.13	2067707	0.61	29.07
7	74730297	22.17	13869596	4.11	14.01	2.38	2352174	0.69	28.35
8	75802199	22.48	15337370	4.55	14.93	2.66	2847437	0.78	30.46
9	68168829	20.22	14431166	4.28	15.38	2.55	2663388	0.79	27.84
10	67677710	20.07	15367196	4.56	16.11	2.80	2912376	0.86	28.29
11	66104489	19.61	16148363	4.79	16.96	2.92	3122008	0.92	28.24
12	62521337	18.54	16017035	4.75	17.48	2.94	3185904	0.94	27.16
13	61344716	18.20	16523008	4.84	17.90	3.05	3288132	0.97	27.08
14	64494261	19.13	17746199	5.26	18.22	3.39	3732030	1.10	28.88
15	63106250	18.72	17440434	5.26	18.42	3.45	3865479	1.14	28.57
16	61202670	18.15	17896143	5.31	18.84	3.55	3952353	1.17	28.18
17	59932012	17.78	17866029	5.30	19.02	3.59	4052158	1.20	27.86
18	58904241	17.47	18352565	5.44	19.56	3.70	4110232	1.21	27.83
19	55232819	16.38	17273312	5.12	19.49	3.57	4118397	1.21	26.29
20	55955681	16.60	18040745	5.35	19.87	3.70	4335321	1.25	26.93
21	52290271	15.51	17143181	5.08	19.98	3.61	4254619	1.25	25.46
22	56612980	16.79	18671094	5.60	20.15	3.99	4775008	1.41	27.78
23	53184023	15.78	18068041	5.36	20.35	3.85	4586632	1.35	26.34
24	52755565	15.65	18239630	5.41	20.50	3.96	4674108	1.38	26.39
25	54344027	16.12	19149670	5.68	20.67	4.18	5107283	1.51	27.48
26	52967773	15.71	18689635	5.60	20.75	4.18	5117081	1.51	27.00
27	53627437	15.91	19392621	5.75	20.92	4.30	5217813	1.54	27.50
28	51672078	15.33	18997789	5.64	21.05	4.28	5190988	1.53	26.77
29	52067831	15.44	19114858	5.67	20.98	4.34	5321785	1.57	27.03
30	54689771	16.22	20476634	6.07	21.22	4.62	5789464	1.71	28.62

Glucuraltaldehyde Cross-linked Biotactase F. Stirred-Batch Reaction

Date - 30/3/1999
 [lactose monohydrate] - 30%^{w/v}
 Cross-linked [Biotactase F] - 1.25 mg cm⁻³ (free-enzyme equivalent)
 Temperature - 40°C
 Run Time - 0-30 minutes
 Reaction volume - 100 cm³
 Stirrer speed - 200 rpm
 Sample volume - 1 cm³
 Quench - 0.05M sodium hydroxide (1 cm³) + water (1 cm³)

Abbreviations:
 %OTS - % Oligosaccharides of Total Sugar
 %GlUTS - % Glucose of Total Sugar
 %GalTS - % Galactose of Total Sugar
 (tri+tet) - trisaccharides+tetrasaccharides
 Oligo - oligosaccharides

* - lactose peak area used for oligo value.

40% Lactose monohydrate

Time (mins)	1%*/v Lactose peak area		1%*/v Oligo* peak area		1%*/v Glucose peak area		1%*/v Galactose peak area		Mass Balance
	Lactose peak area	% Lactose (*/v)	Oligo peak area (tr+tet)	% Oligo (tr+tet)*/v	Glucose peak area	% Glucose (*/v)	Galactose peak area	% Galactose (*/v)	
0	94150086	40.94	1252470	0.54	1.31	0	0.00	0.00	41.48
1	90035937	39.15	2473538	1.08	2.67	0	0.00	0.00	40.23
2	89467403	38.90	4159813	1.81	4.44	0	0.00	0.00	40.71
3	85252621	37.07	5789312	2.52	6.34	0	0.00	0.13	39.72
4	83271576	36.21	7094662	3.08	7.76	0	0.00	0.48	39.77
5	83167568	36.16	8371948	3.64	9.02	0	0.00	0.67	40.37
6	82058376	35.68	9284941	4.04	10.00	0	0.00	0.57	40.38
7	79433265	34.54	9905252	4.31	10.88	0	0.00	0.73	39.56
8	78388839	34.08	10566175	4.60	11.65	0	0.00	0.76	39.44
9	69239524	30.11	11031976	4.80	12.20	7326093	3.58	9.10	39.31
10	68550498	29.81	11886091	5.17	12.96	8205642	4.01	10.05	39.87
11	67420303	29.32	12398333	5.39	13.33	8952046	4.37	10.81	40.43
12	66796349	29.04	13175436	5.73	14.17	9493405	4.64	11.47	40.44
13	63368369	27.55	12978714	5.64	14.51	9535291	4.66	11.98	38.88
14	64536984	28.06	13705959	5.96	14.81	10432324	4.66	11.57	40.24
15	61546641	26.76	13782383	5.99	15.17	10577993	5.17	13.08	39.51
16	63662163	27.68	14866393	6.39	15.37	11682658	5.71	13.74	41.54
17	64024681	27.84	15305394	6.66	15.74	12456613	6.08	14.39	42.29
18	59600141	25.92	14649237	6.37	15.95	11889030	5.81	14.54	39.94
19	62111463	27.01	15623484	6.79	16.24	12811035	6.26	14.96	41.84
20	59000496	25.65	15211925	6.61	16.48	12524089	6.12	15.24	40.14
21	58732967	25.56	15632918	6.80	16.81	12851888	6.28	15.52	40.44
22	62207714	27.05	17237957	7.50	17.26	14075397	6.87	15.83	43.43
23	58652278	25.50	16297337	7.09	17.17	13726681	6.70	16.24	41.27
24	54574077	23.73	15885975	6.91	17.75	13050624	6.37	16.38	38.92
25	57428462	24.97	16518123	7.18	17.47	14102503	6.89	16.76	41.10
26	59234624	25.76	17381981	7.56	17.65	14863110	7.26	16.95	42.83
27	54381173	23.65	16643517	7.24	18.21	13880118	6.78	17.06	39.74
28	54171442	23.36	16851253	7.33	18.30	14287475	6.98	17.43	40.03
29	56883814	24.73	17991272	7.82	18.44	15388473	7.52	17.72	42.42
30	54144862	23.54	17344633	7.54	18.46	15180802	7.41	18.15	40.85

Glutaraldehyde Cross-linked Biotactase F Stirred-Batch Reaction

Date - 8/4/1999
 [lactose monohydrate] - 40%*/v
 Cross-linked [Biotactase F] - 1.25 mg cm³ (free-enzyme equivalent)
 Temperature - 40°C
 Run Time - 0-30 minutes
 Reaction volume - 100 cm³
 Sample volume - 1 cm³
 Stirrer speed - 200 rpm
 Quench - 0.05M sodium hydroxide (2 cm³) + water (2 cm³)

Abbreviations:
 %OTS - % Oligosaccharides of Total Sugar
 %GlUTS - % Glucose of Total Sugar
 %GalTTS - % Galactose of Total Sugar
 (tr+tet) - trisaccharides+tetracosaccharides
 Oligo - oligosaccharides
 * - lactose peak area used for oligo value.

NS: High lactose concentration lead to the masking of the initial glucose peaks, until a high enough threshold value enabled detection.
 Therefore, the initial lactose conversion values will be inaccurate.

Appendix A-2

(Kinetic model Excel spreadsheet calculations)

Soluble β -galactosidase from *Aspergillus oryzae*
(Biolactase F) spreadsheets

Initial lactose monohydrate concentration (mM)	K_m	K_i	$(1-k_m/k_i)$	$[L_0]$	$(K_m \cdot [L_0]/K_i) + K_m$	V_{max} (mM min ⁻¹)
139	74	4.3	-16.21	139	2466.09	76.3
[L]	$[L_0]-[L]$	$\ln([L_0]/[L])$	$V_{max} \cdot t$	% Lactose monohydrate conversion	t (minutes)	
139.00	0.00	0.00	0.00	0.00	0.0	
132.05	6.95	0.05	13.84	5.00	0.2	
125.10	13.90	0.11	34.52	10.00	0.5	
118.15	20.85	0.16	62.82	15.00	0.8	
111.20	27.80	0.22	99.67	20.00	1.3	
104.25	34.75	0.29	146.18	25.00	1.9	
97.30	41.70	0.36	203.67	30.00	2.7	
90.35	48.65	0.43	273.77	35.00	3.6	
83.40	55.60	0.51	358.51	40.00	4.7	
76.45	62.55	0.60	460.43	45.00	6.0	
69.50	69.50	0.69	582.82	50.00	7.6	
62.55	76.45	0.80	729.99	55.00	9.6	
55.60	83.40	0.92	907.80	60.00	11.9	
48.65	90.35	1.05	1124.45	65.00	14.7	
41.70	97.30	1.20	1391.94	70.00	18.2	
34.75	104.25	1.39	1728.91	75.00	22.7	
27.80	111.20	1.61	2166.55	80.00	28.4	
20.85	118.15	1.90	2763.35	85.00	36.2	

Soluble β -galactosidase (1.25 mg cm⁻³) incubated with 5% w/v lactose monohydrate at 40°C

Initial lactose monohydrate concentration (mM)	K_m	K_i	$(K_m \cdot [L_0]/K_i) + K_m$	$[L_0]$	$(K_m \cdot [L_0]/K_i) + K_m$	V_{max} (mM min ⁻¹)
278	74	4.3	4858.19	278	4858.19	76.3
[L]	$[L_0] - [L]$	$\ln([L_0]/[L])$	$V_{max} \cdot t$	% Lactose monohydrate conversion	t (minutes)	
278.00	0.00	0.00	0.00	0.00	0.0	
264.10	13.90	0.05	23.88	5.00	0.3	
250.20	27.80	0.11	61.24	10.00	0.8	
236.30	41.70	0.16	113.62	15.00	1.5	
222.40	55.60	0.22	182.84	20.00	2.4	
208.50	69.50	0.29	271.07	25.00	3.6	
194.60	83.40	0.36	380.94	30.00	5.0	
180.70	97.30	0.43	515.66	35.00	6.8	
166.80	111.20	0.51	679.21	40.00	8.9	
152.90	125.10	0.60	876.62	45.00	11.5	
139.00	139.00	0.69	1114.34	50.00	14.6	
125.10	152.90	0.80	1400.90	55.00	18.4	
111.20	166.80	0.92	1747.80	60.00	22.9	
97.30	180.70	1.05	2171.21	65.00	28.5	
83.40	194.60	1.20	2694.79	70.00	35.3	
69.50	208.50	1.39	3355.24	75.00	44.0	
55.60	222.40	1.61	4214.00	80.00	55.2	
41.70	236.30	1.90	5386.30	85.00	70.6	

Soluble β -galactosidase (1.25 mg cm⁻³) incubated with 10% w/v lactose monohydrate at 40°C

Initial lactose monohydrate concentration (mM)	K_m	K_i	$(K_m \cdot [L_0]/K_i) + K_m$	V_{max} (mM min ⁻¹)
417	74	4.3	417	76.3
[L]	$\ln([L_0]/[L])$	$V_{max} \cdot t$	% Lactose monohydrate conversion	t (minutes)
417.00	0.00	0.00	0.00	0.0
396.15	0.05	33.93	5.00	0.4
375.30	0.11	87.97	10.00	1.2
354.45	0.16	164.42	15.00	2.2
333.60	0.22	266.00	20.00	3.5
312.75	0.29	395.96	25.00	5.2
291.90	0.36	558.21	30.00	7.3
271.05	0.43	757.55	35.00	9.9
250.20	0.51	999.92	40.00	13.1
229.35	0.60	1292.81	45.00	16.9
208.50	0.69	1645.87	50.00	21.6
187.65	0.80	2071.80	55.00	27.2
166.80	0.92	2587.80	60.00	33.9
145.95	1.05	3217.97	65.00	42.2
125.10	1.20	3997.64	70.00	52.4
104.25	1.39	4981.56	75.00	65.3
83.40	1.61	6261.45	80.00	82.1
62.55	1.90	8009.26	85.00	105.0

Soluble β -galactosidase (1.25 mg cm⁻³) incubated with 15% w/v lactose monohydrate at 40°C

Initial lactose monohydrate concentration (mM) 556
 $(K_m/[L_0]/K_i)+K_m$ 9642.37
 V_{max} (mM min⁻¹) 76.3

K_m 74
 K_i 4.3

$(1-K_m/k_i)$ -16.21
 $[L_0]$ 556

[L]	$[L_0]-[L]$	$\ln([L_0]/[L])$	$V_{max} \cdot t$	% Lactose monohydrate conversion	t (minutes)
556.00	0.00	0.00	0.00	0.00	0.0
528.20	27.80	0.05	43.97	5.00	0.6
500.40	55.60	0.11	114.69	10.00	1.5
472.60	83.40	0.16	215.21	15.00	2.8
444.80	111.20	0.22	349.16	20.00	4.6
417.00	139.00	0.29	520.84	25.00	6.8
389.20	166.80	0.36	735.48	30.00	9.6
361.40	194.60	0.43	999.44	35.00	13.1
333.60	222.40	0.51	1320.62	40.00	17.3
305.80	250.20	0.60	1709.00	45.00	22.4
278.00	278.00	0.69	2177.40	50.00	28.5
250.20	305.80	0.80	2742.70	55.00	35.9
222.40	333.60	0.92	3427.79	60.00	44.9
194.60	361.40	1.05	4264.73	65.00	55.9
166.80	389.20	1.20	5300.49	70.00	69.5
139.00	417.00	1.39	6607.89	75.00	86.6
111.20	444.80	1.61	8308.90	80.00	108.9
83.40	472.60	1.90	10632.22	85.00	139.3

Soluble β -galactosidase (1.25 mg cm⁻³) incubated with 20% w/v lactose monohydrate at 40°C

Initial lactose monohydrate concentration (mM)	K_m	K_i	$(1-K_m/K_i)$	$[L_0]$	$(K_m \cdot [L_0]/K_i) + K_m$	V_{max} (mM min ⁻¹)
695	74	4.3	-16.21	695	12034.47	76.3
[L]	$[L_0]-[L]$	$\ln([L_0]/[L])$	$V_{max} \cdot t$	% Lactose monohydrate conversion	t (minutes)	
695.00	0.00	0.00	0.00	0.00	0.0	
660.25	34.75	0.05	54.01	5.00	0.7	
625.50	69.50	0.11	141.41	10.00	1.9	
590.75	104.25	0.16	266.01	15.00	3.5	
556.00	139.00	0.22	432.32	20.00	5.7	
521.25	173.75	0.29	645.73	25.00	8.5	
486.50	208.50	0.36	912.75	30.00	12.0	
451.75	243.25	0.43	1241.33	35.00	16.3	
417.00	278.00	0.51	1641.33	40.00	21.5	
382.25	312.75	0.60	2125.19	45.00	27.9	
347.50	347.50	0.69	2708.92	50.00	35.5	
312.75	382.25	0.80	3413.61	55.00	44.7	
278.00	417.00	0.92	4267.79	60.00	55.9	
243.25	451.75	1.05	5311.50	65.00	69.6	
208.50	486.50	1.20	6603.34	70.00	86.5	
173.75	521.25	1.39	8234.21	75.00	107.9	
139.00	556.00	1.61	10356.35	80.00	135.7	
104.25	590.75	1.90	13255.18	85.00	173.7	

Soluble β -galactosidase (1.25 mg cm⁻³) incubated with 25% w/v lactose monohydrate at 40°C

Initial lactose monohydrate concentration (mM)	K_m	K_i	$(1-k_m/k_i)$	$[L_0]$	$(K_m \cdot [L_0]/K_i) + K_m$	V_{max} (mM min ⁻¹)
834	74	4.3	-16.21	834	14426.56	76.3
[L]	$[L_0]-[L]$	$\ln([L_0]/[L])$	$V_{max} \cdot t$	% Lactose monohydrate conversion	t (minutes)	
834.00	0.00	0.00	0.00	0.00	0.0	
792.30	41.70	0.05	64.06	5.00	0.8	
750.60	83.40	0.11	168.13	10.00	2.2	
708.90	125.10	0.16	316.81	15.00	4.2	
667.20	166.80	0.22	515.48	20.00	6.8	
625.50	208.50	0.29	770.62	25.00	10.1	
583.80	250.20	0.36	1090.02	30.00	14.3	
542.10	291.90	0.43	1483.22	35.00	19.4	
500.40	333.60	0.51	1962.03	40.00	25.7	
458.70	375.30	0.60	2541.38	45.00	33.3	
417.00	417.00	0.69	3240.45	50.00	42.5	
375.30	458.70	0.80	4084.51	55.00	53.5	
333.60	500.40	0.92	5107.79	60.00	66.9	
291.90	542.10	1.05	6358.26	65.00	83.3	
250.20	583.80	1.20	7906.19	70.00	103.6	
208.50	625.50	1.39	9860.54	75.00	129.2	
166.80	667.20	1.61	12403.80	80.00	162.6	
125.10	708.90	1.90	15878.14	85.00	208.1	

Soluble β -galactosidase (1.25 mg cm⁻³) incubated with 30% w/v lactose monohydrate at 40°C

Initial lactose monohydrate concentration (mM)	K_m	K_i	$(1-K_m/k_i)$	$[L_0]$	$(K_m \cdot [L_0]/K_i) + K_m$	V_{max} (mM min ⁻¹)
1112	74	4.3	-16.21	1112	19210.74	76.3
[L]	$[L_0]-[L]$	$\ln([L_0]/[L])$	$V_{max} \cdot t$	% Lactose monohydrate conversion	t (minutes)	
1112.00	0.00	0.00	0.00	0.00	0.0	
1056.40	55.60	0.05	84.15	5.00	1.1	
1000.80	111.20	0.11	221.58	10.00	2.9	
945.20	166.80	0.16	418.40	15.00	5.5	
889.60	222.40	0.22	681.80	20.00	8.9	
834.00	278.00	0.29	1020.40	25.00	13.4	
778.40	333.60	0.36	1444.57	30.00	18.9	
722.80	389.20	0.43	1967.00	35.00	25.8	
667.20	444.80	0.51	2603.44	40.00	34.1	
611.60	500.40	0.60	3373.76	45.00	44.2	
556.00	556.00	0.69	4303.50	50.00	56.4	
500.40	611.60	0.80	5426.32	55.00	71.1	
444.80	667.20	0.92	6787.78	60.00	89.0	
389.20	722.80	1.05	8451.78	65.00	110.8	
333.60	778.40	1.20	10511.89	70.00	137.8	
278.00	834.00	1.39	13113.19	75.00	171.9	
222.40	889.60	1.61	16498.70	80.00	216.2	
166.80	945.20	1.90	21124.05	85.00	276.9	

Soluble β -galactosidase (1.25 mg cm⁻³) incubated with 40% w/v lactose monohydrate at 40°C

Insolubilised β -galactosidase from *Aspergillus oryzae*
(Biolactase F) spreadsheets

Initial lactose monohydrate concentration (mM)	K_m	K_i	$(1-K_m/K_i)$	$[L_0]$	$(K_m/[L_0]/K_i)+K_m$	V_{max} (mM min ⁻¹)
139	104	2.5	-40.60	139	5886.40	43.5
[L]	$\ln([L_0]/[L])$	$V_{max} \cdot t$	% Lactose monohydrate conversion	t (minutes)		
139.00	0.00	0.00	0.00	0.0		
132.05	6.95	19.76	5.00	0.5		
125.10	13.90	55.85	10.00	1.3		
118.15	20.85	110.14	15.00	2.5		
111.20	27.80	184.83	20.00	4.2		
104.25	34.75	282.56	25.00	6.5		
97.30	41.70	406.51	30.00	9.3		
90.35	48.65	560.57	35.00	12.9		
83.40	55.60	749.56	40.00	17.2		
76.45	62.55	979.58	45.00	22.5		
69.50	69.50	1258.44	50.00	28.9		
62.55	76.45	1596.47	55.00	36.7		
55.60	83.40	2007.61	60.00	46.2		
48.65	90.35	2511.46	65.00	57.7		
41.70	97.30	3136.69	70.00	72.1		
34.75	104.25	3927.73	75.00	90.3		
27.80	111.20	4959.08	80.00	114.0		
20.85	118.15	6370.32	85.00	146.4		

Insolubilised β -galactosidase (1.25 mg cm⁻³) incubated with 5% w/v lactose monohydrate at 40°C

Initial lactose monohydrate concentration (mM) $[L_0]$ $(K_m + [L_0]/K_i) + K_m$ V_{max} (mM min⁻¹)
 278 278 11668.80 43.5

K_m K_i
 104 2.5

$(1 - K_m/k_i)$
 -40.60

$[L]$	$[L_0] - [L]$	$\ln([L_0]/[L])$	$V_{max} \cdot t$	% Lactose monohydrate conversion	t (minutes)
278.00	0.00	0.00	0.00	0.00	0.0
264.10	13.90	0.05	34.19	5.00	0.8
250.20	27.80	0.11	100.75	10.00	2.3
236.30	41.70	0.16	203.38	15.00	4.7
222.40	55.60	0.22	346.46	20.00	8.0
208.50	69.50	0.29	535.20	25.00	12.3
194.60	83.40	0.36	775.93	30.00	17.8
180.70	97.30	0.43	1076.34	35.00	24.7
166.80	111.20	0.51	1446.00	40.00	33.2
152.90	125.10	0.60	1896.98	45.00	43.6
139.00	139.00	0.69	2444.80	50.00	56.2
125.10	152.90	0.80	3109.89	55.00	71.5
111.20	166.80	0.92	3919.93	60.00	90.1
97.30	180.70	1.05	4913.74	65.00	113.0
83.40	194.60	1.20	6148.16	70.00	141.3
69.50	208.50	1.39	7711.29	75.00	177.3
55.60	222.40	1.61	9750.77	80.00	224.2
41.70	236.30	1.90	12543.33	85.00	288.4

Insolubilised β -galactosidase (1.25 mg cm⁻³) incubated with 10% w/v lactose monohydrate at 40°C

Initial lactose monohydrate concentration (mM)	K_m	K_i	$(1-k_m/k_i)$	$[L_0]$	$(K_m[L_0]/K_i)+K_m$	V_{max} (mM min ⁻¹)
417	104	2.5	-40.60	417	17451.20	43.5
[L]	$[L_0]-[L]$	$\ln([L_0]/[L])$	$V_{max}t$	% Lactose monohydrate conversion	t (minutes)	
417.00	0.00	0.00	0.00	0.00	0.0	
396.15	20.85	0.05	48.62	5.00	1.1	
375.30	41.70	0.11	145.65	10.00	3.3	
354.45	62.55	0.16	296.62	15.00	6.8	
333.60	83.40	0.22	508.08	20.00	11.7	
312.75	104.25	0.29	787.85	25.00	18.1	
291.90	125.10	0.36	1145.35	30.00	26.3	
271.05	145.95	0.43	1592.11	35.00	36.6	
250.20	166.80	0.51	2142.44	40.00	49.3	
229.35	187.65	0.60	2814.38	45.00	64.7	
208.50	208.50	0.69	3631.15	50.00	83.5	
187.65	229.35	0.80	4623.31	55.00	106.3	
166.80	250.20	0.92	5832.25	60.00	134.1	
145.95	271.05	1.05	7316.03	65.00	168.2	
125.10	291.90	1.20	9159.63	70.00	210.6	
104.25	312.75	1.39	11494.85	75.00	264.2	
83.40	333.60	1.61	14542.46	80.00	334.3	
62.55	354.45	1.90	18716.35	85.00	430.3	

Insolubilised β -galactosidase (1.25 mg cm⁻³) incubated with 15% w/v lactose monohydrate at 40°C

Initial lactose monohydrate concentration (mM)	K_m	K_i	$(1-K_m/K_i)$	$[L_0]$	$(K_m \cdot [L_0]/K_i) + K_m$	V_{max} (mM min ⁻¹)
556	104	2.5	-40.60	556	23233.60	43.5
[L]	$\ln([L_0]/[L])$	$V_{max} \cdot t$	% Lactose monohydrate conversion	t (minutes)		
556.00	0.00	0.00	0.00	0.0		
528.20	0.05	63.05	5.00	1.4		
500.40	0.11	190.54	10.00	4.4		
472.60	0.16	389.86	15.00	9.0		
444.80	0.22	669.71	20.00	15.4		
417.00	0.29	1040.49	25.00	23.9		
389.20	0.36	1514.76	30.00	34.8		
361.40	0.43	2107.88	35.00	48.5		
333.60	0.51	2838.88	40.00	65.3		
305.80	0.60	3731.79	45.00	85.8		
278.00	0.69	4817.50	50.00	110.7		
250.20	0.80	6136.73	55.00	141.1		
222.40	0.92	7744.57	60.00	178.0		
194.60	1.05	9718.31	65.00	223.4		
166.80	1.20	12171.10	70.00	279.8		
139.00	1.39	15278.41	75.00	351.2		
111.20	1.61	19334.16	80.00	444.5		
83.40	1.90	24889.37	85.00	572.2		

Insolubilised β -galactosidase (1.25 mg cm⁻³) incubated with 20% w/v lactose monohydrate at 40°C

Initial lactose monohydrate concentration (mM)	K_m	K_i	$V_{max} \cdot t$	% Lactose monohydrate conversion	t (minutes)	$(1 - k_m/k_i)$	$[L_0]$	$(K_m \cdot [L_0]/K_i) + K_m$	V_{max} (mM min ⁻¹)
695	104	2.5	$\ln([L_0]/[L])$			-40.60	695	29016.00	43.5
[L]	$[L_0] - [L]$	$\ln([L_0]/[L])$	$V_{max} \cdot t$	% Lactose monohydrate conversion	t (minutes)				
695.00	0.00	0.00	0.00	0.00	0.0				
660.25	34.75	0.05	77.48	5.00	1.8				
625.50	69.50	0.11	235.44	10.00	5.4				
590.75	104.25	0.16	483.10	15.00	11.1				
556.00	139.00	0.22	831.33	20.00	19.1				
521.25	173.75	0.29	1293.13	25.00	29.7				
486.50	208.50	0.36	1884.18	30.00	43.3				
451.75	243.25	0.43	2623.65	35.00	60.3				
417.00	278.00	0.51	3535.32	40.00	81.3				
382.25	312.75	0.60	4649.19	45.00	106.9				
347.50	347.50	0.69	6003.86	50.00	138.0				
312.75	382.25	0.80	7650.15	55.00	175.9				
278.00	417.00	0.92	9656.89	60.00	222.0				
243.25	451.75	1.05	12120.59	65.00	278.6				
208.50	486.50	1.20	15182.57	70.00	349.0				
173.75	521.25	1.39	19061.97	75.00	438.2				
139.00	556.00	1.61	24125.85	80.00	554.6				
104.25	590.75	1.90	31062.38	85.00	714.1				

Insolubilised β -galactosidase (1.25 mg cm⁻³) incubated with 25% w/lactose monohydrate at 40°C

Initial lactose monohydrate concentration (mM)	K_m	K_i	$(1-k_m/k_i)$	$[L_0]$	$(K_m[L_0]/K_i)+K_m$	V_{max} (mM min ⁻¹)
834	104	2.5	-40.60	834	34798.40	43.5
$[L]$	$[L_0]-[L]$	$\ln([L_0]/[L])$	$V_{max}t$	% Lactose monohydrate conversion	t (minutes)	
834.00	0.00	0.00	0.00	0.00	0.0	
792.30	41.70	0.05	91.90	5.00	2.1	
750.60	83.40	0.11	280.34	10.00	6.4	
708.90	125.10	0.16	576.34	15.00	13.2	
667.20	166.80	0.22	992.96	20.00	22.8	
625.50	208.50	0.29	1545.78	25.00	35.5	
583.80	250.20	0.36	2253.60	30.00	51.8	
542.10	291.90	0.43	3139.42	35.00	72.2	
500.40	333.60	0.51	4231.75	40.00	97.3	
458.70	375.30	0.60	5566.59	45.00	128.0	
417.00	417.00	0.69	7190.21	50.00	165.3	
375.30	458.70	0.80	9163.57	55.00	210.7	
333.60	500.40	0.92	11569.21	60.00	266.0	
291.90	542.10	1.05	14522.87	65.00	333.9	
250.20	583.80	1.20	18194.05	70.00	418.3	
208.50	625.50	1.39	22845.53	75.00	525.2	
166.80	667.20	1.61	28917.54	80.00	664.8	
125.10	708.90	1.90	37235.40	85.00	856.0	

Insolubilised β -galactosidase (1.25 mg cm⁻³) incubated with 30% w/v lactose monohydrate at 40°C

Initial lactose monohydrate concentration (mM) 1112 K_m 104 K_i 2.5 $(1-k_m/k_i)$ -40.60 $[L_0]$ 1112 $(K_m[L_0]/K_i)+K_m$ 46363.20 V_{max} (mM min⁻¹) 43.5

$[L]$	$[L_0]-[L]$	$\ln([L_0]/[L])$	$V_{max} \cdot t$	% Lactose monohydrate conversion	t (minutes)
1112.00	0.00	0.00	0.00	0.00	0.0
1056.40	55.60	0.05	120.76	5.00	2.8
1000.80	111.20	0.11	370.13	10.00	8.5
945.20	166.80	0.16	762.82	15.00	17.5
889.60	222.40	0.22	1316.21	20.00	30.3
834.00	278.00	0.29	2051.06	25.00	47.2
778.40	333.60	0.36	2992.43	30.00	68.8
722.80	389.20	0.43	4170.95	35.00	95.9
667.20	444.80	0.51	5624.63	40.00	129.3
611.60	500.40	0.60	7401.40	45.00	170.1
556.00	556.00	0.69	9562.92	50.00	219.8
500.40	611.60	0.80	12190.41	55.00	280.2
444.80	667.20	0.92	15393.85	60.00	353.9
389.20	722.80	1.05	19327.43	65.00	444.3
333.60	778.40	1.20	24216.99	70.00	556.7
278.00	834.00	1.39	30412.64	75.00	699.1
222.40	889.60	1.61	38500.93	80.00	885.1
166.80	945.20	1.90	49581.43	85.00	1139.8

Insolubilised β -galactosidase (1.25 mg cm⁻³) incubated with 40% w/v lactose monohydrate at 40°C

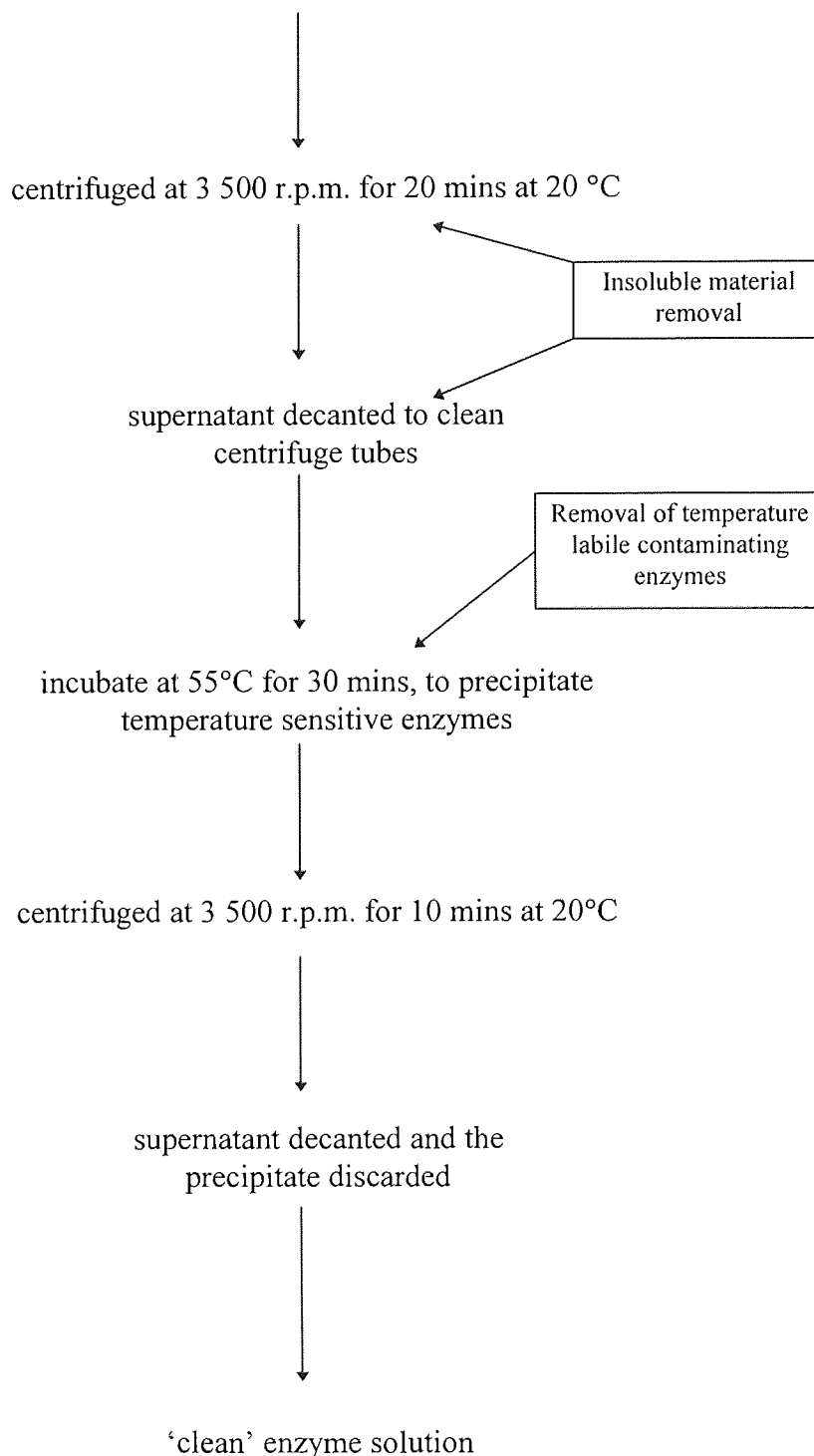
Appendix A-3

(Preparation of glutaraldehyde insolubilised β -galactosidase)

Preparation of insoluble β -galactosidase from *Aspergillus oryzae* (Biolactase F) using glutaraldehyde as a cross-linking Agent

Enzyme Preparation

1g of Biolactase F dissolved in 100 cm³ of degassed HPLC-grade water (10 mg cm⁻³), pH adjusted to 5.2



Glutaraldehyde Cross-linking

20 cm³ of 'clean' enzyme placed in a 100 cm³ medicine flat bottle and 10 cm³ of 4%^{v/v} glutaraldehyde added, and well mixed by shaking the bottle

See Figure 7.4

incubated at 25 °C for 18 hours

precipitated material re-dispersed by shaking bottle and placed in a centrifuge tube

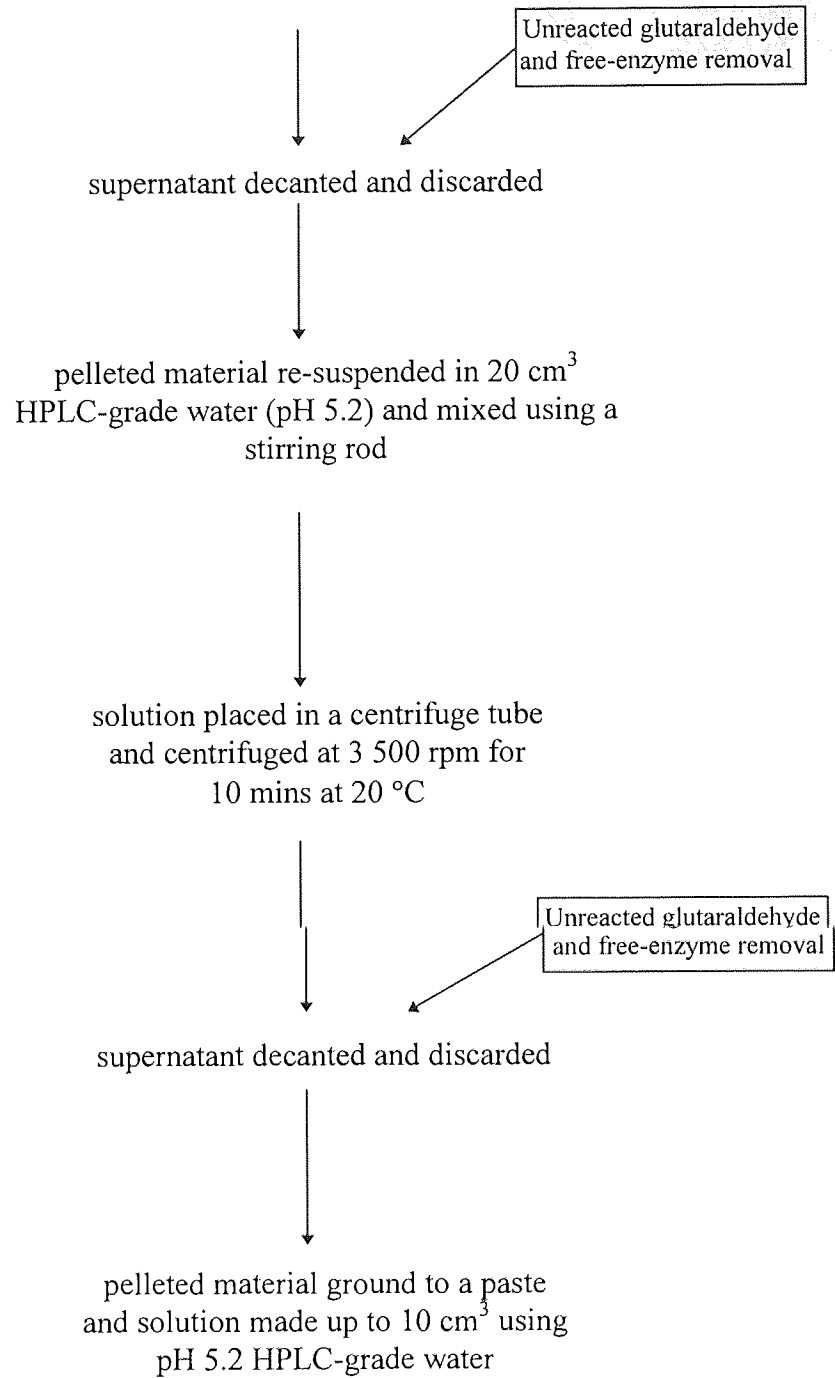
centrifuged at 3 500 r.p.m. for 10 mins at 20 °C

Unreacted glutaraldehyde and free-enzyme removal

supernatant decanted and discarded

pelleted material re-suspended in 20 cm³ of degassed HPLC-grade water pH 5.2 and mixed thoroughly using a stirring rod


solution centrifuged at 3 500 r.p.m. for 10 mins at 20°C




Final Solution Preparation

re-suspended pelleted material whirly-mixed for 1 min and left for 30 mins to allow largest particulate material to settle to bottom of tube


← See Figure 7.6



supernatant decanted and
sedimented material discarded



insoluble, cross-linked enzyme suspension



activity assay performed as described in 7.2.1.2,
and suspension diluted to the desired stirred-batch
or top-layering solution concentration

Appendix A-4

- A - Published in the proceedings of the International Conference on Process Innovation and Intensification, IChemE Research Event, 21-22 October 1999 held at the G-Mex Centre, Manchester, UK.

- B - Published in The Transactions of the Institution of Chemical Engineers, Part C, 2000, Number C1, Volume 78: 35. Special Topic Issue - Biochemical Engineering at Research 2000.

A

ENZYMATIC PRODUCTION OF OLIGOSACCHARIDES IN CENTRIFUGAL FIELDS

P. A. TACK and E. L. SMITH

Department of Chemical Engineering and Applied Chemistry,
Aston University, Birmingham, UK



Aston University

Content has been removed for copyright reasons

B

ENZYMATIC PRODUCTION OF OLIGOSACCHARIDES IN CENTRIFUGAL FIELDS

P.A. Tack and E.L. Smith

Department of Chemical Engineering and Applied Chemistry, Aston University, Birmingham, B4 7ET, UK.

Oligosaccharides are naturally



Aston University

Content has been removed for copyright reasons